Author:
Fraser, Donald

Title:
Circadian Regulation of Plant Responses to Shade and UVB

Circadian Regulation of Plant Responses to Shade and UVB

Donald Peter Fraser

A dissertation submitted to the University of Bristol in accordance with the requirements for award of the degree of Doctor of Philosophy in the Faculty of Life Sciences

School of Biological Sciences

September 2018

Word Count: 41206

Abstract

Plants are sessile organisms and must adapt their development to the environment. Light quality is a primary informational signal that plants sense and respond to. Specialised photoreceptor proteins perceive changes in light quality that indicate the presence of neighbouring vegetation and the risk of shade. Shade avoiding species respond through stem elongation and elevation of leaves. Many plant environmental responses are regulated by the circadian clock through a process called circadian gating. This thesis shows that the inhibition of hypocotyl elongation by UV-B appears to be under circadian regulation in *Arabidopsis thaliana*. This is likely achieved through a temporal coincidence of 1) the circadian-gated peak of UV-B-induced GA catabolism genes with 2) the greatest UV-B-induced reductions in auxin signaling. Shade avoidance can have detrimental effects on yield in commercial growing environments, so knowledge of circadian regulation of plant responses to light quality provides a toolset for product quality improvements. This thesis shows that UV-B inhibits shade avoidance in the commercially important crop, *Coriandrum sativum*, though there are only marginal differences when UV-B is delivered at different times of day. Although shade avoidance can provide plants with a competitive advantage in fast growing stands, excessive stem elongation can be detrimental to plant survival. As such, plants have evolved multiple feedback mechanisms to attenuate photoreceptor-mediated shade avoidance signalling. The combination of a very low red to far red ratio (R:FR) and low levels of photosynthetically active radiation (PAR) present in deep canopy shade can, together, trigger phytochrome A (phyA) signalling; inhibiting shade avoidance and promoting plant survival. This thesis also shows that very low R:FR in a background of low PAR increases expression of the circadian clock component TIMING OF CAB EXPRESSION1 (TOC1) in a phyA-dependent manner at dusk and that TOC1 antagonises shade avoidance in these conditions.

Acknowledgements

In the production of this thesis I have been graced with the support of many great people. I firstly thank my primary supervisor, Prof Kerry Franklin for her mentorship, encouragement and inspiration. I thank also Dr Antony Dodd, for our many insightful discussions, the opportunities that he has given me and for integrating me with his research group and journal club. I also would like to thank my collaborators at Vitacress, Simon Budge and Chris Moncrieff - this project would not have happened without their support and continued interest in my work. I thank colleagues from around the world who have generously provided materials and methods: Prof Gareth Jenkins, Prof Peter Quail, Prof Elena Monte and Prof Rob McClung. In Bristol, special thanks go to: Dr Ashutosh Sharma, who is a fount of knowledge on molecular biology and taught me everything I know about protein work; Fiona taught me how to use the luciferase assay system; and in the Physics workshop, Adrian and Bart, who can build anything and were a pleasure to work with. Many thanks go to my colleagues in the plant lab for their patience, good humour and for indulging my penchant for philosophizing - Dora, Ashley, Katie, Beth, Alex, Noriane, Kelly, Matt... There are so many others, who I have not mentioned here, but collectively their company made my time in Bristol the highlight of my education. Outside of the lab, my best friends - Guy, Andrew, Adam, Liam and Jacob helped me unwind: thanks guys. I thank my family for providing a nurturing environment where I was able to pursue my interests. And finally, I thank my partner, Helena, for her unwavering support and companionship.

This thesis was supported by a BBSRC CASE studentship, in collaboration with Vitacress Herbs Ltd.

I declare that the work in this dissertation was carried out in accordance with the requirements of the University's Regulations and Code of Practice for Research Degree Programmes and that it has not been submitted for any other academic award. Except where indicated by specific reference in the text, the work is the candidate's own work. Work done in collaboration with, or with the assistance of, others, is indicated as such. Any views expressed in the dissertation are those of the author.

SIGNED ____________________ DATE ____________________

Contents

List of Figures

List of Tables

Nomenclature

12L:12D 12 hour light : 12 hour dark photocycle

ABA Abscisic acid

ABI ABA-INSENSITIVE

ADO Adagio Protein - blue light photoreceptor

AFB1 AUXIN SIGNALLING F-BOX PROTEIN 1

ARF AUXIN RESPONSE FACTOR

B Blue

BES1 BRI1-EMS-SUPPRESSOR1

bHLH basic Helix-Loop-Helix

BIM1 BES1-INTERACTING MYC-LIKE 1

BR brassinosteroid

BRI1 BRASSINOSTEROID INSENSITIVE 1

BZR1 BRASSINAZOLE-RESISTANT 1

CAB CHLOROPHYLL A/B BINDING

CCA1 CIRCADIAN CLOCK ASSOCIATED 1

cDNA complementary DNA

ChIP Chromatin Immuno Precipitation

CHS CHALCONE SYNTHASE

CK2 CASEIN KINASE II

COP1 CONSTITUTIVELY PHOTOMORPHOGENIC 1

cry cryptochrome

CUL4 CULLIN4

DDB1 DAMAGED DNA BINDING PROTEIN1

DPBA 2-Aminoethyl diphenyborinate

EC evening complex

EE evening element

ELF3 EARLY FLOWERING 3

ELF4 EARLY FLOWERING 4

FAD flavin adenine dinucleotide

FAR1 FAR-RED IMPAIRED RESPONSE 1

FFT-NLLS fast Fourier transform-nonlinear least-squares

FHL FHY1-LIKE

FHY1 FAR-RED ELONGATED HYPOCOTYL 1

FHY3 FAR-RED ELONGATED HYPOCOTYL 3

FKF1 Flavin-binding Kelch Repeat F-box 1

FR Far Red

GA Gibberellic Acid

GAI GA-INSENSITIVE 1

GC-MS GAS CHROMATOGRAPHY - MASS SPECTROSCOPY

GFP GREEN FLUORESCENT PROTEIN

GI GIGANTEA

GSK3 GLYCOGEN SYNTHASE KINASE3

HFR1 LONG HYPOCOTYL IN FAR RED 1

HIR High irradiance response

HLH Helix-Loop-Helix

HY5 ELONGATED HYPOCOTYL 5

HYH HY5 HOMOLOGUE

IR Infra-Red

LBL low blue light

LD Driven cycle (Light : Dark)

LED Light Emitting Diode

LFR Low fluence response

LHY LATE ELONGATED HYPOCOTYL

LKP2 LOV Kelch Protein 2

LL Continuous Light (Light : Light)

LNK NIGHT LIGHT-INDUCIBLE AND CLOCK-REGULATED

LOV light-oxygen-voltage-sensing

LRB Light-Response Bric-a-Brack/Tramtrack/Broad

LUC LUCIFERASE

LUX LUX ARRHYTHMO

OPM	Output Module
PAR	Photosynthetically Active Radiation (400-700 nm)
PAR1	PHYTOCHROME RAPIDLY REGULATED 1
phot	phototropin
phyA	phytochrome A
PIF	PHYTOCHROME INTERACTING FACTOR
PIL	PIF3-like
PIN3	PIN-FORMED 3
PP2A	PROTEIN PHOSPHATASE 2 ALPHA
PRD	PAS-related domain
PRR	PSEUDO RESPONSE REGULATOR
PSM	Photosensory Module
R:FR	Red : Far-Red ratio
RAE	Relative Amplitude Error
RCC1	REGULATOR OF CHROMATIN CONDENSATION 1
RGA	REPRESSOR OF ga1-3
ROS	Reactive Oxygen Species
RVE8	REVEILLE 8
SAS	Shade Avoidance Syndrome
SOD	Super Oxide Dismutase
SOM	SOMNUS
SPA	SUPPRESSOR OF PHYA-105

SPT	SPATULA
SUMO	small ubiquitin-like modifier
TAA1	TRYPTOPHAN AMINOTRANSFERASE OF ARABIDOPSIS1
TBS	Tris Buffered Saline
TLC	Thin layer chromatography
TMG	TOC1 MINI-GENE
TOC1	TIMING OF CAB EXPRESSION 1 (PRR1)
Trp	Tryptophan - 3 letter code
TT4	TRANSPARENT TESTA 4
TT7	TRANSPARENT TESTA 7
UV-B	Ultraviolet-B radiation (280-315 nm)
UVR8	UV-B RESISTANCE 8
VLFR	Very low fluence response
W	Tryptophan - 1 letter code
WL	White Light
XTH	XYLOGLUCAN ENDOTRANSGLUCOSYLASE/HYDROLASE
YFP	YELLOW FLUORESCENT PROTEIN
ZTL	Zeitlupe

Chapter 1

Introduction

PLANTS have evolved a plethora of environmental responses to allow them to adapt their development and physiology to the conditions around them. A particularly well-studied environmental adaptation that can occur when plants are grown in dense stands is a suite of responses termed *shade avoidance*. Light quantity and quality are the primary environmental cues that regulate shade avoidance. Plants are known to perceive and respond physiologically to a range of wavelengths of electromagnetic radiation, from UV-B (280-315 nm) through to near infra red (725-735 nm), using specialised photoreceptors. Alongside responding to external environmental cues, plant physiology is also regulated by the endogenous circadian clock, which is thought to allow plants to anticipate and prepare for the predictable transitions associated with Earth's 24 h light-dark cycle in order to optimise their growth and fitness. This introductory chapter will firstly discuss the known plant photoreceptors and the shade avoidance syndrome before discussing the plant circadian clock and its interactions with light signalling.

1.1 Photoreceptors

An array of photoreceptor molecules that detect discrete wavebands of electromagnetic radiation have been identified in plants. In the majority of cases these photoreceptors rely on a light-absorbing chromophore.

1.1.1 Phytochromes: Red Light Photoreceptors

Early Phytochrome Research

The naissance of phytochrome research can be traced back to work studying the involvement of light in flowering and germination. The promotion of lettuce seed germination by red (R) light was immediately reversible by short exposure to far-red (FR) radiation, and this photoreversibility was also found in the flowering processes (Borthwick et al., 1952a,b). Subsequently, by using a spectrophotometric assay, Butler et al. (1959) chemically isolated the photoreversible pigment by then known as phytochrome.

Phytochrome Structure

Phytochromes exist in two photo-convertible isomers - a biologically inactive P_r form that absorbs red light and a biologically active P_{fr} form that absorbs far-red light. In natural light, phytochromes exist in a dynamic equilibrium of P_r and P_{fr}, with the proportions of each isoform largely determined by the ratio of Red : Far-Red light (R:FR). R:FR has been formally defined as the 660 - 670 nm photon irradiance/the 725 - 735 nm photon irradiance, which corresponds with the P_{fr}:P_r ratio (equation 2.4).

The crystal structure of an *Arabidopsis thaliana* phytochrome photosensory unit was recently reported by Burgie et al. (2014), with their findings consistent with previous predicted structures from amino acid sequences. Phytochrome structure is conserved between multiple taxa and is proposed to consist of an N-terminal photosensory module (PSM) that cradles the light-absorbing bilin chromophore followed by an output module (OPM) that presumably promotes dimerisation and signalling. Phytochromes in land plants associate into homo- and hetero-dimers *via* interaction between the carboxy-terminal ends of two independently reversible polypeptide subunits (Kim et al., 2006; Sharrock and Clack, 2004; Clack et al., 2009). The C-terminal histidine kinase-related domains of the OPM are reminiscent of bacterial two-component receptor mechanisms, leading to the suggestion that these domains participate in signalling interactions with downstream effectors (Shin et al., 2016).

Following synthesis in the cytoplasm, the *c.* 124 kDa phytochrome apoprotein covalently binds to a plastid-synthesised linear tetrapyrrole phytochromobilin chromophore *via* a thioether linkage (Furya and Song, 1994). The resulting holoprotein folds into the stable red light absorbing P_r form. The proposed key light-sensing step, which converts the biologically inactive P_r form to the P_{fr} state, involves a light-actuated *Z* to *E* isomerisation of the C15=C16 double bond in phytochromobilin that rotates the D pyrrole ring. This initiates conformational changes in the bilin binding pocket and subsequently causes a conformational change to the OPM (Rockwell et al., 2006). P_{fr} rapidly converts back to P_r on absorbtion of Far-Red light or slowly by spontaneous thermal reversion, allowing phytochromes to act as both short and long-lived photoswitches. The rate of thermal reversion is sensitive to temperature, which has led to the hypothesis that phytochromes may also act as thermal sensors (Jung et al., 2016; Legris et al., 2016).

Five Phytochromes

In the model plant species, *Arabidopsis thaliana*, five phytochromes have been sequenced and characterised, all of which belong to a small gene family (Sharrock and Quail, 1989; Clack et al., 1994). Across the angiosperms in general there are three conserved phytochromes; phyA, phyB and phyC, encoded by the genes *PHYA*, *PHYB* and *PHYC* (Mathews et al., 1995). Meanwhile, dicotyledonous plants have two additional phytochromes, phyD and phyE, which likely exist as products of relatively recent gene duplication events (Mathews and Sharrock, 1997). *PHYB*, *PHYD* & *PHYE* share sequence homology (up to *c.* 80% between *PHYB* & *PHYD*) and hence are considered to form a distinct subgroup of "type II" phytochromes within the arabidopsis *PHY* gene family (Goosey et al., 1997). Due to their relative stability in their P_{fr} form, photoreversible responses are mediated by this "type II" subgroup and are termed Low Fluence Responses (LFRs) (Sharrock and Clack, 2002).

phyB mutants resemble the growth of wild-type plants grown in low R:FR (Nagatani et al., 1991; Somers et al., 1991). Furthermore, a study using immunoblot analysis by Sharrock and Clack (2002) found that in light-grown seedlings, phyB is the most abundant; as such phyB is thought to be the primary mediator of responses to low R:FR by antagonising shade avoidance responses under high R:FR. A naturally occuring *phyD* mutation, which displays a phenotype weakly reminiscent of the *phyB* mutant was isolated in the Wassilewskija (Ws) accession of *Arabidopsis* (Aukerman et al., 1997). Consistent with the *PHYB* & *PHYD* sequence homology, *phyBphyD* double mutants displayed longer hypocotyls, longer petioles and earlier flowering than the monogenic parents, implying that phyD and phyB act redundantly to suppress shade avoidance (Devlin et al., 1999). In addition, a mutant screen by Devlin et al. (1998) identified a *phyAphyBphyE* triple mutant that was a phenocopy of the accelerated flowering and elongation of internodes between rosette leaves characteristic of the response of *phyAphyB* double mutants to end-of-day (EOD) FR treatments[1]. Thus, phyE was implicated in having a regulatory role in this response; the *phyBphyE* double mutant flowered earlier and had longer petioles than *phyB* mutants, suggesting that phyE acts redundantly with phyB and to a lesser extent, phyD in the suppression of shade avoidance under high R:FR (Halliday et al., 1994; Devlin et al., 1998, 1999).

Contrasting with the other phytochromes, phyA accumulates to high levels in

[1]EOD FR treatments are an artificial way of mimicing shade avoidance: FR at the end of the day establishes a greater pool of P_r that will persist during the dark period, which will result in a strong shade avoidance phenotype.

etiolated seedlings and can signal during rapid photoconversion between P_r and P_{fr}, but on transfer to light that establishes a high proportion of P_{fr} (*e.g.* R), phyA is rapidly degraded to low steady-state levels (Clough and Vierstra, 1997). The highly sensitive non-reversible responses of phyA to low quantities of light have been termed Very Low Fluence Responses (VLFRs), this function can also be interpreted as an "antenna" that promotes germination and photomorphogenesis of buried seeds following a brief exposure to light on emergence from the soil (Franklin and Quail, 2010). Meanwhile, the continuous irradiation of wavelengths that establish a low proportion of P_{fr} (*e.g.* FR) and results in the photo-cycling of phyA between its Pr and Pfr forms signals *via* the High Irradiance Reponse (HIR) mode (Hennig et al., 2000). Plants deficient in phyA are unable to de-etiolate in continuous FR, which formed the basis for screens to identify *phyA* mutants (Nagatani et al., 1993; Parks and Quail, 1993). Additionally, the observations that *phyA* mutant seedlings displayed enhanced hypocotyl elongation when compared to wild type when grown in continuous low R:FR led to the suggestion that phyA antagonises phyB-mediated shade avoidance by limiting hypocotyl extension. This was supported by observations that *phyAphyB* double mutants display enhanced hypocotyl elongation compared to monogenic *phyB* mutants (Johnson and Bradley, 1994) and a report that phyA antagonism of shade avoidance takes on greater significance in conditions of low PAR (Martínez-García et al., 2014). A role for phyC in the mediation of shade-avoidance responses was excluded with the observation that *phyBphyDphyE* triple mutants were blind to reductions in the R:FR ratio and EOD FR treatments. Isolation of *phyC* mutants suggested that phyC performs a small, redundant role in seedling photomorphogenesis (Franklin et al., 2003a,b; Monte et al., 2003) and is a source of natural variation in flowering and growth responses (Balasubramanian et al., 2006).

Mechanism of Phytochrome Signalling

On the basis that phyB contained putative nuclear localisation signals within its C-terminal region, Sakamoto and Nagatani (1996) investigated the signal transduction activity of phyB. Using a transgenic phyB-GUS fusion protein and immunoblot analysis, the authors demonstrated that phyB localised to the nucleus in R, while nuclear levels of phyB were reduced on dark adaptation and FR irradiation. Additional evidence of the nuclear localisation mechanism for phytochrome signalling came from work by Kircher et al. (1999): Using GREEN FLUORESCENT PROTEIN (GFP) fusion proteins and R & FR light treatments, they showed that phyA-GFP and phyB-GFP are translocated to the nucleus under R light. FR light appeared to inhibit phyB-GFP nuclear transport but not that of phyA-GFP, which by contrast translocated to the nucleus under FR light alone. Further work extended this mechanism to phytochromes C, D & E and revealed that light quality differentially regulated this mechanism of translocation between the five phytochromes (Kircher et al., 2002). In general, following photoconversion from Pr to the active Pfr form, phytochromes translocate to the nucleus where they have been shown to bind directly to eight members in a family of basic Helix-Loop-Helix (bHLH) transcription factors, termed PHYTOCHROME INTERACTING FACTORS (PIFs1 - 8), which will be discussed in more detail in section 1.1.4 (Pham et al., 2018). Pfeiffer et al. (2012) showed that phyB P_{fr} migration to the nucleus is facilitated by selective binding to PIF transcription factors. In contrast, phyA migrates to the nucleus after binding FAR-RED ELONGATED HYPOCOTYL 1 (FHY1) and FHY1-LIKE (FHL) (Genoud et al., 2008). Once in the nucleus it is released from FHY1 and FHL by transformation to P_r , it is then back-transformed to P_{fr} for its nuclear activity (Rausenberger et al., 2011). PIF1 and PIF3 have been reported to bind phyA (Shen et al., 2005; Bauer et al., 2004), while another study reported that phyA binds to AUX-IAA repressors to inhibit auxin signalling (Yang et al., 2018). Chen et al. (2014) have shown that phyA directly associates with numerous promoters to regulate the transcription of target genes. Taken together, these data result in a complex, and not fully clarified, picture for how phyA signals in the nucleus.

On import into the nucleus, phyA and phyB localise into "photobodies" (Van Buskirk et al., 2012): phyB forms two types; early photobodies are formed within 15 mins of light exposure and co-localise with PIFs, late photobodies are larger, more stable and are observed after longer 2-3 h R light treatments once PIFs are degraded (Bauer et al., 2004). phyA co-localizes with CONSTITUTIVE PHOTOMORPHOGENIC 1 (COP1) in early nuclear bodies and the direct interaction of the phyA PAS-related domain (PRD) and COP1 WD40-repeat domains mediates rapid ubiquitination and destabilisation of phyA in R light (Seo and Watanabe, 2004; Saijo et al., 2008). In addition, several photomorphogenesis promoting factors are targeted for proteasomal degradation by the COP1/SUPPRESSOR OF PHYA-105 (SPA) E3 ligase complex, but are stabilised in light by the inactivation of COP1 by phytochromes (Lau and Deng, 2012; de Lucas and Prat, 2014).

1.1.2 Blue Light Sensors

In plants, three flavoprotein classes (cryptochromes, phototropins and Zeitlupe) sense Blue (B) and UV-A wavelengths (300-500 nm).

Cryptochromes

Cryptochromes (cry) are blue-light and UV-A sensing photoreceptors. They are bound to a flavin adenine dinucleotide (FAD) light-sensitive subunit and bear amino acid sequence similarity to DNA photolyases, which catalyse B and UV-A light-dependent repair of UV-induced DNA lesions (Sancar, 1990). The *Arabidopsis* mutant, *hy4* was found to have elongated hypocotyls when grown under B light (Koorneef et al., 1980). HY4 similarity to DNA photolyases (Ahmad and Cashmore, 1993), its binding to FAD and the hypersensitivity of transgenic tobacco expressing *Arabidopsis HY4* cDNA to B and UV-A light indicated that HY4 was a cryptochrome and hence was renamed cry1 (Lin et al., 1995). cry2 was identified through the screening of Arabidopsis cDNA libraries with *cry1* cDNA probes (Hoffman et al., 1996; Ahmad et al., 1996) and subsequent studies demonstrated that cry2 primarily regulates the photoperiodic promotion of floral initiation (Guo et al., 1998; El-Assal et al., 2001). In addition, cry2 is thought to enhance light sensitivity due to its promotion of photomorphogenesis in low intensities of B light (Lin et al., 1998). A third cryptochrome, cry3 has also been identified, but it role remains unclear; a T-DNA insertional *cry3* mutant showed no obvious phenotypic alteration, leading to speculation that cry3 is most likely involved in the protection of organellar genomes in Arabidopsis from DNA damage due to its mitochrondial and plastid localisation and biochemical activity (Yu et al., 2010). In addition to their respective roles in B-light-induced de-etiolation and photoperiodic control of flowering-time, cry1 and cry2 have also been shown to regulate several other light responses including but not limited to: circadian rhythms, tropic growth, root development, guard cell development, stomatal opening, pathogen responses, abiotic stress responses, cell cycles, apoptosis, apical dominance and seed development (reviewed by Yu et al. (2010)). Cryptochromes also have an established role in low B (LBL)-mediated shade avoidance through their perception of B light depletion. Indeed, the mechanism of cryptochrome modulation of plant architecture has begun to be elucidated by the finding that both cry1 and cry2 interact with PIF4 and PIF5 (Pedmale et al., 2015; Ma et al., 2015).

Phototropins

Phototropins are B-light and UV-A-activated serine/threonine protein kinases that have two LOV domains bound to two flavin mononucleotide chromophores. Phototropins control responses that optimise plant photosynthetic efficiency through phototropism, stomatal opening and chloroplast movements (Christie, 2007). Prior to the isolation of the first phototropin gene (Huala et al., 1997), a plasma-membrane-associated protein was identified by Gallagher et al. (1988) in dark-grown pea epicotyls that became phosphorylated upon B-light irradiation. The correlation between phosphorylation and phototropism indicated that this protein was a candidate phototropism photoreceptor that underwent autophosphorylation in response to B-light treatment (Short and Briggs, 1990; Hager and Brich, 1993; Palmer et al., 1993; Hager, 1996). The *nph* mutants of *Arabidopsis thaliana* show impaired hypocotyl phototropism. The *nph1* mutant lacks the activity of the plasma membrane-associated phosphoprotein. Initially designated NPH1, the encoded protein was confirmed to be a phototropic receptor that undergoes autophosphorylation in response to B light and was renamed phot1 (Liscum and Briggs, 1995; Christie et al., 1999; Briggs et al., 2001).

Genetic analysis of phot-deficient *Arabidopsis* mutants established the partially overlapping roles of the two phototropins, phot1 and phot2. Both phot1 and phot2 regulate hypocotyl phototropism responses to high intensity B light (Sakai et al., 2001), whereas the phototropic response to low intensity light is solely mediated by phot1 (Liscum and Briggs, 1995; Sakai et al., 2000, 2001). In addition, phot1 and phot2 redundantly mediate B-light-induced opening of stomatal pores equally across the the same light intensities (Kinoshita et al., 2001). Phototropins also mediate the movement of chloroplasts in response to differing light intensities. Under low light, phot1 and phot2 promote light capture by inducing chloroplast accumulation at the upper cell surface (Sakai et al., 2001). In high intensity light, phot2 mediates the chloroplast movement away from the irradiation sites to prevent photosynthetic apparatus photo-damage (Kasahara et al., 2002). It has also been shown that phot1 is responsible for the B-light-induced rapid inhibition of hypocotyl elongation in dark grown seedlings (Folta and Spalding, 2001). Phototropins have also been reported in the promotion of cotyledon (Ohgishi et al., 2004) and leaf (Sakamoto and Briggs, 2002) expansion. It has also been suggested that phototropism plays a role in light foraging within dense canopies (Pierik and De Wit, 2014; Goyal et al., 2016).

Zeitlupe

The light-sensitive LOV domain has also been identified in a new class of B and UV-A receptors called the ZEITLUPE/ADAGIO (ZTL/ADO) protein family (see Ito et al. (2012) for review). This class comprises three members; Zeitlupe (ZTL), Flavin-binding Kelch Repeat F-box 1 (FKF1) and LOV Kelch Protein 2 (LKP2) (Banerjee and Batschauer, 2005). These proteins share an F-box motif typically found in E3 ubiquitin ligases and evidence now indicates that ZTL/ADO members mediate light-dependent proteasome-dependent protein degradation (Nelson et al., 2000; Somers et al., 2000; Schultz et al., 2001). Analysis of these proteins have so far demonstrated roles in circadian clock function and photoperiodic dependent flowering in *Arabidopsis* by controlling the accumulation of key regulator proteins in the clock and flowering pathways (Más et al., 2003; Kiba et al., 2007; Fornara et al., 2009).

1.1.3 UVR8: The UV-B Photoreceptor

UV-B mediates regulatory responses in plants

Ultra-violet (UV) light is split into three wavebands of the electromagnetic spectrum, UV-A (315-400 nm), UV-B (280-315 nm) and UV-C (100-280 nm). The stratospheric ozone layer absorbs UV light below 290 nm, which includes UV-C and much of the UV-B waveband. Sunlight that has filtered through, therefore, contains UV-A and a part of UV-B. While UV-B is only a small portion of the daylight spectrum, it has major impacts on virtually all organisms. UV-B radiation can damage molecules like DNA, which could impair cellular processes and result in death. Organisms have evolved strategies to avoid and repair UV-B-induced damage. In plants, UV-B exposure stimulates the synthesis of flavonoid "sun-screen" compounds and the production of reflective surface waxes and hairs, while repair is carried out by anti-oxidants and DNA damage repair enzymes. (Caldwell et al., 1983; Jordan, 2002; Rozema et al., 1997; Frohnmeyer and Staiger, 2003; Jenkins, 2009). It was discovered that low doses of UV-

B could stimulate photomorphogenic reponses that were not a consequence of UV-B-induced damage nor could they be explained by known photoreceptors. Responses include inhibition of hypocotyl elongation, root growth and promotion of cotyledon opening (Wellmann, 1976; Ballaré et al., 1995; Kim et al., 1998; Boccalandro et al., 2001; Suesslin and Frohnmeyer, 2003; Tong et al., 2008; Conte et al., 2010). The finding that plants respond to UV-B independent of known photoreceptors indicated the existence of a specific UV-B photoreceptor.

UVR8 Discovery

In a genetic screen for plants hyper-sensitive to UV-B, Kliebenstein et al. (2002) identified the *Arabiopsis thaliana* mutant *uvr8-1* in Landsberg *erecta*. This mutant had greatly reduced expression of the flavonoid biosynthesis enzyme, CHALCONE SYNTHASE (CHS) and increased expression of the stress-related PATHOGENESIS RELATED1 (PR1) and PR5 proteins. Observations that *uvr8-1* differed from other mutants in the screen, due to altered gene regulation following UV-B exposure, indicated the involvement of ULTRA-VIOLET RESISTANCE 8 (UVR8) in the UV-B signalling pathway. UVR8 was finally identified as the UV-B photoreceptor by a study demonstrating that UVR8 dimers monomerise on perception of UV-B and that UVR8 monomers interact with COP1, which is a central regulator of light signalling (Rizzini et al., 2011).

Structure

Crystallographic and solution structures of the UVR8 protein (Christie et al., 2012) were consistent with the predicted structure (Rizzini et al., 2011) and revealed the mechanism for UV-B perception by UVR8. *UVR8* encodes a seven-bladed β-propellor protein with structural, though not functional, homology to human REGULATOR OF CHROMATIN CONDENSATION1 (RCC1) (Brown et al., 2005). Christie et al. (2012) reported a number of aromatic residues and charged side chains at the dimer interface key to UV-B perception and signalling. The aromatic tryptophan (Trp/W) residues form a cross-dimer excitonically-coupled Trp pyramid, while the off-set arrangement of arginine and carboxylate side chains form a network of salt bridges across the dimer interface. The Trp residue absorbs wavelengths in the UV-B range and *Arabidopsis* UVR8 has 14 Trp residues; one in the C-terminal region, six in the β-propellor core and seven at the dimer interface. Mutation of the pyramid Trps revealed their roles in UV-B perception with W285 emerging as the principle UV-B sensor in the Trp pyramid (Christie et al., 2012). The authors proposed that photoreception of UV-B by the excitonically-coupled Trp pyramid results in the transfer of an electron from the Trp pyramid to adjacent arginines. This causes charge neutralisation and disrupts the cross-dimer salt bridges, which results in monomerisation of the UVR8 homodimer. Dynamic crystallography captured early UV-B induced structural changes in UVR8. The absorption of UV-B by Trp233 caused a 10º turn and a 30º tilt in Trp285, which lead to the ejection of a water molecule that weakens the bonds at the dimer interface (Zeng et al., 2015). Thus, unlike all other photoreceptors identified to date, UVR8 does not rely on a light-sensitive chromophore subunit to perceive light.

UVR8 Signaling

Most UVR8 is localised to the cytosol in plants prior to UV-B irradiation (Brown et al., 2005; Kaiserli and Jenkins, 2007). On UV-B exposure, UVR8 was shown to accumulate in the nucleus. COP1 also accumulates in the nucleus in plants after UV-B exposure, and transient expression experiments found that CFP-UVR8 colocalises with YFP-COP1 in nuclear bodies after UV-B irradiation (Favory et al., 2009). COP1 interacts with UVR8 in a UV-B-dependent manner and is thought to be the primary signaling partner of UVR8 (Favory et al., 2009; Rizzini et al., 2011; Cloix et al., 2012). COP1-regulated genes are largely the same as those regulated by UV-B, indicating that COP1 and UVR8 act together to mediate photomorphogenic UV-B responses. It was previously thought that this positive function of COP1 contrasts with its well-characterised activity as a repressor of photomorphogenesis in dark-grown seedlings where it targets positive regulators of photomorphogenesis *e.g.* ELONGATED HYPOCOTYL 5 (HY5), for destruction *via* its role in an E3 ubiquitin ligase complex (Osterlund et al., 2000; Lau and Deng, 2012). Recent opinion suggests instead that UVR8 sequesters COP1, which prevents it from degrading transcription factors (Podolec and Ulm, 2018).

Huang et al. (2013) showed that UV-B exposure reduced the association of the CULLIN4 (CUL4)-DAMAGED DNA BINDING PROTEIN1 (DDB1) E3 ubiquitin ligase complex with COP1 and SPA proteins. After UV-B exposure SPA proteins associate with COP1 and UVR8, with this UVR8-COP1-SPA complex acting to positively regulate UV-B-induced photomorphogenesis (Heijde et al., 2013; Huang et al., 2013). Their observations were consistent with a model whereby the presence of the UVR8-COP1-SPA complex under UV-B resulted in stabilisation of the HY5 protein; while in the absence of UV-B, COP1-SPA is recruited to the CUL4-DDB1 complex, which likely promotes degradation of HY5 (Favory et al., 2009; Huang et al., 2013). Observations that this is not abolished in the *cop1* mutant suggest that an E3 ubiquitin ligase other than COP1 is also involved in degradation of HY5 . The accumulation of HY5 is, therefore, promoted by the UVR8-COP1-SPA protein complex through both post-translational stabilisation and transcriptional stimulation (Jenkins, 2014).

Deletion of a 27-amino acid region of UVR8 towards the protein's C-terminus (C27) prevented interaction with COP1 in yeast two-hybrid assays and *in planta* Cloix et al. (2012). The WD40 domain of COP1 interacts with UVR8, perhaps *via* a motif in the C27 domain (Rizzini et al., 2011; Cloix et al., 2012; Wu et al., 2013), but this does not preclude interactions between other regions of UVR8 and COP1 (Jenkins, 2014). Association of COP1 with UVR8 leads to COP1 stabilisation and accumulation (Favory et al., 2009; Heijde et al., 2013). COP1 and HY5 form a negative feedback loop: UV-B stimulates the transcription of *COP1* in a mechanism that requires the HY5 and FAR-RED ELONGATED HYPOCOTYL 3 (FHY3) transcription factors, which bind elements in the COP1 promoter (Huang et al., 2012b).

HY5 and the closely related HY5 HOMOLOG (HYH) act with partial redundancy downstream of UVR8 and COP1 in UV-B responses although HY5 is the major effector of UVR8-mediated gene expression (Brown et al., 2005; Brown and Jenkins, 2008; Favory et al., 2009). The induction of *HY5* and *HYH* expression in response to UV-B is very rapid and HY5 regulates many UV-B photomorphogenic gene targets (Brown et al., 2005; Oravecz et al., 2006). Many HY5-regulated UV-B response genes are involved in growth, as evinced by the impairment of UVR8-mediated growth suppression in the *hy5* mutant (Oravecz et al., 2006; Cloix et al., 2012). In addition, HY5-regulated UV-B response genes also include transcription factors like MYB12, which is involved in flavonol biosynthesis (Stracke et al., 2010a). However, the UV-B induction of the clock genes, *CIRCADIAN CLOCK ASSOCIATED 1* (*CCA1*) and *PSEUDO RESPONSE REGULATOR 9* (*PRR9*) is HY5- and HYH- independent, showing that not all UVR8-regulated genes are controlled by HY5/HYH (Fehér et al., 2011). Mechanistically, there is much still to discover about how the UVR8 protein signals. However, a recent study reports that UVR8 directly interacts with BRI1-EMS-SUPPRESSOR 1 (BES1) and BES1-INTERACTING MYC-LIKE 1 (BIM1), two key transcription factors in the brassinosteroid (BR) signalling pathway. The authors argue that nuclear-localised UVR8 sequesters BES1 and BIM1, preventing their DNA-binding and transcriptional activity (Liang et al., 2018).

UVR8-Mediated Regulation of Transcription

The mechanism of transcriptional regulation by UVR8 and COP1 has yet to be fully clarified, but there is evidence that UVR8 could associate with chromatin. Alongside its structural homology to RCC1, UVR8 appears to bind histone-agarose beads *in vitro* (Brown et al., 2005), preferentially interacts with histone H2B, can be detected in plant chromatin preparations and histones are present in immunoprecipitated (with anti-GFP) GFP-UVR8 material (Cloix and Jenkins, 2008). Taken together, these findings suggested that UVR8 associates with chromatin *in vivo via* histones, but UV-B may or may not stimulate UVR8 chromatin association as association was constitutive (Cloix and Jenkins, 2008). The role of COP1 in UVR8-chromatin binding is unclear as binding occurs in both the *cop1-4* mutant (Favory et al., 2009) as well as the ΔC27UVR8 truncated protein (Cloix et al., 2012). There is currently no evidence that COP1 binds directly to chromatin. Data from Chromatin Immuno Precipitation (ChIP) experiments indicate that UVR8 associates with some but not all of the genes that it regulates: Chromatin fragments containing the UVR8-regulated *HY5*, *MYB12* and *CRYD* genes were immunoprecipitated using anti-GFP antibodies in GFP-UVR8-expressing plants and similar results were achieved with anti-UVR8 in wild-type plants (Brown et al., 2005; Cloix and Jenkins, 2008). The promoter regions of other UVR8-regulated genes, *HYH* and *CHS* were, however, not found in these experiments (Cloix and Jenkins, 2008). It remains unclear why some target genes and not others associate with UVR8 from these particular ChIP experiments (Jenkins, 2014). In addition, the knock-down of select chromatin remodelling genes using RNAi resulted in plants hyper-sensitive to UV-B and altered the expression of UV-B regulated genes (Casati et al., 2006), while the acetylation of particular histones in maize (Casati et al., 2008) and *Arabidopsis* (Cloix and Jenkins, 2008) correlated with increased transcription of several genes in response to UV-B exposure. Jenkins (2014) conjectured that the mechanism by which UVR8 regulates transcription may involve the promotion or activation of transcription factors and the remodeling of chromatin at target gene loci. Recently, and in contrast with previous ChIP experiments, Binkert et al. (2016) found no *in vitro* association of UVR8 with nucleosomes and noted a lack of conservation of histone and DNA-interaction residues compared with *Drosophila melanogaster* RCC1. Binkert et al. (2016) instead propose that UVR8-COP1 effects gene expression primarily through HY5 and HYH as HY5 is both stabilised by the UVR8-COP1-SPA complex (Favory et al., 2009; Huang et al., 2013) and binds to and positively regulates the activity of its own promoter Abbas et al. (2014); Binkert et al. (2014, 2016). There is, therefore, no comprehensive answer for how UVR8 regulates transcription beyond the increased stabilisation and expression of the main effectors of UV-B signalling, HY5 and HYH.

Regulation of UVR8 Signalling

REPRESSOR OF UV-B PHOTOMORPHOGENESIS 1 (*RUP1*) and *RUP2* encode two small WD40-repeat proteins, which have sequence similarity to COP1 and SPA WD40 domains (Gruber et al., 2010). The *rup1rup2* double mutant was hyper-responsive to UV-B, showing enhanced hypocotyl growth suppression and increased UVR8-mediated *HY5* and *CHS* gene expression as well as elevated levels of flavonoids when compared to WT plants under UV-B. Over-expressing RUP2 suppressed UV-B-induced *HY5* and *CHS* expression. *RUP1* and *RUP2* expression was UV-B-induced in a mechanism that required UVR8, COP1 and HY5, which suggested that RUP1 and RUP2 form a negative feedback mechanism for UVR8 signaling. Data from bimolecular fluorescence complementation and yeast two-hybrid assays support a model whereby RUP proteins negatively regulate UVR8 *via* physical interaction with the UVR8 C27 region (Gruber et al., 2010; Cloix et al., 2012; Heilmann and Jenkins, 2013). Consistent with these findings, Heijde and Ulm (2013) have shown that RUP1 and RUP2 proteins mediate the redimerisation of UVR8; *rup1rup2* double mutant plants have a slower rate of UVR8 dimer reversion than WT, while RUP2 overexpressing plants have reduced levels of monomeric UVR8 due to enhanced dimer reversion. The RUP-mediated dimerisation of UVR8 appears to be independent of COP1 as mutating RUPs in the *cop1* background slowed, but did not inhibit, dimer formation (Heijde and Ulm, 2013). CULLIN-4 (CUL4) also appears to be a negative regulator of UVR8 signaling. In plants with reduced levels of CUL4, the UV-B-induction of UVR8-regulated transcripts (not including *HY5*) was increased. Observations that these plants had increased levels of HY5 protein after UV-B, but without increases in *HY5* transcripts suggest that CUL4 may repress HY5 accumulation through mediating proteolysis (Huang et al., 2013).

1.1.4 Phytochrome Interacting Factors (PIFs)

Phytochromes control gene expression through their interaction with different families of transcription factors, of which the PIFs are the best characterised. The PIF family comprises of 15 known members (Toledo-Ortiz et al., 2003), which are mostly found in light signaling. Alongside PILs (PIF3-like), PIFs are members of the bHLH (basic helix-loop-helix) family of transcription factors. Early work using yeast two-hybrid screens to isolate phy-interacting proteins yielded the founder member of this gene family, PIF3 (Ni et al., 1998; Fankhauser et al., 1999; Choi et al., 1999). *In vitro* assays demonstrated that complete chromophore-conjugated molecules of phyA and phyB bind to PIF3, but only after light-induced conversion to the active P_{fr} form (Ni et al., 1999; Zhu et al., 2000). PIF3 constitutively localises to the nucleus, and binds to the G-box DNA sequence, CACGTG, present in various light-regulated promoters. Additionally, Martínez-García et al. (2000) showed that phyB can bind specifically and photoreversibly to PIF3 already bound to its cognate DNA-binding site. Taken together, it was initially inferred from these data that PIFs operate as positive regulators that induce light-regulated genes (Duek and Fankhauser, 2005). However, recent analyses have led to the conclusion that PIFs act as negative regulators of phytochrome signaling due to the photomorphogenic phenotype of most dark-grown PIF mutants and the exaggerated skotomorphogenic phenotype of PIF over-expressors. Dark-grown *pif* mutants display short hypocotyls, open cotyledons, and the accumulation of chlorophyll precursors. PIF over-expressors display long hypocotyls, negative hypocotyl gravitropic growth, unopened cotyledons, sustained apical hook and inhibition of chlorophyll biosynthesis (de Lucas and Prat, 2014). A small number of bHLH proteins, *e.g.* PIF6, which promotes germination (Penfield et al., 2010) and LONG HYPOCOTYL IN FAR RED 1 (HFR1), which inhibits shade avoidance by forming non DNA binding heterodimers with PIF4 and PIF5 (Hornitschek et al., 2009), have been reported to act as positive regulators of phytochrome signaling.

phyB has been reported to interact with PIFs 1 through 8 of this gene family (Pham et al., 2018) whereas phyA has been reported to bind with PIF1 and PIF3, (Huq et al., 2004; Khanna et al., 2004). Sequestration by phyB inhibits PIF function as Park et al. (2012) demonstrated that phyB prevented PIFs from binding to their target promoters. Binding to phytochromes triggers the ultimate degradation of PIF proteins, with 10 minutes of R light sufficient for the initial phosphorylation step for PIF3 (Bauer et al., 2004). Ni et al. (2013) found that phosphorylation triggers rapid ubiquitination and degradation of PIF3, yet the mutation of these residues did not affect phyB interaction or DNA binding ability. Indeed, phosphorylation state did not affect the formation of PIF3 nuclear aggregates either, but was required for negative feedback modulation of phyB levels. Recently, Sadanandom et al. (2015) revealed an additional layer of phytochrome light signaling modulation; the small ubiquitin-like modifier (SUMO) is responsible for the reversible SUMOylation of phyB, which is proposed to block its binding with PIF5.

Phosphorylation, which primes PIF polyubiquitination and degradation, is the primary phytochrome triggered event (Al-Sady et al., 2006) and recent work has begun to elucidate some potential kinases and phosphatases responsible for this phospho-regulation. Bu et al. (2011) showed that CASEIN KINASE II (CK2) is necessary for the phosphorylation and light-induced degradation of PIF1. Bernardo-García et al. (2014) found that mutation of a GLYCOGEN SYNTHASE KINASE3 (GSK3)-like kinase, BRASSINOSTEROID INSENSITIVE 2 (BIN2), phosphorylation consensus sequence stabilised PIF4. Recent work has shown that BLADE-ON-PETIOLE (BOP1 & 2) proteins physically interact with PIF4 in a CULLIN3-BOP1-BOP2 E3 ubiquitin ligase complex (Zhang et al., 2017). Yue et al. (2016) reported the indentification of a type 1 protein phosphatase, TOPP4, which directly interacts with and dephosphorylates PIF5 to block its red light induced ubiquitination and degradation in photomorphogenesis. Finally, Ni et al. (2014) identified the Light-Response Bric-a-Brack/Tramtrack/Broad (LRB) E3 ubiquitin ligase that promotes the polyubiquitination and mutually assured destruction of the signaling partners, PIF3 and phyB.

Major roles in plant development have been described for PIF1, PIF3, PIF4 and PIF5 (Ni et al., 1998; Huq et al., 2000; Oh et al., 2004). PIF1/PIL5 controlled by phyB has been reported to play a pivotal role in the R/FR reversible response of germination of imbibed *Arabidopsis* seeds (Shinomura et al., 1994) by regulating the expression of Abscisic acid (ABA) and Gibberellic Acid (GA) related genes (Oh et al., 2007). PIL5 binds to G-box motifs in the promoters of *GA-INSENSITIVE 1* (*GAI*) and *REPRESSOR OF ga1-3* (*RGA*) (Oh et al., 2007), while indirectly promoting ABA biosynthesis and GA catabolic gene expression through the activation of SOMNUS (*SOM*) (Kim et al., 2008) and *ABA-INSENSITIVE* (*ABI*) 3 & 5 gene targets (Oh et al., 2009). In the light, phyB destabiliation of PIL5 reduces PIL5 action and hence reduces ABA levels while increasing GA synthesis, which leads to DELLA destabilisation and the triggering of seed germination (Oh et al., 2007). Penfield et al. (2005) demonstrated that cold temperatures and light act synergistically to promote seed germination *via* the SPATULA (SPT) bHLH factor. Furthermore, PIF6 was reported to play a role in dormancy release; *pif6* mutants exhibited increased primary seed dormancy while over-expression of a splice variant lacking the DNA-binding domain reduced dormancy (Penfield et al., 2010).

PIF1 and PIF3 in darkness have been reported to inhibit photomorphogenesis through the negative regulation of chloroplast development and chlorophyll synthesis. *pif1* and *pif3* mutants accumulate a phototoxic intermediate from the chlorophyll biosynthesis pathway, protochlorophyllide, which causes photo-oxidative damage on illumination: PIF1 directly activates the expression of protochlorophyllide oxidoreductase (*PORC*), while PIF1 and PIF3 repress the *HEMA1* and *GUN4* genes involved in tetrapyrrole synthesis (Moon et al., 2008; Stephenson et al., 2009). Chen et al. (2013) reported that PIF1 and PIF3 can inhibit ROS signalling during de-etiolation by forming heterodimers with the HY5 and HYH bZIP transcription factors. Although PIF1, PIF3, PIF4 and PIF5 are redundant in their regulation of etiolated dark-grown seedling development; PIF1 is thought to have the greatest contribution (Shen et al., 2005; Leivar et al., 2008). In de-etiolated seedlings, PIF4, PIF5 & most recently PIF7 are the main regulators of auxin synthesis in shade avoidance, discussed in section 1.2 (Lorrain et al., 2008; Hornitschek et al., 2012; Li et al., 2012a). Nozue et al. (2007) showed that PIF4 and PIF5 accumulate to high levels at the end of the night, which along with PIF3 (Soy et al., 2012), accounted for rhythmic growth of hypocotyls in short day photoperidos, where the window of highest elongation rate is at the end of the night. Apical hook formation is controlled by PIF5's regulation of ethylene biosynthesis (Khanna et al., 2007), and, in the light, ethylene induces PIF3-dependent hypocotyl elongation (Zhong et al., 2012). PIFs have also been implicated in sucrose signaling with *PIF1*, *PIF3*, *PIF4* and *PIF5* transcript levels shown to be upregulated during sucrose-induced, GA-dependent hypocotyl elongation in the dark (Liu et al., 2011). To further underline their ubiquity in plant growth and development; PIF3, PIF4 and PIF6 have also been implicated in light-mediated regulation of stomatal development and opening (Casson et al., 2009; Wang et al., 2010). The PIFs have been shown to play a role in blue light induced phototropism (Sun et al., 2013) and Franklin et al. (2011) identified PIF4 as the primary regulator of auxin biosynthesis during high temperature-induced hypocotyl elongation. Indeed, through their G-box and PIF-binding E-box (PBE) variant (CACATG) preferred binding motifs (Hornitschek et al., 2012; Zhang et al., 2013), PIFs regulate the expression of many different classes of transcription factor and are thus thought of as integrators of multiple signaling pathways (Duek and Fankhauser, 2005; Franklin, 2009; de Lucas and Prat, 2014).

1.2 Shade Avoidance

Plants compete with their neighbours for sunlight. When plants grow in close proximity to each other, whether in nature or agriculture, they run the risk of mutual shading, which threatens photosynthesis, productivity and hence fitness.

1.2.1 Early Work

It was not until the second half of the century that phytochromes and their detection of R:FR were linked to Shade Avoidance. Experiments on the seeds of *Chenopodium rubrum* demonstrated that germination was sensitive to R:FR, which led to speculation that this may optimise germination in the presence of shade from neighbouring vegetation (Cumming, 1963). Kasperbauer (1971) subsequently noted that, in the field, *Nicotiana tabacum* leaves transmitted more FR light relative to red or blue light and shaded leaves consequently received more FR light than unshaded leaves. The same study demonstrated that *N. tabacum* treated with FR irradiation resembled plants that had been shaded by other plants.

Smith and Holmes (1977) quantitatively related natural variations in R:FR radiation spectra (ξ) (Holmes and Smith, 1975, 1977) to phytochrome photoequilibria, P_{fr}/P_r (φ). They proposed that R:FR be defined as the ratio of two 10 nm wave bands that centre around the absorption maxima of the two photoreversible forms of phytochrome, P_r and P_{fr} (R, 660-670nm : FR, 725-735nm). These values are now commonly used as the parameters to characterise the R:FR levels (equation 2.4). Moreover, using the relationship between φ and ξ (Smith and Holmes, 1977), Morgan and Smith (1976) estimated φ from ξ; and using artificial light sources (that provided uniform photosynthetically active radiation (PAR (400-700 nm)) but varied R:FR) reported that there was a linear relationship between stem elongation rate and φ, the phytochrome photoequilibrium, thus establishing phytochrome in the perception of R:FR (Morgan and Smith, 1978, 1981).

1.2.2 Perception of Shade

Plants can detect their neighbours through physical touching of leaf tips and the sensing of volatile phyto-chemicals (Pierik and De Wit, 2014). However, changes in light quality and quantity dominate as neighbour detection cues. The R:FR of unfiltered natural sunlight ranges from *c.* 1.15 at midday to *c.* 0.7-0.8 at dawn and dusk due to atmospheric absorption, with scattering and refraction at solar elevations below 10° resulting in the enrichment of longer wavelengths (Linkosalo and Lechowicz, 2006). Vegetation dramatically alters ambient spectral quality as photosynthetic pigments absorb light over the PAR (400-700 nm) spectrum, while radiation in the FR region is poorly absorbed, resulting in an enrichment of FR radiation in reflected and transmitted light. Indeed, the typical reported R:FR from underneath vegetational canopies are in the range of 0.09-0.7 (Smith, 1982). This reduction in R:FR is detected by neighbouring vegetation *via* their phytochrome photoreceptors, which is subsequently interpreted as a signal that competitors are nearby. This can also be thought of as an "early warning signal" for shade, with plants altering their architecture or life cycle as a response to the threat of anticipated shade (Ballaré et al., 1990). Post canopy closure, in direct shade conditions, plants can experience a further reduction in R:FR ratio and PAR alongside a depletion of blue-light and an enrichment of green light to additionally give a reduced B:G ratio, which is perceived by cryptochromes cry1 and cry2 (Sellaro et al., 2010). Low blue light, detected by the cry photoreceptor has also been shown to enhance phytochrome-mediated shade avoidance responses through PIF interactions (Pedmale et al., 2015; de Wit et al., 2016). Given that the phototropin blue light sensors phot1 and phot2 mediate re-orientation of cotyledons and leaves as well as chloroplast re-positioning towards blue light illuminated surfaces it has been suggested that phototropins may also play a role in plant competition in very low light conditions (Pierik and De Wit, 2014). Goyal et al. (2016) showed that phototropism is enhanced in shade, which is due to PIF promotion of YUCCA-mediated auxin production. They also proposed that shade-induced phototropism is inhibited by phyB in open environments. UV-B is additionally depleted in shade. Due to UV-B suppression of *Arabidopsis* elongation growth this depletion was also suggested to derepress elongation growth and thus promote shade avoidance (Pierik and De Wit, 2014). However, recent work has revealed that UV-B sensed by UVR8 regulates PIFs to directly antagonise shade avoidance (Hayes et al., 2014).

1.2.3 Physiological Responses to Shade

In hindsight, Borthwick et al. (1952b)'s seminal work on R/FR-reversible promotion of lettuce seed germination initially established germination as a shade avoidance response as it prevents the generation of seedlings that will be immediately exposed to limiting PAR levels at the base of deep canopies. *Arabidopsis* seed germination has been shown to be repressed by shade light, but seeds can subsequently germinate on exposure to sunlight *e.g.* through canopy disturbance. Under dense canopies, however, *Arabidopsis* seeds can also germinate after sensitisation by dark incubation, which is a condition experienced by buried seeds (Shinomura et al., 1996; Botto et al., 1996). Phytochromes mediate the germination of *Arabidopsis* seeds; *phyB* mutants have reduced sensitivity to red light, while *phyA* mutants do not germinate in continuous FR (Shinomura et al., 1994). In addition, action spectra for seed germination performed in WT, *phyA* and *phyB* mutants demonstrated a typical R/FR reversible LFR mediated by phyB (Shinomura et al., 1996). Seed dormancy and germination is beyond the scope of this review and readers are therefore directed to Bentsink and Koornneef (2008) for further detail. Exposure to shade light conditions accelerates time to flowering, which perhaps can be explained as shortening the generation time so that seeds are produced before the canopy becomes too closed giving offspring a greater chance of escaping shade (Casal, 2012). Plants grown under shade light conditions flower after producing fewer leaves than plants grown in sunlight (Sanchez et al., 2011). *phyB* mutants, further exacerbated by *phyD* & *phyE* mutations, have earlier flowering than WT (Halliday et al., 1994; Devlin et al., 1999, 1998) and the effects of these mutations is caused by increased expression of *FLOWERING LOCUS T* (FT) (Cerdán and Chory, 2003; Halliday et al., 2003).

As seedlings, the major shade avoidance architectural responses in Arabidopsis include the promotion of hypocotyl elongation and the upward angling of cotyledons (hyponasty), which places the cotyledons and first true leaves in an elevated position in the canopy. Light gradients caused by the difference between foliar shade and sun flecks in a canopy can also trigger phototropic responses as seedlings forage for light (Casal, 2012). At the rosette stage, architectural responses include: reduced branching, internode elongation, leaf hyponasty and the elongation of petioles, which together efficiently elevate leaves above the canopy or toward canopy gaps to facilitate light capture (Casal, 2012). Elongation responses to low R:FR can be rapid, with changes in gene expression within 8 minutes (Salter et al., 2003) and changes in hypocotyl elongation rate within 15 minutes (Morgan et al., 1980). Other physiological responses include: reduced chlorophyll content in leaves and increased apical dominance (Smith and Whitelam, 1997); reductions in leaf area, biomass and harvest yield (Keiller and Smith, 1989; Robson et al., 1993; Devlin et al., 1999). Together with reduced branching, these additional responses are thought to be a result of a phytochrome-mediated re-allocation of resources (Yang et al., 2016).

1.2.4 Photoreceptors regulate PIFs to antagonise Shade Avoidance

A low R:FR establishes a higher proportion of inactive phyB Pr in the cytoplasm, which therefore releases growth-promoting PIF transcription factors from their phyB-mediated suppression. It has been shown that PIF4, PIF5 and PIF7 play major roles in shade avoidance (Lorrain et al., 2008; Hornitschek et al., 2012; Li et al., 2012a). PIF4 and PIF5 are stabilised in low R:FR primarily as a consequence of a reduction in phyB-triggered phosphorylation and degradation

(Lorrain et al., 2008). PIF7 stably accumulates in its phosphorylated form in high R:FR, but is dephosphorylated in low R:FR (Li et al., 2012a).

It was shown that cryptochromes 1 and 2 physically interact with PIF4 and PIF5 (Pedmale et al., 2015; Ma et al., 2015). The elongated phenotype of *cry* mutants in low blue light (LBL) suggest that crys antagonise shade avoidance (Keuskamp et al., 2011; Pedmale et al., 2015). As Pedmale et al. (2015) report that PIF5, though not PIF4, abundance increases in LBL together with cry2, it is a possibility that cry2 may be operating as a negative regulator of PIF activity to prevent over-elongation. Another study argues that LBL augments low R:FR-induced shade avoidance through increasing PIF5 abundance, and reducing the inhibition of COP1, which is then freed to promote the degradation of negative regulators of PIFs, such as HFR1 (de Wit et al., 2016).

A number of PIF negative regulators are upregulated by the PIFs themselves. These include the bHLH protein HFR1 and the Helix-Loop-Helix (HLH) proteins PHYTOCHROME RAPIDLY REGULATED 1 (PAR1) and PAR2, all of which are hypothesised to inhibit elongation through the formation of non-DNA binding complexes with PIFs (Hornitschek et al., 2009; Galstyan et al., 2011; Hao et al., 2012). Another PIF negative regulator is HY5, which is negatively regulated by the COP1/SPA1 E3 ubiquitin ligase complex. Active phyB has been shown to bind SPA proteins and inhibit their interaction with COP1 (Sheerin et al., 2015). Mutant analyses have suggested that COP1/SPA positively regulate shade avoidance (Rolauffs et al., 2012), it is therefore possible that reduced phyB Pfr in low R:FR releases suppression of the COP1/SPA complex allowing it to degrade PIF negative regulators (*e.g.* HY5). The DELLA family is another class of negative regulator, which forms non DNA-binding complexes with PIFs (Lucas et al., 2008; Feng et al., 2008). DELLA stability appears to be photoreceptor-regulated. Achard et al. (2007) showed that GFP-RGA stability increased in etiolated hypocotyls transferred to light and Djakovic-Petrovic et al. (2007) reported that DELLAs inhibit shade avoidance in hypocotyls through increased GA-dependent DELLA turnover in low R:FR.

It has also been shown that UV-B, perceived by UVR8, inhibits shade avoidance through the antagonism of auxin signalling (Hayes et al., 2014). The mechanisms for the strong antagonism of shade avoidance by UV-B are not fully elucidated, but appear to involve increased PIF turnover and increased DELLA stability (Hayes et al., 2014). Other potential mechanisms may include reductions in *PIF* relative transcript abundance (Hayes et al., 2017), increased HY5 stability, which competes with PIFs at target promoters (Toledo-Ortiz et al., 2014; Gangappa and Kumar, 2017) and perhaps the downregulation of brassinosteroid signalling through the UVR8-BES1-BIM1 interaction (Liang et al., 2018).

1.2.5 Hormonal regulation of shade avoidance

Comparison of low R:FR- and LBL-grown seedlings has revealed that despite sharing similar shade avoidance phenotypes, their hormonal signalling cascades are only partially shared. In low R:FR, auxin biosynthesis, transport and signalling plays a dominant role, whereas in LBL, brassinosteroid signalling is additionally required to achieve full shade avoidance phenotypes (Keller et al., 2011; Keuskamp et al., 2011; Pedmale et al., 2015).

Auxin

PIFs 4, 5 and 7, in a manner requiring TRYPTOPHAN AMINOTRANSFERASE OF ARABIDOPSIS1 (TAA1), upregulate auxin biosynthesis through increasing the expression of YUCCA enzymes, which control the rate-limiting step of the tryptophan-dependent auxin biosynthesis pathway (Tao et al., 2008; Hornitschek et al., 2012; Li et al., 2012a). This low R:FR - induced increase in auxin biosynthesis is thought to mediate the re-localisation and increased expression of the auxin efflux carrier PIN-FORMED 3 (PIN3) protein to promote auxin distribution to the hypocotyl (Keuskamp et al., 2010). At high PAR, *in silico* modelling indicates that increased tryptophan-dependent auxin biosynthesis is primarily responsible for shade avoidance. Hersch et al. (2014) show, however, that under low PAR, PIF4 and PIF5 are responsible for up-regulating auxin sensitivity to counter decreases in auxin production, arguing that increasing auxin sensitivity is more resource-efficient than increasing auxin biosynthesis. Intriguingly, Yang et al. (2018) recently demonstrated that phyA, which had accumulated to high levels in shaded plants, directly interacted with and stabilised AUX/IAA auxin signalling repressors. The authors argue that by competing with the TIR1 auxin receptor to bind to AUX/IAA proteins, phyA reduces auxin sensitivity and, therefore, antagonises shade avoidance in deep shade. While this finding substantially contributes to the mechanistic understanding of phyA antagonism of shade-induced hypocotyl elongation (Martínez-García et al., 2014), it is likely that there are further components yet to be established.

Brassinosteroids

Keller et al. (2011) reported that plants impaired in brassinosteroid signalling or brassinosteroid biosynthesis had an attenuated response or no response respectively to LBL treatment. The XYLOGLUCAN ENDOTRANSGLYCOSYLASE/HYDROLASE (XTH) family of cell wall loosening enzymes increase in abundance in low R:FR and LBL and are regulated by both auxin and BR (Sasidharan et al., 2010; Keuskamp et al., 2011). Interestingly, Keuskamp et al. (2011) showed that auxin and brassinosteroid independently regulate different subsets of the XTH family. Brassinosteroid perception by BRI1 (BRASSINOSTEROID INSENSITIVE 1) leads to the activation of the HLH BES1 and BRASSINAZOLE-RESISTANT 1 (BZR1) transcription factors which play major roles in the regulation of brassinosteroid-regulated expression (Kim and Wang, 2010). BES1 and BZR1 have also been shown to interact with both DELLAs and PIFs (Gallego-Bartolome et al., 2012; Li et al., 2012b; Oh et al., 2012). DELLAs form non DNA binding complexes with BES1 and BZR1 to inhibit their activity (Gallego-Bartolome et al., 2012) whereas BZR1 and PIF4 have been reported to heterodimerise and co-regulate auxin and cell wall-related targets (Oh et al., 2012).

Gibberellin

Observations that GA 20-oxidase expression increases in vegetational shade may result in an elevation of Gibberellic Acid concentration (Salter et al., 2003; Sessa et al., 2005). GA increases turnover of DELLAs (Djakovic-Petrovic et al., 2007), which reduces PIF inhibition. With UV-B irradiation, however, increases in transcripts of GA catabolism genes have been recorded, with *GA2ox1* relative transcript abundance strongly induced by UV-B (Hayes et al., 2014). It has been suggested that reduced GA concentrations, through increased GA catabolism, likely promotes DELLA stabilisation and hence PIF inhibition (Hayes et al., 2014). The requirements for PIF4, PIF5 and PIF7 for low R:FR and LBL shade avoidance, together with observations that GA and brassinosteroid signalling partners directly interact with PIFs has led to the suggestion that PIFs form a signalling module with DELLAs and BZR1 where hormone signalling pathways converge to regulate growth (de Lucas and Prat, 2014).

Ethylene

Low R:FR treatment has also been shown to enhance levels of the volatile plant hormone ethylene (Finlayson et al., 1999). As ethylene application induces shade avoidance-like responses (Pierik et al., 2004), it has been argued that ethylene also plays a role in neighbour detection (Kegge and Pierik, 2010). The extent to which the shade avoidance response depends on ethylene remains unresolved. While shade-induced petiole elongation is impaired in ethylene-insensitive mutants (Pierik et al., 2009), hypocotyls retain a full shade avoidance response (Das et al., 2016).

1.3 The Circadian Clock

The rotation of the planet Earth about its polar axis produces a cycle of day and night with a period of 24 h. This day - night cycle is characterised by a warmer light period followed by a dark period with cooler temperatures. Organisms occuring in all domains of life have evolved internal mechanisms that resonate with these external day and night rhythms. These endogenous circadian mechanisms oscillate with self-sustaining rhythmicity, are entrainable to external conditions and compensate for temperature changes. Through the circadian clock, plants anticipate and adjust their biology to the predictable environmental changes associated with dawn and dusk. Studies have shown that correctly entrained and functioning circadian clocks confer fitness advantages to plants through increased photosynthesis, carbon fixation, biomass and faster growth (Dodd et al., 2005).

1.3.1 Circadian Clock Architecture

The majority of knowledge about plant circadian clock architecture has been derived from experiments on Arabidopsis. However, until the development of the luciferase assay system, observations of circadian behaviour in plants were limited to analyses of physiological changes such as leaf movements and stomatal movements; or labour-intensive RNA gel blotting time-courses. Firefly luciferase (LUC) offers a noninvasive and versatile reporter of circadian rhythms. LUC catalyzes the ATP-dependent oxidative decarboxylation of luciferin, which releases a 560 nm photon that can be quantified using sensitive electron-multiplying charge-coupled device (EMCCD) cameras (Welsh et al., 2005). A 320 base pair fragment of the Arabidopsis *CHLOROPHYLL A/B BINDING* (*CAB2*) protein promoter fused to the firefly luciferase, initially transformed into tobacco, was shown to drive rhythmic expression of *LUC* mRNA. LUC expression, driven by the *CAB2* promoter could then be detected as rhythmic light emission (Millar et al., 1992). Extension of this system into Arabidopsis allowed screening for circadian clock mutants, with the first isolated plant circadian clock mutant *timing of cab2 expression1* (*toc1-1*) (Millar et al., 1995a).

Taking the form of a network of interlocked transcription-translation feedback loops (McClung, 2006), the oscillator in Arabidopsis shares concepts with circadian clocks studied in other organisms, but appears to be highly complex. One transcription-translation feedback loop contains the MYB-like transcription factors CIRCADIAN CLOCK ASSOCIATED 1 (CCA1) and LATE ELONGATED HYPOCOTYL (LHY), which form a reciprocal regulatory loop with TOC1, also known as PRR1, (PSEUDO RESPONSE REGULATOR 1). *CCA1* and *LHY* transcripts peak in the morning and their protein products suppress *TOC1* transcription through binding to its promoter (Alabadí et al., 2001). As CCA1 and LHY protein abundance decreases towards the end of the day, *TOC1* is transcribed and TOC1 protein accumulates, which represses *CCA1* and *LHY* transcription (Gendron et al., 2012; Huang et al., 2012a; Adams et al., 2015). Another loop is formed by the other members of the *PRR* gene family: *PRR9*, *PRR7* and *PRR5*, which are expressed sequentially during the day (Nakamichi et al., 2005). PRR9, PRR7 and PRR5 have partial functional redundancy, are homologs of TOC1 and also inhibit *CCA1* and *LHY* transcription (Nakamichi et al., 2010). LHY and TOC1 appear to repress the expression of *PRR9*, *PRR7* and *PRR5* (Huang et al., 2012a; Adams et al., 2015). *PRR9* expression is also inhibited by the evening complex (EC) (Nagel and Kay, 2012). This is a trimeric protein complex containing LUX ARRHYTHMO (LUX), EARLY FLOWERING3 (ELF3) and ELF4 that also represses *TOC1* transcription, which alleviates the inhibition of *CCA1* and *LHY* transcription to indirectly promote their expression (Nagel and Kay, 2012; Adams et al., 2015). CCA1 and LHY have been shown to repress the expression of EC components, and have been further suggested to auto-regulate their own and each other's transcription (Adams et al., 2015). A recently described loop of the plant circadian clock incorporates the *REVEILLE* (*RVE*) gene family, a set of morning-expressed MYB-like homologs of *CCA1* and *LHY*. Unlike CCA1 and LHY, RVE8 and its partially redundant homologs RVE6 and RVE4 induce the transcription of afternoon and evening-phased genes (Rawat et al., 2011; Hsu et al., 2013). RVE8 associates with the promoter of evening element (EE) containing genes such as *PRR5*, *TOC1*, *LUX* and *ELF4* and promotes histone acetylation, an epigenetic mark that promotes open chromatin, and hence transcriptional activity (Hsu et al., 2013). RVE8 has also been shown to interact with another family of morning-expressed genes, NIGHT LIGHT-INDUCIBLE AND CLOCK-REGULATED (LNK1, 2, 3 and 4), which are reported to coactivate as well as antagonise RVE8 (Xie et al., 2014; Pérez-García et al., 2015). *GIGANTEA* (*GI*) is repressed by CCA1, LHY and TOC1 but also promotes the expression of *CCA1* and *LHY* (Park et al., 1999; Huang et al., 2012a; Adams et al., 2015). It is not considered to be among the core clock components, but has been suggested to play a role in connecting the oscillator to downstream physiological processes (Mishra and Panigrahi, 2015).

The architecture of the core plant circadian clock is, therefore, made up of several interlocking transcription-translation feedback loops. It is conceptually possible to expand the architecture of the plant circadian clock to include components beyond the core oscillator described above. Sanchez and Kay (2016) highlight that while the central clock regulates metabolic processes including carbohydrate metabolism, and the homeostasis of nitrogen, calcium, iron and copper; all the processes involving these nutrients have been documented to feedback to the central oscillator. Feedback regulation between the circadian clock and phytohormones has also been described (Sanchez and Kay, 2016). Furthermore, the circadian clock regulates the transcript abundance of *PIF*s (Nusinow et al., 2011), which have in turn been suggested to communicate sucrose signals to the central oscillator (Shor et al., 2017). It is highly likely that there are more circadian clock components to be identified, which will add further layers to the complexity of the circadian system. *In silico* modelling found that changing photoperiods coupled with environmental stochasticity selects for circadian clocks with a high degree of complexity through multiple feedback loops (Troein et al., 2009). In agreement with this, Shalit-Kaneh et al. (2018) recently combined *in silico* and experimental approaches to suggest that the complexity of the plant circadian network evolved to provide a mechanism that oscillates robustly in the wide range of environmental extremes that could be experienced in nature.

1.3.2 Circadian Clock Entrainment by Light

At dawn, the transition from dark to light serves as a time-setting cue (Millar et al., 1995b; Oakenfull and Davis, 2017). Light entrains the circadian clock through the photoreceptor network (Somers et al., 1998; Wenden et al., 2011; Fehér et al., 2011) and metabolic entrainment (Haydon et al., 2013). The signalling of photoreceptors to the clock is consistent with Aschoff's rule, where increases in light intensity accelerate the pace of the oscillator to cause a shortening of period (Aschoff, 1979). The phytochrome and cryptochrome photoreceptors mediate circadian entrainment to R and B light (Somers et al., 1998). Increasing fluences of B light, sensed by cry1 at lower fluence rates and additively with cry2 at higher fluence rates, progressively shortens circadian period (Somers et al., 1998). Similarly, increasing R light fluence rates shortens circadian period. PhyB appears to be the primary high-fluence R light photoreceptor to the clock, whereas phyA participates in both low fluence R and B light signalling to the clock (Somers et al., 1998). The UV-B photoreceptor, UVR8 (Rizzini et al., 2011), also influences the pace of the circadian clock. Higher fluence rates and pulses of UV-B have been shown to increase the pace and shift the phase of the circadian oscillator (Fehér et al., 2011). In contrast to most other UVR8-mediated responses, however, the entrainment of the circadian oscillator by UV-B does not require HY5 or HYH, (Fehér et al., 2011).

Little is known, however, about the mechanisms by which photoreceptors communicate light information to the oscillator. Wenden et al. (2011) used a FR only system to isolate photoreceptor activity to phyA. Under these conditions, oscillator gene expression was profoundly altered, with evening genes having elevated expression and morning genes having suppressed expression. This study also identified ELF4 as a candidate for mediating FR light inputs to the oscillator, whilst another study identified that phyA signalling partners FHY3, FAR1 & HY5 directly activate ELF4 (Wenden et al., 2011; Li et al., 2011).

Independently of photoreceptors, light can indirectly entrain the circadian oscillator. In a mechanism involving PRR7, sugars produced through photosynthesis provide a "metabolic dawn" (Haydon et al., 2013). A recent study has also suggested that PIFs participate in the metabolic entrainment of the circadian oscillator (Shor et al., 2017). *PIF* transcript abundance is regulated by the circadian clock (Nusinow et al., 2011), but may also form a major mechanism of light input to the circadian oscillator. PIFs have been shown to interact with phytochromes and cryptochromes and may, therefore, input photoreceptor signals to the circadian clock through direct associations with G-box motif-containing clock promoters such as *CCA1*, *LHY*, *PRR5*, *PRR7 PRR9* and *LUX* (Martínez-García et al., 2000).

Light also influences the circadian oscillator through post-translational mechanisms. ZEITLUPE (ZTL) is a LOV domain blue-light sensitive protein that, alongside its homologs FLAVIN BINDING KELCH REPEAT, F-BOX (FKF1) and LOV KELCH PROTEIN 2 (LKP2), ubiquitinates TOC1 and PRR5 and targets them for proteasomal degradation (Baudry et al., 2010). Blue light promotes an interaction between ZTL and GI, preventing it from binding protein targets. In comparison, the affinity of ZTL for GI is weakened in darkness, resulting in dissociation of GI-ZTL and the degradation of PRR5 and TOC1 (Kim et al., 2007).

1.3.3 Circadian-regulated processes and gating of environmental responses

A primary mechanism through which the circadian clock regulates physiological processes is transcriptional control. In Arabidopsis it has been reported that up to 31% of the transcriptome is circadian-regulated (Harmer et al., 2000; Michael et al., 2008). Clock transcriptional regulation occurs through specific circadian-regulated promoter motifs, which are associated with different phases of the circadian cycle (Harmer et al., 2000; Michael et al., 2008). For instance, Myb-like transcription factors such as CCA1, LHY and RVE8 bind to the evening element promoter motif in genes like *TOC1* and *PRR5* to suppress (Alabadí et al., 2001) or, in some cases, promote transcriptional activity (Hsu et al., 2013). Clock components directly regulate genes outside of the core circadian oscillator in a similar manner. The two most well-characterised circadian clock components CCA1 and TOC1 are reported to bind to 449 genomic loci (Kamioka et al., 2016) and 867 genomic loci (Huang et al., 2012a) respectively. It is thought that by rhythmically limiting or promoting transcriptional activity (and therefore cellular processes) to particular times of the day, the circadian clock provides a fitness advantage to correctly entrained plants (Dodd et al., 2005; Greenham and Mcclung, 2015). For instance, the clock appears to participate in the management of the growth and defence trade-off (Huot et al., 2014) by timing pathogen and environmental defences to the morning (Wang et al., 2011; Takeuchi et al., 2014) and growth to the night (Nozue et al., 2007; Nusinow et al., 2011).

Circadian gating is where applying a stimulus of set magnitude at different times of day to an organism can elicit a different magnitude of response (Hotta et al., 2007). Limiting transcriptional activity to particular times of day is one way in which the circadian clock can gate responses and through circadian regulation of photoreceptor expression and accumulation, it has been suggested that the clock gates its own sensitivity to entrainment (Tóth et al., 2001). Downstream of the rhythmic regulation of photoreceptor expression, the circadian clock exerts control over individual light-responsive pathways. Fehér et al. (2011) showed that the circadian clock gates the UV-B-induced accumulation of *HYH* and *CHS* transcripts to the morning. Salter et al. (2003) reported that the rapid shade avoidance response is circadian gated, with transcripts of *PIL1* encoding a TOC1-interacting protein, strongly induced by low R:FR at subjective dawn and weakly at subjective dusk. The mechanisms of circadian gating of transcription have not yet been fully clarified, but may involve changes in chromatin structure (Más, 2008; Hsu et al., 2013). Recent work has highlighted a novel mechanism of circadian gating through interactions between PIFs and PRRs (Soy et al., 2016; Zhu et al., 2016; Martín et al., 2018). TOC1, PRR5, PRR7 and PRR9 have been reported to directly interact with PIF3 and PIF4 and co-bind to target promoters to inhibit their transcriptional activity. The PRRs are hypothesised to sequentially inhibit PIF activity during the night to gate hypocotyl elongation to the end of the night in short day conditions (Martín et al., 2018). There is, however, much still to discover about the mechanisms of circadian gating and its adaptive significance in natural environments.

1.4 Aims

The aim of this project was to investigate the co-regulation of plant architecture by light quality and the circadian clock. An over-arching objective was to apply the finding that UV-B inhibits shade avoidance (Hayes et al., 2014) to a commercial growing environment using the potted herb *Coriandrum sativum* (Coriander) as a model. Using the Arabidopsis model, focus was placed upon the possible circadian regulation of the inhibition of shade avoidance by UV-B, and the potential for temporally-targeted UV-B treatments at the time-of-day when plants are most sensitive to UV-B-mediated inhibition of hypocotyl elongation. Giving short dose UV-B may limit the exposure of workers to harmful radiation and deliver an economical and environmentally-friendly solution that could lead to improvements in product quality. Through a combination of morphological, genetic and biochemical techniques, this thesis aims to contribute to the understanding of how the circadian clock regulates light responses in plants to optimise their growth in shade.

Chapter 2

Materials and Methods

2.1 Plant Material

2.1.1 *Arabidopsis thaliana*

Mutant and transgenic lines used in this thesis are as follows. In the Columbia-0 (Col-0) background: *uvr8-6* (Favory et al., 2009), *toc1-101* (Kaczorowski, 2004) (donated by Prof Peter Quail and Prof Elena Monte), *elf3-1* (Zagotta et al., 1996), *rve8-1* (Rawat et al., 2011), *TOC1 MINIGENE (TMG)* (Más et al., 2003), *tt4* (Winkel-Shirley et al., 1995), *tt7* (Winkel-Shirley et al., 1995), *CCA1::LUC* and *TOC1::LUC* were both produced as part of the ROBUST project and were donated by Anthony Hall. The *prr5-3*, *prr7-3*, *prr9-1* mutant alleles were donated by Prof Rob McClung (Michael et al., 2003). In the Wassilewskija (Ws) background: *hy5KS50* (Oyama et al., 1997), *hyh* (Holm et al., 2002), *hy5KS50hyh* (Holm et al., 2002), *uvr8-7* (Favory et al., 2009). In the Landsberg *erecta* background: *phyA-1* (Whitelam et al., 1993), *phyB-1* (Koorneef et al., 1980)and *uvr8-1* (Kliebenstein et al., 2002).

2.1.2 *Coriandrum sativum*

Coriandrum sativum (Coriander) “Slow Bolt” and “Cruiser” cultivars were provided by Vitacress Herbs Ltd.

2.2 Growth Conditions

2.2.1 Seed Treatment

Arabidopsis thaliana

Arabidopsis seeds were surface sterilised with a 70% v/v EtOH wash followed by a 20% v/v Sodium Hypochlorite wash for 20 min. The seeds were then washed three times with freshly autoclaved water before suspension in freshly autoclaved 0.1% w/v agar. Seeds were individually placed on compost or agar using a pipette then stratified in darkness at 4 °C for 72 h, then germinated in White Light (WL) at 20°C and 70% humidity in 12 h light, 12 h dark photocycles.

Coriandrum sativum

Coriandrum sativum seeds were scarified to break dormancy and synchronise germination. Fruit were manually split into two mericarps through gentle abrasion with a mortar and pestle and soaked in H_2O for 48 h. Seeds were germinated on damp tissue in the same conditions as *Arabidopsis thaliana*. After 3 days in these conditions, germinated seeds were selected for potting on to compost media and placed at a depth of 10 mm.

2.2.2 Media

Compost Media

A 3:1 v/v mixture of compost (Levingtons F2) and silver sand was used for all experiments except for luciferase assays and physiology experiments on *Coriandrum sativum* carried out at the Vitacress glasshouses.

Agar Media

0.5 X Murashige and Skoog medium (Murashige and Skoog, 1962) was prepared by autoclaving 0.215% w/v MS Basal Salts (Melford) and 0.8% w/v agar (Melford) in distilled H_2O at pH 5.7.

2.2.3 Controlled Climate Chambers

Experiments were carried out in controlled climate chambers (Microclima 1600E, Snijder Scientific). Temperature was maintained at 20°C with 70% humidity. White light (WL) was provided using fluorescent bulbs (Philips cool white fluorescent tubes 400-700 nm). PAR (400-700 nm) was adjusted in the range of 70 to 5 µmol m^{-2} s^{-1} as specified in the experiments using neutral density filters (Lee Filters). Supplementary Far-Red (+ FR) LEDs (peak at 730 nm) were used to adjust the Red : Far-Red (R:FR) ratio within a range of 0.05 to 5 as specified in experiments. R:FR ratio was calculated using equation 2.4. Supplementary UV-B (+ UV-B) filtered to 1.5 µmol m^{-2} s^{-1}(0.6 W m^{-2}) using heat-resistant copper tape was provided with Philips TL100W/01 narrow band UV-B bulbs. Polycarbonate filters (6 mm thickness) were used to attenuate UV-B for plants grown in control -UV-B conditions. Unless otherwise specified, plants were germinated and entrained in 12 h light 12 h dark photocycles. For light spectra used in UV-B experiments, see figure 2.1. For deep shade light spectra, see figure 2.2.

2.2.4 EM-CCD Camera Chamber

A customised LED chamber (Photek) was utilised for collecting luciferase data. LEDs were modulated to produce PAR in the range 47 - 5 µmol m^{-2} s^{-1} and R:FR in the range of 1.62 - 0.05. For LED light spectra used in experiments, see figure 2.3. The chamber itself had no temperature control, but laboratory air conditioning was set to 19°C. Plants were grown in sealed plates.

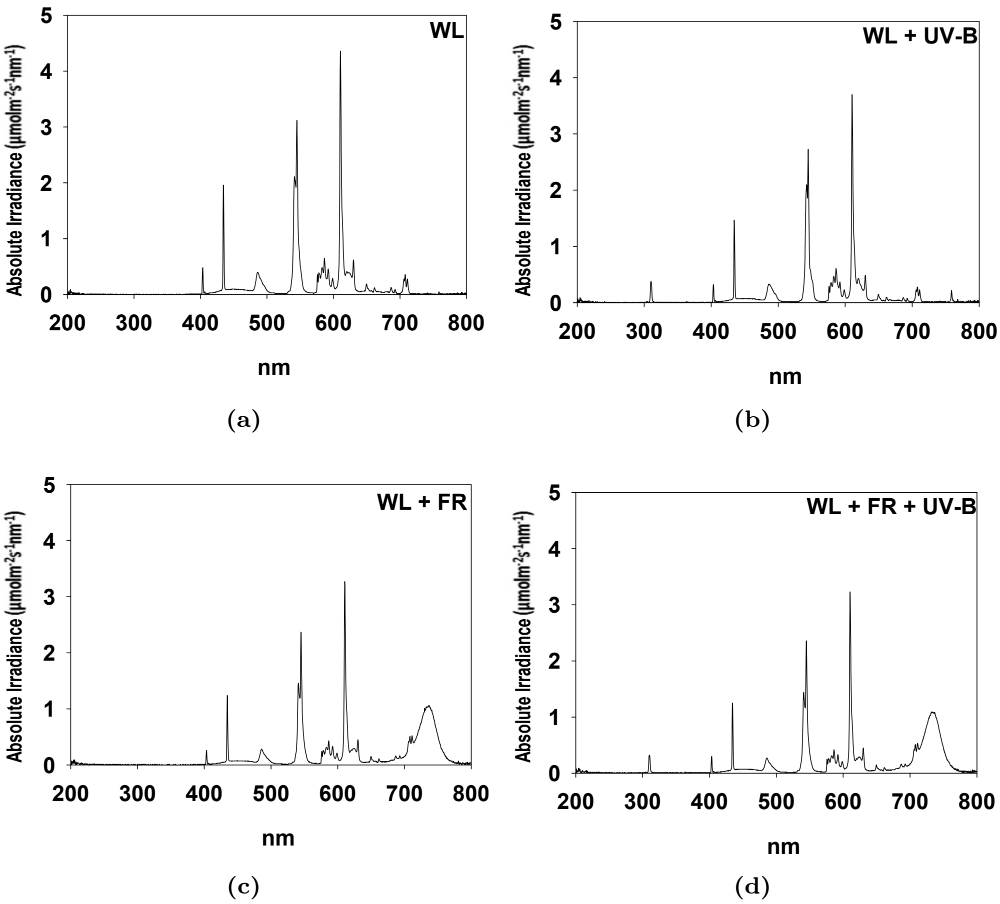

Figure 2.1: Light spectra from high PAR experimental conditions. Measurements were recorded in controlled cabinets. 70 µmol m^{-2} s^{-1} white light supplied with fluorescent bulbs either (2.1a) without supplemental FR or UV-B, (2.1b) supplemented with UV-B at an intensity of 1.5 µmol m^{-2} s^{-1}using narrow band fluorescent bulbs, (2.1c) supplemented with FR LEDs to achieve a R:FR of 0.05 and (2.1d) supplemented with FR and UV-B.

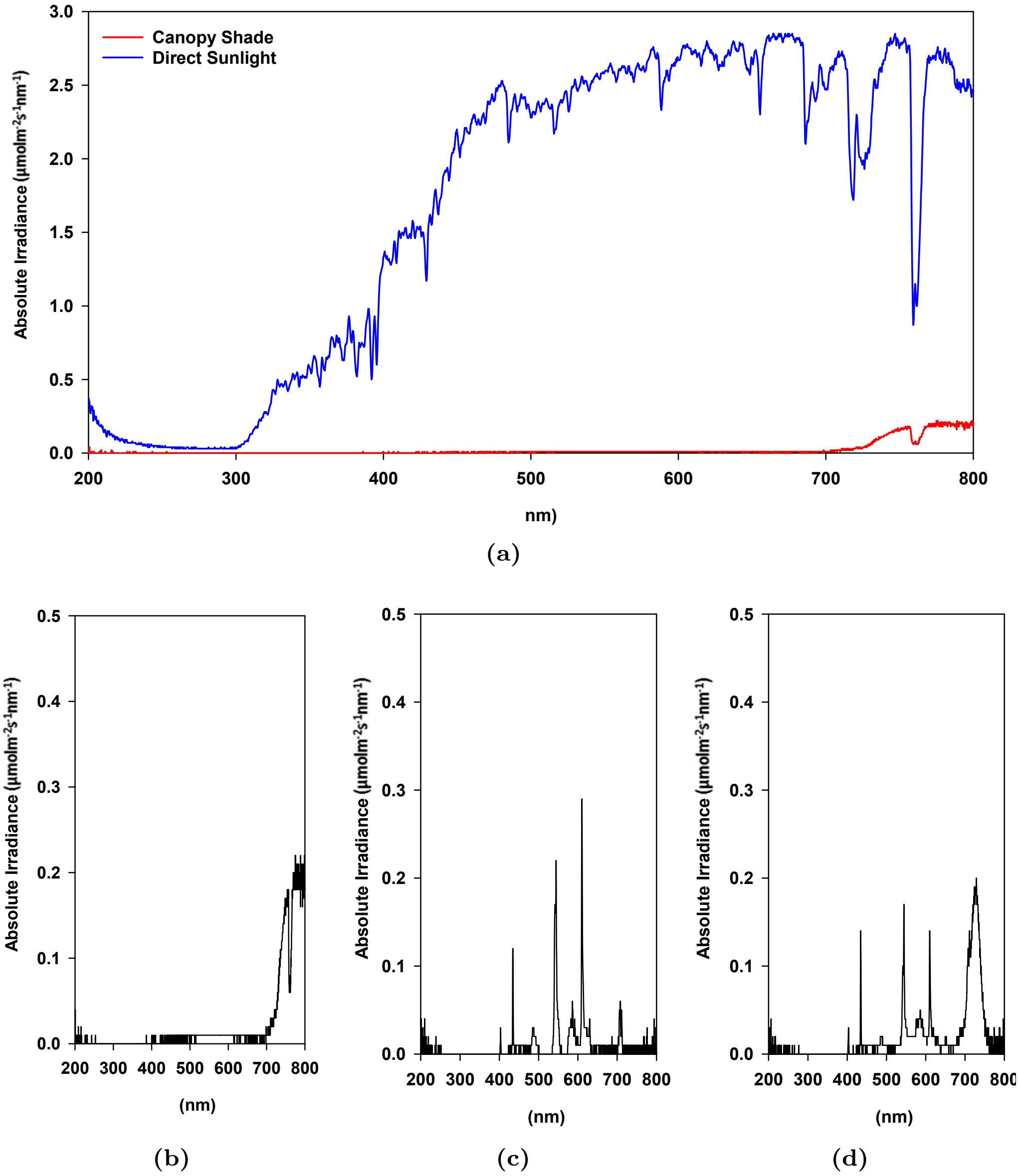

Figure 2.2: Light spectra from natural and low PAR experimental conditions. (2.2a) Outdoor light spectra recorded in Bristol in September, in direct sunlight (PAR = 1022.32 µmol m^{-2} s^{-1}, R:FR = 1.27) and canopy shade (PAR = 14.04 µmol m^{-2} s^{-1}, R:FR = 0.1). (2.2b) Canopy shade on an expanded scale. (2.2c) Low PAR, high R:FR light conditions (PAR = 5.01 µmol m^{-2} s^{-1}, R:FR = 1.62). (2.2d) Low PAR, low R:FR light conditions (PAR = 5.01 µmol m^{-2} s^{-1}, R:FR = 0.06).

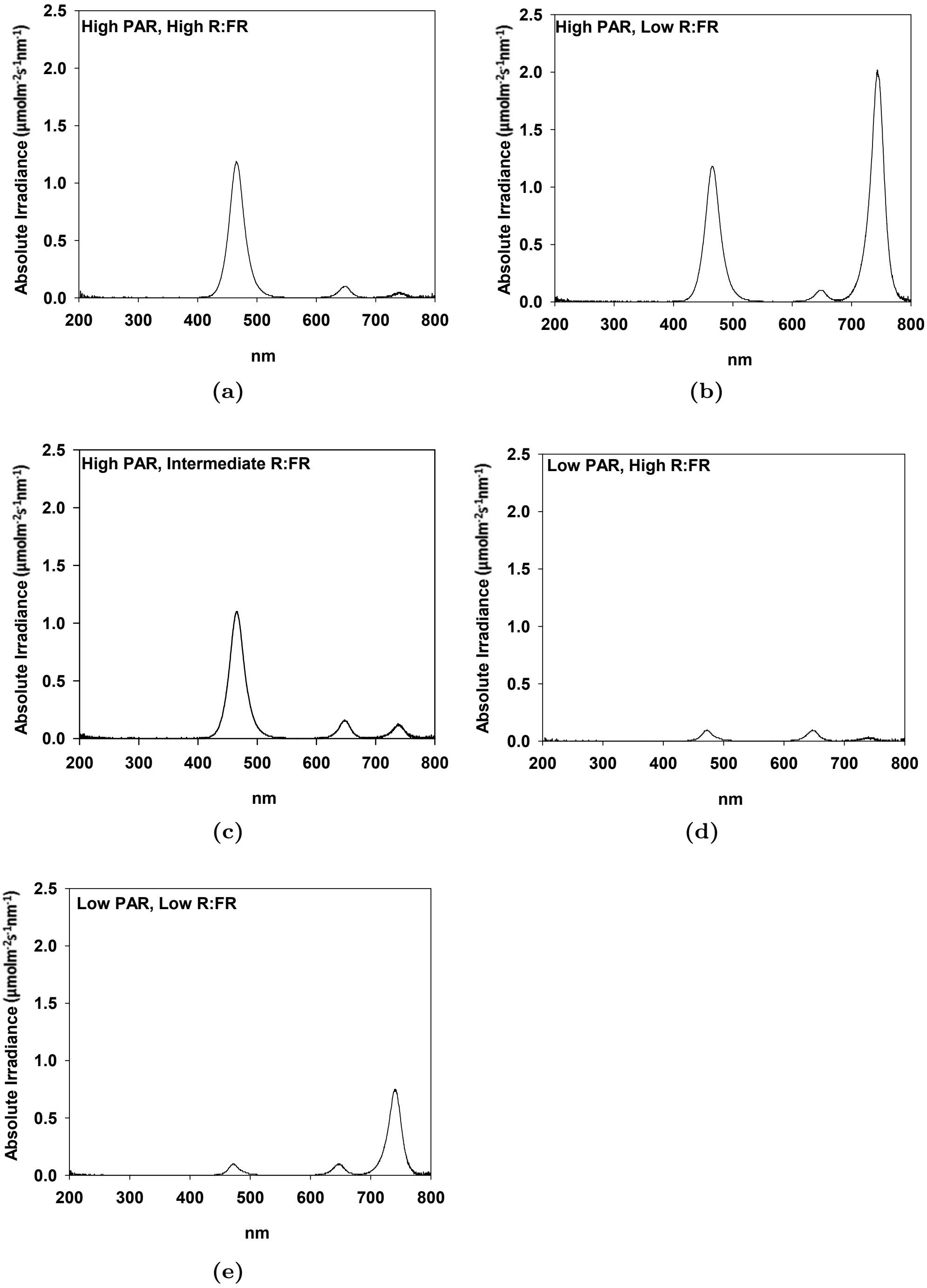

Figure 2.3: Light spectra traces in EM-CCD camera chamber. (2.3a) High PAR, high R:FR (PAR = 47 µmol m^{-2} s^{-1}, R:FR = 1.2). (2.3b) High PAR, low R:FR (PAR = 47 µmol m^{-2} s^{-1}, R:FR = 0.05). (2.3c) High PAR, intermediate R:FR (PAR = 47 µmol m^{-2} s^{-1}, R:FR = 0.5). (2.3d) Low PAR, high R:FR (PAR = 5 µmol m^{-2} s^{-1}, R:FR = 1.62). (2.3e) Low PAR, low R:FR (PAR = 5 µmol m^{-2} s^{-1}, R:FR = 0.05).

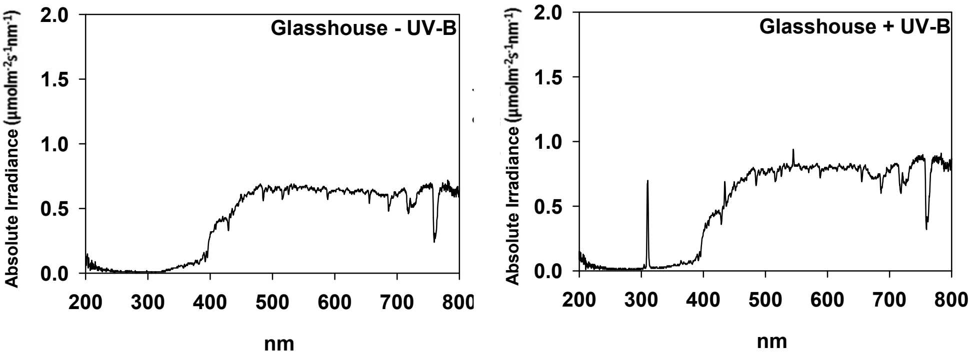

(a) (b)

Figure 2.4: Light spectra from Old Park Hill Glasshouse experiments. In the Glasshouse, plants were exposed to ambient light levels typical of Spring in Bristol. (2.4a) Glasshouse light spectra with UV-B bulb attenuated with 6 mm acrylic filter. (2.4b) Ambient light was supplemented with UV-B at an intensity of 1.5 µmol m^{-2} s^{-1} using narrow band fluorescent bulbs.

2.2.5 Glasshouse

In experiments conducted in the Old Park Hill Experimental Glasshouse (University of Bristol, UK), plants were exposed to ambient PAR levels which ranged from 60 to 800 µmol m^{-2} s^{-1} throughout the experiment. A minimum PAR of 165 µmol m^{-2} s^{-1} and 16 h photoperiods were maintained using supplementary fluorescent lamps (Plug and Grow compact 200 W) that switched off when ambient light exceeded 230 µmol m^{-2} $s^{-1}$and came on when ambient light dropped below 140 µmol m^{-2} s^{-1}. UV-B supplementation filtered to 1.5 µmol m^{-2} s^{-1} was provided using Philips TL100W/01 narrow band UV-B bulbs (figure 2.4). Temperature was programmed to 18 °C day and night, but in practice values fell within a range of 22°C (day) and 16°C (night) due to varying daily and seasonal temperatures.

2.3 Image Analysis

Morphological data from *Arabidopsis thaliana* and *Coriandrum sativum* was extracted from images using FIJI (Schindelin et al., 2012). Hypocotyls were measured from the shoot apical meristem to the shoot-root junction. Petiole lengths were measured from the shoot apex to the base of the leaf blade. Visible leaf area was measured by counting pixels from binarized images of flattened leaf blades.

2.4 Timelapse Imaging

For Time-Lapse Infra Red (IR) photography, a custom built 8 × 8 array of 880 nm IR LEDs were controlled with a 24 h timer. Timelapse images were captured with a modified Nikon D80 DSLR camera with its IR blocking filter removed, a SIGMA 105 mm macro lens and an IR pass filter (>850 nm) (Zomei, Jiangsu, China) operated with digiCamControl v2.0.0 remote camera tethering freeware (downloaded in 2017)[1]. Timelapse image capture intervals, start and duration were as specified in the experiment. Hypocotyl lengths from individual images and time lapse image stacks were manually measured from images using FIJI.

2.5 Chlorophyll Abundance

Coriandrum sativum leaf chlorophyll content was determined as described by Witham et al. (1971). 100 mg fresh tissue from leaf 2 of 28-day-old *Coriandrum sativum* was snap frozen in liquid nitrogen and stored at –80 °C. Samples were homogenised using stainless steel beads and a TissueLyser (Qiagen). Chlorophyll from homogenised tissue was extracted in 80% (v/v) acetone and loaded into a quartz crystal cuvette. Absorbances were recorded at 663, 645 and 652 nm with 80% acetone used as a blank. Chlorophyll abundance was given in mg g^{-1} by normalising to tissue fresh weight and volume of extract using equations 2.1, 2.2 & 2.3.

$$ChlA\,(mg\,g^{-1} fresh\,weight) = (12.7(A_{663}) - 2.69(A_{645})) \times \frac{V\,(ml)}{W\,(mg)} \qquad (2.1)$$

[1] digiCamControl software is freely available from http://digicamcontrol.com

$$ChlB\,(mg\,g^{-1} fresh\,weight) = (22.9(A_{645}) - 4.68(A_{663})) \times \frac{V\,(ml)}{W\,(mg)} \tag{2.2}$$

$$ChlA + B\,(mg\,g^{-1} fresh\,weight) = (20.2(A_{645}) + 8.02(A_{663})) \times \frac{V\,(ml)}{W\,(mg)} \tag{2.3}$$

2.6 Total anti-oxidant capacity

Total antioxidant capacity of *Coriandrum sativum* was analysed using a Total Antioxidant Capacity Assay kit, MAK187 (Sigma-Aldrich). 100 mg of leaf tissue from leaf 3 was snap frozen in liquid nitrogen and stored at −80 °C. Samples were homogenised using stainless steel beads and a TissueLyser (Qiagen). Samples were extracted in 1 ml of ice cold 1 X Phosphate Buffered Saline (PBS) and the supernatant was diluted 1:100 to bring values within range of kit standards. Samples were assayed according to the manufacturer's protocol, by comparing the absorbances of diluted extracts at 570 nm with a standard curve prepared from Trolox standards. Values were then normalised to tissue fresh weight.

2.7 Flavonol glycoside detection by thin layer chromatography

Flavonol glycoside extraction and thin layer chromatography were carried out as described previously (Stracke et al., 2010b). 100 mg of leaf tissue was homogenised and extracted in 0.4 ml 80% (v/v) MeOH. Samples were incubated for 15 min at 70 °C then centrifuged for 10 min. Supernatants were vacuum-dried at 65 °C and dried pellets dissolved in 1 µl 80% MeOH mg^{-1} fresh weight. 1 µl of methanolic extracts were spotted onto HPTLC silica gel 60 glass plates (Millipore). Chromatography was performed in a closed glass tank (with a mobile phase of ethyl acetate, formic acid, acetic acid and water (100:26:6:12 v/v). After separation, plates were air dried and flavonols detected by spraying 2 ml of 1% (w/v) 2,3-dibromopropanal (DPBA) (Sigma-Aldrich) in MeOH 3 times with 5 min between sprayings. This was followed by 2 ml of 5% (w/v) PEG 4000 (AppliChem) in MeOH 3 times with 5 min between sprayings. After 15 min, the stained HPTLC plate was visualized under UV (365 nm). Flavonol glycoside-DPBA derivatives fluoresce under UV light. Liquid chromatography-Mass Spectrometry (LC-MS) has been used in previous studies to profile these flavonol glycosides and assign them to different colours (Stracke et al., 2010b).

2.8 Quantitative Reverse Transcription Polymerase Chain Reaction

2.8.1 RNA Extraction

Arabidopsis thaliana RNA was extracted using the Spectrum Plant Total RNA Kit (STRN250-1KT, Sigma-Aldrich) and eluted into RNAse-free water according to manufacturer's protocols. DNA was removed from the eluted RNA using the Amplification Grade DNAse I kit (AMPD1, Sigma-Aldrich).

2.8.2 cDNA Synthesis

RNA yield and integrity were checked using a Nanodrop ND 1000 spectrophotometer (Thermo Fisher Scientific). 1 µg RNA was used for cDNA synthesis using the Applied Biosystems High Capacity cDNA Reverse Transcription kit (4368814, Thermo Fisher Scientific).

2.8.3 Quantitative Polymerase Chain Reaction

Quantitative PCR was carried out using the Brilliant III Ultra-Fast SYBR Green QPCR Master Mix kit according to manufacturer's protocols in 10 µl reactions

(600882, Agilent Technologies). Appropriate cDNA dilutions for qPCR were determined using standard curve and primer efficiency analysis. Relative quantitation was calculated using the $2^{-\Delta\Delta Ct}$ algorithm (Pfaffl, 2001), normalised to the expression of *Actin-2* or *PP2A* as specified in the figures. For list of qPCR primers, refer to table.

2.9 Western Blot

2.9.1 UVR8 native polyclonal antibody

Arabidopsis Col-0 and Coriander *cv.* Slow Bolt plant tissue was extracted in freshly prepared extraction buffer (20 mM HEPES pH 7.8, 450 mM NaCl, 50 mM NaF, 0.2 mM EDTA, 25% glycerol, 0.5 mM PMSF, 1 mM DTT and 1 tablet/10 ml Protease Inhibitor (Complete Mini, Roche)). Samples were centrifuged at maximum speed for 10 min at 4 °C, with the supernatant transferred to a fresh sample tube. Total protein concentration was quantified from the supernatants using the Bradford Assay (Biorad) (Bradford, 1976). SDS-PAGE 4x loading buffer (250 mM Tris-HCL pH6.8, 2% SDS, 20% β-mercaptoethanol, 40% glycerol, 0.5% bromophenol blue) was added to supernatant to a final dilution of 1x. 25 μg unboiled protein was loaded into each lane. SDS-PAGE resolving conditions were: 120 V for 120 min in 8% polyacrylamide gel. Transfer to PVDF membrane was 400 mA for 45 min. A Ponceau stain for 5 min was followed by a H_2O rinse. The membrane was destained with TBS (Tris Buffered Saline: 25 mM Tris-HCl pH 8, 150 mM NaCl, 2.7 mM KCl) then blocked with 8% milk in TBS for 60 min at room temperature. Incubation with UVR8 polyclonal antibody generously provided by Prof. Gareth Jenkins (Findlay and Jenkins, 2016) at 1:10000 dilution in 8% milk in TBS was carried out overnight at 4°C. The following morning the membrane was washed twice with TBS-TT (TBS with 0.1% v/v of 100% Triton X-100 (SIGMA-ALDRICH) and 0.05% v/v of 100% Tween-20) for 5 min each followed by a 5 min wash in TBS. The blot was then

Primer Name	Sequence
Actin-2 Forward	TCAGATGCCCAGAAGTGTTGTTCC
Actin-2 Reverse	CCGTACAGATCCTTCCTGATATCC
PP2A Forward	GTTCTCCACAACCGCTTGGT
PP2A Reverse	TAACGTGGCCAAAATGATGC
CCA1 Forward	GCACTTTCCGCGAGTTCTTG
CCA1 Reverse	TGACTCCTTTCTTACCCTGTTATTCTG
TOC1 Forward	TCTTCGCAGAATCCCTGTGAT
TOC1 Reverse	GCTGCACCTAGCTTCAAGCA
RVE8 Forward	GGGAAGCTCAAGCCGAACAGTATC
RVE8 Reverse	GGCCTCTCGTTTCAGGATCAAAGA
ELF3 Forward	GGAAAGCCATTGCCAATCAA
ELF3 Reverse	ATCCGGTGATGCAATAAGT
ELF4 Forward	CGACAATCACCAATCGAGAATG
ELF4 Reverse	AATGTTTCCGTTGAGTTCTTGAATC
LUX Forward	CGGATTCGAAGAAGCAAAAG
LUX Reverse	TCATCTCCATCACCCTTTGA
PIF4 Forward	GCCGATGGAGATGTTGAGAT
PIF4 Reverse	CCAACCTAGTGGTCCAAACG
PIF5 Forward	CAGATGGCTATGCAAAGTCAGATGC
PIF5 Reverse	AGATTTGGTTCTGTGCTTGGAGCTG
HY5 Forward	CGGAGAAAGTCAAAGGAAG
HY5 Reverse	CCAACTCGCTCAAGTAAG
HYH Forward	GGAAGAAACCCTGTTGATAAAGA
HYH Reverse	GCATTGTGTTCTCGTTCGT
GA2ox1 Forward	CCTTCGGATACGGGAACAGTAAGATTG
GA2ox1 Reverse	GTGTACTCTTCCAATGCGTTTCTGAAAG
IAA29 Forward	ATCACCATCATTGCC CGTAT
IAA29 Reverse	ATTGCCACACCATCCATCTT
YUCCA8 Forward	ATCAACCCTAAGTTCAACGAGTG
YUCCA8 Reverse	CTCCCGTAGCCACCACAAG

Table 2.1: List of qPCR primers

incubated with the secondary antibody (anti-rabbit conjugated to horseradish peroxidase) at 1:20000 dilution in 8% milk in TBS for 60 min at room temperature. The membrane was finally washed 5 times with TBS-TT for 5 min each time, followed by 5 min in TBS. Blot visualisation is described below (2.9.2).

2.9.2 Chemiluminescence

Blots were visualised using chemiluminescence. The SuperSignal West Femto Maximum Sensitivity Substrate (Thermo Fisher Scientific) was used according to manufacturer's protocols, with 200 µl of mixed substrate sufficient for a 80 x 55 mm blot.

2.10 Luciferase Imaging

Images of Luciferase bioluminescence were captured using a Lumintek EM-CCD imaging system (Photek Ltd, St Leonards on Sea, UK) controlled by Image32 software (Photek) and custom control scripts (45 sec integrations, EM gain setting 2700). Monochromatic blue, red and far-red LEDs were modulated to deliver PAR at 47 or 5 µmol m^{-2} s^{-1} and R:FR ratios of 1.2, 0.9, 0.5 or 0.05 as indicated in the experiments. 7-day-old plants were moved to specified experimental conditions 72 h before image acquisition to entrain for three cycles of 12 h light : 12 h dark cycles. 100 µl sterile 5 mM luciferin (potassium salt of D-luciferin; Melford Laboratories Ltd, Ipswich, UK) was added 24 h before data acquisition. Images were captured at 60 min intervals, preceded by a dark delay of 2 min to eliminate chlorophyll autofluorescence from the bioluminescence signal. For time courses in PAR = 47 µmol m^{-2} s^{-1}, 48 h of images were captured in driven conditions before transfer to continuous light. For time courses in PAR = 5 µmol m^{-2} s^{-1}, images were captured in driven conditions.

Imaging data were analysed using Image32 software (Photek), with time courses in continuous light further analysed using the fast Fourier transform-nonlinear least-squares (FFT-NLLS) algorithm within Brass (Southern and Millar, 2005) downloaded in 2015 from http://millar.bio.ed.ac.uk.

2.11 Light Measurements

Data were recorded using FLAME and USB2000 spectrophotometers (Ocean Optics) and analysed using Oceanview software (Ocean Optics) and SigmaPlot v13 (Systat Software Inc.). Light spectra were measured at the soil surface unless otherwise specified. PAR, R:FR ratio and UV-B intensity ratio were calculated from full collected spectra. R:FR was calculated according to equation 2.4.

$$R:FR \quad ratio = \frac{photon\,irradiance\,at\,660-670nm}{photon\,irradiance\,at\,725-735nm} \tag{2.4}$$

2.12 Statistical Analyses

SigmaPlot v13 was used to plot & analyse quantitative data (Systat Software Inc.). Where used, boxplots represent 1st quartile, median and 3rd quartile, whiskers represent the 10th and 90th percentiles with outliers plotted individually.

Chapter 3

Circadian Gating of UV-B Signalling and Shade Avoidance Antagonism

3.1 Introduction

PLANTS compete with their neighbours for sunlight; when plants grow in close proximity to each other, whether in nature or agriculture, they run the risk of mutual shading, which threatens photosynthesis and hence productivity. In these conditions, plants try to overtop each other *e.g.* by elongation of hypocotyls and petioles, or raising of leaves (hyponasty). These architectural alterations are part of a suite of responses collectively termed the "shade avoidance syndrome" (SAS) (Casal, 2012), which has evolved as a counter to the perceived threat of shade. Plants perceive the quantitative and qualitative changes in light related to over-crowding through a complex photoreceptor network that modulates growth largely through the regulation of the PHYTOCHROME INTERACTING FACTOR (PIF) family of basic helix-loop-helix transcription factors (reviewed in Fraser et al. (2016)).

Vegetation absorbs light in the visible 400-700 nm waveband, but reflects and transmits light of longer wavelengths in the FR waveband, thus light in dense vegetation is both depleted in R and B light as well as enriched in Far-Red radiation. Plants monitor the R:FR ratio through the phytochrome photoreceptors, which exhibit photoreversibility between their inactive P_r and active P_{fr} forms on absorbtion of R and FR light respectively (Casal, 2012). Of the phytochromes, phyB, which shares sequence homology and functional redundancy with phyD & phyE in dicots (Mathews and Sharrock, 1997; Franklin et al., 2003a), has long been regarded as the dominant phytochrome in SAS regulation. High R:FR establishes a high proportion of active phyB P_{fr} (Holmes and Smith, 1975; Morgan and Smith, 1976; Smith and Holmes, 1977), which is translocated to the nucleus (Sakamoto and Nagatani, 1996; Yamaguchi et al., 1999; Kircher et al., 1999) where it triggers the phosphorylation, ubiquitination and degradation of PIFs by the 26s proteasome (Lorrain et al., 2008; Ni et al., 2014). Conversely, in dense vegetation, a low R:FR ratio reverses the P_r/P_{fr} photoequilibrium to establish a high proportion of inactivated phyB P_r, which releases PIF suppression to allow their stabilisation, accumulation and promotion of growth by binding to CACGTG G-box motifs in a broad range of target genes *e.g. PIL1* (Salter et al., 2003) & *ATHB2* (Steindler et al., 1999), which are often used as SAS marker genes (Leivar and Monte, 2014).

Major roles in SAS have been described for PIFs 4, 5 & 7 alongside relatively minor roles for PIFs 1 & 3 (Lorrain et al., 2008; Li et al., 2012a; Leivar et al., 2012a,b). PIFs control hypocotyl cell elongation *via* the transcriptional regulation of the TAA & YUCCA family enzymes that are involved in auxin synthesis (Lorrain et al., 2008; Hornitschek et al., 2012; Li et al., 2012a). Low R:FR-induced auxin signalling drives the expression and re-localisation of the auxin efflux regulator PIN-FORMED 3 (PIN3) to direct an increase of auxin levels in the hypocotyl (Keuskamp et al., 2010). Following low R:FR exposure, auxin accumulates in the first hour, but not in *pif7* mutants, suggesting a role for PIF7 in this process. Uniquely among the PIFs, PIF7 is poised for early SAS growth as it accumulates in a stable phosphorylated form that on inactivation of phy signalling is rapidly dephosphorylated (Li et al., 2012a). PIFs also promote the transcription of bHLH TFs: *HFR1*, *PAR1*, *PAR2* and the DELLA protein *GAI,* which complex with PIFs and negatively regulate their activity either through sequestration of their DNA-recognition domains or targetting them for degradation *via* the ubiquitin-proteasome system, to form a negative feedback loop (Hornitschek et al., 2009; Galstyan et al., 2011; Hao et al., 2012; Leivar et al., 2012b; Li et al., 2016). The stability of DELLA proteins, however, is reduced in canopy shade and neighbour detection conditions, likely through increased gibberellic acid (GA) levels (Djakovic-Petrovic et al., 2007).

Most of the sun's ultra-violet (UV) light is absorbed by the stratospheric ozone layer such that only UV of wavelengths above 295 nm reach the Earth's surface. Of this, 95% is the longer wavelength, lower energy UV-A (315-400 nm) while the rest is UV-B (280-315 nm) radiation. In spite of UV-B making up only a very small proportion of the light plants receive, it has major effects on their life history (reviewed in Jenkins (2009). In Arabidopsis, UV-B is detected by the seven-bladed β-propellor UV RESISTANCE LOCUS 8 (UVR8) protein, which in its ground state is a dimer that monomerises in response to UV-B photons (Rizzini et al., 2011). Monomeric UVR8 binds to its primary signalling partner, the E3 Ubiquitin Ligase COP1 and promotes the expression of *HY5* and *HYH*, which are required for the regulation of a substantial proportion of known UVR8-regulated genes (Brown et al., 2005; Oravecz et al., 2006; Brown and Jenkins, 2008). Following UV-B irradiation, UVR8 regulates the transcription of a set of genes involved in photoprotection including flavonoid biosynthesis, anti-oxidant production and DNA damage repair enzymes (Caldwell et al., 1983; Jordan, 2002; Rozema et al., 1997; Frohnmeyer and Staiger, 2003; Jenkins, 2009, 2014). At the same time, low dose UV-B detected by UVR8 can stimulate photomorphogenic responses including the inhibition of hypocotyl elongation and root growth while also promoting cotyledon opening (Wellmann, 1976; Ballaré et al., 1995; Kim et al., 1998; Boccalandro et al., 2001; Suesslin and Frohnmeyer, 2003; Tong et al., 2008; Conte et al., 2010; Hayes et al., 2014). UV-B is also filtered by plant canopies so may provide environmental cues to a plant on the level of competition it faces. Recent data indicate that non-stressful low dose UV-B perceived by UVR8 is a potent inhibitior of low R:FR- and LBL-induced shade avoidance through the suppression of the activity of plant hormones auxin and GA (Hayes et al., 2014; Mazza and Ballaré, 2015). The UVR8-mediated mechanism by which UV-B inhibits shade avoidance has not yet been fully elucidated, but while UVR8 antagonises auxin signalling, it does not appear to directly interact with PIFs (Hayes et al., 2014). UV-B increases DELLA stabilisation, likely through UVR8-mediated increases in expression of GA catabolism genes like *GA2ox1* (Hayes et al., 2014). Increased DELLA stabilisation could lead to the formation of inactive DELLA:PIF complexes (Lucas et al., 2008; Feng et al., 2008). Similar hypothesised mechanisms include the increased stabilisation of HFR1 through UVR8 sequestration of COP1 (Huang et al., 2013), or the direct inhibition of PIFs by HY5 (Toledo-Ortiz et al., 2014). Other potential mechanisms seem to involve reductions in PIF abundance either through protein degradation (Hayes et al., 2014), which could occur through DELLA interactions (Li et al., 2016), or the suppression of *PIF* transcript abundance by UV-B (Hayes et al., 2017). Recent data has shown that UVR8 directly interacts with BRI1-EMS-SUPPRESSOR1 (BES1) and BES1-INTERACTING MYC-LIKE 1 (BIM1) to mediate the UVR8-dependent inhibition of brassinosteroid (BR)-promoted hypocotyl elongation (Liang et al., 2018). Brassinosteroid signaling has been shown to dominate in LBL-mediated shade avoidance (Keller et al., 2011; Keuskamp et al., 2011; Pedmale et al., 2015), but UVR8-BR signaling interactions in shade avoidance remain to be elucidated.

Plants also respond to internal regulators such as the circadian clock. The circadian clock is an endogenous biological timer and, in plants, consists of a network of interlocking transcription-translation feedback loops in a mechanism that oscillates with a period of *c.* 24 h (Sanchez and Kay, 2016). The clock is entrained by external stimuli, *e.g.* light/dark cycles or temperature cycles such that it is synchronised to match the 24 h environmental cycle. It has been shown that plants that correctly match their circadian period to the external light/dark cycle are at a competitive advantage over plants with a period differing from their environment (Dodd et al., 2005). Thus, the circadian clock allows plants to anticipate predictable changes in their environment and hence synchronize their metabolism to allow for the optimal phasing of molecular and physiological responses with the time of day. To achieve this, the circadian clock adjusts the outcome of signalling pathways in a process called circadian gating. One consequence of circadian gating is where stimuli of the same magnitude applied at different times during a 24 h cycle elicit differing magnitudes of response (Hotta et al., 2007; Greenham and Mcclung, 2015). Recent data suggest that response to UV-B stress is gated by the circadian clock (Fehér et al., 2011; Takeuchi et al., 2014), but notably, a central circadian gating mechanism for UV-B-induced gene induction has not been identified: While UVR8 is transcribed rhythmically, neither protein abundance nor dimer/monomer status showed daily oscillations and the circadian gating of UV-B induced genes likely occurs on a gene-by-gene basis (Fehér et al., 2011; Findlay and Jenkins, 2016).

In this chapter, the circadian gating of UV-B-induced shade avoidance inhibition is experimentally investigated in Arabidopsis. These experiments aimed to identify what times of day plants are most responsive to UV-B-induced inhibition of shade avoidance and whether or not this is subject to circadian regulation. Circadian gating may yield the opportunity to design a light regime for use in glasshouses for the precise timing of the application of supplemental low dose UV-B at periods of maximum plant sensitivity. Such a light regime may provide an economical and environmentally friendly solution for the manipulation of plant architecture without the pleiotropic effects associated with long-term exposure. If successful, targeted UV-B supplementation may also have applications in the ornamental plant industry to replace the use of chemical growth inhibitors.

3.2 Diurnal regulation of UV-B-mediated inhibition of shade avoidance

End-point hypocotyl assays were employed to assess the time of day when UV-B is most effective at inhibiting shade avoidance. Plants were grown- and treatments given- in 12 h light 12 h dark photocycles (12L:12D) under simulated high (R:FR = 5) and low (R:FR = 0.05) R:FR ratios. Equal UV-B doses of 4 h at 1.5 µmol m^{-2} s^{-1} were given at three sequential times of day corresponding to morning (0 - 4 h), midday (4 - 8 h) and afternoon (8 - 12 h) to three different groups of plants for 4 d in each R:FR ratio.

3.2.1 The greatest UVR8 -dependent and -independent inhibition of hypocotyl elongation by UV-B occurs towards the middle of the day

Consistent with previous reports (Hayes et al., 2014), in wild type plants, UV-B treatment for the duration of the photoperiod (12 h) significantly inhibited hypocotyl elongation in high (figure 3.1a,3.3a) and low (figure 3.2a,3.4a) R:FR. Mutants deficient in the UVR8 protein had an attenuated response to UV-B; the *uvr8-1* mutant exhibited a small but significant UV-B-induced inhibition of hypocotyl elongation in a background of low R:FR (figure 3.2b) while the *uvr8-6* mutant had no significant difference between control and 12 h UV-B treatment at high and low R:FR (figure 3.3b,3.4b).

The efficacy of UV-B treatments for the inhibition of hypocotyl elongation varied to a small degree depending on the time of day of the dose. In L. *er*, the midday and evening doses were equally more effective than the morning dose in a background of high R:FR (figure 3.1a), while in low R:FR, the middle of the day dose was significantly more effective than the morning or evening doses (figure 3.2a). The same experiment in Col-0 gave slightly different results. In high R:FR there was no significant difference between treatments, with all being equally as effective as UV-B given for 12 h (figure 3.3a). In low R:FR the midday dose was only marginally more effective than the morning or evening doses (figure 3.4a). The *uvr8-1* mutant exhibited similar time of day effects to the L. *er* controls in low R:FR, with the middle of the day dose being the most effective compared to morning and evening doses (figure 3.2b). In the *uvr8-6* mutant (Col-0), differences in effectiveness of UV-B doses at different times was less pronounced, with no significant differences between the 4 h treatments in either high (figure 3.3b) or low (figure 3.4b) R:FR.

In general, the short dose (4 h) UV-B treatments were less effective than the 12 h UV-B treatment for inhibition of hypocotyl elongation, which suggests that the magnitude of UV-B-induced inhibition of hypocotyl elongation is dose-dependent. Additionally, there was overall a small trend for the middle of the day treatment to be the most effective of the short dose treatments in both the L. *er* and Col-0 ecotypes. While the *uvr8-6* mutation largely removed the UV-B-mediated inhibition of hypocotyl elongation, the *uvr8-1* mutation only partially attenuated the magnitude of the response. These plants still showed a similar time of day response to wild type controls, which may reflect UVR8-independent effects (Biever et al., 2014) that could also be subject to time of day differences.

3.2.2 The period of maximal hypocotyl growth inhibition by UV-B is dependent on a functioning circadian clock

Fehér et al. (2011) previously demonstrated that UV-B signalling is circadian gated, with photo-protective responses, such as the upregulation of *CHS* expression in the flavonoid biosynthesis pathway, having their UV-B induction gated to the start of the day. The trend described in section 3.2.1 where a 4 h UV-B dose during the middle of the day gave the greatest inhibition of hypocotyl elongation may, therefore, be due to circadian regulation. To test this hypothesis,

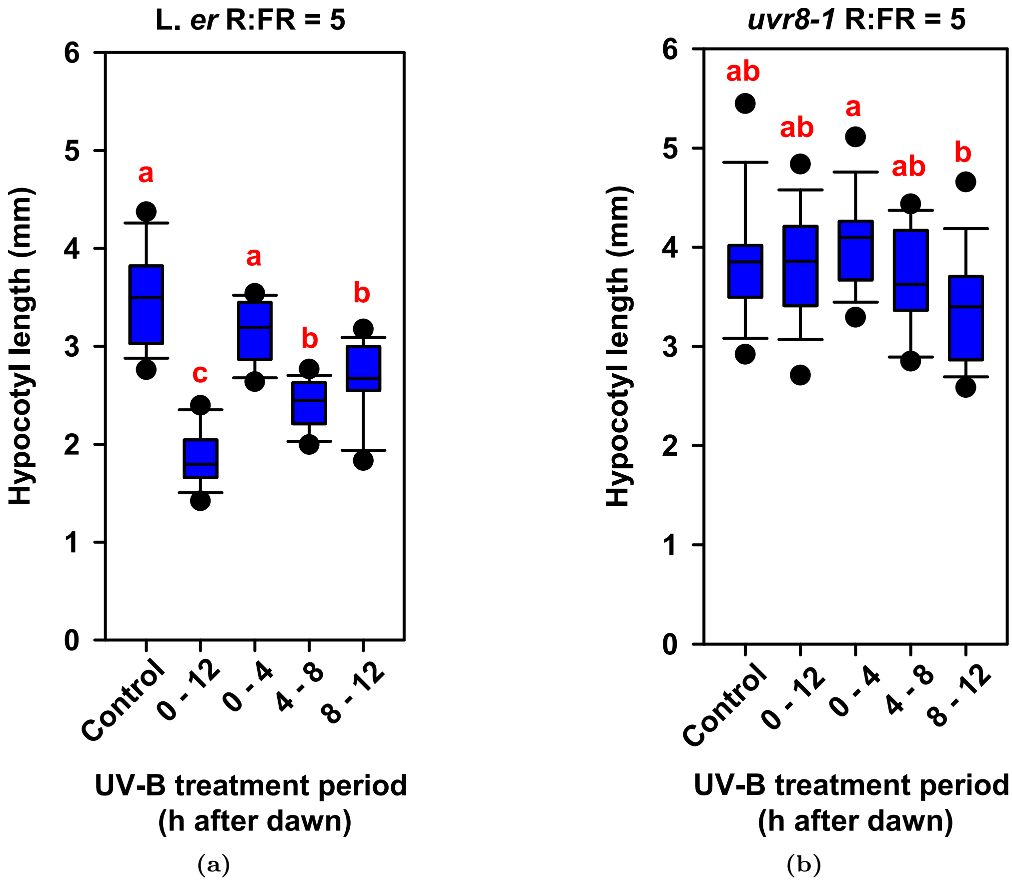

Figure 3.1: In high R:FR, UVR8-mediated inhibition of hypocotyl elongation is time-of-day dependent. L. *er* and *uvr8-1* plants were grown under 12L:12D cycles, with R:FR = 5. Groups of 3-day-old seedlings were treated with UV-B at 1.5 µmol m^{-2} s^{-1} at 0 - 4 h, 4 - 8 h, 8 - 12 h and 0 - 12 h after dawn for 4 d. 7-day-old seedlings were sampled for hypocotyl elongation analysis. Data are shown as box plots representing the 1st, 2nd and 3rd quartiles with whiskers representing the 10th and 90th percentile. Different red letters indicate statistically significant differences by Tukey's post hoc at $p < 0.05$, $n = 25$.

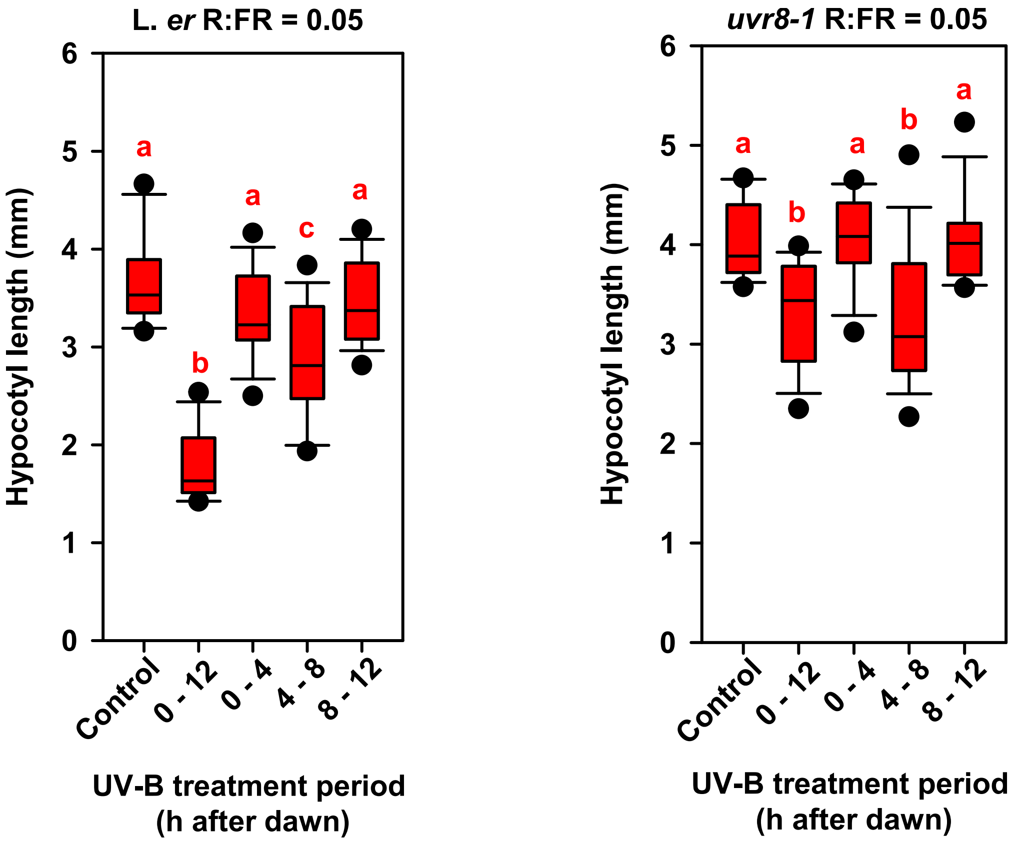

(a) (b)

Figure 3.2: In low R:FR, UVR8-mediated inhibition of hypocotyl elongation is time-of-day dependent. L. *er* and *uvr8-1* plants were grown under 12L:12D cycles, with R:FR = 0.05. Groups of 3-day-old seedlings were treated with UV-B at 1.5 µmol m^{-2} s^{-1} at 0 - 4 h, 4 - 8 h, 8 - 12 h and 0 - 12 h after dawn for 4 d. 7-day-old seedlings were sampled for hypocotyl elongation analysis. Data are shown as box plots representing the 1st, 2nd and 3rd quartiles with whiskers representing the 10th and 90th percentile. Different red letters indicate statistically significant differences by Tukey's post hoc at $p < 0.05$, n = 25.

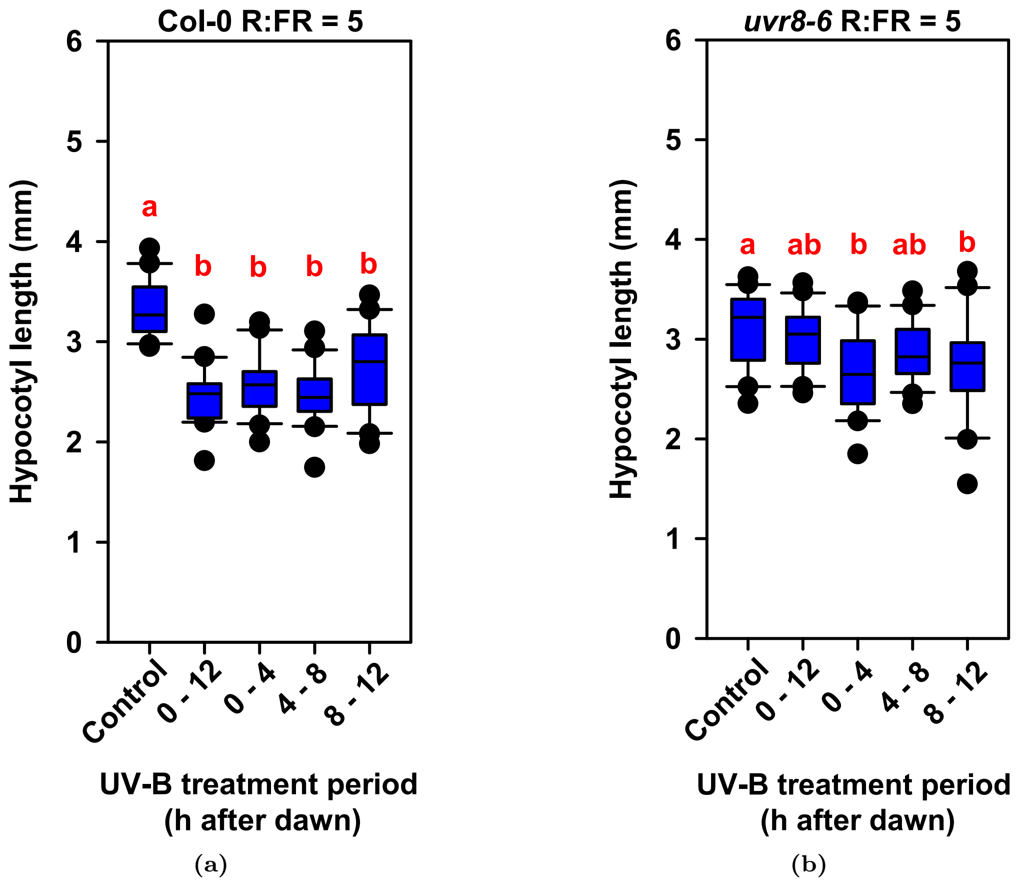

Figure 3.3: In the Col-0 background in high R:FR, UVR8-mediated inhibition of hypocotyl elongation is not time-of-day dependent. Col-0 and *uvr8-6* plants were grown under 12L:12D cycles, with R:FR = 5. Groups of 3-day-old seedlings were treated with UV-B at 1.5 μmol m^{-2} s^{-1} at 0 - 4 h, 4 - 8 h, 8 - 12 h and 0 - 12 h after dawn for 4 d. 7-day-old seedlings were sampled for hypocotyl elongation analysis. Data are shown as box plots representing the 1st, 2nd and 3rd quartiles with whiskers representing the 10th and 90th percentile. Different red letters indicate statistically significant differences by Tukey's post hoc at $p < 0.05$, n = 25.

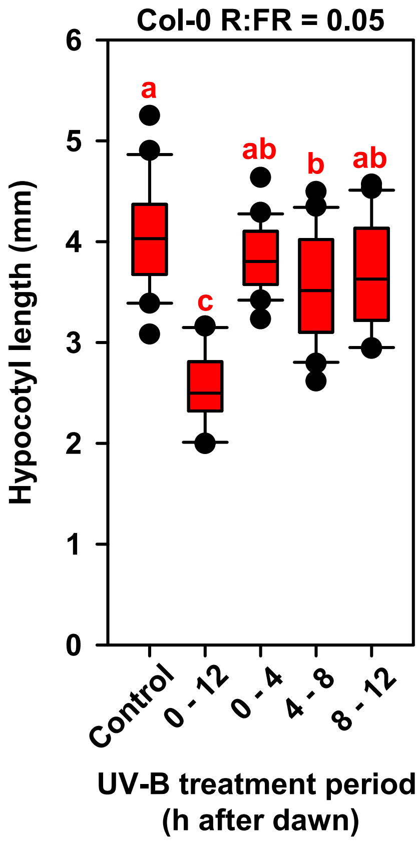

(a)

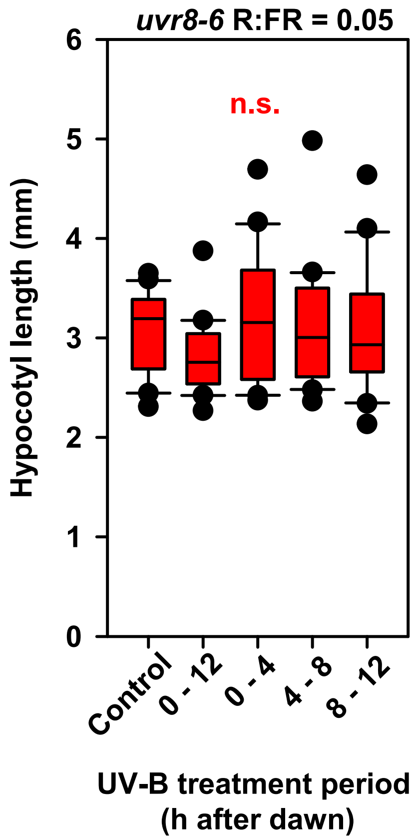

(b)

Figure 3.4: In the Col-0 background in low R:FR, UVR8-mediated inhibition of hypocotyl elongation is not time-of-day dependent. Col-0 and *uvr8-6* plants were grown under 12L:12D cycles, with R:FR = 0.05. Groups of 3-day-old seedlings were treated with UV-B at 1.5 µmol m^{-2} s^{-1} at 0 - 4 h, 4 - 8 h, 8 - 12 h and 0 - 12 h after dawn for 4 d. 7-day-old seedlings were sampled for hypocotyl elongation analysis. Data are shown as box plots representing the 1st, 2nd and 3rd quartiles with whiskers representing the 10th and 90th percentile. Different red letters indicate statistically significant differences by Tukey's post hoc at $p < 0.05$, n = 25.

plants with disrupted circadian clocks were tested in the same conditions as in section 3.2.1. CCA1 is a morning-phased central repressor of the plant circadian clock and its over-expression results in arrhythmia in LL (Wang and Tobin, 1998). ELF3 is a component of the evening complex, which is responsible for transcriptional repression in early night, *elf3-1* mutants are also arrhythmic in LL (Hicks et al., 1996).

In both high and low R:FR, the *elf3-1* mutant and a transgenic line constitutively expressing *CCA1* displayed elongated hypocotyls when compared to Col-0 controls. Furthermore, UV-B treatment for the duration of the light period significantly inhibited hypocotyl elongation of *elf3-1* and *CCA1-OX* in both high and low R:FR (figure 3.5,3.6). In high R:FR, the *elf3-1* mutant exhibited a similar pattern of effectiveness of UV-B treatment to Col-0, with no significant differences between UV-B for the duration of the photoperiod and 4 h doses given at different times of day (figure 3.5b). In *CCA1-OX*, the evening dose was as effective as giving UV-B for the duration of the photoperiod and resulted in significantly shorter hypocotyls than plants given the morning and midday doses (figure 3.5c). In low R:FR, the *elf3-1* mutant exhibited a similar pattern of time-of-day differences to Col-0 but with significant differences between treatment times, with the midday UV-B dose as effective as UV-B for the duration of the photoperiod, and significantly shorter hypocotyls than the other short-dose UV-B treatments (figure 3.6b). In *CCA1-OX*, plants treated with the evening UV-B dose were significantly shorter than plants given the morning UV-B dose while the hypocotyl lengths of plants given the midday dose showed an intermediate phenotype (figure 3.6c). Additionally, *CCA1-OX* displayed shorter hypocotyls in low R:FR than high R:FR, which is the opposite phenotype to wild type controls (figure 3.5,3.6).

Collectively, the results in figures 3.5 and 3.6 indicate that disrupting the circadian clock alters the timing of the responsiveness of hypocotyl elongation to UV-B inhibition, which may suggest that the inhibition of hypocotyl elongation by UV-B is gated by the circadian clock. Whereas the *elf3-1* mutation did not alter the timing of the response from that of wild type, over-expression of *CCA1* shifted the timing of maximum response to later in the day. The difference in behaviour of the two arrhythmic lines may reflect the pleiotropic effects of over-expressing a central repressor of the circadian clock versus a mutation whose effects may be diminished through functional redundancies.

3.2.3 Mutation of *HY5* and *HYH* alters the timing of the responsiveness of hypocotyl elongation to UV-B inhibition in high but not low R:FR.

The photomorphogenic transcription factor, HY5 and the closely related HYH are rapidly upregulated after UV-B irradiation and are the major effectors of UVR8 signalling, regulating the transcription of numerous downstream target genes (Brown et al., 2005; Brown and Jenkins, 2008; Favory et al., 2009). Reports that the UV-B induced expression of *HYH*, but not *HY5* is gated by the circadian clock (Fehér et al., 2011), and the involvement of HY5 and HYH in UV-B mediated inhibition of shade avoidance inhibition (Hayes et al., 2014), raises the possibility that HYH and/or HY5 could be involved in regulating the timing of responsiveness of hypocotyl elongation to UV-B inhibition.

Consistent with previously reported data (Hayes et al., 2014); in high and low R:FR, the *hy5* mutant had an elongated phenotype when compared to Ws, though UV-B still inhibited hypocotyl elongation when given for the full length of the photoperiod. The *hyh* mutant was also still responsive to UV-B treatment, but with shorter hypocotyls than the *hy5* mutant. The *hy5/hyh* double mutant was partially responsive to UV-B treatment and had long hypocotyls (figure 3.7,3.8).

In high R:FR, the midday UV-B treatment resulted in significantly shorter hypocotyls than the morning and evening treatments in Ws. In the *hy5* mutant, midday treatment resulted in significantly shorter hypocotyls than the evening treatment, with the morning treatment showing an intermediate response (fig-

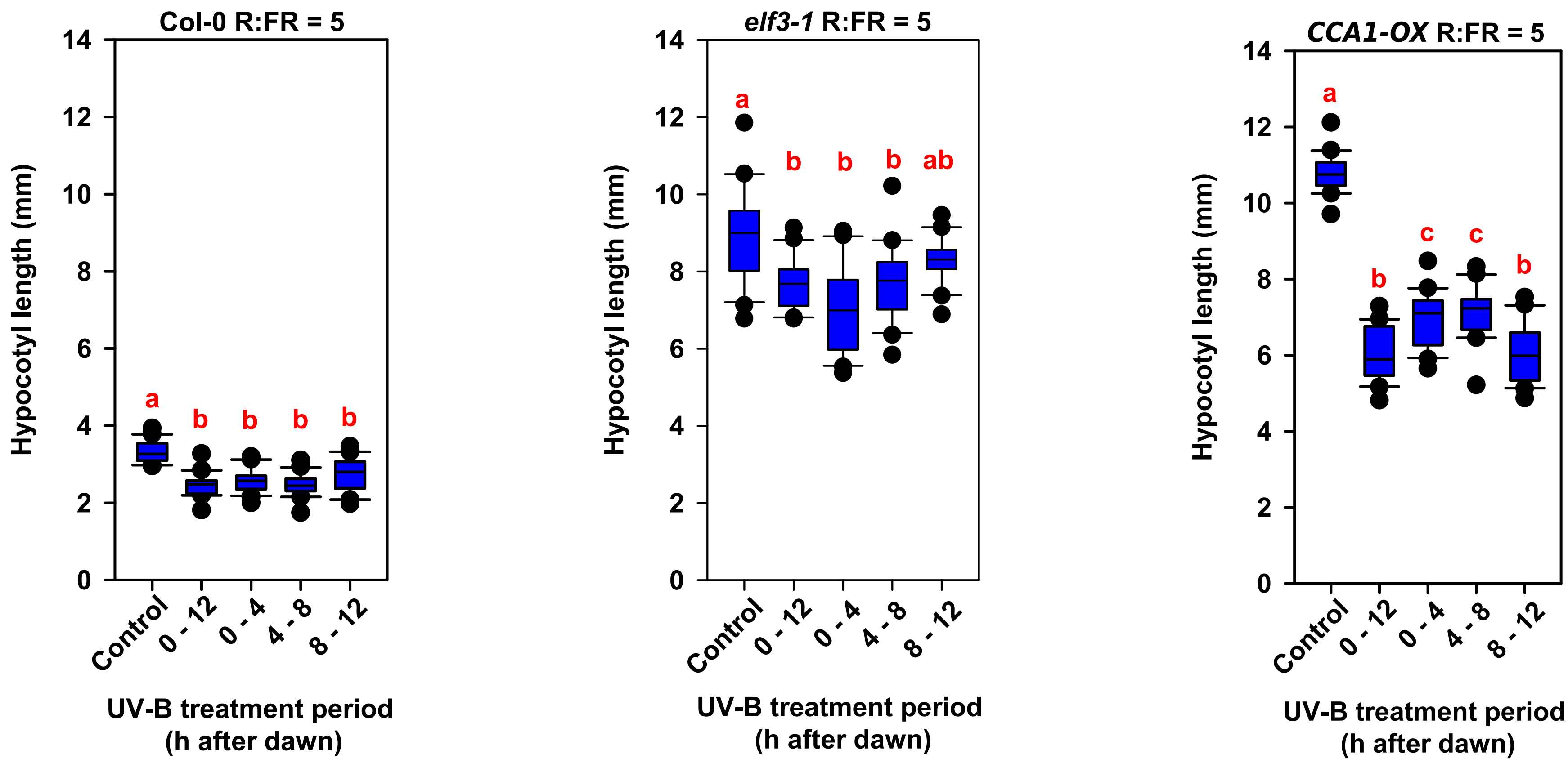

(a) (b) (c)

Figure 3.5: In high R:FR the time-of-day-dependence of UV-B-mediated inhibition of hypocotyl elongation requires a functioning circadian clock. Col-0, *elf3-1* and CCA1-OX plants were grown under 12L:12D cycles, with R:FR = 5. Groups of 3-day-old seedlings were treated with UV-B at 1.5 µmol m^{-2} s^{-1} at 0 - 4 h, 4 - 8 h, 8 - 12 h and 0 - 12 h after dawn for 4 d. 7-day-old seedlings were sampled for hypocotyl elongation analysis. Data are shown as box plots representing the 1st, 2nd and 3rd quartiles with whiskers representing the 10th and 90th percentile. Different red letters indicate statistically significant differences by Tukey's post hoc at $p < 0.05$, n = 25.

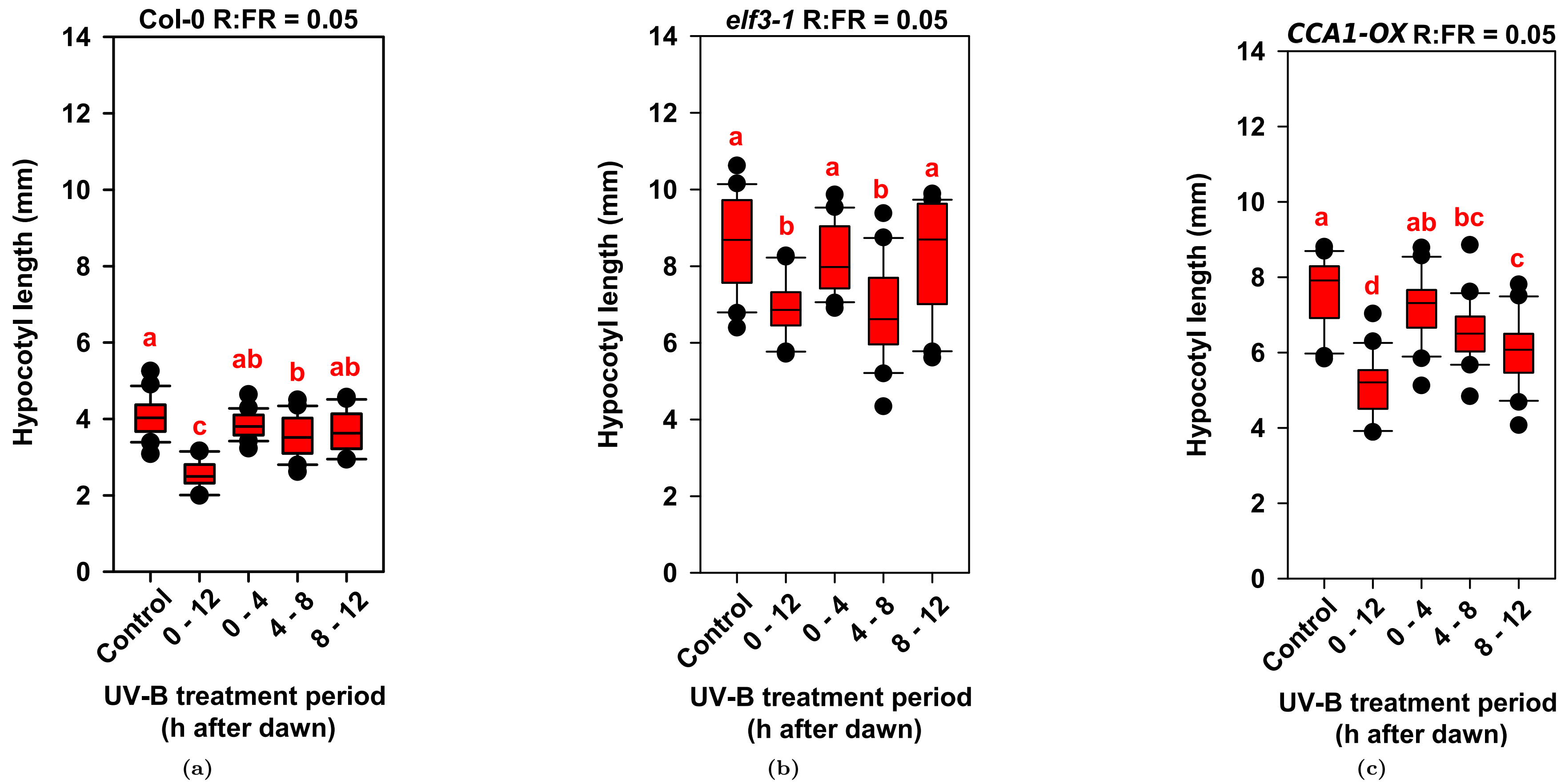

Figure 3.6: In low R:FR the time-of-day dependence of UV-B-mediated inhibition of hypocotyl elongation requires a functioning circadian clock. Col-0, *elf3-1* and CCA1-OX plants were grown under 12L:12D cycles, with R:FR = 0.05. Groups of 3-day-old seedlings were treated with UV-B at 1.5 µmol m^{-2} s^{-1} at 0 - 4 h, 4 - 8 h, 8 - 12 h and 0 - 12 h after dawn for 4 d. 7-day-old seedlings were sampled for hypocotyl elongation analysis. Data are shown as box plots representing the 1st, 2nd and 3rd quartiles with whiskers representing the 10th and 90th percentile. Different red letters indicate statistically significant differences by Tukey's post hoc at $p < 0.05$, $n = 25$.

ure 3.7b). In the *hyh* mutant, the morning and midday UV-B doses resulted in significantly shorter hypocotyls than the evening dose (figure 3.7c). In the *hy5/hyh* double mutant there were no significant differences between the treatment times (figure 3.7d), which suggests that HY5 and HYH may redundantly mediate the timing of the maximum sensitivity of hypocotyl elongation to UV-B inhibition. However, in low R:FR, neither Ws nor the mutants demonstrated significant differences between short dose UV-B treatment times (figure 3.8). Contrary to the results in high R:FR, this observation suggests that neither HY5 nor HYH play a major role in mediating the timing of the responsiveness of elongating hypocotyls to UV-B inhibition in low R:FR.

3.3 UV-B-regulation of transcripts involved in shade avoidance is rhythmic in circadian and nycthemeral conditions

It was previously shown that UV-B induces the expression of genes involved in the inhibition of shade avoidance (Hayes et al., 2014). According to proposed models, one signalling pathway by which UV-B antagonises shade avoidance is through the upregulaton of *GA2ox1*, a GA catabolism gene. This happens in a *HY5/HYH*-dependent manner and promotes the stabilisation of DELLAs that form non DNA-binding heterodimers with PIFs (Hayes et al., 2014). Another signalling pathway by which UV-B inhibits hypocotyl elongation is likely through the suppression of *PIF4* expression (Hayes et al., 2017). The relative transcript abundance of these genes and their auxin-related downstream targets were therefore assayed for rhythmicity and circadian gating of induction by UV-B.

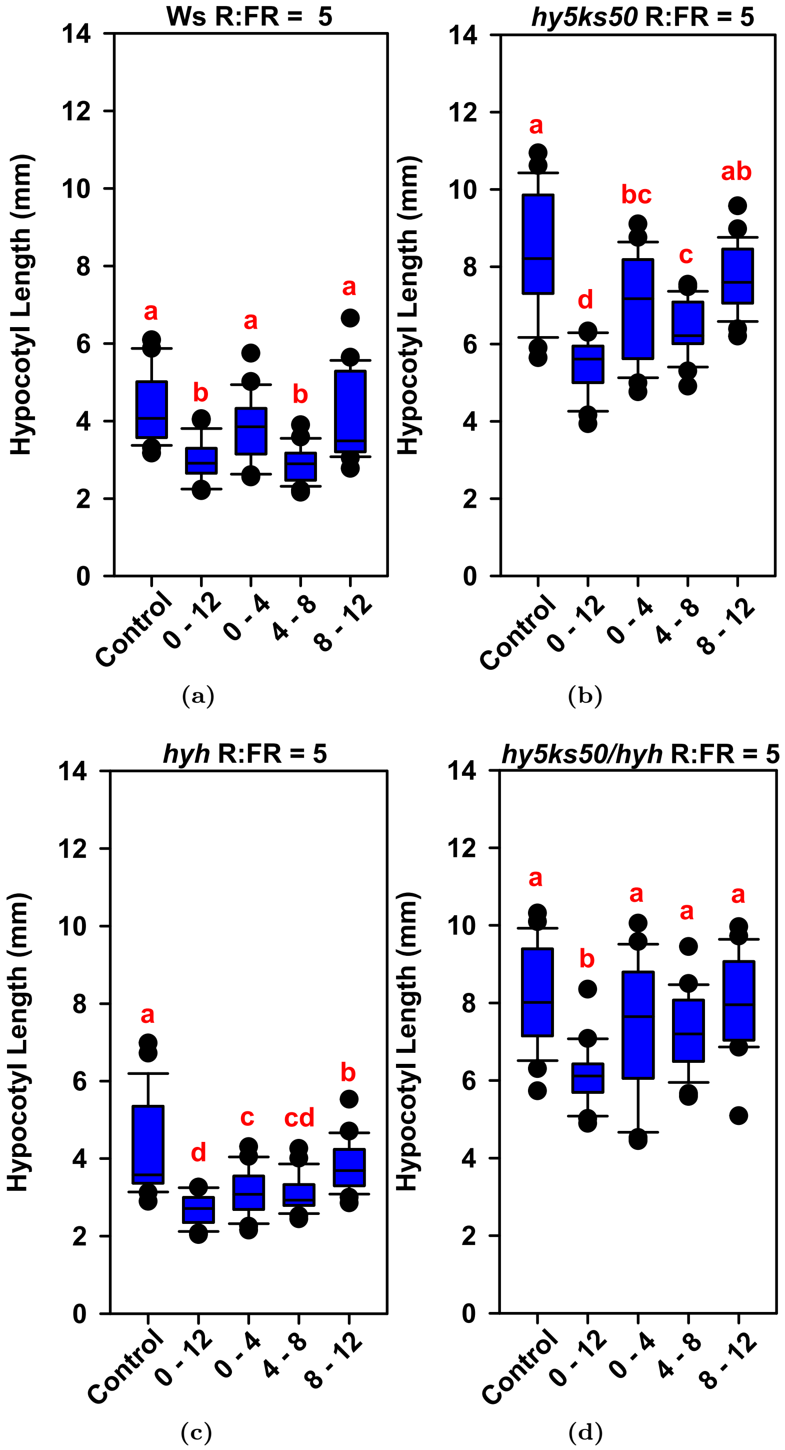

Figure 3.7: In high R:FR, the time-of-day dependence of UV-B-mediated inhibition of hypocotyl elongation is dependent on the presence of HY5 and HYH. Ws (3.7a), *hy5ks50* (3.7b), *hyh* (3.7c) and *hy5ks50/hyh* (3.7d) plants were grown under 12L:12D cycles, with R:FR = 5. Groups of 3-day-old seedlings were treated with UV-B at 1.5 μmol m^{-2} s^{-1} at 0 - 4 h, 4 - 8 h, 8 - 12 h and 0 - 12 h after dawn for 4 d. 7-day-old seedlings were sampled for hypocotyl elongation analysis. Data are shown as box plots representing the 1st, 2nd and 3rd quartiles with whiskers representing the 10th and 90th percentile. Different red letters indicate statistically significant differences by Tukey's post hoc at $p < 0.05$, n = 25.

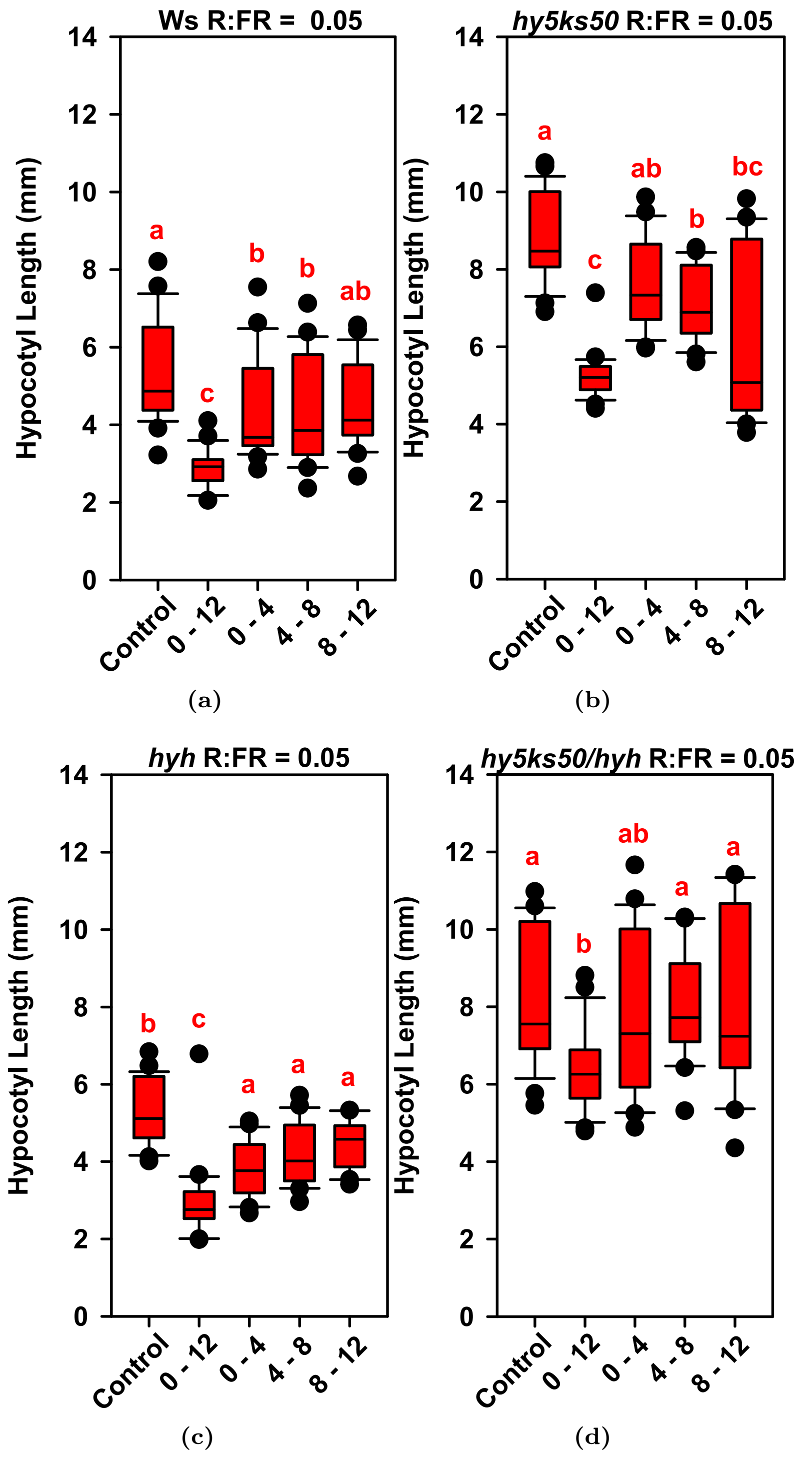

Figure 3.8: In low R:FR, the time-of-day dependence of UV-B-mediated inhibition of hypocotyl elongation is independent of HY5 and HYH. Ws (3.8a), *hy5ks50* (3.8b), *hyh* (3.8c) and *hy5ks50/hyh* (3.8d) plants were grown under 12L:12D cycles, with R:FR = 0.05. Groups of 3-day-old seedlings were treated with UV-B at 1.5 µmol m^{-2} s^{-1} at 0 - 4 h, 4 - 8 h, 8 - 12 h and 0 - 12 h after dawn for 4 d. 7-day-old seedlings were sampled for hypocotyl elongation analysis. Data are shown as box plots representing the 1st, 2nd and 3rd quartiles with whiskers representing the 10th and 90th percentile. Different red letters indicate statistically significant differences by Tukey's post hoc at $p < 0.05$, n = 25.

3.3.1 Circadian gating of UV-B-induced gene expression is R:FR-dependent in continuous light

Landsberg *erecta* plants were entrained in either high (5) or low (0.05) R:FR in 12L:12D for 4 days. On day 5, plants were placed into LL high and low R:FR conditions for a further 24 h before treatments. At 4 h intervals over a 48 h period, treated plants were subjected to a single 2 h UV-B treatment at 1.5 µmol m^{-2} s^{-1} and were harvested alongside untreated controls immediately afterwards.

In LL high R:FR, maximum induction of *GA2ox1*, *HY5* and *HYH* by UV-B was rhythmic (figure 3.9a,3.10a,3.11a) suggesting gating by the circadian clock. These data both agree and contrast with the findings of Fehér et al. (2011) who reported that only the UV-B induction of *HYH* was circadian gated. In LL low R:FR, however, the maximum induction of *GA2ox1*, *HY5* and *HYH* by UV-B lost its rhythmicity (figure 3.9b,3.10b,3.11b), suggesting that the gating of these genes is lost when the R:FR ratio is lowered in LL.

Together these data suggest that the circadian clock gates the UV-B-induction of *GA2ox1*, *HY5* and *HYH*. Unexpectedly, the circadian gating of these genes was lost in LL low R:FR. A possible explanation for this loss of circadian gating is examined in chapter 5. While assays carried out in LL are informative for investigations of circadian regulation, they are not representative of natural conditions characterised by day/night cycles. The following section (3.3.2), therefore, analyses the effect of UV-B treatment on gene expression in LD conditions that more closely reflect real world conditions.

3.3.2 In nycthemeral conditions regulation of gene expression by UV-B is time-of-day-dependent

For experiments in LD, Landsberg *erecta* plants were grown in 5 cycles of 12L:12D at high (5) or low (0.05) R:FR. On day 6, plants were treated at 2 h intervals with a single 2 h UV-B dose at 1.5 µmol m^{-2} s^{-1} and were sampled

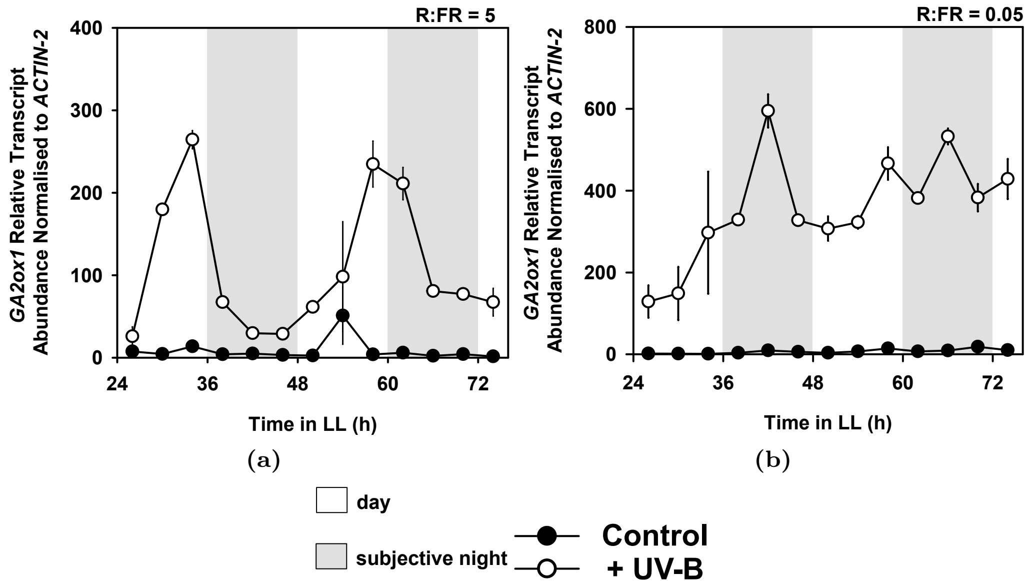

Figure 3.9: In LL, the circadian gating of the UV-B induction of *GA2ox1* is R:FR-dependent. L. *er* plants were entrained in 4 cycles of 12L:12D in either high (3.9a) or low (3.9b) R:FR before transfer to LL. After 24 h in LL, UV-B treatments of 1.5 µmol m^{-2} s^{-1} for 2 h were carried out on 6-, 7- and 8-day-old plants. Treated plants (unfilled circles) were given a single 2 h UV-B dose at 4 h intervals and were sampled at the plotted time points alongside untreated controls (filled circles). Plotted are means +/- 1 S.E.M. of two independent experiments carried out on different occasions (n = 2).

alongside untreated controls at the plotted time points.

The UV-B induction of *GA2ox1* peaked at 6 h after dawn in high R:FR and 8 h after dawn in low R:FR (figure 3.12, which was a few hours earlier than the peak of circadian gating expression in LL (figure 3.9a). In LD, *HY5* did not have a clear peak of UV-B-induced transcript abundance in high or low R:FR (figure 3.13a,3.13b), which contrasts with the data reported in figure 3.10a, but is consistent with Fehér et al. (2011). UV-B-induced *HYH* relative transcript abundance peaked at the start of the day in both high and low R:FR (figure 3.14a,3.14b), which is consistent with Fehér et al. (2011) and the data collected in LL (figure 3.11a).

PIF4 expression has daily rhythms and is regulated by the circadian clock (Nusinow et al., 2011). It was recently shown that *PIF4* transcript is strongly reduced by UV-B (Hayes et al., 2017). Consistent with previous reports, *PIF4* transcript abundance peaked 6 h after dawn and its expression was reduced by UV-B at

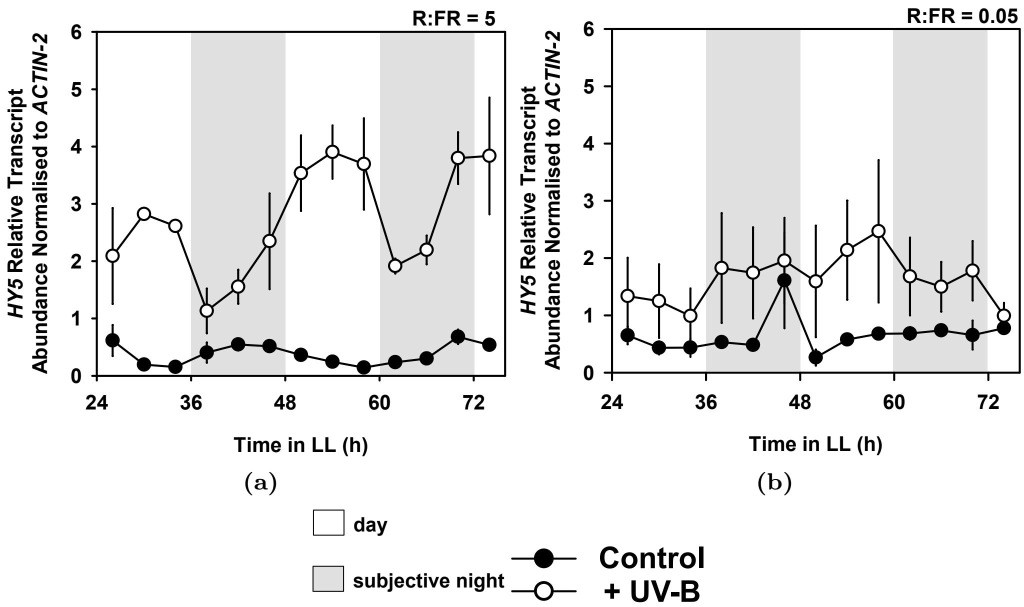

Figure 3.10: In LL, the circadian gating of the UV-B induction of *HY5* is R:FR-dependent. L. *er* plants were entrained in 4 cycles of 12L:12D in either high (3.10a) or low (3.10b) R:FR before transfer to LL. After 24 h in LL, UV-B treatments of 1.5 µmol m^{-2} s^{-1} for 2 h were carried out on 6-, 7- and 8-day-old plants. Treated plants (unfilled circles) were given a single 2 h UV-B dose at 4 h intervals and were sampled at the plotted time points alongside untreated controls (filled circles). Plotted are means +/- 1 S.E.M. of two independent experiments carried out on different occasions (n = 2).

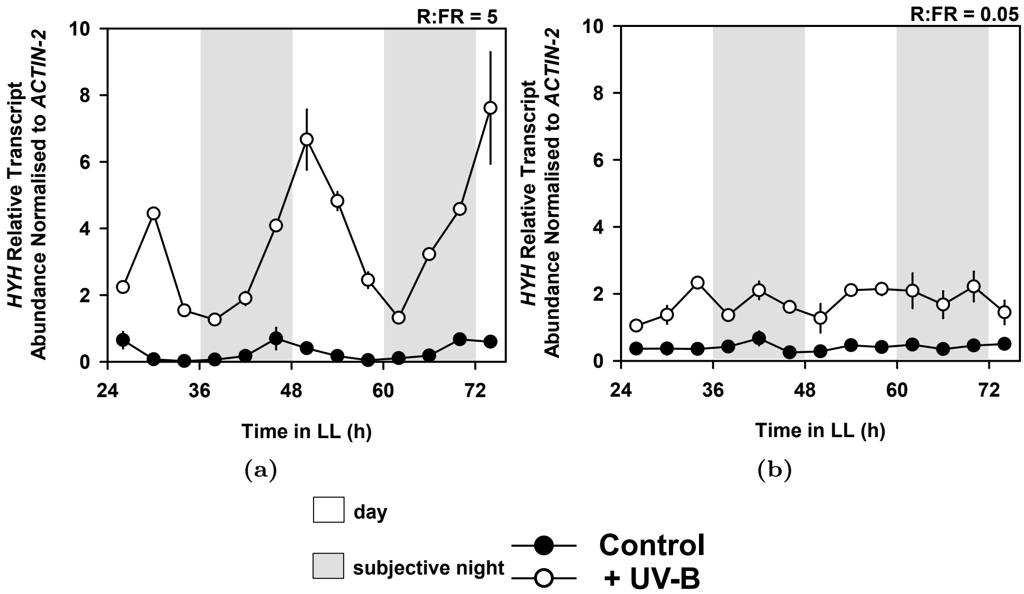

Figure 3.11: In LL, the circadian gating of the UV-B induction of *HYH* is R:FR-dependent. L. *er* plants were entrained in 4 cycles of 12L:12D in either high (3.11a) or low (3.11b) R:FR before transfer to LL. After 24 h in LL, UV-B treatments of 1.5 µmol m^{-2} s^{-1} for 2 h were carried out on 6-, 7- and 8-day-old plants. Treated plants (unfilled circles) were given a single 2 h UV-B dose at 4 h intervals and were sampled at the plotted time points alongside untreated controls (filled circles). Plotted are means +/- 1 S.E.M. of two independent experiments carried out on different occasions (n = 2).

all tested time points (figure 3.15a,3.15b).

Low R:FR promotes hypocotyl elongation, in part, through increases in auxin biosynthesis. This is achieved by the upregulation of the expression of YUCCA enzymes, which control the rate-limiting step of a major auxin biosynthesis pathway (Hornitschek et al., 2012; Li et al., 2012a). In LD, *YUCCA8* relative transcript abundance peaked at 6 h after dawn, accumulated to a higher abundance in low R:FR and was strongly suppressed by UV-B at all tested time points (figure 3.16a,3.16b). In a similar fasion, the expression of *IAA29*, an auxin-responsive gene, peaked at 6 - 8 h after dawn in high and low R:FR and was also strongly suppressed by UV-B treatment at all tested time points (figure 3.17a,3.17a).

The transcript abundance data in this section report that unlike in LL, the patterns and relative transcript abundances of *GA2ox1*, *HY5* and *HYH* in response to UV-B did not dramatically differ between high and low R:FR in LD, suggesting that the unexpected loss of circadian gating observed in section 3.3.1 may be an artefact of carrying out experiments in LL low R:FR. Observations that the UV-B-induced relative transcript abundance of *GA2ox1* showed a clear peak around 6 - 8 h after dawn whereas *HYH* peaked at the start of the day and *HY5* did not show a clear peak suggest that the time-of-day regulation of *GA2ox1* is unlikely to be fully dependent on the time-of-day regulation of *HY5* and *HYH*. Observations that *PIF4*, *YUCCA8* and *IAA29* transcripts all peak at or around the middle of the day in both high and low R:FR (6 - 8 h after dawn), and are strongly suppressed by UV-B irradiation at all points, taken alongside the midday peak of UV-B-induced *GA2ox1* transcript, may explain the trend in hypocotyl assays for middle of the day UV-B treatments to elicit the greatest inhibition of hypocotyl elongation (section 3.2.1).

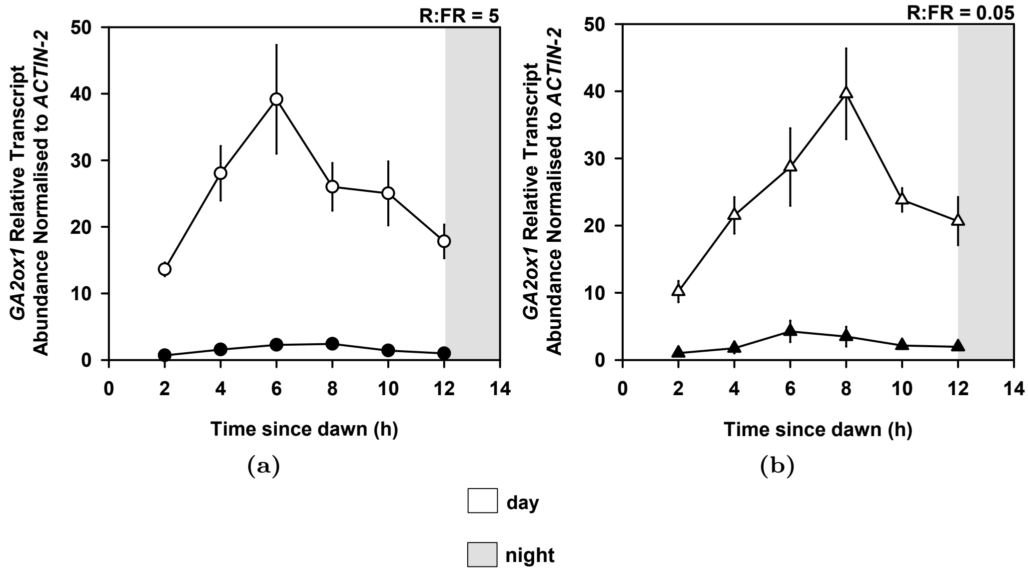

Figure 3.12: In LD, UV-B induction of *GA2ox1* is time-of-day-dependent and peaks 6 - 8 h after dawn. L. *er* plants were grown in 5 cycles of 12L:12D in either high (3.12a) or low (3.12b) R:FR. UV-B treatments of 1.5 µmol m^{-2} s^{-1} for 2 h were carried out on 6-day-old plants. Treated plants (unfilled markers) were given a single 2 h UV-B dose at 2 h intervals and were sampled at the plotted time points alongside untreated controls (filled markers). Plotted are means +/- 1 S.E.M. of three independent experiments carried out on different occasions (n = 3).

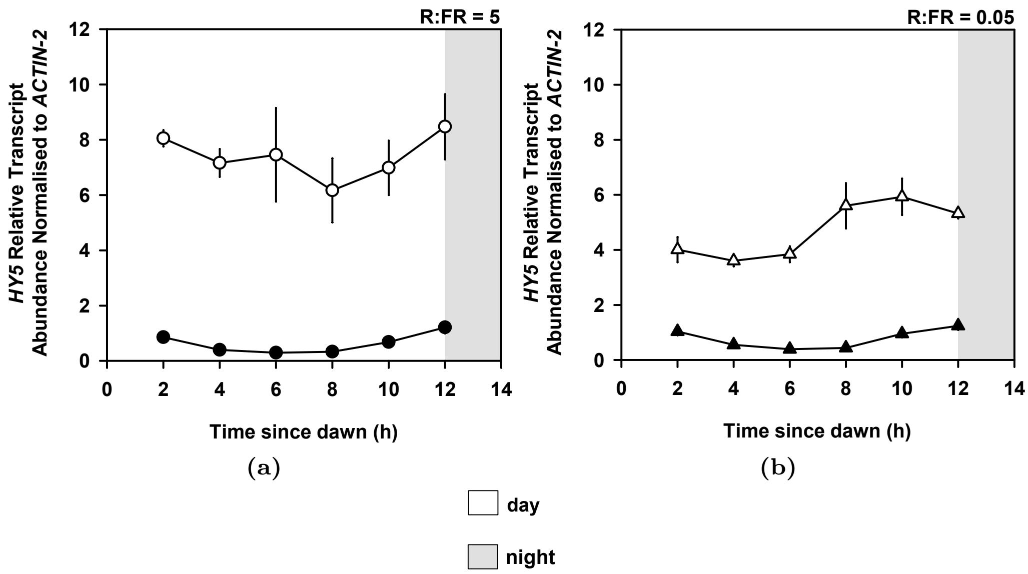

Figure 3.13: In LD, UV-B induction of *HY5* is not time-of-day dependent. L. *er* plants were grown in 5 cycles of 12L:12D in either high (3.13a) or low (3.13b) R:FR. UV-B treatments of 1.5 µmol m^{-2} s^{-1} for 2 h were carried out on 6-day-old plants. Treated plants (unfilled markers) were given a single 2 h UV-B dose at 2 h intervals and were sampled at the plotted time points alongside untreated controls (filled markers). Plotted are means +/- 1 S.E.M. of three independent experiments carried out on different occasions (n = 3).

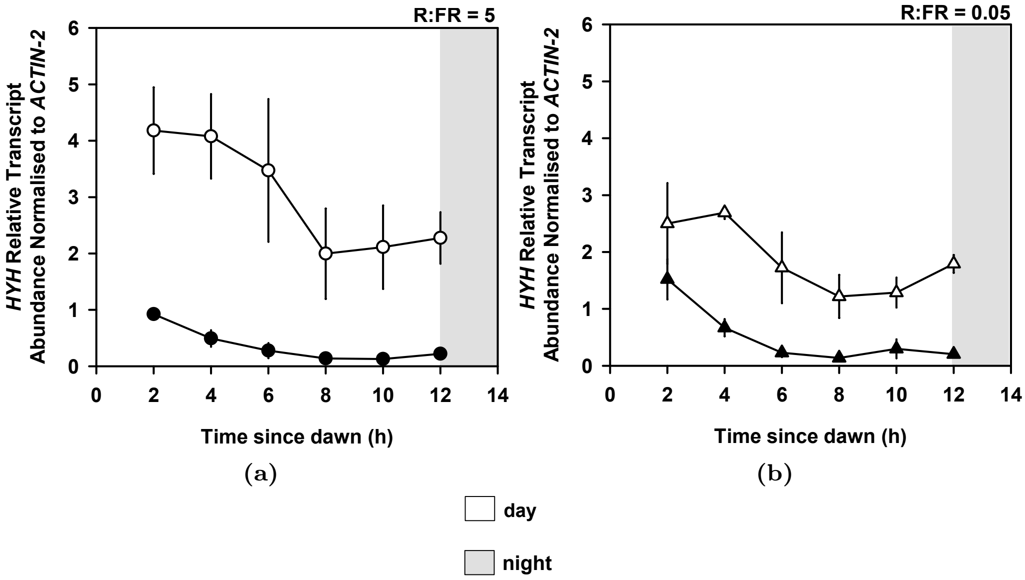

Figure 3.14: In LD, UV-B induction of *HYH* is time-of-day-dependent and peaks 2 - 4 h after dawn. L. *er* plants were grown in 5 cycles of 12L:12D in either high (3.14a) or low (3.14b) R:FR. UV-B treatments of 1.5 µmol m^{-2} s^{-1} for 2 h were carried out on 6-day-old plants. Treated plants (unfilled markers) were given a single 2 h UV-B dose at 2 h intervals and were sampled at the plotted time points alongside untreated controls (filled markers). Plotted are means +/- 1 S.E.M. of three independent experiments carried out on different occasions (n = 3).

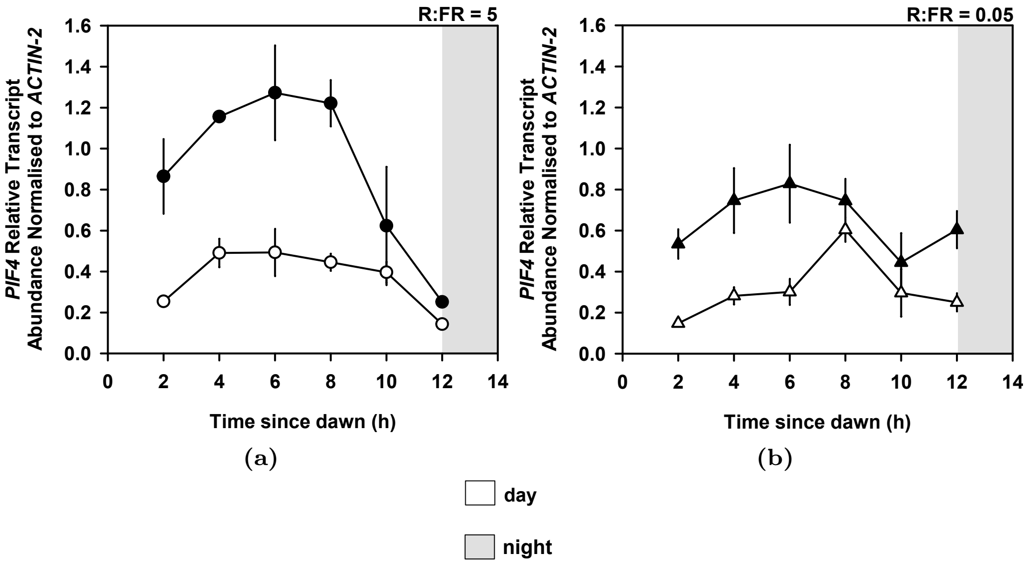

Figure 3.15: In LD, *PIF4* transcript abundance peaks 6 h after dawn and is suppressed by UV-B. L. *er* plants were grown in 5 cycles of 12L:12D in either high (3.15a) or low (3.15b) R:FR. UV-B treatments of 1.5 µmol m^{-2} s^{-1} for 2 h were carried out on 6-day-old plants. Treated plants (unfilled markers) were given a single 2 h UV-B dose at 2 h intervals and were sampled at the plotted time points alongside untreated controls (filled markers). Plotted are means +/- 1 S.E.M. of three independent experiments carried out on different occasions (n = 3).

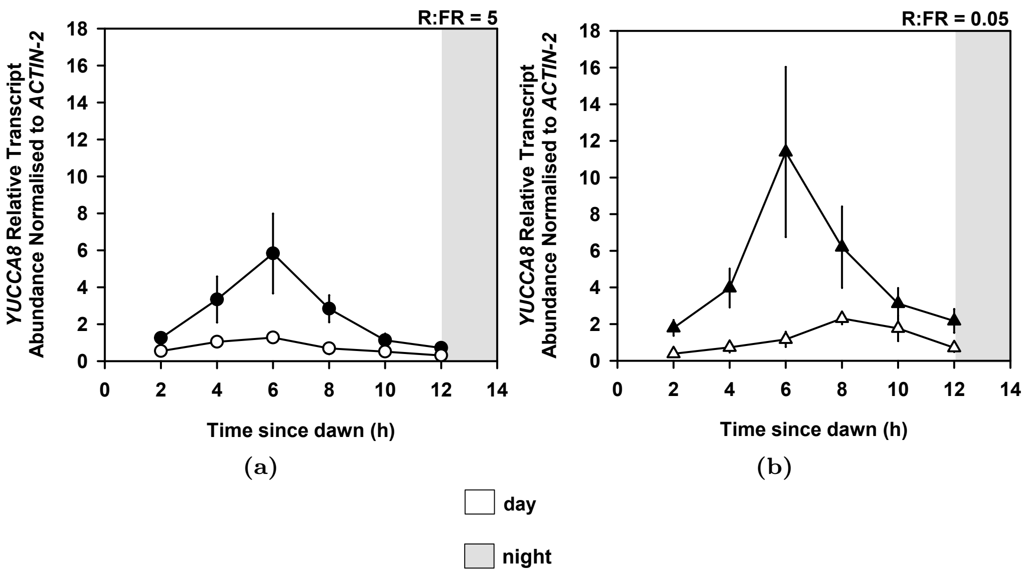

Figure 3.16: In LD, *YUCCA8* transcript abundance peaks 6 h after dawn, is elevated in low R:FR and is suppressed by UV-B. L. *er* plants were grown in 5 cycles of 12L:12D in either high (3.16a) or low (3.16b) R:FR. UV-B treatments of 1.5 µmol m^{-2} s^{-1} for 2 h were carried out on 6-day-old plants. Treated plants (unfilled markers) were given a single 2 h UV-B dose at 2 h intervals and were sampled at the plotted time points alongside untreated controls (filled markers). Plotted are means +/- 1 S.E.M. of three independent experiments carried out on different occasions (n = 3).

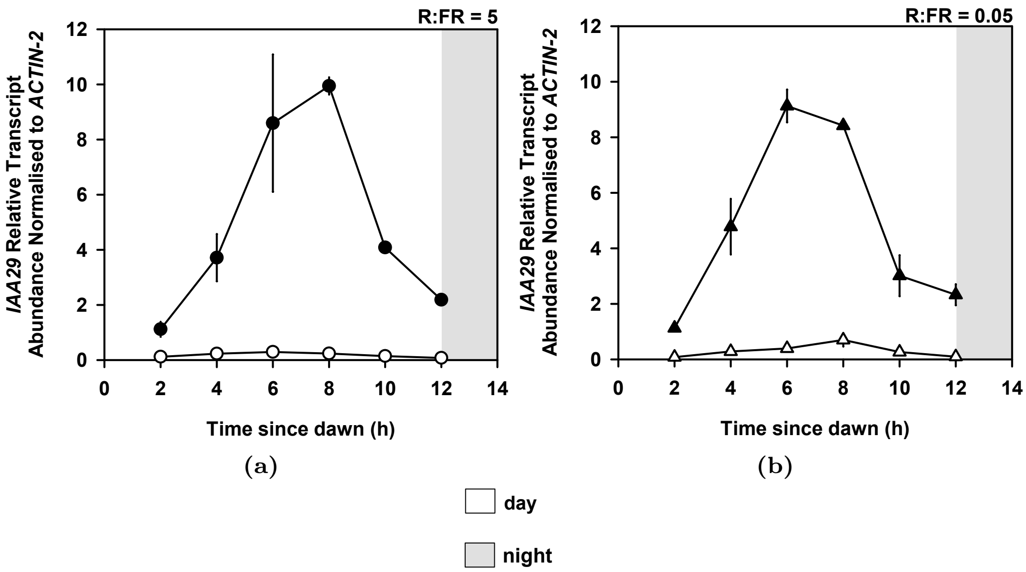

Figure 3.17: In LD, *IAA29* transcript abundance peaks 6 - 8 h after dawn and is suppressed by UV-B. L. *er* plants were grown in 5 cycles of 12L:12D in either high (3.17a) or low (3.17b) R:FR. UV-B treatments of 1.5 µmol m^{-2} s^{-1} for 2 h were carried out on 6-day-old plants. Treated plants (unfilled markers) were given a single 2 h UV-B dose at 2 h intervals and were sampled at the plotted time points alongside untreated controls (filled markers). Plotted are means +/- 1 S.E.M. of three independent experiments carried out on different occasions (n = 3).

3.3.3 PSEUDO-RESPONSE-REGULATORS may mediate the circadian gating of UV-B-induced target gene expression

Recent ChIP-seq studies on the clock's PRR transcriptional repressors (Liu et al., 2016) raise the possibility that PRRs regulate the circadian gating of *HY5*, *HYH* and *GA2ox1* through the association with G-box-like motifs within promoters. Preliminary relative transcript abundance data from mutants is consistent with this notion. Col-0, *prr5-3* and *prr7-3* plants were entrained in 12L:12D at high R:FR (5) for 6 cycles and then placed into LL for UV-B treatments and sampling. While data for *HY5* and *HYH* is inconclusive (figure 3.18b,3.18c), *GA2ox1* relative transcript abundance after UV-B treatment was clearly increased in the *prr5-3* and *prr7-3* mutants at the start and middle of the day compared to Col-0 (figure 3.18a). As the results of a single experimental repeat are reported, these preliminary data require repetition to confirm the findings. In addition, reported ChIP-seq data suggests that PRR5, PRR7 and PRR9 may act redundantly in transcriptional regulation (Liu et al., 2016), it may therefore be informative to test the *prr579* mutant for circadian gating of UV-B responses.

3.4 Discussion

The results reported in this chapter show that UV-B treatments applied at different times of a day have different magnitudes of shade avoidance inhibition. The data also suggest that the differences in effect size at different times-of-day are due to both circadian regulation through modulation of the transcriptional response to UV-B and the underlying rhythmicity of hypocotyl elongation.

Section 3.2.1 provides evidence that UV-B, both detected by- and independent of- UVR8, when given at the middle of the day, gave the greatest inhibition of hypocotyl elongation compared to UV-B in the morning or at the end of the

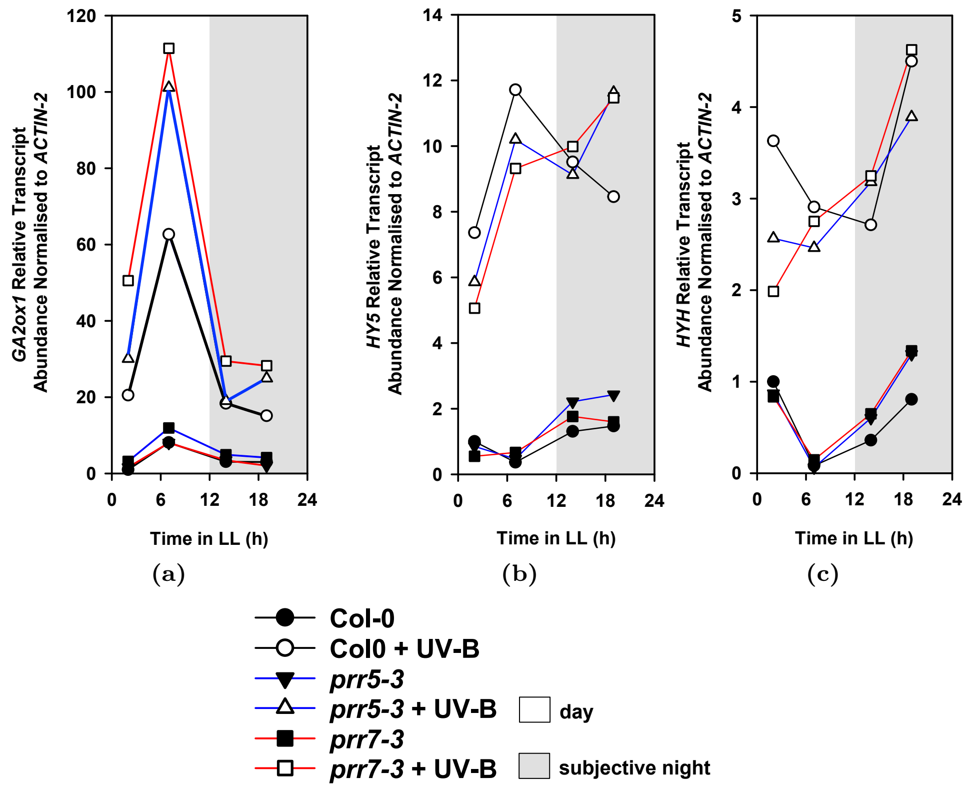

Figure 3.18: PRRs may mediate the circadian gating of UV-B responsive genes. Col-0, *prr5-3* and *prr7-3* plants were entrained in 12L:12D at R:FR = 5 for 6 cycles then placed into LL for treatments and sampling. Treated plants were given 2 h UV-B at 1.5 µmol m^{-2} s^{-1} and sampled for (3.18a) *GA2ox1*, (3.18b) *HY5* and (3.18c) *HYH* RNA abundance at the plotted times. Plotted is the relative transcript abundance of one experimental replicate (n = 1).

day. This effect is most prominent in L. *er* (figure 3.1a,3.2a) and Ws (figure 3.7a,3.8a) but is diminished in Col-0 (figure 3.3a,3.4a), which may result from natural genetic variation between ecotypes (van Zanten et al., 2009; Aukerman et al., 1997). The *uvr8-1* mutant still exhibited an inhibition of shade avoidance after UV-B treatment, which is consistent with the suggestion that there are UVR8-independent UV-B-induced hypocotyl inhibition responses, perhaps through photo-dimer accumulation (Biever et al., 2014) or the accumulation of ROS (Jenkins, 2014). The *uvr8-6* mutant, however, completely abolished the inhibition of hypocotyl elongation by UV-B and removed temporal differences in both high and low R:FR (figure 3.3b,3.4b). The observation that absence of UVR8 removed the temporal differences in effectiveness of the UV-B treatment in some, but not all cases, raises the possibility that another factor mediating the time-of-day differences in UV-B inhibition of hypocotyl elongation could be the rhythmic regulation of hypocotyl elongation rather than the UV-B signaling pathway itself.

In the *CCA1-OX* line, which has a disrupted circadian clock (Wang and Tobin, 1998), the time-of-day when UV-B most inhibited hypocotyl elongation was shifted to the final third of the day (8 - 12 h after dawn) (figure 3.6). This observation suggests that the UV-B-induced inhibition of hypocotyl elongation is subject to some form of circadian regulation. A later treatment of UV-B in *CCA1-OX* could establish an augmented level of transcriptional and post-translational inhibition of PIF4 and 5 that persists throughout the night. Plants receiving an earlier UV-B treatment, however, may have more time for PIF inhibition to return to background levels before dark, meaning that PIFs are freer to accumulate and function during night-time elongation. To investigate this hypothesis, PIF4 and PIF5 protein abundance analysis could be performed to analyse PIF stability in the hours after the three UV-B treatments at different time points. Similarly, the stability of growth-repressing DELLA proteins, which inhibit PIF activity through sequestration of PIF DNA-recognition domains (Lucas et al., 2008; Feng et al., 2008) as well as degradation (Li et al., 2016), could be affected by the time of day that the UV-B treatment is given. In addition, *CCA1-OX* plants exhibited long hypocotyls when grown under high R:FR, yet under low R:FR, hypocotyls were shorter than under high R:FR. This may be due to altered phyA activity or stability in *CCA1-OX* plants. phyA signals in low R:FR and is thought to antagonise the phyB-mediated shade avoidance response (Martínez-García et al., 2014). Salter et al. (2003) reported a small transient inhibition of hypocotyl elongation at subjective dawn by a low R:FR pulse, which they hypothesised was a phyA-mediated effect, citing circadian cycling of phyA levels to peak at dawn. Supposing that *CCA1-OX* plants have their circadian clocks paused at the morning part of the cycle, it is possible that increases in *PHYA* transcript, protein abundance and activity might be observed.

Time-course transcript abundance assays in LL confirmed that the UV-B-induction of genes involved in the inhibition of shade avoidance (Hayes et al., 2014) is gated by the circadian clock (section 3.3.1). Observations that the peaks of UV-B-induced transcript abundance differ in position (*GA2ox1* peaks at the end of the day, *HY5* at midday and *HYH* at the start of the day) between the three genes suggests that their expression may be gated to different times of day by different clock components. Additionally, in LL low R:FR, rhythms of *GA2ox1* induction by UV-B damp high (figure 3.9b), whereas rhythms of *HY5* and *HYH* induction by UV-B damp low (figure 3.10b,3.11b). Were it the same mechanism that gates the UV-B induction of *GA2ox1*, *HY5* and *HYH* transcript, then the rhythms of UV-B induction of these genes in LL low R:FR should all damp either high or low. These observations agree with the suggestion that there may be no central system for the circadian gating of UV-B responses, rather, the clock gates the expression of these genes on a *gene-by-gene* basis (Fehér et al., 2011; Takeuchi et al., 2014). There is also the possibility that the gating of *HY5*, *HYH* & *GA2ox1* transcription is modulated by direct protein interaction of HY5/HYH and a clock component (*e.g.* CCA1 has been shown to interact with HY5 in yeast (Andronis et al., 2008)), similar to the co-binding of PRRs and PIF3 to promoters to constrain its growth-promoting activity to pre-dawn (Soy et al., 2016; Martín et al., 2018). Taken together with the evidence that HY5 binds to its own promoter (Abbas et al., 2014) and in response to UV-B to drive *HY5* transcription (Binkert et al., 2014, 2016), this conjecture could provide an explanation for the gating of the UV-B response.

Surprisingly, under LL low R:FR, the circadian gating of *HY5*, *HYH* and *GA2ox1* was lost. An explanation for this observation is examined in the following chapter (5), but it was reasoned that the loss of gating may be countered by carrying out experiments in LD. Experiments in LD may also be more informative for explaining the physiology results in section 3.2 as growth in LD will also reduce any effects of phase delays and period differences that become exacerbated in LL.

In section 3.3.2, therefore, experiments were carried out in LD conditions. As predicted, rhythms of UV-B-induction for *HY5*, *HYH* and *GA2ox1* were similar in both high and low R:FR. Interestingly, the peak of UV-B-induction of *GA2ox1* occurred around the middle of the light period (6 - 8 h after dawn) (figure 3.12), which correlates with the observation that 4 h UV-B delivered around the middle of the day was most effective at inhibiting hypocotyl elongation (section 3.2). Peak *HYH* transcript abundance occurred at 2 h after dawn and declined over the course of the day, whereas *HY5* transcript did not have a clear peak, which is consistent with previous reports (Fehér et al., 2011). This result, taken together with the observation that *hy5*, *hyh* and *hy5/hyh* mutants did not have their optimal time of day for UV-B-mediated hypocotyl inhibition shifted in low R:FR (section 3.2.3), suggests that the timing of UV-B induction of *HY5* and *HYH* does not play a major role in the timing of peak *GA2ox1* induction nor the timing of the maximum sensitivity of shade avoidance hypocotyl elongation to UV-B inhibition.

PIF4 is transcribed rhythmically due to circadian regulation (Nusinow et al., 2011). In figure 3.15, *PIF4* relative transcript abundance peaked around 6 - 8 h after dawn in high R:FR and to a lower abundance in low R:FR. Lower

PIF4 expression in low R:FR compared to high R:FR may be a result of negative feedback regulation or perhaps augmented evening complex transcriptional control in low R:FR (Nusinow et al., 2011). UV-B treatment strongly reduced *PIF4* relative transcript abundance, with the greatest UV-B-induced reduction in *PIF4* transcript occurring around 6 - 8 h after dawn in high R:FR and 6 h after dawn in low R:FR. Similarly, the relative transcript abundances of a flavin mono-oxygenase gene, *YUCCA8,* which catalyses a rate-limiting step of auxin biosynthesis (Tao et al., 2008) and the auxin-response gene *IAA29* peaked at 6 h after dawn and 6 - 8 h after dawn respectively. Again, UV-B treatment strongly reduced the relative transcript abundances of these auxin-related genes. The coincidence of peak timings of UV-B induction of *GA2ox1* with maximum UV-B-induced repression of genes that promote hypocotyl elongation in section 3.3.2, may therefore explain the result that a middle-of-day (4 - 8 h) UV-B treatment gave the greatest inhibition of hypocotyl elongation in 12L:12D (section 3.2). It is intuitive that as UV-B has been shown to be such a strong inhibitor of hypocotyl elongation (Hayes et al., 2014, 2017), application at the time-of-day when elongation rate is at its greatest gives the greatest effect. It would, therefore, be informative to analyse hypocotyl elongation and its response to UV-B using time-lapse imagery to derive elongation rate. As the experiments in this chapter have been carried out under a 12L:12D regime, it would be interesting to see if the time-of-day when hypocotyl elongation is most sensitive to inhibition by UV-B shifts under different day lengths: It is well-documented that short day photoperiods (8L:16D) promote hypocotyl elongation (Niwa et al., 2009), shifting peak hypocotyl elongation rate to the end of night as the timing of peak PIF abundance is moved into the night when PIFs are not targeted by active photoreceptors (Nozue et al., 2007).

In conclusion, the data reported in this chapter present evidence that the inhibition of hypocotyl elongation by UV-B is gated by the circadian clock such that UV-B applied at different times-of-day elicit different magnitudes of response. It appears that both UV-B up-regulated genes and the pathways that promote elongation, which UV-B signaling antagonises, are subject to rhythmic regulation by the circadian clock as well as R:FR. It is, therefore, possible that the underlying rhythmic regulation of hypocotyl elongation is the main influence for time-of-day sensitivity of the hypocotyl to UV-B inhibition. While the data presented here are broadly consistent with the findings that genes up-regulated by UV-B are circadian gated (Fehér et al., 2011; Takeuchi et al., 2014), preliminary data are also presented which suggests the involvement of the PRR family of transcriptional repressors in the circadian regulation of the previously identified UV-B-induced shade avoidance antagonist, *GA2ox1* (Hayes et al., 2014). Future study of the circadian gating of UV-B responses should, therefore, examine the transcriptional (Liu et al., 2016) and possibly post-translational (Martín et al., 2018) role that the PRRs may have in the modulation of responses to UV-B.

Chapter 4

The Effect of UV-B Supplementation on Shade-Avoiding *Coriandrum sativum*

4.1 Introduction

Coriander (*Coriandrum sativum*) is one of the United Kingdom's best-selling culinary herbs, and for Vitacress Herbs Ltd (the UK's largest fresh herb supplier) it is the top selling herb, with sales exceeding £18 million in 2015[1]. Maintaining high standards of product quality is expensive and can lead to the rejection of many plants before they get to retail. The production of aesthetically pleasing, compact and dark green plants is a key objective for the potted herb industry.

In commercial glasshouses, Coriander is often planted densely with around 60

[1] http://www.vitacress.com/news-centre/herb-sales-boost;-Coriander-remains-top-seller/

seedlings per pot (Simon Budge (Vitacress), *pers. comm.*). Crowded conditions can promote shade-avoidance, which may contribute to Coriander's elongated phenotype. In natural conditions, plants are exposed to UV-B radiation from sunlight. UV-B has previously been shown to limit the elongation of hypocotyls and petioles in both shade avoidance and thermomorphogenesis (Hayes et al., 2014, 2017). However, many materials used in glasshouse construction such as glass or clear acrylic attenuate or completely filter out UV-B radiation. Thus, plants growing in glasshouses may not be receiving this natural brake on elongation that they would be receiving outdoors and such a situation could further exacerbate stem elongation driven by shade avoidance.

An emerging area of research is the manipulation of light quality in commercial growth environments (Wargent, 2016; Thomas T.T. and Puthur, 2017). Red, blue, green and yellow LEDs have been used to control the architecture and antioxidant content of sweet basil (Carvalho et al., 2016) and Coriander (Naznin et al., 2016). Manivannan et al. (2015) showed that red and blue LED lights could enhance the antioxidant capacity of Chinese floxglove while another study found that blue LEDs enhanced proline accumulation and the activity of antioxidant enzymes such as super oxide dismutase (SOD) in tomato (Kim et al., 2013). Reactive oxygen species (ROS) such as superoxide anion radicals and hydrogen peroxide are produced by the human body as products of normal cellular functions (Orient et al., 2007). The effects of ROS on human health are mixed, in some instances, low-level oxidative stress can be beneficial (Pizzino et al., 2017). However, a large body of evidence has linked ROS imbalances to neuro-degenerative diseases such as Alzheimer's and Parkinson's (Uttara et al., 2009) as well as numerous forms of cancer (Liou and Storz, 2010). Consumption of antioxidants can protect the human body from the effects of destructive ROS free radicals and as most dietary antioxidants are derived from plants, it follows that increasing the antioxidant capacity of crops could have appreciable health benefits (Dou et al., 2017). There have also been a number studies that have manipulated UV-B levels. Mazza et al. (2013) showed that in the

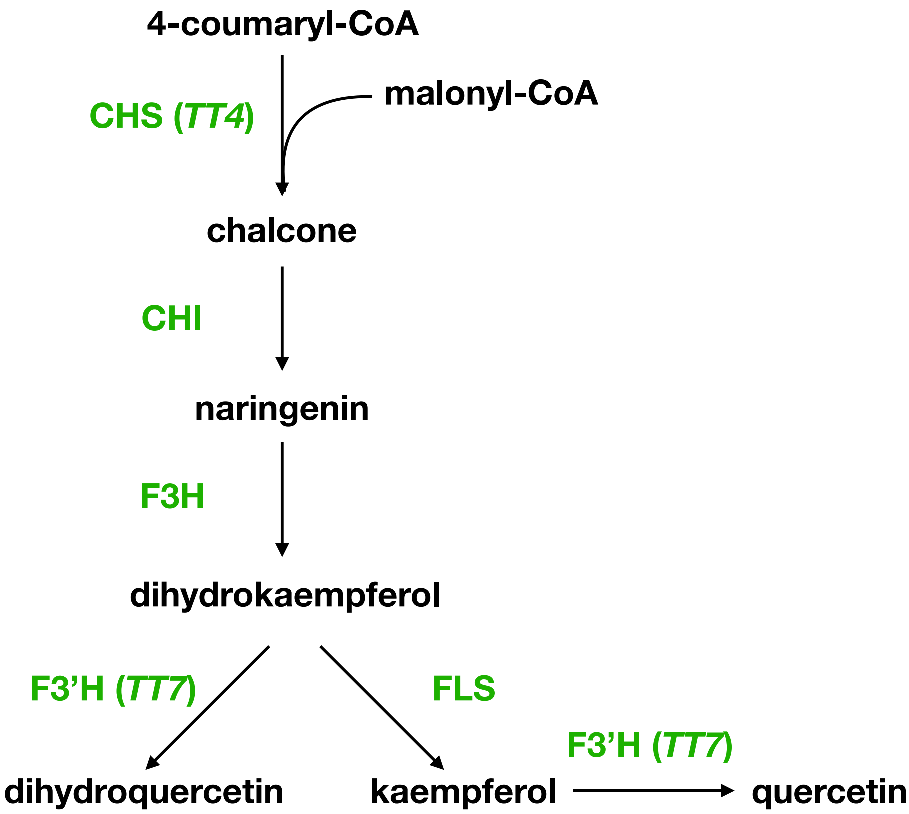

Figure 4.1: Simplified schematic of a section of the Arabidopsis flavonoid biosynthesis pathway. Enzymes are highlighted in green, with encoding genes included for CHS and F3'H. Figure adapted from Winkel-Shirley (2001).

field, solar UV-B irradiation increased soybean crop yield through reduced insect herbivory. Another study found that post transplantation to field, UV-B pre-treated lettuce produced greater harvestable yield than lettuce grown in a UV-B-excluding environment (Wargent et al., 2011). UV-B supplementation has been shown to increase leaf area, biomass, antioxidant capacity and chlorophyll content of sweet basil (Sakalauskaite et al., 2012). The most extensively studied response to UV-B in plants is flavonoid biosynthesis (Caldwell et al., 1983; Lois, 1994). Flavonols are among the most abundant plant flavonoids, they absorb UV light in the 280-320 nm waveband and thus act as a sunscreening filter for UV-B . In Arabidopsis, it has been shown that low dose UV-B strongly upregulates the expression of key enzymes in the flavonoid biosynthesis pathway (figure 4.1) such as CHALCONE SYNTHASE (CHS) (Fuglevand et al., 1996;

Jenkins et al., 2001). The accumulation of flavonols has both potential health benefits (Yao et al., 2004) and impacts on plant flavour (Roland et al., 2013). In Coriander, high dose narrowband UV-B has been shown to induce chomosomal abnormalities while decreasing pigment and carbohydrate content (Kumar and Pandey, 2017). However, the impact of low dose, non-stressful levels of UV-B on Coriander development remains relatively unstudied.

This chapter describes experiments carried out in collaboration with Vitacress Herbs Ltd. The main aim was to investigate if UV-B supplementation could improve Coriander product quality by promoting a more compact growth habit and the accumulation of desirable metabolites. Another objective was to test if there were an optimal time of day to deliver a UV-B dose to Coriander to achieve improvements in plant architecture. Temporally targetting a short UV-B dose (rather than continuous UV-B irradiation) to a time of day when the crop is most sensitive in a commercial glasshouse could reduce costs related to energy consumption, as well as limiting the exposure of glasshouse workers to potentially harmful UV-B radiation. What follows is an analysis of the effects of low dose, non-stressful levels of UV-B on Coriander architecture, pigment and antioxidant content in controlled climate chambers and glasshouse trials.

Most of the data in this chapter are published in a peer reviewed journal:

Fraser, D.P., Sharma, A., Fletcher, T., Budge, S., Moncrieff C., Dodd, A.N., Franklin, K., 2017. UV-B antagonises shade avoidance and increases levels of the flavonoid quercetin in coriander (Coriandrum sativum). Scientific Reports, 7(1), p.17758.

4.2 Coriander germination

To control for plant developmental stage it is favourable to have synchronous germination of plants for laboratory experiments. Established germination and seed sterilisation protocols for Arabidopsis (Weigel and Glazebrook, 2002) led to asynchronous germination in Coriander over the course of 7 to 14 days. Even

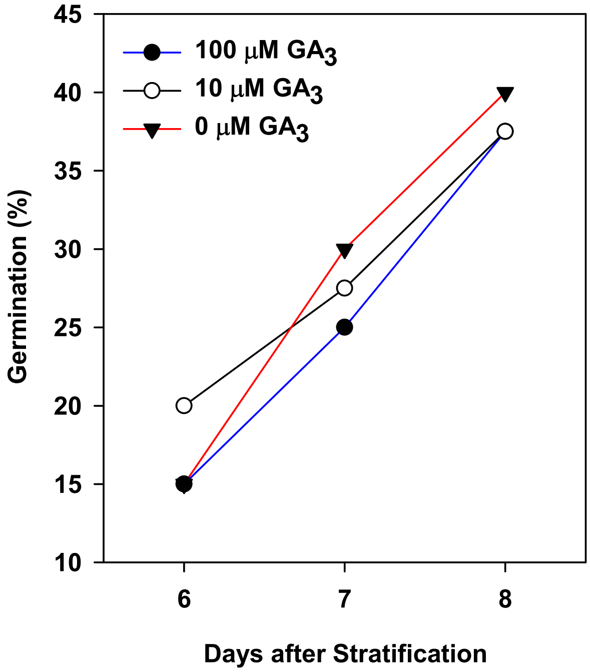

Figure 4.2: Coriander germination is insensitive to GA_3. Stratified Coriander seeds were imbibed in three different concentrations of GA_3 in water as indicated in the figure.

with stratification, within-fruit germination was asynchronous. Gibberellic Acid (GA_3) is well documented for breaking dormancy in many species (reviewed in Miransari and Smith (2014)). In a pilot experiment where Coriander seeds were imbibed in different concentrations of GA_3, Coriander appeared to be insensitive to GA_3 treatment (figure 4.2), which is consistent with observations from the commercial glasshouse (Simon Budge (Vitacress), *pers. comm.*). Rather than optimising a protocol for breaking dormancy, germination was synchronised through scarification, imbibition in H_2O and manual selection for potting on as described in 2.2.1.

4.3 Supplemental UV-B antagonises shade-avoidance in Coriander

4.3.1 UV-B inhibits hypocotyl elongation in shade-avoiding Coriander

Coriander seedlings were grown under high (5) and low (0.05) R:FR ratio conditions in 12 hour light 12 hour dark photocycles with and without UV-B supplementation (figure 4.3a,4.3b). Seedling hypocotyls were measured 13 days after germination. Plants grown in low R:FR ratio achieved by supplementing white light with far red LEDs (WL + FR) were significantly elongated when compared to plants grown in high R:FR ratio white light (WL), showing that Coriander displays shade avoidance (Fraser et al., 2016) (figure 4.3b). Coriander seedlings supplemented with low intensity (1.5 µmol m^{-2} s^{-1}) UV-B in a background of high R:FR (WL + UV-B) were not significantly different compared to WL controls. However, hypocotyl lengths of UV-B treated Coriander in a low R:FR ratio background (WL + FR + UV-B) were significantly shorter than Coriander grown in WL + FR, similar to responses observed in Arabidopsis (Hayes et al., 2014) (figure 4.3b). The addition of low dose UV-B only had a significant effect in low R:FR grown plants, which suggests that UV-B mediated effects on Coriander hypocotyl elongation may only be observed in crowded conditions.

Different Coriander cultivars exhibit different stem-elongation phenotypes

In this study, the magnitude of shade avoidance was cultivar-dependent. Slow Bolt is a variety of Coriander that has been the industry standard, characterised by its long time to flowering, distinctive aroma and superior flavour. However, a new variety, Cruiser, is now being widely grown by horticulturalists and this recently developed cultivar is described as:

> "... *a new variety of Coriander particularly distinguished by its*

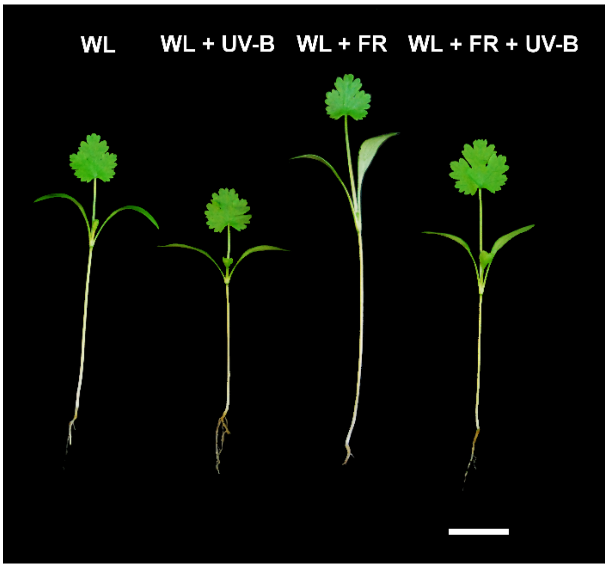

(a)

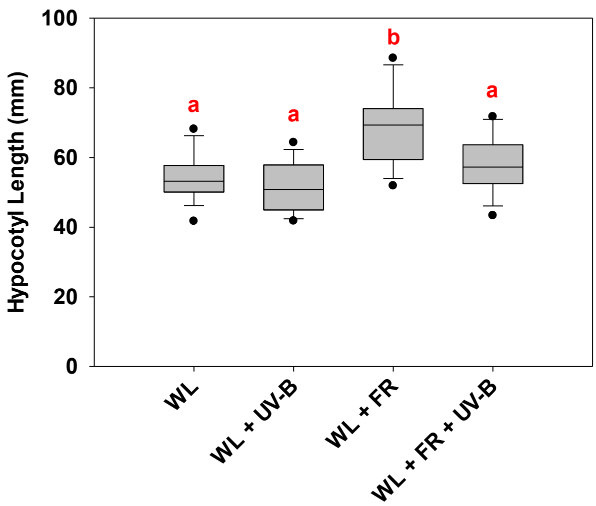

(b)

Figure 4.3: UV-B inhibits hypocotyl elongation in shade-avoiding Coriander. (4.3a) Coriander were germinated in WL for 3 days and then placed into WL, WL + UV-B, WL + FR & WL + FR + UV-B conditions as indicated for a further 10 days. Scale bar = 20mm. (4.3b) Coriander Hypocotyl Lengths (mm) as grown in 4.3a ANOVA (F(3,60) = 13.865 $p < 0.001$) n = 16. Different red Letters indicate statistically significant differences by Tukey's post hoc test at $p<0.05$.

> *slow bolting, large round leaves with bright, shiny, dark green color and fewer serrated margins, a distinctive upright, but basal branching habit, long shelf life and good vigour indexing...*" (Shrestha and Warren, 2016)

Both the Slow Bolt and Cruiser cultivars displayed elongated hypocotyls in WL + FR compared to WL controls, though hypocotyl lengths for Slow Bolt were significantly longer than Cruiser in WL + FR (figure 4.4). UV-B supplementation at 1.5 μmol m^{-2} s^{-1} inhibited low R:FR-induced hypocotyl elongation of both cultivars, though again the Slow Bolt cultivar displayed significantly longer hypocotyls compared to Cruiser. Due to its enhanced elongation phenotype in low R:FR ratio conditions, the Slow Bolt cultivar was used for subsequent experiments.

4.3.2 UV-B supplementation increases compactness of mature shade avoiding Coriander

Seedling phenotypes can be a reasonable predictor of mature plant phenotypes, so the effect of low R:FR and UV-B on mature Coriander plant phenotypes were also examined. Coriander plants were grown until they were 28 days old, a developmental stage when they produce multiple petioles with variable leaf phenotypes, and a similar age to commercially grown Coriander when it is transported to customers (figure 4.5).

Shade-avoiding Arabidopsis has been shown to produce fewer and smaller leaf blades when compared to controls as resources are diverted toward elongation (Nagatani et al., 1991; Finlayson et al., 2010). In addition, Hayes et al. (2014) reported a complex interaction where low R:FR and UV-B delivered separately inhibit leaf expansion, but low R:FR in a background of UV-B promotes leaf expansion in a UVR8-dependent manner. The effect of these light signals on Coriander leaf morphology and production was assessed through comparison of total visible leaf area in plants grown in high and low R:FR, with and without

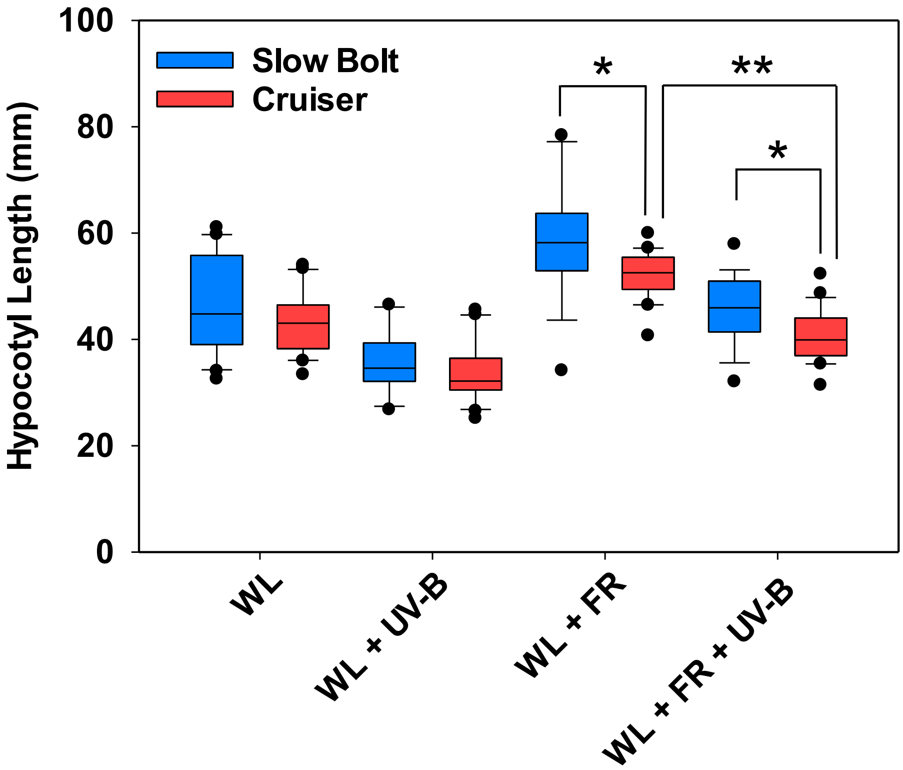

Figure 4.4: Hypocotyl elongation in different Coriander cultivars. 'Slow Bolt' (Blue) and 'Cruiser' (Red) were germinated and grown as in Figure 4.3. n = 18 – 21 seedlings. Student's T-tests were performed to test for differences between cultivars in the indicated conditions. * indicates significant difference between cultivars at $p < 0.05$. WL + FR ($t(37) = 2.624$, $p = 0.0126$), WL + FR + UV-B ($t(38) = 2.541$, $p = 0.0153$). ** indicates significant difference between WL + FR and WL + FR + UV-B in the Cruiser Cultivar at $p < 0.05$ ($t(39) = 7.988$, $p < 0.001$).

UV-B supplementation. WL- and WL + UV-B-treated plants did not differ significantly in their total visible leaf areas, whereas WL + FR-treated plants had significantly reduced total visible leaf area when compared to other treatments. WL + FR + UV-B-treated plants were not significantly different to either groups, being rather variable and lying between them (figure 4.6a). Each petiole has varying numbers of leaf blades, so it follows that total visible leaf area could be linked to the number of petioles. WL + FR-treated plants had a significantly reduced petiole count compared to plants grown in WL and WL + UV-B. WL + FR + UV-B-grown plant petiole counts did not differ significantly from the other groups, lying between WL and WL + FR-grown plants (figure 4.6b). Thus, UV-B did not significantly increase total visible leaf area or petiole number in either R:FR ratio. UV-B-treated plants did, however, appear more compact, which was reflected in the lengths of the longest petioles. WL + UV-B-treated plants did not significantly differ from WL controls, yet the significantly elongated petioles of WL + FR treated plants were significantly reduced by supplemental UV-B (figure 4.6c). In order to give a measure of plant *compactness*, the ratio between total visible leaf area and total petiole lengths (that is, a *leaf blade to stalk ratio*) was analysed. This comparison showed that plants grown in WL + FR had a significantly reduced leaf blade to stalk ratio compared to plants grown in WL and that the addition of UV-B to the low R:FR condition significantly increased this parameter, but not sufficiently to return to the level of high R:FR-grown plants (figure 4.6d).

Taken together, light quality has dramatic effects on Coriander architecture. A low R:FR ratio drives elongation of hypocotyls in seedlings and elongation of petioles in adult plants, both of which are inhibited by UV-B. On the other hand, the reduction in leaf area and number of petioles caused by low R:FR were not significantly alleviated by UV-B. Nevertheless, UV-B treated plants (WL + FR + UV-B) were still more compact than their low R:FR (WL + FR) controls as demonstrated by the ratio of total visible leaf area to total petiole lengths.

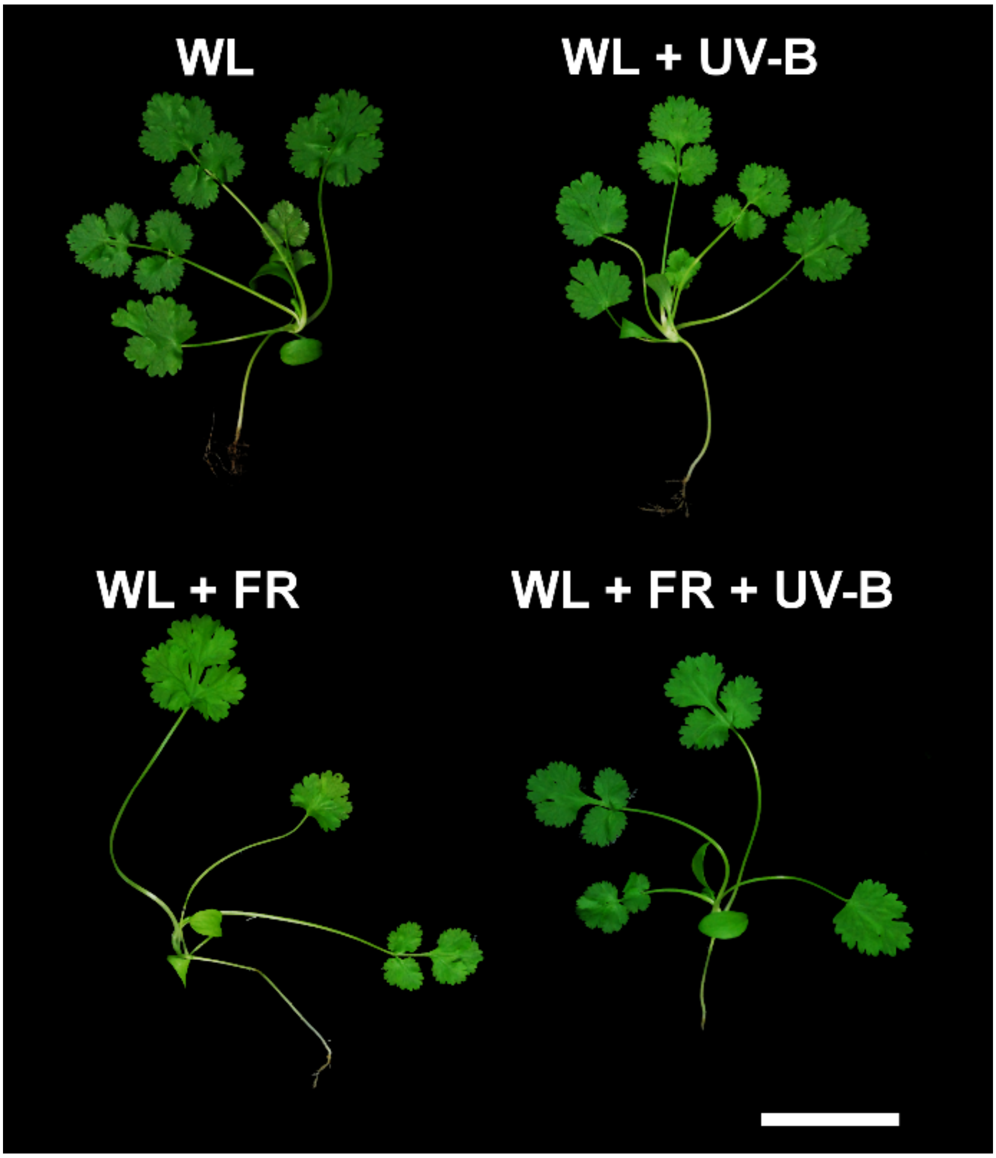

Figure 4.5: Phenotypes of 28-day-old Coriander (Slow Bolt) grown in 12h photoperiods. Seedlings were germinated in WL for 3 days and then placed into WL, WL + UV-B, WL + FR & WL + FR + UV-B conditions as indicated for a further 25 days. Scale bar = 50 mm

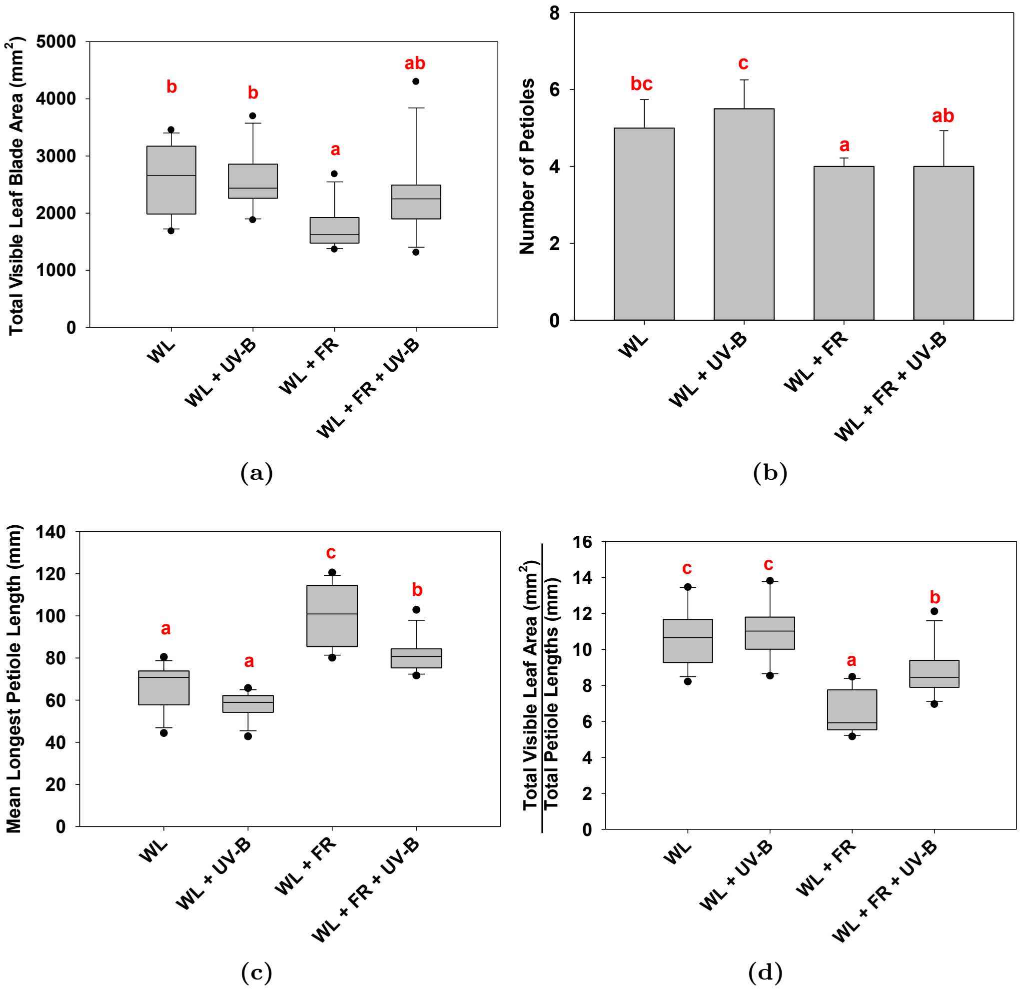

Figure 4.6: UV-B inhibits petiole elongation but does not significantly increase leaf blade area or number of petioles in mature shade-avoiding Coriander. Morphological data were gathered from 28-day-old Coriander grown as in Figure 4.5. (4.6a) Total Visible Leaf Blade Area, ANOVA ($F(3,44) = 5.696$, $p = 0.002$. (4.6b) Number of Petioles, Median +/- 1 S.D., ANOVA ($F(3,44) = 19.319$, $p < 0.001$). (4.6c) Mean Longest Petiole length, ANOVA ($F(3,44) = 32.694$, $p < 0.001$ (4.6d) Ratio of Total Visible Leaf Area to Total Petiole Lengths, ANOVA ($F(3,44) = 25.926$, $p < 0.001$. $n = 12$. Different Letters indicate statistically significant differences by Tukey's post hoc test at $p<0.05$.

4.4 Is there an optimum time of day for UV-B-mediated inhibition of shade avoidance in Coriander?

Considering that greenhouse materials such as glass or clear acrylic filter UV-B radiation, the data described in section 4.3 indicate that supplementation with UV-B could be a way of improving the compactness and hence the aesthetic quality of Coriander in commercial glasshouse settings. However, UV-B exposure may present health and safety concerns for workers and continuous illumination would not be economically or environmentally favourable. In Arabidopsis it has previously been shown that aspects of the UVR8 signalling pathway are gated by the circadian clock, seemingly on a *"gene-by-gene basis"* (Fehér et al., 2011). Thus, there could be a time-of-day when plants are most sensitive to UV-B for the inhibition of elongation, which may give the opportunity to deliver UV-B for short doses yet still give meaningful effects on physiology. For Vitacress, this could be a solution that improves Coriander product quality while limiting workers' risk of exposure to harmful UV-B radiation and reducing economical and environmental costs associated with energy usage.

4.4.1 Coriander hypocotyl elongation rate is rhythmic in light/dark cycles

The rate of hypocotyl elongation in Arabidopsis is rhythmic; in continuous light the peak rate occurs at c. 8h after subjective dawn whereas in short days (8 h light : 16 h dark) it peaks at the end of the night (Nozue et al., 2007). The mechanistic basis for rhythmic hypocotyl growth has been described by an external coincidence model (Nozue et al., 2007).

To analyse growth rate in Coriander, infra-red time-lapse photography was employed (figure 4.7). As before (section 4.3.1), UV-B supplementation clearly inhibited elongation in backgrounds of WL and WL + FR (figure 4.7a,4.7b). Similar to Arabidopsis, Coriander displayed rhythmic hypocotyl elongation. The daily peak of elongation rate for Coriander in all tested conditions tended to occur during the light period (figure 4.7c,4.7d), this is likely to result from growth in 12 h light, 12 h dark cycles. Peak elongation rate in the WL + FR condition occured around the middle of the day and the plants supplemented with UV-B in a low R:FR background clearly had this peak curtailed (figure 4.7d). Taken together these data suggest that the major time to target for UV-B inhibition of hypocotyl elongation is during the light period. Doing so avoids giving monochromatic UV-B during the night period, an unrealistic condition that would not be experienced in nature that may have effects (*e.g.* on entrainment (Fehér et al., 2011)) that are difficult to predict and interpret.

4.4.2 Short doses of UV-B at different times of day marginally affects the magnitude of inhibition of shade avoidance

A single short (4 h) 1.5 µmol m^{-2} s^{-1} UV-B treatment given at three different times-of-day to three separate groups of shade-avoiding Coriander (0-4 h, 4-8 h, 8-12 h) was sufficient to significantly inhibit hypocotyl elongation compared to the WL + FR-grown control (figure 4.8). The timing of treatments, however, had only marginal effects on response magnitude: The 8-12 h treatment resulted in the greatest decrease in mean hypocotyl length (17% decrease), followed by UV-B treatment at the start of day (13% decrease), while the treatment given at the middle of the day was least effective (8% decrease). Unsurprisingly, the 12 h UV-B treatment (for the length of the photoperiod) resulted in the shortest hypocotyls (25% shorter), indicating that the total UV-B dose is the most important factor for mediating the inhibition of shade avoidance.

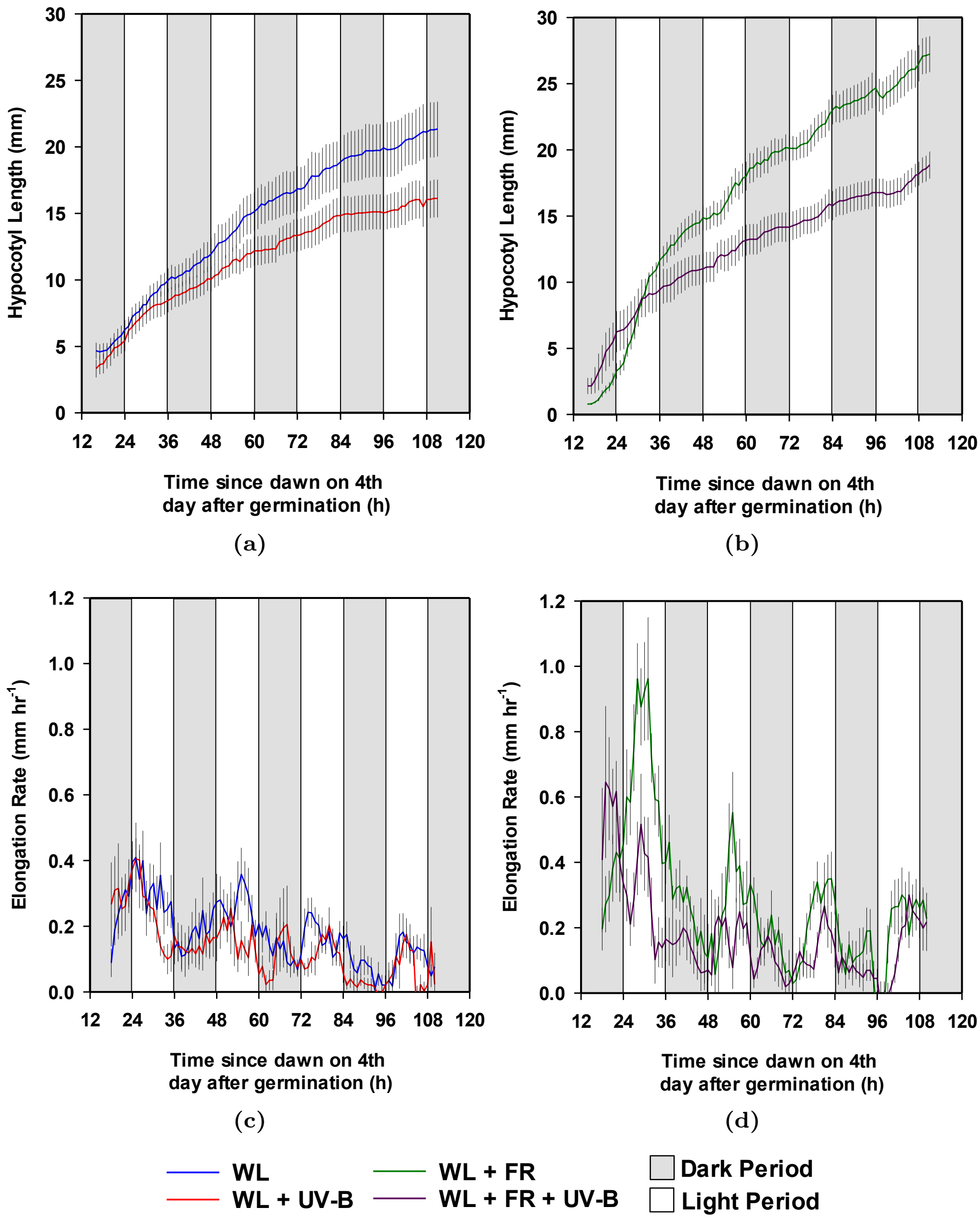

Figure 4.7: Shade-avoiding Coriander exhibits rhythmic hypocotyl growth, which is suppressed by UV-B. Coriander were germinated in WL for 3 days then placed into the indicated conditions for timelapse IR photography. Hourly hypocotyl length and growth rate of Coriander in WL (4.7a,4.7c) and WL + FR (4.7b,4.7d) n = 8 +/- 1 S.E.M.

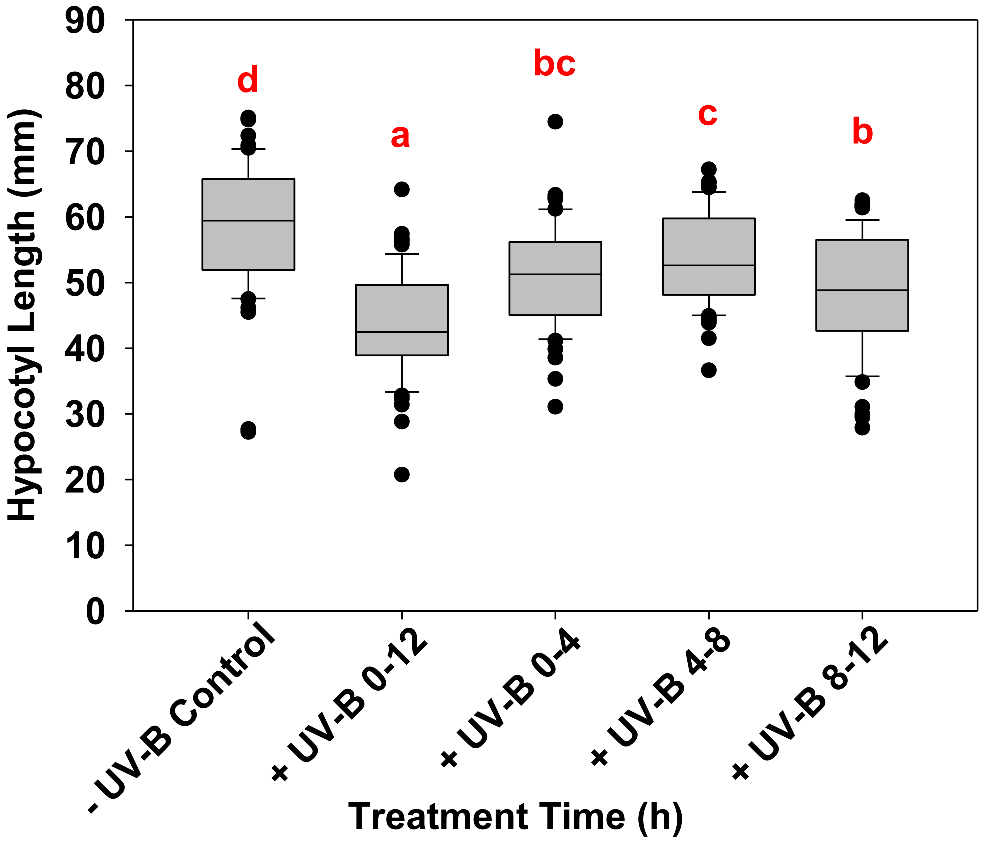

Figure 4.8: The timing of UV-B supplementation is unimportant for inhibition of shade-avoidance. Coriander were germinated in WL for 3 days and then placed into WL + FR & WL + FR supplemented with UV-B at the indicated times for a further 10 days. n = 57-61. ANOVA ($F(4,288) = 25.484$, $p < 0.001$) Different Letters indicate statistically significant differences by Tukey's post hoc test at $p<0.05$.

	PAR 400-700 nm (µmol m^{-2} s^{-1})	R:FR ratio
Glasshouse	421	1.34
Glasshouse Canopy	192	0.86
Growth Cabinet	70	5
Growth Cabinet Shade	70	0.05

Table 4.1: A summary of typical PAR and R:FR ratio measurements in glasshouse and growth cabinet lighting from this study.

4.5 Supplemental UV-B inhibits Coriander stem elongation in greenhouse environments

As would be expected, the light spectra given by fluorescent bulbs in growth cabinets differs greatly from natural light in the glasshouse in its quality and quantity (figure 4.9 and table 4.1). In addition, the R:FR ratio measured in dense stands within the Coriander canopy was less extreme than the treatments provided in the growth cabinets (table 4.1). Due to the substantial differences between light conditions in artificial versus natural light conditions, it is prudent to assess the effectiveness of UV-B supplementation for the manipulation of Coriander architecture in commercial glasshouses. Plants were exposed to sunlight levels of PAR, which ranged from 60 to > 800 µmol m^{-2} s^{-1} depending on time of day and cloud cover. A minimum PAR of 165 µmol m^{-2} s^{-1} and 16 h photoperiods were maintained using supplementary fluorescent lamps (Plug and Grow compact 200 W). UV-B supplementation was provided using Philips TL100W/01 narrow band UV-B bulbs.

4.5.1 The UV-B-mediated inhibition of Coriander hypocotyl elongation in the glasshouse is density-dependent

When planted at a density of 1 seedling per 16 cm^2, *i.e.* one seedling per pot, UV-B supplementation did not have a significant effect on hypocotyl length whether given for the length of the day (16 h) or for just 4 h at midday when

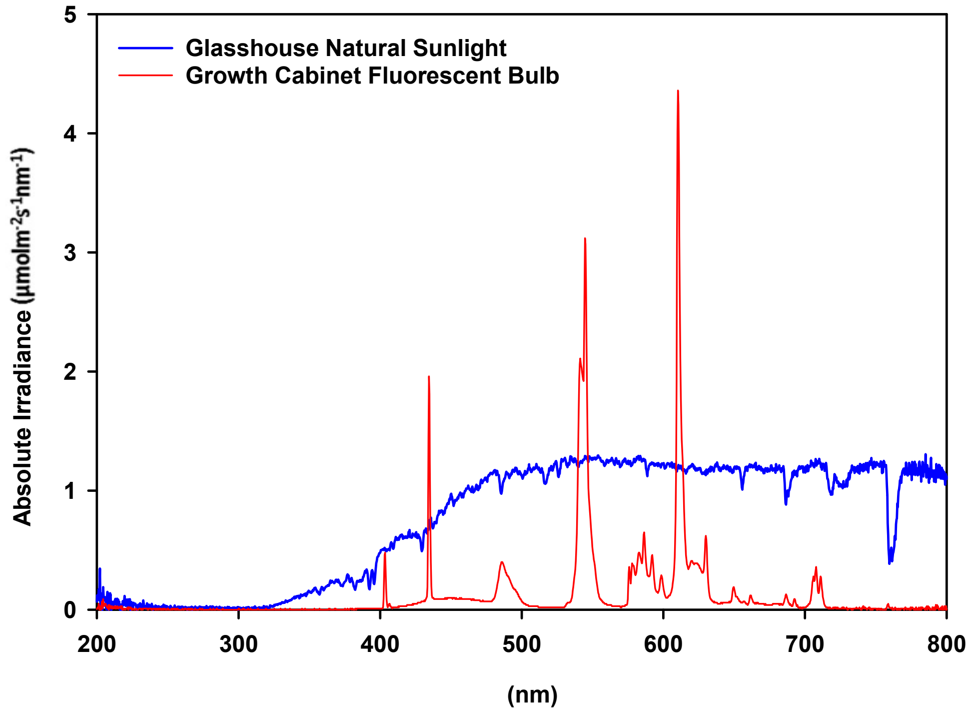

Figure 4.9: Typical light spectra traces in glasshouse and growth cabinet lighting.

compared to control seedlings (figure 4.10). Interestingly, when seedlings were planted at a higher density of 4 seedlings per 10 cm^2 (approaching the density that they are grown at Vitacress), 4 h UV-B supplementation at midday was sufficient to significantly inhibit hypocotyl elongation (figure 4.11), though giving a longer UV-B treatment for the duration of the photoperiod (16 h) had a greater effect (figure 4.11). These observations are consistent with previous data that showed UV-B supplementation to have an effect on hypocotyl elongation only under low R:FR ratio (simulated crowding) conditions (section 4.3).

When Coriander plants were grown for 32 days in the glasshouse, 4 h and 16 h UV-B treatments were similarly effective in inhibiting of hypocotyl elongation (figure 4.12a). However, significant inhibition of petiole elongation was only found in plants treated with the longer (16 h) UV-B treatment (figure 4.12b).

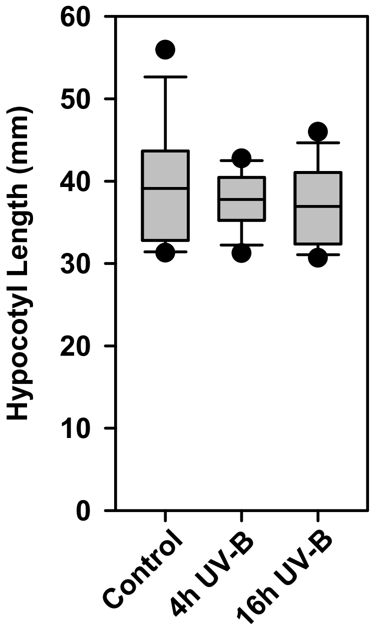

Figure 4.10: UV-B supplementation did not inhibit the hypocotyl elongation of seedlings in the glasshouse when grown at low density. Coriander seedlings were grown for 10 days with 16h photoperiods maintained with supplemental white light bulbs. UV-B was provided by narrow band UV-B bulbs for either the entire photoperiod (16 h) or for 4 h at the middle of the day. 1 seed 16 cm^{-2}, n = 12, ANOVA ($F(2,33) = 0.656$, $p = 0.526$).

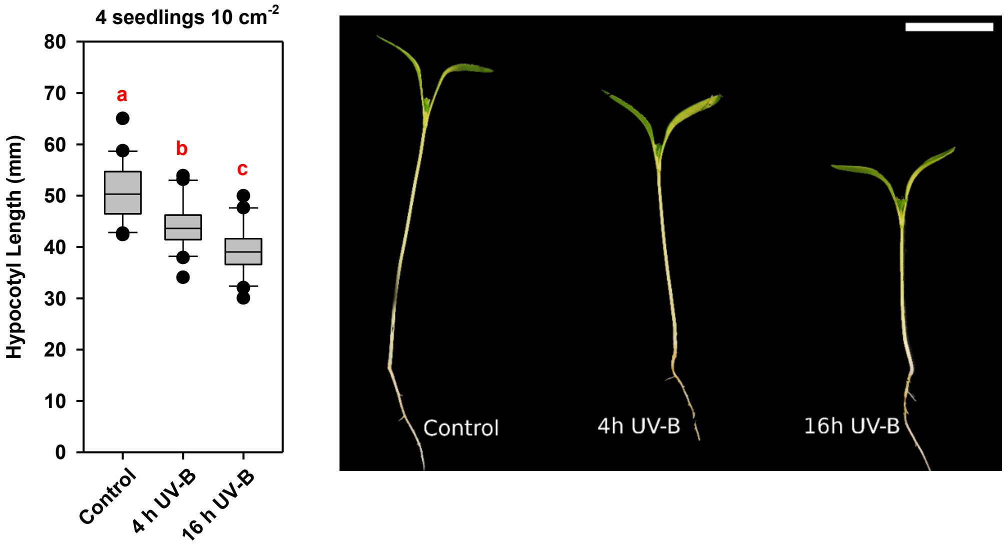

(a) (b)

Figure 4.11: UV-B supplementation inhibited hypocotyl elongation of seedlings in glasshouses when grown at high density. Coriander seedlings were grown for 10 days with 16h photoperiods maintained with supplemental white light bulbs. UV-B was provided by narrow band UV-B bulbs for either the entire photoperiod (16 h) or for 4 h at the middle of the day. (4.11a) Shared pots at a density of 4 seedlings 10 cm^{-2}, n = 20, ANOVA ($F(2,57) = 23.106$, $p < 0.001$), different letters indicate statistically significant differences by Tukey's post hoc test at $p < 0.05$. (4.11b) Phenotype of representative seedlings. Scale bar = 20 mm.

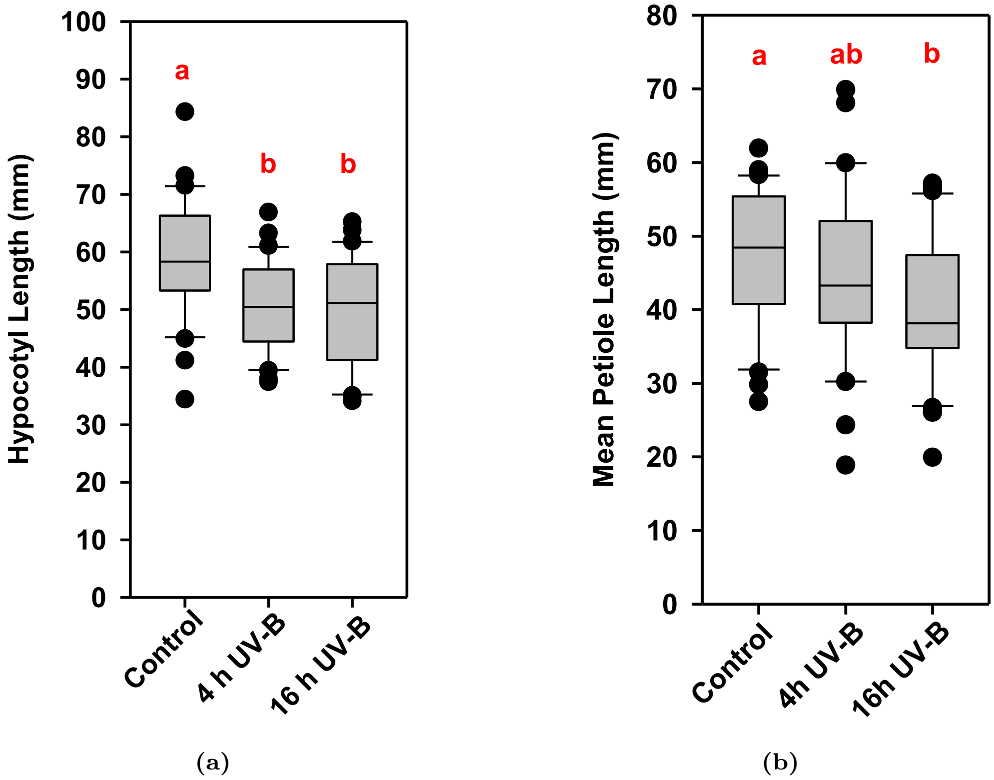

Figure 4.12: UV-B inhibited mean petiole elongation in mature Coriander grown at high density (4 seedlings 10 cm^{-2}) in the glasshouse. Coriander was grown for 32 days with 16 h photoperiods maintained with supplemental white light bulbs. UV-B was provided by narrow band UV-B bulbs for either the entire photoperiod (16 h) or for 4 h at the middle of the day. Plotted are morphological data from 32 day old plants 4.12a Hypocotyl Lengths, ANOVA ($F(2,87) = 8.551$, $p < 0.001$). 4.12b Mean Petiole Length ANOVA ($F(2,87) = 4.015$, $p = 0.021$). N = 30. Different red letters indicate statistically significant differences at $p < 0.05$.

4.5.2 Varying the intensity of UV-B irradiance did not significantly vary the magnitude of hypocotyl elongation inhibition in the Vitacress Glasshouse

On site experiments were conducted in the trial area of the Vitacress Runcton glasshouses to investigate the application of knowledge to a commercial horticulture setting. Potted Coriander were taken direct from the production line at 7 days after potting and placed in the experimental conditions. As before, plants were exposed to sunlight levels of PAR, which ranged from 60 to $>$ 800 µmol m^{-2} s^{-1} depending on time of day and cloud cover, but a minimum PAR of 200 µmol m^{-2} s^{-1} and 16 h photoperiods were maintained using supplementary fluorescent lamps. UV-B supplementation was provided using Philips TL100W/01 narrow band UV-B bulbs.

PAR over the course of the experiment was highly variable due to cloud cover and the height of the sun. It has been shown in numerous studies that modulation of PAR (400-700 nm) alters the sensitivity of plant responses to UV-B (reviewed in Krizek (2004), who noted that "*In general, one observes a reduction in total biomass and plant height with decreasing PAR and increasing UV-B.*"). Thus, the ratio of UV-B : PAR, which would be artificially high in laboratory experiments compared to the field due to technical limitations of the growth cabinets, could be important for the magnitude of inhibition of shade avoidance in Coriander. Three different intensities of UV-B corresponding to low (1 µmol m^{-2} s^{-1}), medium (2 µmol m^{-2} s^{-1}) and high (3 µmol m^{-2} s^{-1}) were trialled. After 10 days all three UV-B intensities had significantly inhibited hypocotyl elongation, however between the different intensities there was no significant difference, suggesting that UV-B at 1 µmol m^{-2} s^{-1}could be just as effective as 3 µmol m^{-2} s^{-1} at inhibiting hypocotyl elongation in the glasshouse (4.13).

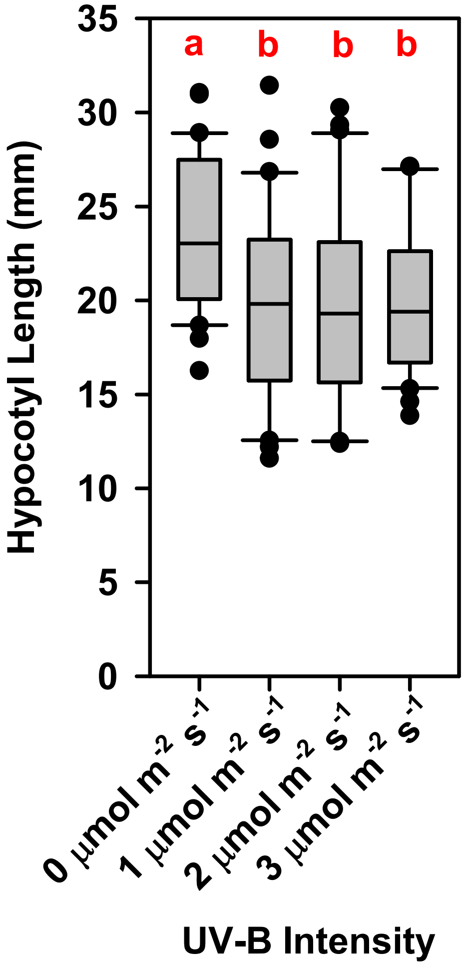

Figure 4.13: The magnitude of UV-B-mediated inhibition of hypocotyl elongation in the glasshouse is not dependent on UV-B intensity. Supplemental UV-B was delivered for the length of the photoperiod (16h, maintained by incandescent bulbs in the Vitacress glasshouse). Three intensities of UV-B irradiation were given, corresponding to low (1 µmol m^{-2} s^{-1}), medium (2 µmol m^{-2} s^{-1}) and high (3 µmol m^{-2} s^{-1}) doses for 10 days. ANOVA ($F(3,116) = 4.933$, $p = 0.003$), n = 30 different red letters indicate statistically significant differences by Tukey's post hoc at $p < 0.05$.

4.6 UV-B and R:FR effects on Coriander chlorophyll and phytonutrient content

4.6.1 R:FR ratio and UV-B treatment have no significant effect on leaf chlorophyll abundance

An objective for the potted herb industry is the production of aesthetically appealing products with dark green leaves. As it has been previously reported that R:FR ratio and UV-B irradiation can have impacts on chlorophyll abundance (Bartoli et al., 2009) and photosynthetic efficiency (Davey et al., 2012), the leaf blade chlorophyll content of plants grown in WL, WL +UV-B, WL +FR and WL +FR + UV-B were quantified using the Witham et al. (1971) method. In the tested conditions neither R:FR ratio nor UV-B treatment significantly affected chlorophyll content in the leaf blades of 28-day-old Coriander (figure 4.14).

4.6.2 UV-B elevates leaf antioxidant capacity

Early studies of plant responses to UV-B explored its role as a stressor that causes damage to DNA and tissues through photodimer formation and oxidative stress in photosynthetic machinery (Jansen et al., 1998). Due to the recovery of the Earth's stratospheric ozone layer since the Montreal protocol (Strahan and Douglass, 2018), concerns about the effects of high intensity UV-B have lessened, with recent experiments testing the hypothesis that UV-B signalling acts as an acclimating "eustress" that activates antioxidant defences prior to the onset of oxidative pressures caused by exposure to high "distress" levels of UV-B (Hideg et al., 2013; Czégény et al., 2016a,b).

Total antioxidant capacity was assayed in leaf blades from 28-day-old Coriander that had been grown under supplemental UV-B at high and low R:FR ratio. In high R:FR, plants treated with UV-B displayed significantly greater total antioxidant capacity compared to plants grown just under WL (figure 4.15). As

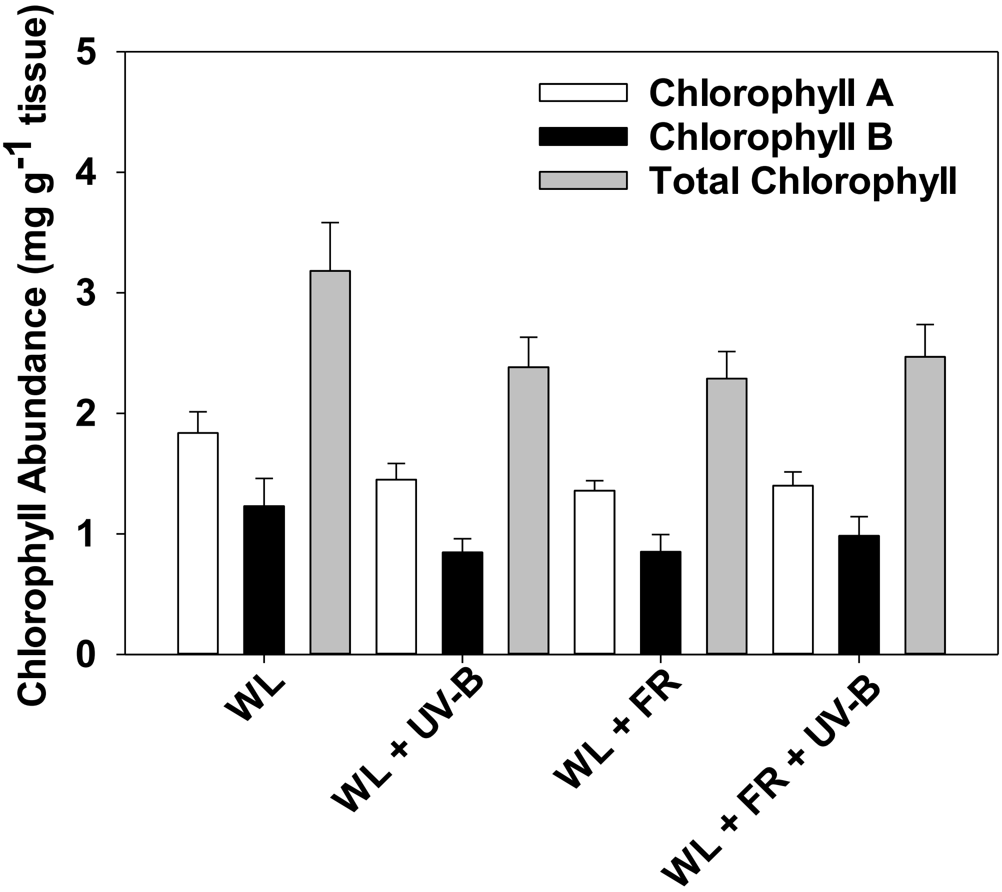

Figure 4.14: Low intensity UV-B and low R:FR do not significantly alter chlorophyll content. Leaf tissue was sampled from 28-day-old Coriander *cv.* Slow Bolt grown in 12h photoperiods. Seedlings were germinated in WL for 3 days and then placed into WL, WL + UV-B, WL + FR & WL + FR + UV-B conditions as indicated for a further 25 days. Chlorophyll A & B content in the different light conditions as determined by the Witham et al. (1971) method. Chlorophyll A, ANOVA ($F(3,12)=2.84, p=0.083$); Chlorophyll B, ANOVA ($F(3,12)=2.84, p=0.363$); Chlorophyll A&B, ANOVA ($F(3,12)=1.918, p=0.181$) $n = 4$. Means +/- 1 S.E.M..

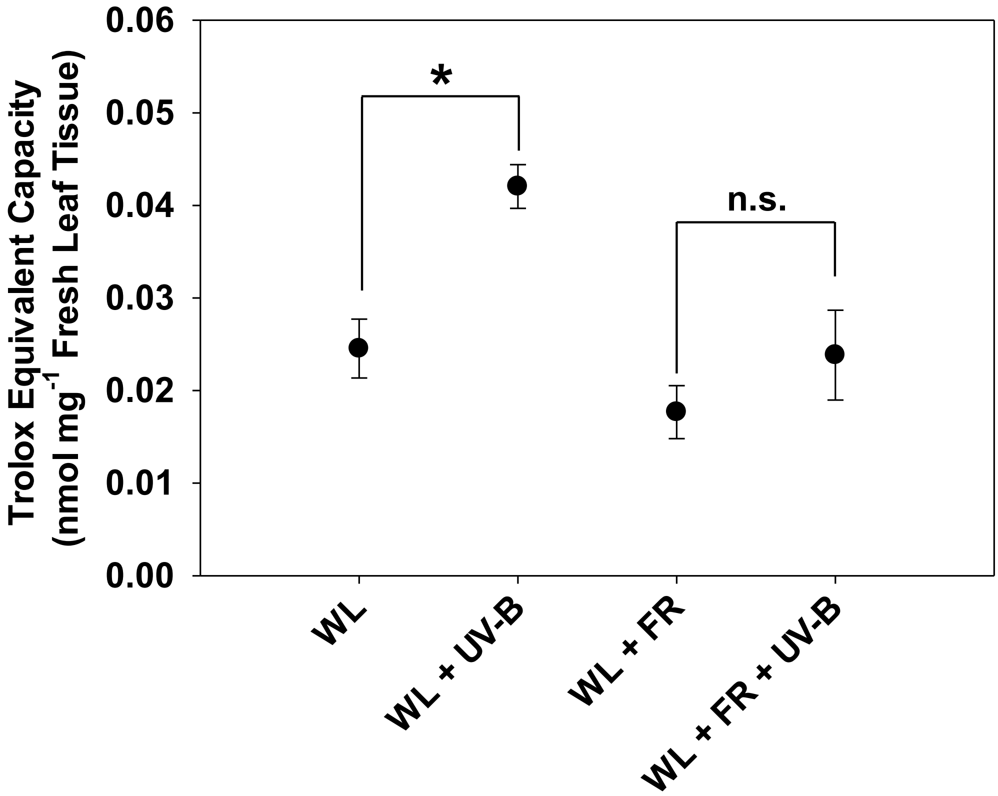

Figure 4.15: UV-B supplementation elevated leaf anti-oxidant capacity in high R:FR but not low R:FR. Leaf tissue was sampled from 28-day-old Coriander *cv.* Slow Bolt grown in 12h photoperiods. Seedlings were germinated in WL for 3 days and then placed into WL, WL + UV-B, WL + FR & WL + FR + UV-B conditions as indicated for a further 25 days. Anti-oxidant activity (in Trolox equivalent nmol mg^{-1} fresh leaf tissue) in UV-B treated plants, n = 8. Plotted are means +/- 1 S.E.M. At high R:FR, $t(14) = -4.419$, $p = 0.000584$. * indicates statistically significant differences at $p < 0.05$.

seen in other species (Bartoli et al., 2009), Coriander grown in WL + FR had a reduced antioxidant capacity compared to WL-grown plants. Leaf antioxidant capacity was not significantly elevated by UV-B in a background of low R:FR, suggesting that low dose UV-B is not sufficient to alleviate the low R:FR ratio-induced reduction in antioxidant capacity.

4.6.3 UV-B elevates leaf flavonoid content

Coriander leaves were qualitatively assayed for changes in flavonol glycoside content in response to UV-B in different R:FR ratio backgrounds using thin layer chromatography (TLC) and DPBA derivation as previously described (Stracke et al., 2010b). Under UV-illumination at 365 nm, DPBA-conjugated methanolic flavonol glycoside extracts fluoresce as follows: green - kaempferol derivatives, orange - quercetin derivatives, blue - sinapate derivatives and unknown substances, dark red - chlorophyll. Arabidopsis mutants deficient in flavonoid biosynthesis were included as controls: *TT4* encodes CHALCONE SYNTHASE and it catalyses the first step in the flavonol biosynthesis pathway, whereas FLAVONOID 3'-HYDROXYLASE (encoded by *TT7*) catalyses the conversion of kaempferol and dihydrokaempferol to quercetin and dihydroquercetin respectively (Winkel-Shirley et al., 1995) (figure 4.1).

Mobile Phase Optimisation

Initially, the Stracke et al. (2010b) protocol was followed exactly, with a mobile phase system of ethyl acetate/formic acid/acetic acid/water (100:26:12:12 v/v/v/v). However, with the equipment available, after derivation with DPBA the separation of flavonol glycoside bands in the Arabidopsis controls was less than optimal (figure 4.16a). Reducing the polarity of the mobile phase by altering the composition of the mobile phase to 100:26:6:12 (v/v/v/v) resulted in improved band separation in Arabidopsis (figure 4.16b). In the Coriander samples, separation was also improved by altering the mobile phase (figure 4.16c to 4.16d). There is scope to further improve separation of the bands, but separation was sufficient to demonstrate differences between treatments (figure 4.17 top panel).

UV-B elevates Coriander leaf quercetin content

Consistent with its role in the first step of the flavonoid biosynthesis pathway (figure 4.1), methanolic extracts from the *tt4* mutants lacked flavonol glycosides when compared to Col-0 in all conditions as indicated by the absence of green and orange derivatives. Similarly, the absence of orange derivatives in the methanolic extracts from *tt7* mutants indicated the absence of quercetin derivatives. Additional orange bands in Col-0 after UV-B illumination indicated that

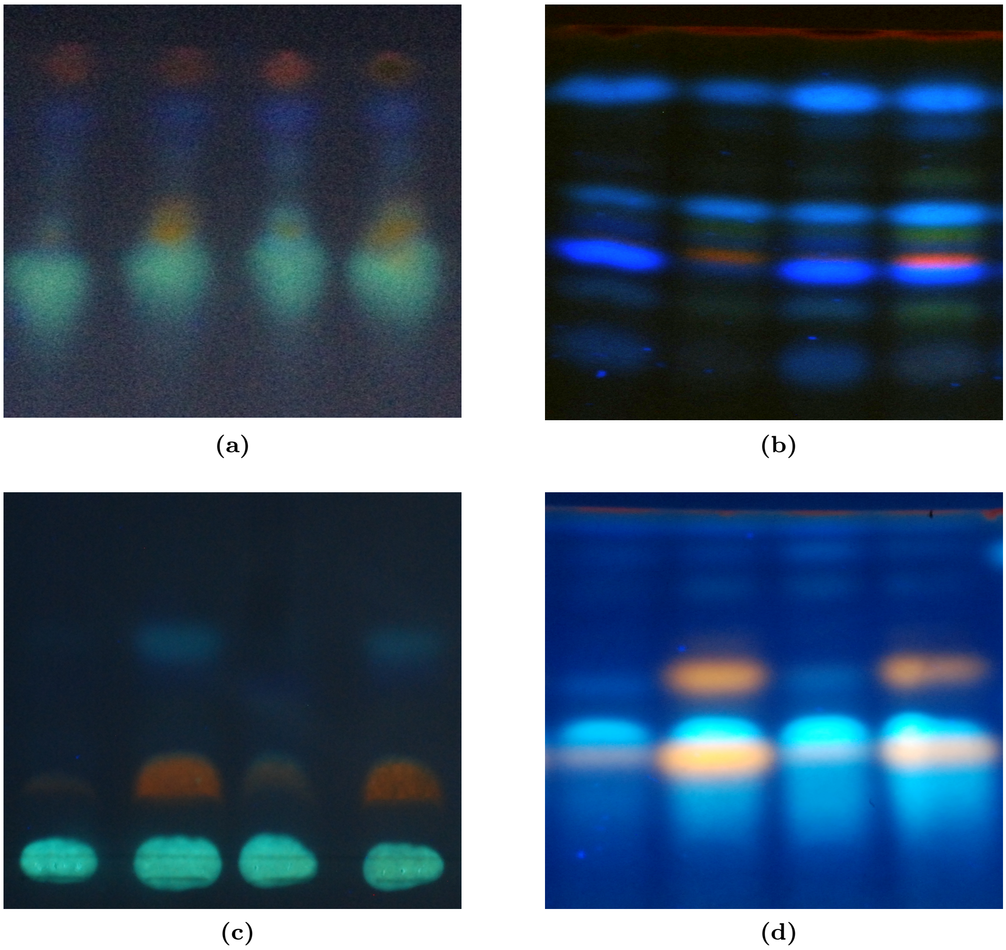

Figure 4.16: Pilot thin layer chromatography experiments to optimise mobile phase. Arabidopsis Col-0 (4.16a,4.16b) and Coriander (4.16c,4.16d) with ethyl acetate/formic acid/acetic acid/water 100:26:12:12 v/v/v/v (4.16a,4.16c) and 100:26:6:12 v/v/v/v ((4.16b),4.16d) mobile phases.

UV-B elevates the accumulation of quercetin derivatives in both high and low R:FR backgrounds. This result correlated with a decrease in sinapate derivatives (as indicated by the disappearance of the dark blue bands in the UV-B treated plants (figure 4.17 bottom panel)). While accumulation of flavonol glycosides in Coriander grown in backgrounds of high and low R:FR did not differ substantially, UV-B treatment elevated the accumulation of quercetin derivatives as indicated by the presence of orange bands in the Coriander methanolic extracts (figure 4.17 top panel).

Flavonoids do not contribute to UV-B - mediated inhibition of shade avoidance

Flavonoids, in particular quercetin, have been shown to modulate auxin transport in plants (Peer and Murphy, 2007). Given that auxin synthesis and transport are central regulators of shade avoidance (Casal, 2012) and its inhibition by UV-B (Hayes et al., 2014), and as UV-B augments flavonoid accumulation as described above in section 4.3.1, the question of whether flavonoids contribute to the inhibition of shade avoidance is thus raised. Analysis of hypocotyl elongation in the *tt4* and *tt7* Arabidopsis mutants grown in high and low R:FR with and without UV-B supplementation did not find a statistically significant interaction with genotype and treatment as factors (figure 4.18) (data collected by Dr Ashutosh Sharma).

4.7 UVR8 in Coriander could not be detected using a polyclonal Arabidopsis UVR8 antibody

UV-B is sensed by the UVR8 photoreceptor, first described in Arabidopsis (Rizzini et al., 2011), but phylogenetic and molecular evidence suggest its functional conservation across multiple taxa and early-diverging lineages (Fernandez et al., 2016; Soriano et al., 2018). As Coriander clearly responded to UV-B ir-

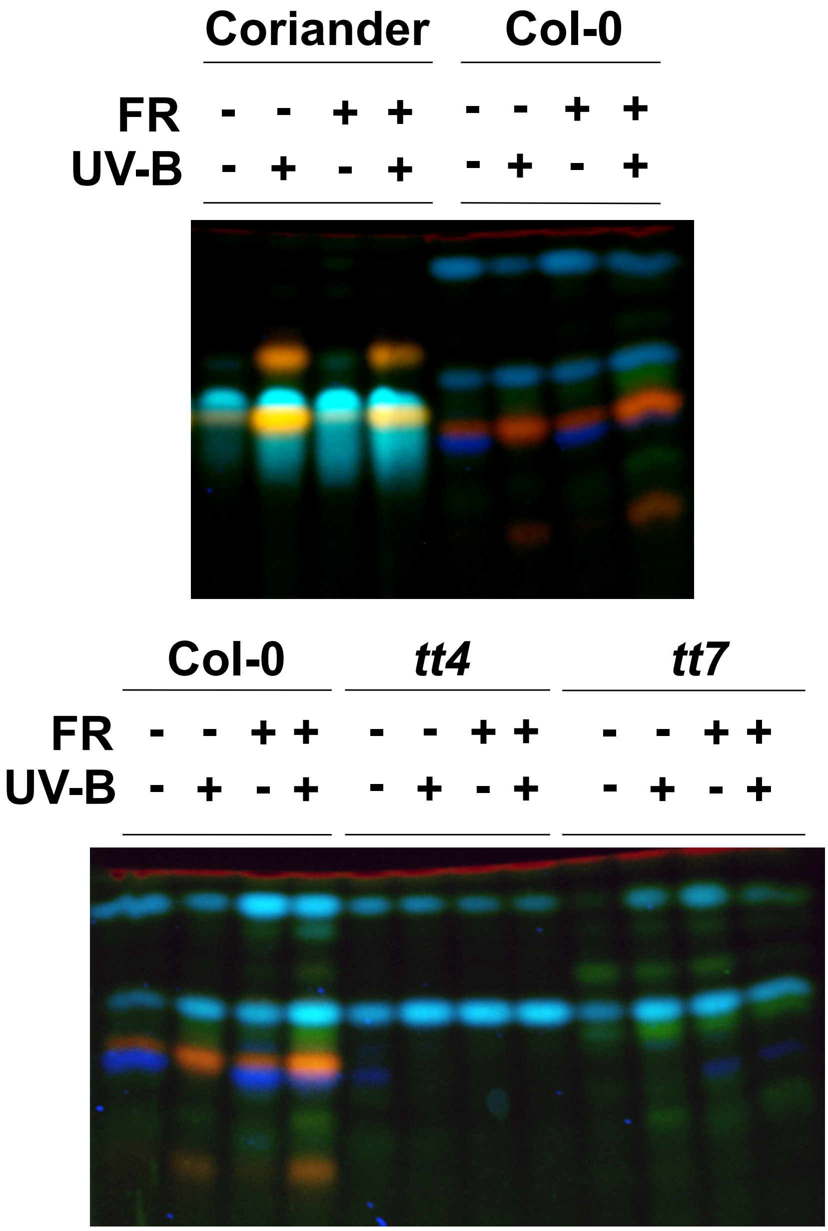

Figure 4.17: UV-B supplementation elevates leaf flavonoid content. Leaf tissue was sampled from 28-day-old Coriander cv. Slow Bolt grown in 12h photoperiods. Seedlings were germinated in WL for 3 days and then placed into WL, WL + UV-B, WL + FR & WL + FR + UV-B conditions as indicated for a further 25 days. Leaf flavonol glycoside accumulation as assayed by high performance thin layer chromatography and derivation with DPBA as described previously (Stracke et al., 2010b). Flavonol glycoside derivatives are imaged with UV-illumination (365nm). Fluorescent Colour key: green, kaempferol derivatives; orange, quercetin derivatives; blue, sinapate derivatives and unknown substances; dark red, chlorophyll.

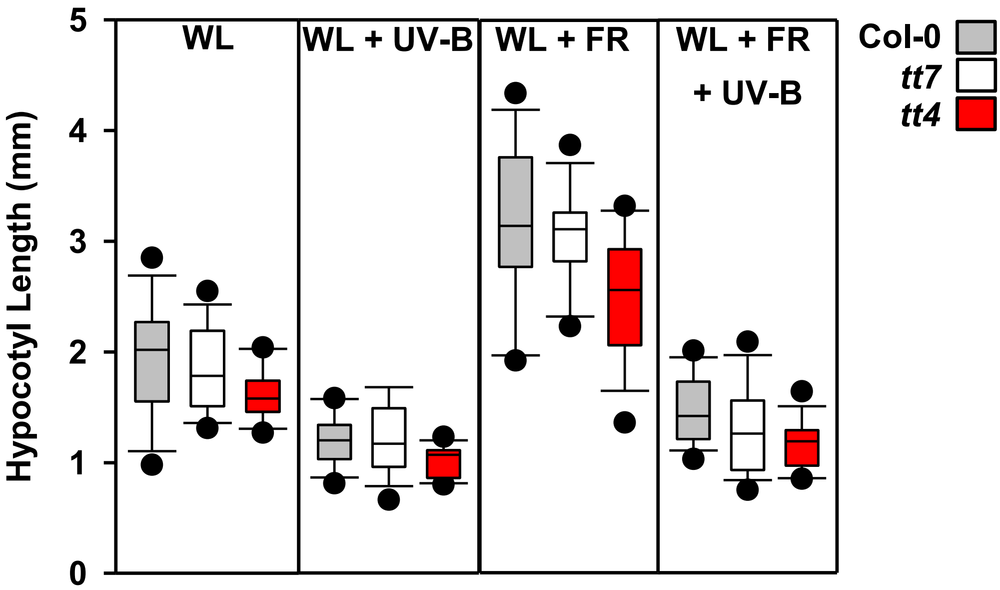

Figure 4.18: Hypocotyl elongation of flavonoid biosynthesis mutants. Plants were grown in long day (16h light/8h dark) for 3 days in WL and then 4 days in the indicated light conditions. Two Way ANOVA interaction with genotype and light condition as factors (F(6,166) = 1.480, p = 0.188). Data for this figure was collected by Dr Ashutosh Sharma.

radiation in a fashion that is canonical with UVR8 signaling (Jenkins, 2017), one might expect Coriander to have a UVR8 homologue. However, an annotated complete nuclear genome sequence for Coriander is not yet available and a BLAST search of the obtainable Coriander sequences in the NCBI database for the AtUVR8 coding sequence did not return any significant sequence similarities. Nor did western blot experiments with a custom made polyclonal antibody raised against Arabidopsis UVR8[2], unambiguously bind to a specific band in the Coriander samples (figure 4.19).

4.8 Discussion

Consistent with previous reports from studies in the Arabidopsis model (Hayes et al., 2014), low R:FR - induced elongation of Coriander stems and petioles was inhibited by supplementation of low dose UV-B (section 4.3). Observations

[2]The custom polyclonal anti-UVR8 antibody was generously provided by Prof. Gareth Jenkins

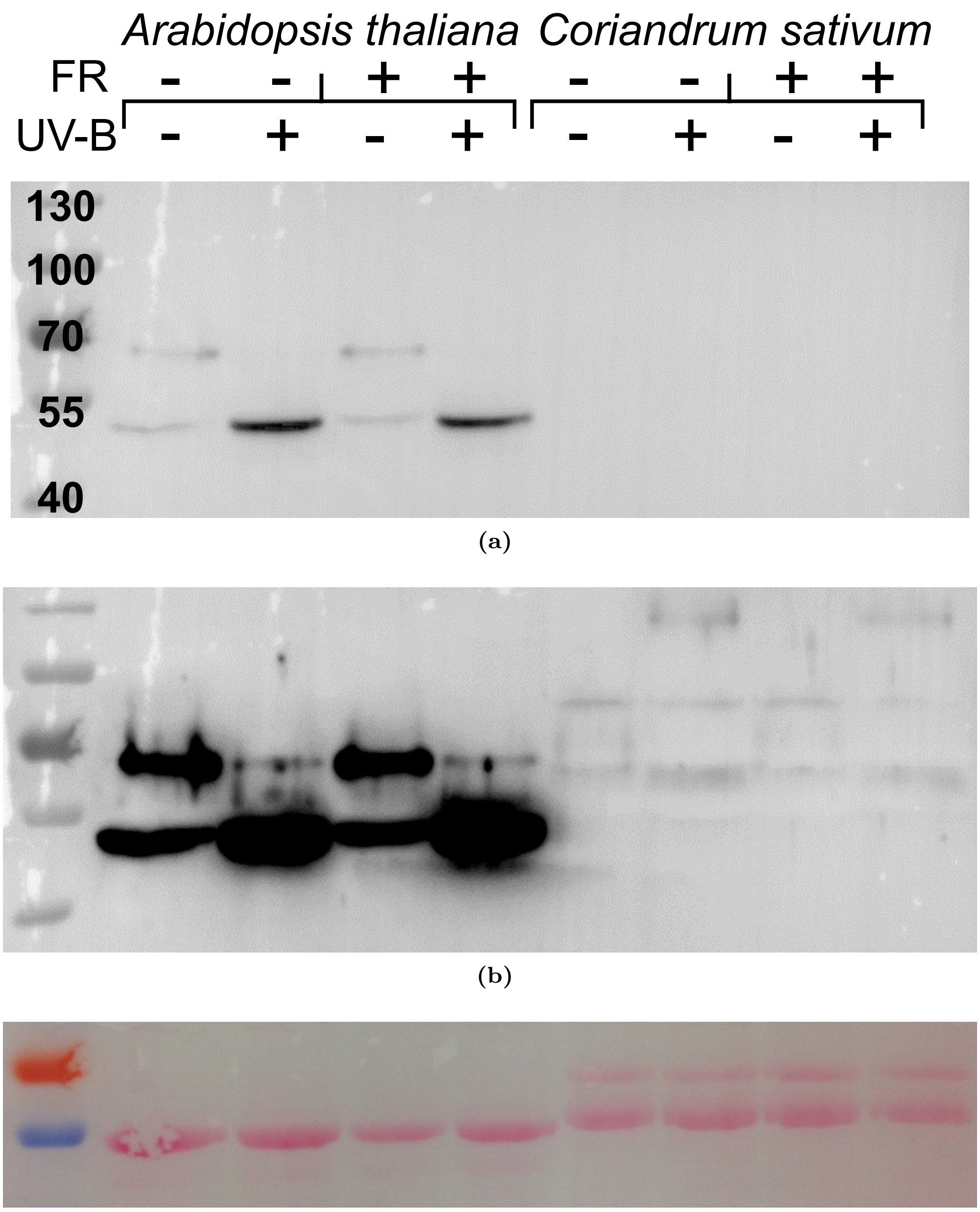

(a)

(b)

(c)

Figure 4.19: A UVR8 polyclonal antibody did not bind to specific bands in Coriander protein samples. Plants were grown in WL and WL + FR. Tissue was sampled from 10 day old Arabidopsis whole seedlings and leaf tissue from 14 day old Coriander. Protein samples suspended in extraction buffer were directly irradiated with 20 µmolm^{-2}s^{-1} UV-B for 10 minutes before 25 µg protein was loaded into each well. (4.19a) 50 second exposure. Numbers in the left lane correspond to molecular weight bands in kDa. (4.19b) 10 minute exposure. (4.19c) Ponceau stain of the RUBISCO large subunit loading control.

that Coriander demonstrated substantial elongation in response to low R:FR suggests Coriander is not a shade tolerant species and may account in part for the observed spindly architecture of the herb as it is often commercially grown in dense stands.

The plant growth hormone auxin plays a key role in promoting stem elongation and has a well established role in shade avoidance (Fraser et al., 2016), whereas UV-B has been shown to down-regulate auxin signaling and biosynthesis in Arabidopsis shade avoidance (Hayes et al., 2014). The similarities in the architectural responses to R:FR ratio and UV-B between Coriander and Arabidopsis suggest that similar signaling mechanisms exist in both species.

In Arabidopsis, shade has been shown to reduce the number of leaves produced due to an increase of the time interval between initiation of new leaves, or plastochron (Cookson and Granier, 2006). As growth in low R:FR reduced the number of petioles produced in Coriander it was hypothesised that UV-B may also alleviate this reduction in leaf initation rate. However, UV-B supplementation did not significantly affect the number of petioles in either high or low R:FR in Coriander. The observation that 28-day-old Coriander plants appeared more compact under UV-B treatment occurred mainly through the inhibition of petiole elongation (section 4.3.2).

Responses to UV-B have previously been shown to be gated by the plant circadian clock in Arabidopsis (Fehér et al., 2011). In nature the level of UV-B varies over the course of the day (Findlay and Jenkins, 2016). Stem elongation in Arabidopsis is rhythmic (Nozue et al., 2007) and analysis of Coriander hypocotyl elongation rate revealed that in 12 h light/12 h dark photoperiod conditions, Coriander displayed maximal growth rate during the light period (section 4.4.1). While a shorter 4 h UV-B dose was sufficient to significantly inhibit hypocotyl elongation in a background of WL + FR, targeting this treatment to different times of day only produced marginal differences (figure 4.8). This may suggest that, unlike many reported UV-B responses, UV-B-induced inhibition of shade avoidance may not be gated by the circadian clock, or the data may be a consequence of differences in circadian and photomorphogenic regulation between Arabidopsis and Coriander. Alternatively, if the inhibition of elongation is circadian gated, then perhaps this gating negates rhythms of UV-B responsiveness (Fehér et al., 2011) to minimise differences caused by the time of day of treatment, thus acting to preserve rhythmic growth (Nozue et al., 2007).

The data presented here focus on the effects UV-B and shade avoidance on Coriander, with the experiments being carried out almost exclusively in 12 h light, 12 h dark photocycles. It would thus be of interest to investigate the effect of UV-B on Coriander architecture in different length photoperiods *i.e.* short (8 h light) and long (16 h light) day conditions. In Arabidopsis, growth in short day photoperiods promotes hypocotyl elongation and produces maximum growth rate at the end of the night due to the coincidence of transcriptional and post-translational regulation of PIF abundance and activity by light signaling and the circadian clock (Nozue et al., 2007; Soy et al., 2016; Martín et al., 2018). Growth in different photoperiods with altering light quality may concomitantly shift the period of maximum elongation and the timing of responsiveness to UV-B inhibition of shade avoidance. Such future experiments could be informative as in winter months, shorter days with more cloud cover may exacerbate the shade avoidance elongation response.

Whilst UV-B supplementation did not significantly inhibit Coriander elongation in a background of WL (PAR = 70 µmol m^{-2} s^{-1}); the data reported here do not exclude the possibility that UV-B supplementation could repress elongation in low PAR environments where blue light and red light are depleted to low levels (de Wit et al., 2016). Nevertheless, at higher (sunlight) PAR levels found in glasshouse growing environments (see table 4.1 for typical values of glasshouse PAR), low dose UV-B supplementation significantly inhibited elongation of Coriander hypocotyls only when grown in dense stands (section 4.5.1), consistent with the inhibition of hypocotyl elongation in a background of WL + FR in growth cabinet conditions (section 4.3.1).

PAR in glasshouses (as opposed to controlled climate growth chambers) is highly variable due to cloud cover and the height of the sun. The importance of the UV-B : PAR ratio for the inhibition of hypocotyl elongation was crudely tested by using 3 different intensities of UV-B for the duration of the photoperiod. Interestingly, all three UV-B treatments significantly inhibited hypocotyl elongation. Observations that the three treatments were similarly effective may reflect the sensitivity of the mechanism of UV-B sensing by UVR8, *i.e.* a 1 µmol m^{-2} s^{-1} treatment for the duration of the photoperiod is as saturating as a 3 µmol m^{-2} s^{-1} treatment. This result does not support the proposition that UVR8-inhibition of hypocotyl elongation is a result of photodimer accumulation (Biever et al., 2014)[3] as were this the case the highest intensity of UV-B should result in the shortest hypocotyls, unless the response is already saturated with lower intensity UV-B irradiation. The data reported here would not be inconsistent with the finding that the UVR8 monomer/dimer equilibrium stays reasonably constant over the course of the day (Findlay and Jenkins, 2016). Considering its conservation in early diverging lineages (Soriano et al., 2018), it seems reasonable to assume that Coriander will have a UVR8 homologue. Yet in this work, a homologue could not be unambiguously identified using the available Arabidopsis antibody (section 4.7). In the absence of an annotated Coriander genome, the question of whether or not Coriander has the UVR8 protein remains open.

Low R:FR ratio light and high intensity UV-B radiation have been reported to reduce leaf chlorophyll content in multiple species (Bartoli et al., 2009; Kumar and Pandey, 2017). With the observed healing of the ozone layer (Solomon et al., 2016), more research emphasis is now being placed on the regulatory effects of low-dose, non-harmful UV-B radiation, which has been found to improve photosynthetic efficiency (Davey et al., 2012). In the tested conditions, neither R:FR ratio nor low intensity UV-B significantly depleted, or promoted, chloro-

[3]The work reported by Biever et al. (2014) investigated photomorphogenesis in etiolated seedlings so is not directly comparable to the data reported here. Nevertheless, it presents a hypothesis that the data in this thesis do not support.

phyll abundance, suggesting that Coriander chlorophyll accumulation may not be as sensitive to light quality as in other species (section 4.6.1).

Following UV-B perception, Arabidopsis upregulates antioxidant defences *via* the UVR8-COP1-HY5 signaling pathway (Ulm et al., 2004; Rizzini et al., 2011; Jenkins, 2017) for the prevention or alleviation of DNA damage and oxidative pressure (Hideg et al., 2013). Consistent with studies in Arabidopsis (Csepregi et al., 2017), for Coriander grown in a background of WL, low dose UV-B significantly increased antioxidant capacity (figure 4.15). However, it was striking that the same UV-B treatment given to Coriander grown in low R:FR ratio did not significantly increase antioxidant capacity. Indeed, Coriander grown in a low R:FR ratio exhibited a drop in antioxidant capacity compared to plants grown in a high R:FR ratio, which is consistent with findings in other species (Bartoli et al., 2009). Observations that antioxidant capacity is inhibited by low R:FR ratio light could be interpreted as plants diverting resources from antioxidant defence toward elongation. Plants may perceive a high R:FR ratio as a signal of direct sunlight, which is associated with high light, and the potential for damage due to excess irradiance. Conversely, a low R:FR ratio is a signal of indirect or reduced light (perhaps due to shade) and hence in this context photoprotective mechanisms are less important. As UV-B is a component of direct sunlight, it was surprising that supplemental UV-B irradiation was insufficient to significantly elevate antioxidant capacity in a low R:FR ratio background, suggesting that low R:FR ratio light blocks UV-B activation of antioxidant defences. While interesting, it should be noted that in a natural context plants would only receive sunlight levels of UV-B in conjunction with a low R:FR ratio on emergence from a canopy.

Analysis of Coriander leaves for changes in flavonol glycoside content using thin layer chromatography suggests that in both a background of WL and WL + FR, UV-B mainly induces the accumulation of quercetin (section 4.6.3). While increases in flavonoids vary from species to species, the increase of quercetin by UV-B has previously been reported in such unrelated taxa as petunia (Ryan et al., 1998), *Brassica napus* (Wilson et al., 1998) and apple (Solovchenko and Schmitz-Eiberger, 2003). Like other flavonoids, quercetin has UV-B absorptive properties, but it also acts as an effective antioxidant (Agati and Tattini, 2010) likely due to multiple hydroxy groups in the A, B & C aromatic rings (Rice-Evans et al., 1996). However, quercetin is not likely to play a large role in Coriander's ROS scavenging as the antioxidant capacity data show that when UV-B is given in a background of WL + FR, there is no significant increase in total antioxidant capacity (figure 4.15) despite the clear increase in quercetin (figure 4.17). In spite of its potential health benefits, quercetin, like other flavonoids is associated with bitter flavours (Drewnowski and Gomez-Carneros, 2000). Thus growers may need to balance aesthetic and health benefits with flavour alterations. Aldehydes are understood to be the main contributor to Coriander's (*polarizing*, due to variants of the *OR6A2* olfactory receptor gene in humans (Eriksson et al., 2012)) flavour. It would be interesting to analyse, perhaps using Gas Chromatography Mass Spectroscopy (GC-MS), the aldehyde content of UV-B-treated Coriander.

In addition to their antioxidant and sunscreening properties, flavonoids have been shown to negatively regulate auxin transport (Peer and Murphy, 2007). Hypocotyl elongation analysis of flavonoid deficient mutants *tt4* and *tt7* found that they behaved similarly to wild type controls (figure 4.18), suggesting that flavonoids do not play a key role in the UV-B mediated inhibition of shade avoidance.

The results reported in this chapter suggest that the inclusion of UV-B into growth regimes can give appreciable benefits to Coriander architecture and alterations to phytonutrient content. While 4 h UV-B delivered daily at 1.5 µmol m^{-2} s^{-1} was sufficient to elicit a significant suppression of hypocotyl elongation even in highly variable glasshouse conditions, the data indicate that the timing and the intensity of the UV-B dose were relatively unimportant compared to the duration of dose. Here, fluorescent narrow band UV-B bulbs were used to deliver supplemental UV-B treatments, but due to advancements in UV-B

LED technology, future research is likely to utilise LEDs (Wargent, 2016). At present, UV-B LEDs are still prohibitively expensive, with short lifespans and fairly high energy requirements. An alternative solution that may also minimise energy consumption could be the construction of greenhouses from materials with relatively high UV-B transmission qualities (Paul et al., 2005). It would thus be interesting to see if such UV-B transparent materials can improve the architecture and alter the phytonutrient content of glasshouse grown Coriander.

Chapter 5

Low R:FR Ratio Damps Rhythms of *CCA1* and *TOC1* Expression

5.1 Introduction

How plants adapt to crowded conditions through stem elongation and the elevation of petioles continues to be intensely studied. A major cue for plants that they are in close proximity to neighbouring vegetation is the relative enrichment of long wavelength FR light, resulting in a low R:FR ratio that is perceived by the phytochrome photoreceptors (reviewed in Casal (2012); Pierik and De Wit (2014); Fraser et al. (2016)). A low R:FR ratio causes the stabilisation of PIFs 4 and 5 (Lorrain et al., 2008) and the dephosphorylation of PIF7 (Li et al., 2012a), resulting in an elevation of auxin synthesis and transport, and ultimately the elongation of hypocotyls and petioles. In addition to controlling stem elongation through direct interactions with PIF proteins, photoreceptors regulate the entrainment of the plant circadian clock (Oakenfull and

Davis, 2017).

At dawn, the transition from dark to light is a vital clock resetting cue (Millar et al., 1995b). The phytochrome and cryptochrome photoreceptors have major roles in the entrainment process (Somers et al., 1998; Wenden et al., 2011) and the UVR8 photoreceptor has also been shown to entrain the circadian clock independently of HY5 and HYH (Fehér et al., 2011). The R-light photoreceptor, phyB, physically interacts with the evening complex component EARLY FLOWERING 3 (ELF3), and through this mechanism may provide a light input pathway into the circadian clock (Liu et al., 2001; Kolmos et al., 2011). PhyA has been shown to mediate low fluence R and B light signalling to the circadian clock (Somers et al., 1998), but there have been no reports of direct interaction between phyA and circadian clock components. Loss of ELF4 function has, however, been shown to curtail FR signalling to the clock, suggesting a role in phyA signalling (Wenden et al., 2011).

The morning-expressed Myb-like transcription factor CCA1 (Wang and Tobin, 1998) along with its close homolog LHY (Schaffer et al., 1998), repress the expression of the evening-phased PSEUDO RESPONSE REGULATOR (PRR) TIMING OF CAB EXPRESSION 1 (TOC1) through interaction with a promoter motif known as the evening element (EE) (Alabadí et al., 2001). Subsequently, TOC1 acts as a transcriptional repressor that represses the expression of *CCA1* and *LHY* (Huang et al., 2012a; Gendron et al., 2012; Pokhilko et al., 2012). Together these genes form a core negative feedback loop within the Arabidopsis circadian clock. CCA1 is regarded as a central transcriptional repressor of the plant circadian clock. Over-expression of CCA1 causes clock arrhythmia in LL, with plants displaying extremely elongated hypocotyls (Wang and Tobin, 1998). TOC1 over-expressors are also arrhythmic in LL (Makino et al., 2002), but, in contrast with CCA1 over-expressors, display short hypocotyls. TOC1 has recently been shown to bind to PIF3 and PIF4 and inhibit the expression of PIF targets, thereby inhibiting hypocotyl elongation (Soy et al., 2016; Zhu et al., 2016).

Through circadian gating, the clock exerts control over the phase of cellular and physiological processes such as hypocotyl elongation to produce rhythmic behaviours and restrict responses to appropriate times of day (Greenham and Mcclung, 2015). The circadian clock provides a competitive advantage, but only if its period matches its environment (Dodd et al., 2005), the clock can therefore only provide its advantage if it is correctly entrained. Dowson-Day and Millar (1999) showed that disruption of the plant circadian clock altered rhythmic patterns of hypocotyl elongation. Experiments by Nozue et al. (2007) demonstrated that, by regulating PIF transcript abundance and PIF protein abundance respectively, the circadian clock and light mediate rhythmic hypocotyl growth in driven conditions, proposing an "external coincidence" model to explain their observations. Nusinow et al. (2011) reported that the evening complex mediates rhythms of PIF transcript abundance, while another report proposed that PIF4 and ELF3 form a non DNA-binding complex, independent of the other evening complex components (Nieto et al., 2015). Other studies have found that the rapid shade avoidance response is gated by the circadian clock (Salter et al., 2003), although Sellaro et al. (2012) report that the evening complex plays only a minor role in the gating of shade avoidance in driven conditions. Reminiscent of the ELF3-PIF4 interaction (Nieto et al., 2015), recent work has revealed that members of the PRR family also mediate the circadian gating of hypocotyl elongation and shade avoidance through direct interaction with PIFs (Soy et al., 2016; Martín et al., 2018).

In chapter 3, rhythms of transcript abundance for *HY5*, *HYH* and *GA2ox1* after UV-B treatment were unexpectedly abolished in free-running low R:FR ratio conditions, suggesting that the circadian gating of the UV-B induction of these genes was lost. The experiments reported in this chapter investigate the hypothesis that this loss of circadian gating could be a consequence of an alteration of the behaviour of the circadian clock.

5.2 Low R:FR ratio damps free-running oscillations of *CCA1* and *TOC1* relative transcript abundance

Experiments were carried out on the same cDNA collected in section 3.3: Plants were entrained in 12 h light/12 h dark photocycles in high R:FR (5) and low R:FR (0.05) at PAR = 70 µmol m^{-2} s^{-1} for four days before transfer to continuous light (LL) on day 5 (while maintaining their respective R:FR ratios). 6-, 7- & 8-day-old seedlings were sampled for RNA analysis every 4 h (figure 5.1). The relative transcript abundance of two well-characterised circadian clock genes was analysed. *CCA1* is a morning - phased repressor, whereas *TOC1* is an evening - phased repressor (reviewed in Hsu and Harmer (2014)). Under high R:FR, *CCA1* (figure 5.1a) and *TOC1* (figure 5.1b) both had rhythms of transcript abundance in LL consistent with previous reports: *CCA1* relative transcript abundance peaked at the start of the subjective day and *TOC1* relative transcript abundance peaked at the end of subjective day. For plants entrained and grown in low R:FR, transcript oscillations were damped to the point that they appeared arrhythmic. Notably, oscillations of *CCA1* transcript damped to a low abundance whereas oscillations of *TOC1* transcript damped to a high abundance (figure 5.1).

5.3 Low R:FR ratio damps free-run oscillations of *CCA1pro::LUC* and *TOC1pro::LUC*

The altered levels of *CCA1* and *TOC1* transcript abundance (figure 5.1) may result from low R:FR-mediated effects on promoter activity. Luciferase assays were employed to analyse the dynamics of *CCA1* and *TOC1* promoter activity at a PAR of 47 µmol m^{-2} s^{-1} in three different R:FR ratios; high = 1.2, intermediate = 0.5 & low = 0.05, which correspond with neighbour detection conditions

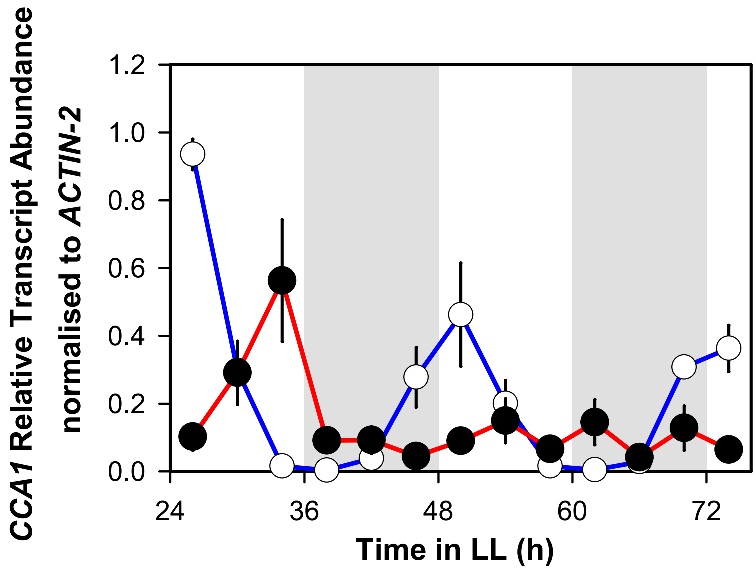

(a)

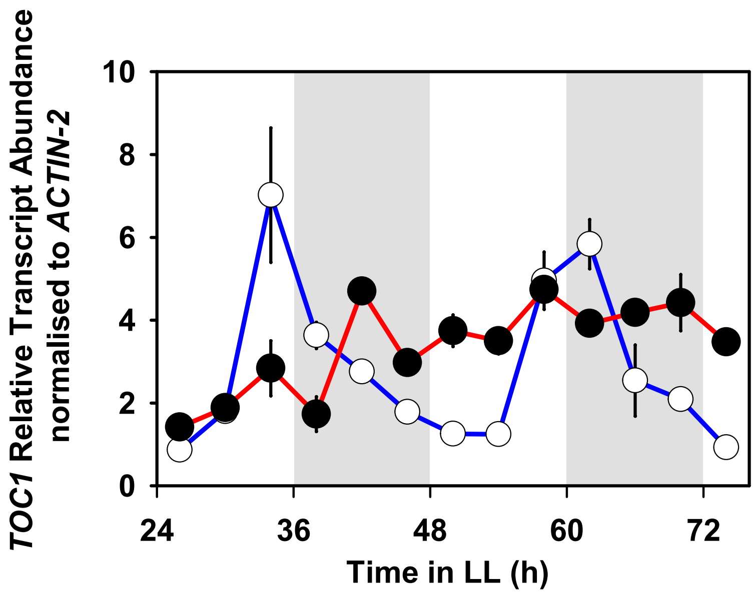

(b)

Figure 5.1: R:FR ratio alters behaviour of *CCA1* and *TOC1* transcript abundance in free run. Wild type Arabidopsis (L.*er*) seedlings were entrained in 12 h L : 12 D in either R:FR = 5 (open circles) or R:FR = 0.05 (filled circles) for 4 d. Plants were transferred to 24 h LL on day 5. 6, 7 & 8 day-old-seedlings were sampled for RNA analysis. Plotted is mean relative transcript abundance of two independent experiments (n = 2) of (5.1a) *CCA1*, (5.1b) *TOC1* normalised to *ACTIN-2* +/- 1 S.E.M.

in nature such as direct sunlight, moderate crowding and densely crowded conditions respectively. Transgenic plants expressing *CCA1pro::LUC* (figure 5.2a) and *TOC1pro::LUC* (figure 5.2b) had strong rhythmic behaviour across the range of R:FR ratios in driven (LD) conditions (first 48 h of data acquisition), which suggests that low R:FR in LD cycles does not disrupt entrainment (figure 5.2). 24 h after transfer to LL low R:FR, *CCA1pro::LUC* and *TOC1pro::LUC* oscillations were damped compared to high and intermediate R:FR (figure 5.2). *CCA1pro::LUC* and *TOC1pro::LUC* signal damped low and high respectively, which is consistent with the transcript abundance data (section 5.2) and their reciprocal transcriptional repression (Gendron et al., 2012; Hsu and Harmer, 2014).

Relative amplitude error (RAE) from Fast Fourier Transform Non Linear Least Squares (FFT-NLLS) analysis indicates the closeness of fit of the experimental data to a sine wave (where 0 is perfect fit, 1 is no fit and values > 0.5 could be interpreted to suggest arrhythmia for luciferase reporters). FFT-NLLS analysis of luciferase data after the initial 24 h in continuous light showed that plants in continuous low R:FR had marginally greater RAEs than plants grown in high and intermediate R:FR. This observation may be due to a drop in the signal to noise ratio as the reduction in R:FR ratio caused a reduction in amplitude so noise becomes a larger portion of the signal, it also suggests damping of promoter activity and that rhythmicity was weakened by low R:FR. Both *CCA1pro::LUC* and *TOC1pro::LUC* still showed robust rhythmicity with RAEs <0.5 (figure 5.3a). With reductions in R:FR ratio from 1.2 to 0.5 to 0.05, both *CCA1pro::LUC* and *TOC1pro::LUC* plants displayed reduced period lengths (figure 5.3b,5.3c), which suggests that lowering R:FR ratio may accelerate the circadian clock in LL. In the first 48 h after transfer to LL, a 5 h delay in phase in *CCA1pro::LUC* and *TOC1pro::LUC* signal was observed in the low R:FR-treated plants that was not observed in the intermediate and high R:FR-treated plants (figure 5.2).

The data described above indicate that the R:FR ratio affects circadian clock function in LL. In particular, low R:FR-grown plants in LL had damped oscillations and shortened periods. In LD, there was no obvious difference in behaviour of the circadian clock between the different R:FR ratios, which suggests that in the presence of a strong entraining signal, that is, the transition from dark to light at the start of the day, clock function is mostly unaffected.

5.4 Discussion

In this chapter, the data reported show that R:FR ratio affects the rhythmic behaviour of central clock components in free-running conditions. Observations that *CCA1* and *TOC1* transcript and promoter activity display damped oscillations (to the point where oscillations in transcript abundance were not visible - possibly due to larger sampling intervals) in low R:FR supports previous findings from experiments using monochromatic FR to entrain the clock (Wenden et al., 2011). Both the transcript abundance and luciferase data suggest that *CCA1* expression damps low whereas *TOC1* expression damps high in low R:FR. Given that both CCA1 and TOC1 act as reciprocal transcriptional repressors (Matsushika et al., 2002; Gendron et al., 2012), one possibility is that low R:FR elevates TOC1 expression in the first instance, which causes a subsequent suppression of CCA1 expression. The extremely low R:FR ratio used here may be acting similarly to the monochromatic FR used in Wenden et al. (2011): where it was surmised that the clock *paused* at a point in its limit cycle. It has been shown that the plant circadian clock displays tissue-specific behaviours, with guard cells, epidermal cells and the vasculature all having distinct circadian clocks (Yakir et al., 2011; Endo et al., 2014). Some tissues also appear to display inter-organ coupling, though the coupling factor has yet to be established (Endo et al., 2014; Endo, 2016), it has been suggested that in roots a photosynthesis-related (James et al., 2008) or perhaps hormonal signal may communicate timing information between the shoot and the root (Gould et al., 2017). The *pause* in the limit cycle could, therefore, happen heterogeneously

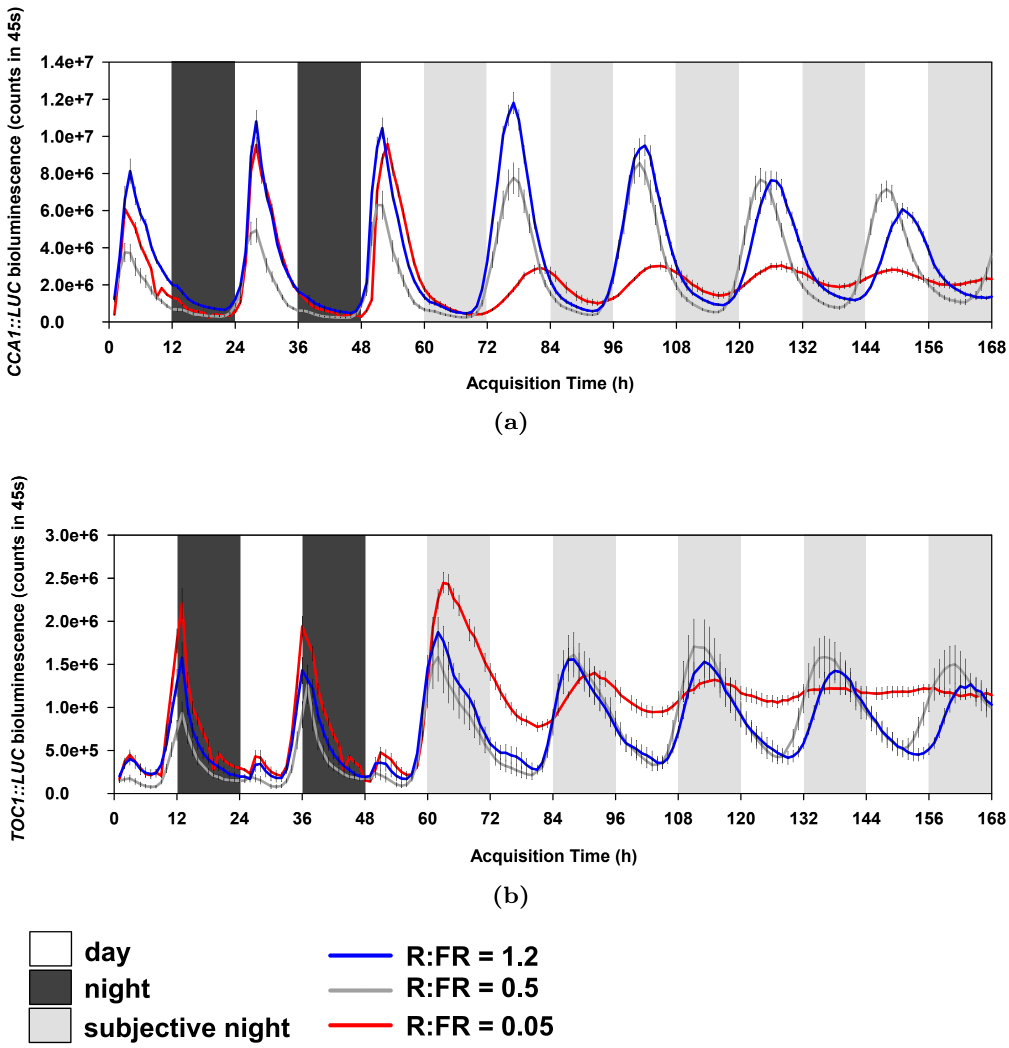

Figure 5.2: R:FR ratio alters behaviour of *CCA1pro::LUC* and *TOC1pro::LUC*. Traces of luciferase activity of (5.2a) *CCA1pro::LUC*, (5.2b) *TOC1pro::LUC* in the Col-0 background in R:FR ratio = 0.05 (red line), 0.5 (grey line) and 1.2 (blue line) as indicated in driven (LD 0 – 48h), followed by free-run (LL 48-168h) conditions. Dark grey shading indicates night while light grey shading indicates subjective night. Plants were grown for 7 d in PAR = 70 µ mol m-^{2} s^{-1} at the R:FR ratio indicated then transferred to PAR = 47 µmol m^{-2} s^{-1}for 3 d to entrain maintaining the same R:FR ratios. 10-day-old plants in clusters of 12 were dosed with luciferin and imaging commenced 24 h later (Time 0 on graph). Plotted are means +/- 1 S.E.M., n = 6.

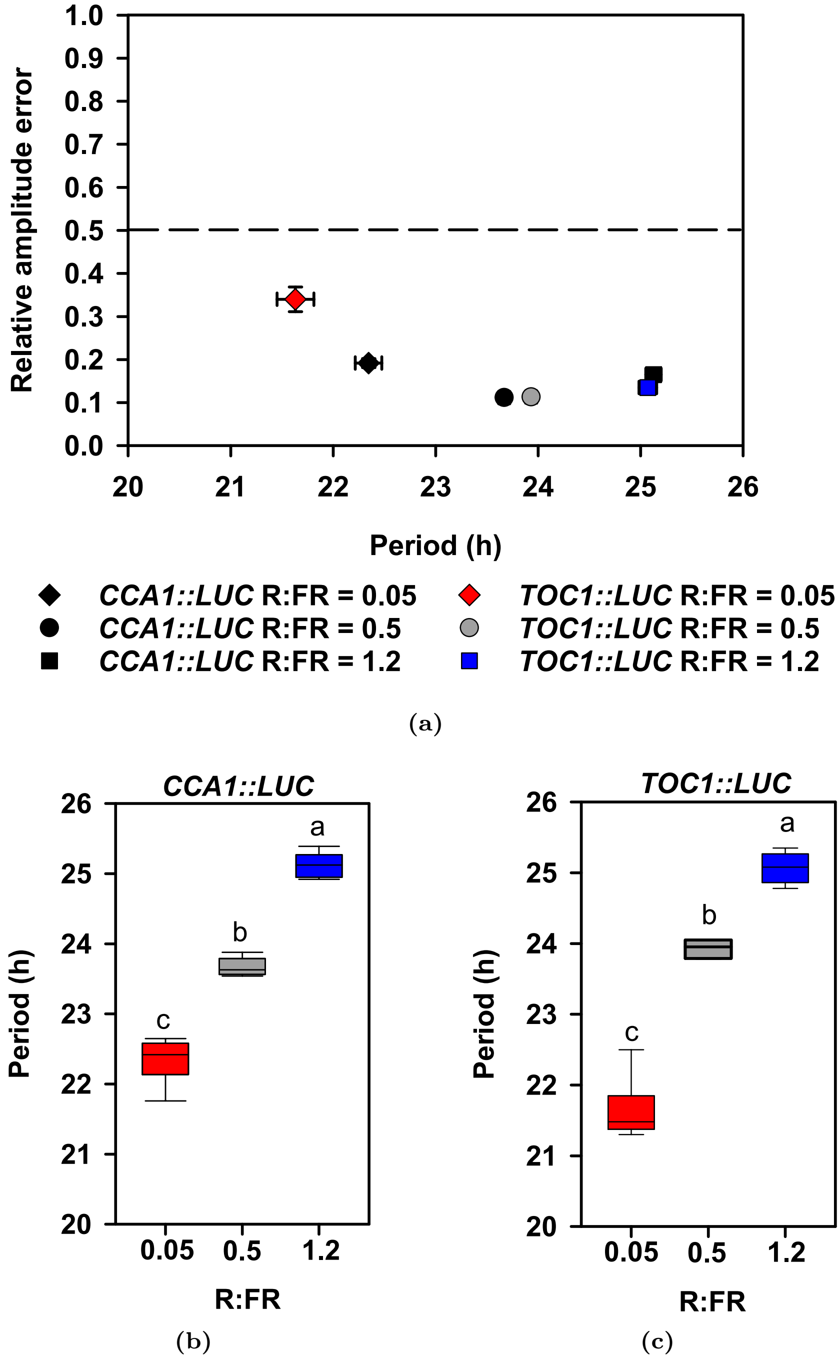

Figure 5.3: Low R:FR ratio reduces period length. (5.3a) Relative Amplitude Error and period length scatter plot, using data derived from FFT-NLLS analysis of *CCA1pro::LUC* and *TOC1pro::LUC* free-run data (Figure 5.2). Plotted are means +/- 1 S.E.M., n = 6. Period length box plots of (5.3b) *CCA1pro::LUC* and (5.3c) *TOC1pro::LUC*. Different letters indicate statistically significant differences by one-way ANOVA at $p < 0.05$ (*CCA1pro::LUC* ($F(2,15) = 230.559$, $p < 0.001$), *TOC1pro::LUC* ($F(2,15) = 215.589$, $p < 0.001$)).

across cells or organs: The damping of oscillations observed in continuous low R:FR reported here may result from a loss of synchronicity between cells or tissues (Yakir et al., 2011; Wenden et al., 2012), maintenance of synchronicity but a reduction in amplitude range, or perhaps a mixture of the two. Unfortunately it was not possible to discern which of these possibilities is the cause as the techniques used here sampled the whole aerial tissue of seedings. Wenden et al. (2011) also showed that the *elf4-1* mutation abolished the damping of rhythms caused by FR. It would therefore be interesting to investigate the role of ELF4 in low R:FR. The low R:FR-induced damping of circadian oscillations in LL is likely not isolated to just *CCA1* and *TOC1* due to the interlocking feedback loop architecture of the circadian clock system and its downstream components, although this remains to be tested. A damping of oscillations of the circadian clock may explain the loss of the circadian gating of the UV-B-induced genes *HY5*, *HYH* and *GA2ox1* reported in chapter 3: Supposing that mechanisms for circadian gating include direct association of rhythmic clock components to proteins and promoters to cause transcriptional repression or chromatin modifications (Hsu et al., 2013; Nieto et al., 2015; Soy et al., 2016; Zhu et al., 2016; Martín et al., 2018), a loss of rhythmicity in the abundance of circadian clock proteins could lead to a loss of rhythmicity in promoter activity, and hence transcript abundance, of target genes. Taken alongside the circadian clock's pervasive control of the transcriptome (Covington et al., 2008), it is likely that the expression and the circadian gating of many other downstream genes will be affected in their expression.

Observations that *CCA1pro::LUC* and *TOC1pro::LUC* exhibited damped oscillations and a phase delay of c. 5 h after 24 h in the lowest R:FR (figure 5.2) raises the possibility that there could be a threshold R:FR ratio below 0.5 where phase is delayed and rhythmicity is damped in LL. In the conditions used here, reducing the R:FR ratio progressively shortened period in LL (figure 5.3), such that in spite of the initial phase delay of c. 5 h, the plants grown in low R:FR ratio came back into phase with plants grown in high and intermediate R:FR after 72-84 h (figure 5.2). In contrast, Jiménez-Gómez et al. (2010) reported that simulated shade increased period length in free-run, but this result may reflect ecotype-specific responses to shade of the Bay-0 and Sha *ELF3* alleles.

As reductions in R:FR ratio were achieved through increasing the intensity of the FR LEDs, this increased clock pace in low R:FR could be a consequence of Aschoff's rule, where increasing the light intensity that a diurnal organism is exposed to shortens its period in free run (Aschoff, 1979). Another possibility is that FR supplementation increases metabolic entrainment of the oscillator: Haydon et al. (2013) showed that the addition of sugar to arabidopsis growth media shortens circadian period in a PRR7-dependent manner. Taken alongside the Emerson effect, where maximum photosynthetic rate is achieved with a combination of 680 and 700 nm wavelengths (Emerson, 1958), it is possible that, as previously described in *Lactuca sativa* by Zhen and van Iersel (2017), the supplementation of FR to the experimental light conditions increases the rate of photosynthesis, which strengthens sugar entrainment of the circadian clock and hence shortens period length in free-run.

Observations that extremely low R:FR ratios caused damping of clock oscillations in free-run, but not in driven conditions suggests that such responses may not occur naturally in diurnal cycles of shade. In addition, an extremely low R:FR ratio would generally be experienced naturally by plants in conditions of very low PAR (figure 2.2). The combination of continuous light and an extremely low R:FR ratio in a background of moderate PAR does therefore not accurately reflect natural light conditions. In order to study circadian behaviour under different R:FR ratios in physiologically relevant conditions, the following chapter (6) investigates the circadian clock in deep shade conditions that more accurately reflect those found in nature.

Chapter 6

Circadian Clock Behaviour and the Regulation of Stem Elongation in Deep Shade

6.1 Introduction

A system commonly used for studying shade avoidance reduces the R:FR ratio while keeping PAR constant by adding FR to a background of (*e.g.*) white light. In doing so, plants can be exposed to realistic R:FR ratios without having to alter environmental features with shade netting or filters, which allows researchers to study proximity perception rather than shade. In controlled climate chambers, the capabilities of FR LED light sources make it possible to achieve R:FR ratios of < 0.1 without reducing R fluence rate, *e.g.* a R:FR ratio of 0.05 in a background of PAR $= 70$ µmol m^{-2} s^{-1} (figure 2.1c). In nature, however, a ratio of R:FR < 0.1 would be found in canopy shade where PAR < 10 µmol m^{-2} s^{-1} (figure 2.2a). Ballaré et al. (1990) showed that, in natural conditions, FR light scattered by vegetation in dense stands is perceived by stems and causes internode elongation in *Sinapis alba* and *Datura ferox.* It is interesting that this early study noted that at greater canopy densities, blocking FR light did not fully cancel the elongation response, suggesting that the additional elongation is attributable, at least in part, to a lower fluence rate of R and B light (due to its absorption by vegetation for photosynthesis) (Ballaré et al., 1990).

Phytochromes perceive R:FR: phyB is photoconverted to the inactive P_r form when R:FR is moderately lowered to mimic dense stands without shading (Franklin, 2008). In deep shade, where both PAR and R:FR ratio are very low, phyA signalling antagonises stem elongation (Martínez-García et al., 2014). phyA is highly light labile, it accumulates to high levels in etiolated seedlings and signals during rapid photoconversion between P_r and P_{fr}, but on transfer to light that establishes a high proportion of P_{fr} (*e.g.* R) phyA is rapidly degraded to low steady-state levels by the proteasome (Clough and Vierstra, 1997; Debrieux and Fankhauser, 2010). The rapid turnover of phyA in light explains why phyA only antagonises shade avoidance when PAR is very low. Yanovsky et al. (1995) reported that in deep shade, *phyA* mutants had impaired de-etiolation, had extremely elongated hypocotyls and died. Perhaps, therefore, the FR-induced antagonism of hypocotyl elongation by phyA in deep shade may prevent excessive elongation in an otherwise light-depleted environment where other photoreceptors would not be expected to signal. To date, only PIF1 and PIF3 have been reported to bind to phyA (Shen et al., 2005; Bauer et al., 2004). A recent study shed new light on the mechanism of phyA signalling, reporting that phyA accumulates in deep shade and competes with SCF^{TIR1} to bind to and stabilise the AUX/IAA repressors of the AUXIN RESPONSE FACTOR (ARF) family to inhibit auxin-induced transcription (Yang et al., 2018). Nevertheless, a comprehensive model for the antagonism of shade avoidance by phyA remains to be established.

Blue light (B) is also attenuated in deep shade. Cryptochromes perceive B light and, in low B light, have been shown to physically interact with both PIF4 and PIF5 and co-associate with PIF target promoters to modulate their activity (Pedmale et al., 2015). de Wit et al. (2016) reported that the combination of low B and low R:FR resulted in longer hypocotyls and petioles than either signal alone, arguing that enhanced PIF abundance and transcriptional activity resulted in increased brassinosteroid and auxin signalling. Other studies propose that in deep and prolonged shade, less auxin is synthesised than in neighbour detection conditions. Instead, auxin sensitivity is enhanced in deep shade through the increased expression of the auxin receptors *AUXIN SIGNALLING F-BOX PROTEIN 1* (*AFB1*) (Hersch et al., 2014), *AFB2* and *TIR1* (Pucciariello et al., 2018). Elongation in deep shade, therefore, is regulated through interactions between photoreceptors and PIFs to modulate the levels of, and sensitivity to, growth hormones including auxin and brassinosteroid. While studies have reported that the circadian clock gates shade avoidance through transcriptional regulation and by direct interactions with PIFs by clock components (Salter et al., 2003; Soy et al., 2016), the role of the circadian clock on elongation in deep shade has yet to be explored.

Light quantity as well as quality influences the behaviour of the plant circadian clock. In constant conditions, the clock demonstrates fluence-rate dependent behaviour with increases in R, B and UV-B fluence rates causing period shortening (Somers et al., 1998; Fehér et al., 2011). As reported by Jiménez-Gómez et al. (2010) and as demonstrated in chapter 5, R:FR ratio also has an impact on the behaviour of the clock. Haydon et al. (2013) showed that the lengthening of circadian period caused by growth in < 10 μmol m^{-2} s^{-1} light (presumably due to a weakening of sugar signalling to the clock) can be reversed in a PRR7-dependent manner through the addition of sugar to arabidopsis growth media. It is possible that in deep shade, metabolic entrainment of the plant circadian clock could also be weakened. In the context of low PAR, phyA accumulates to very high levels, where its minor absorbtion of B light, alongside its absorbtion of R and FR light, may take on an important role in the entrainment of the clock (Somers et al., 1998). The effects and input mechanisms of monochromatic light to the plant circadian clock are well-studied, but the mechanisms and relative contributions of the different photoreceptors to the entrainment of the plant circadian clock in shaded conditions remains unclear.

In chapter 5, the effect of low R:FR ratio on clock function was sufficient to damp oscillations of clock components in continuous light but not in driven conditions (where there is a strong entraining stimulus); it was hypothesised that by weakening the entraining stimulus in driven conditions (by lowering PAR to simulate deep canopy shade), low R:FR - induced damping of oscillations might be observed. By simulating natural light conditions, it might also be possible to assign a physiological significance to the observations of circadian clock behaviour in low R:FR ratio light. This chapter analyses circadian clock behaviour and its regulation of hypocotyl elongation in simulated deep shade conditions.

6.2 In low PAR, low R:FR ratio elevates peak *TOC1* and evening complex expression

CCA1pro::LUC and *TOC1pro::LUC* plants were entrained in 12 h L/12 h D (12L:12D) under R:FR = 5, PAR = 70 µmol m^{-2} s^{-1}at 20 ºC for 7 days then transferred to PAR = 5 µmol m^{-2} s^{-1} for 4 days to entrain in low PAR before imaging. Three cycles of 12L:12D at R:FR = 0.9 were captured followed by three cycles of 12L:12D at R:FR = 0.05 before return to four cycles of R:FR = 0.9 (Figure 6.1). Peak luciferase signal was reduced by an order of magnitude under PAR = 5 µmol m^{-2} s^{-1} (Figure 6.1c,6.1d) compared to plants in PAR = 47 µmol m^{-2} s^{-1} (Figure 5.2) but the luciferase signal from both *CCA1pro::LUC* and *TOC1pro::LUC* was still rhythmic, with luciferase signal traces displaying kurtoses typical of plants in driven conditions (figure 6.1c,6.1d). *CCA1pro::LUC* signal appeared to be unaffected by the altering R:FR ratio light conditions (figure 6.1c). After 12 h in R:FR = 0.05, peak *TOC1pro::LUC* signal showed

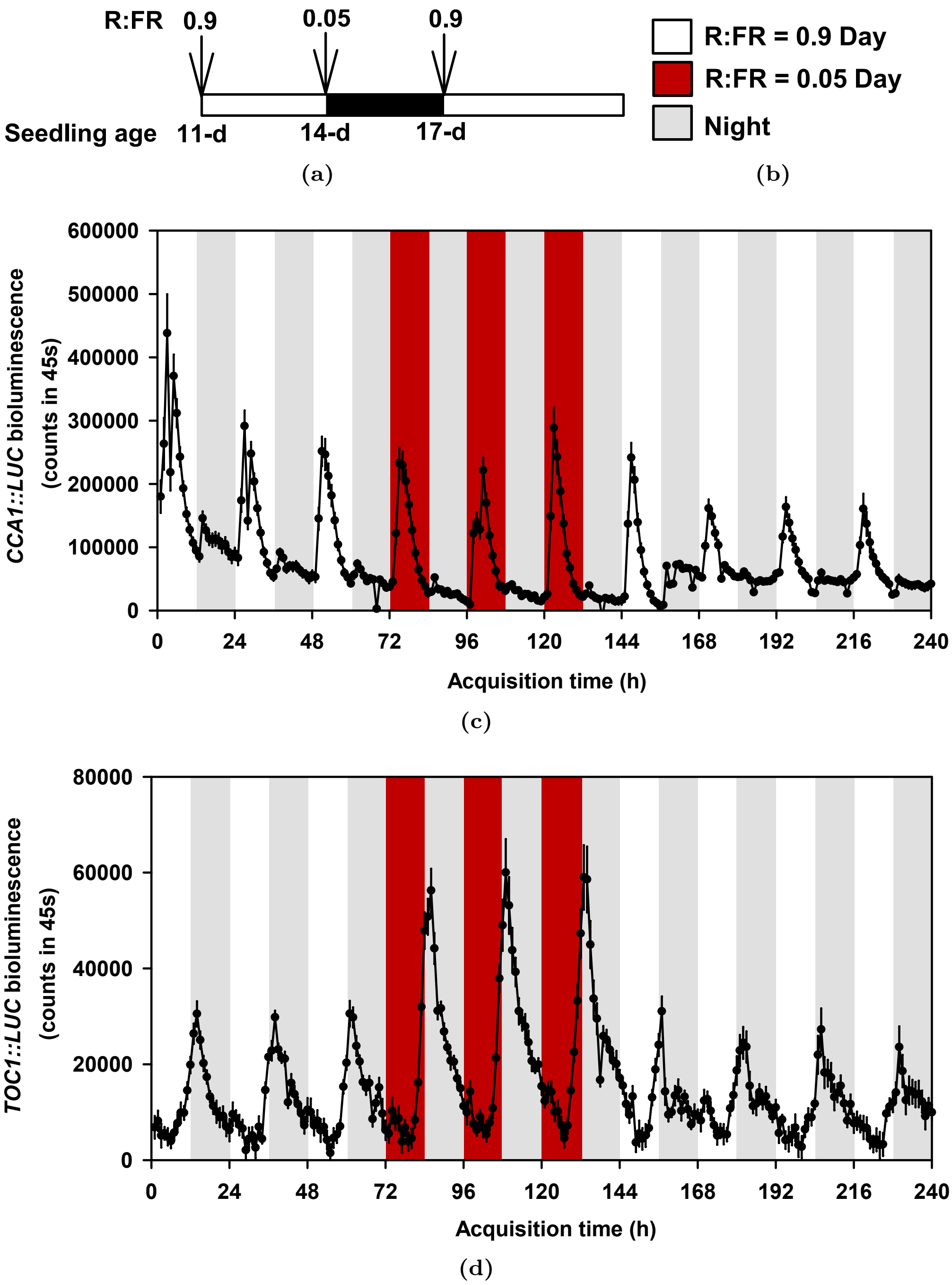

Figure 6.1: In low PAR, low R:FR ratio elevates *TOC1pro::LUC* signal in driven cycles. For luciferase assays in PAR = 5 μmol m^{-2} s^{-1} Plants were grown in WL PAR = 70 μmol m^{-2} s^{-1}, R:FR = 5 for 7 days before transfer to PAR = 5 μmol m^{-2} s^{-1}, R:FR = 0.9 for 4 days. Imaging was carried out during 10 driven cycles of PAR = 5 μmol m^{-2} s^{-1}at R:FR = 0.9 and R:FR = 0.05 as indicated in the experimental design (6.1a). (6.1b) No shading indicates light period at R:FR = 0.9, red shading indicates light period at R:FR = 0.05 and gray shading indicates dark period. (6.1c) *CCA1pro::LUC*, (6.1d) *TOC1pro::LUC*, n = 6, plotted are means +/- 1 S.E.M. .

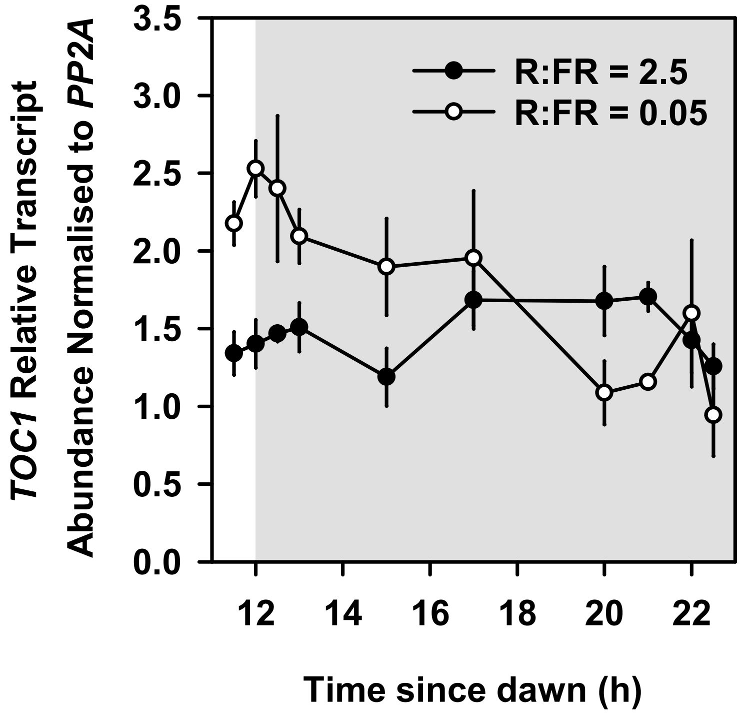

Figure 6.2: *TOC1* relative transcript abundance is elevated by supplemental FR in low PAR . *TOC1* relative transcript abundance normalised to *PP2A* at R:FR = 2.5 and R:FR = 0.05. Col-0 plants were grown in PAR = 5, R:FR = 2.5 or R:FR = 0.05 for 7 days before sampling at the indicated times. Plotted are the means +/- 1 S.E.M. n = 3.

increased amplitude during the night compared to under R:FR = 0.9, while on return to R:FR = 0.9, *TOC1pro::LUC* signal peak amplitude dropped to the level it was before the cycles of R:FR = 0.05 (figure 6.1d). Consistent with the elevation of *TOC1pro::LUC* signal, FR in a background of low PAR also elevated *TOC1* relative transcript abundance, producing a discernible peak in early night that was not present in high R:FR (figure 6.2).

At a higher PAR (47 µmol m^{-2} s^{-1}) (Figure 6.3), FR supplementation did not augment *TOC1* promoter activity. Unlike at low PAR, peak *TOC1pro::LUC* signal steadily increased with time due to increases in leaf area related to plant growth whether it was under low (0.05) or high (1.2) R:FR. Furthermore, peak signal did not decrease after return to high R:FR (figure 6.3). These data suggest that the elevation of *TOC1* promoter activity is a phenomenon that is particular to deep shade.

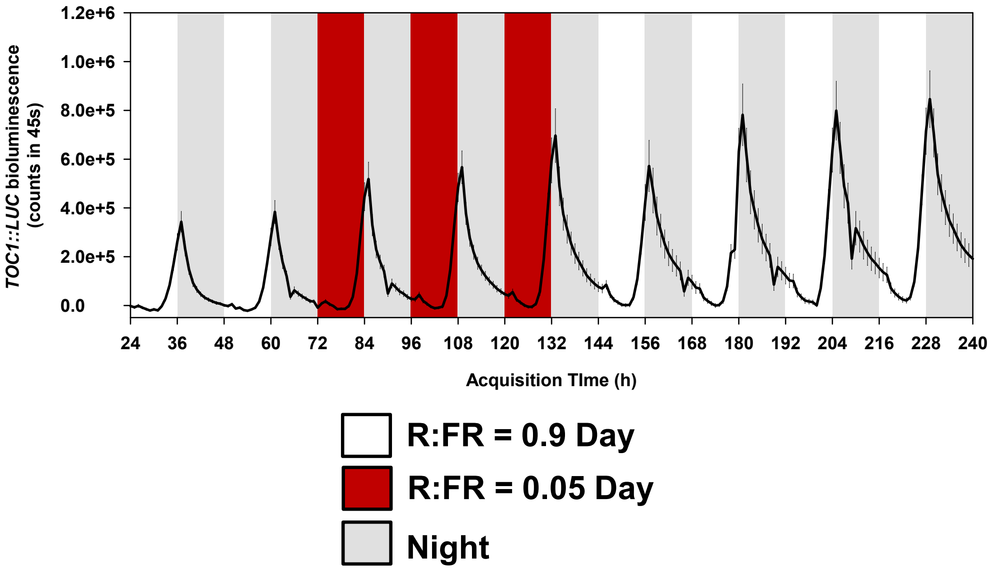

Figure 6.3: At high PAR, supplemental FR does not elevate *TOC1pro::LUC* signal in driven cycles. Plants were germinated in WL PAR = 70 µmol m^{-2} s^{-1}, R:FR = 5 for 7 days before transfer to PAR = 47 µmol m^{-2} s^{-1}, R:FR = 0.9 for 4 days entrainment. Imaging was carried out during two driven cycles of PAR = 47 µmol m^{-2} s^{-1}, R:FR = 0.9 followed by three driven cycles of PAR = 47 µmol m^{-2} s^{-1}, R:FR = 0.05 then a further 4 cycles at PAR = 47 µmol m^{-2} s^{-1}, R:FR = 0.9, as indicated, on clusters of 12 plants. N = 6, plotted are means +/- 1 S.E.M. No shading indicates light period at R:FR = 0.9, red shading indicates light period at R:FR = 0.05 and gray shading indicates dark period.

Given that the *TOC1* promoter contains the evening element motif (AAAATATCT), the transcript abundance of genes encoding evening complex components *ELF3*, *ELF4* and *LUX*, all of which also contain the evening element motif, was also analysed in low PAR and low R:FR. These data were rather variable and did not consistently show alterations in *ELF3*, *ELF4* and *LUX* relative transcript abundance in responses to changes in R:FR in a background of deep shade (figure 6.4)

6.3 phyA and RVE8 regulate TOC1 and evening complex transcript abundance in deep shade

Phytochromes detect the R:FR ratio and communicate information about a plant's environment (Fraser et al., 2016). In particular, phyB is a major regulator of red light signalling whereas FR stimulates phyA signalling in low PAR. phyA has previously been shown to mediate FR entrainment of the plant circadian clock (Wenden et al., 2011), and Tepperman et al. (2001) reported that *TOC1* was upregulated by phyA following FR treatment of etiolated seedlings. Consistent with these data, in low PAR, whereas the *phyB-1* mutant was similar to WT with elevated *TOC1* transcript abundance in low R:FR; the *phyA-1* mutant did not demonstrate the low R:FR - induced elevation of *TOC1* (figure 6.5), suggesting that the elevation of *TOC1* expression in low PAR, low R:FR is phyA-mediated.

To date, there has been no evidence of direct association of phyA with the *TOC1* promoter. The *TOC1* promoter does not appear in a publicly available ChIP-seq and RNA-seq dataset that identified promoters of genes directly targeted by phyA (Chen et al., 2014). There are also very few identified positive regulators in the plant circadian system, which was highlighted by Somers (2012) who lamented the "*dearth of activators*". Recent work has, however, found a new central circadian clock component, REVEILLE 8 (RVE8) to be an activator of

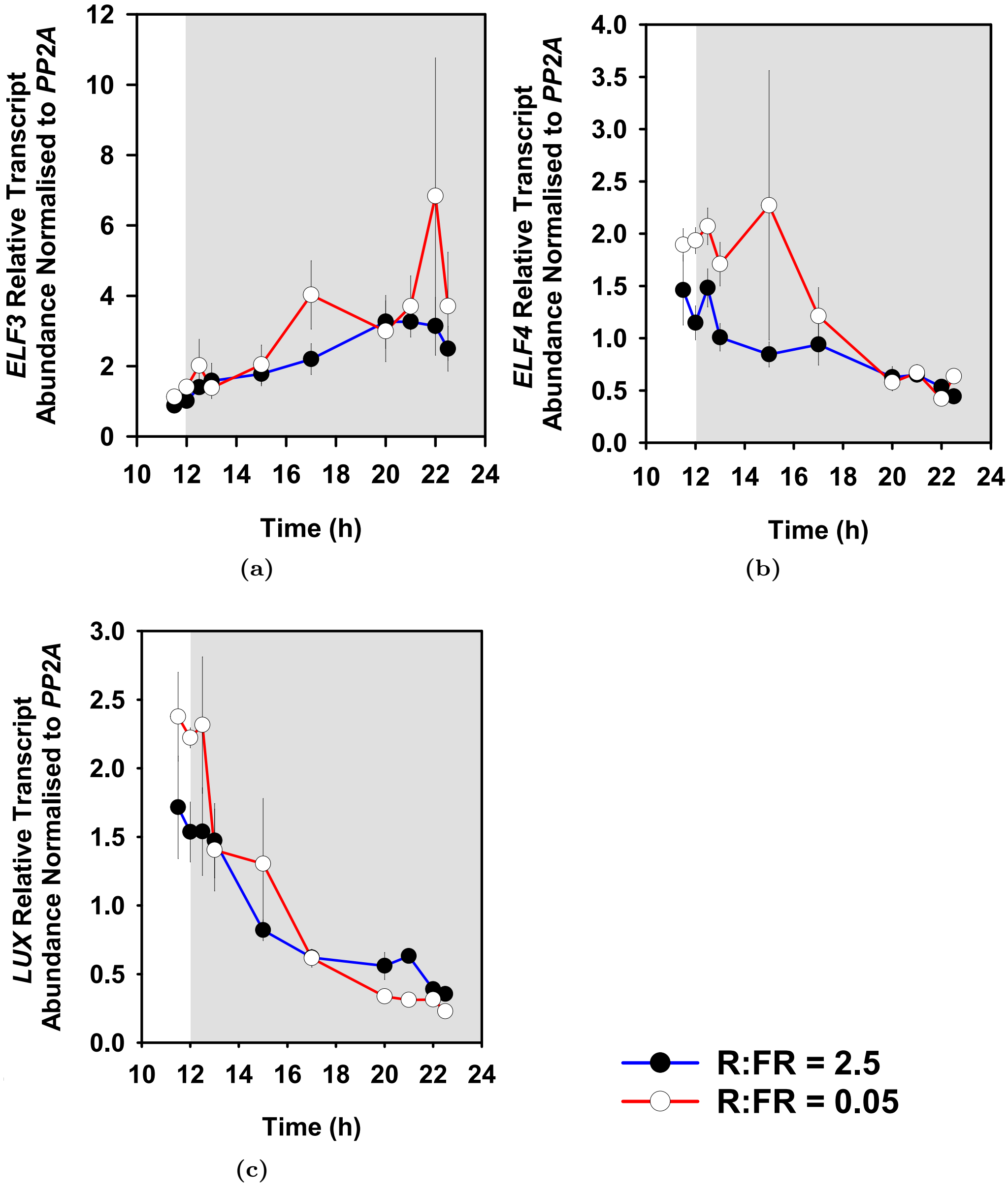

Figure 6.4: Relative Transcript Abundance of evening complex genes under changing R:FR in low PAR. (6.4a) *ELF3*, (6.4b) *ELF4* and (6.4c) *LUX* normalised to *PP2A* at R:FR = 2.5 (blue) and R:FR = 0.05 (red). Col-0 plants were grown in PAR = 5, R:FR = 2.5 or R:FR = 0.05 for 7 days before sampling at the indicated times. Plotted are the means +/- 1 S.E.M. n = 3.

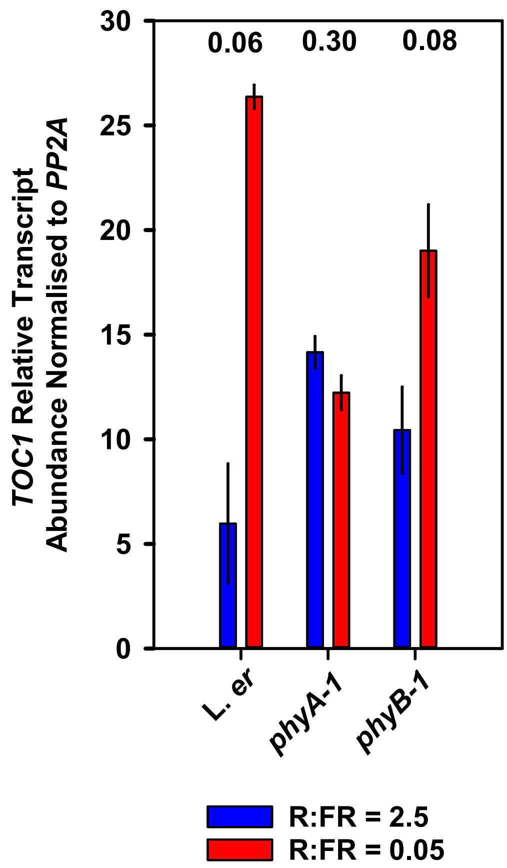

Figure 6.5: In low PAR, low R:FR - induced elevation of *TOC1* transcript is dependent on phyA. Plotted is the mean +/- 1 S.E.M. of *TOC1* relative transcript abundance at dusk normalised to *PP2A* in 3-day-old *phyA-1* and *phyB-1* mutants in the L. *er* background in PAR = 5 µmol m^{-2} s^{-1} at R:FR = 2.5 and R:FR = 0.05, n = 3. Located above the bar charts are p-values from t-tests comparing the $\Delta\Delta$CT values within genotypes.

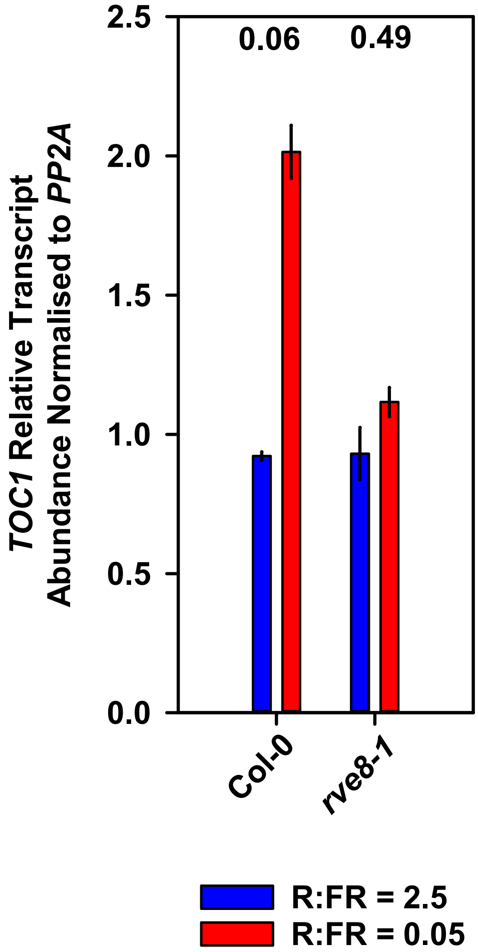

Figure 6.6: In low PAR, low FR - induced elevation of *TOC1* transcript is dependent on RVE8. *TOC1* relative transcript abundance at dusk normalised to *PP2A* in 3 day old *rve8-1* mutant in the Col-0 background in PAR = 5 µmol m^{-2} s^{-1} R:FR = 2.5 and R:FR = 0.05. n = 3, plotted are means +/- 1 S.E.M. Located above the bar charts are p-values from t-tests comparing the ΔΔCT values within genotypes.

gene expression that appears to associate with the evening element of promoters such as *TOC1* to promote histone acetylation, an epigenetic mark associated with gene expression (Rawat et al., 2011; Hsu et al., 2013). In low PAR, the FR-induced elevation in *TOC1* relative transcript abundance was also dependent on the presence of RVE8 (Figure 6.6) . In addition, the evening complex genes *ELF3*, *ELF4* and *LUX*, which also contain the evening element in their promoter regions, had elevated expression at dusk that also appeared to be phyA- and RVE8- dependent (Figure 6.7). Contrasting with Chen et al. (2014), in the conditions used here, *RVE8* relative transcript abundance was not promoted in

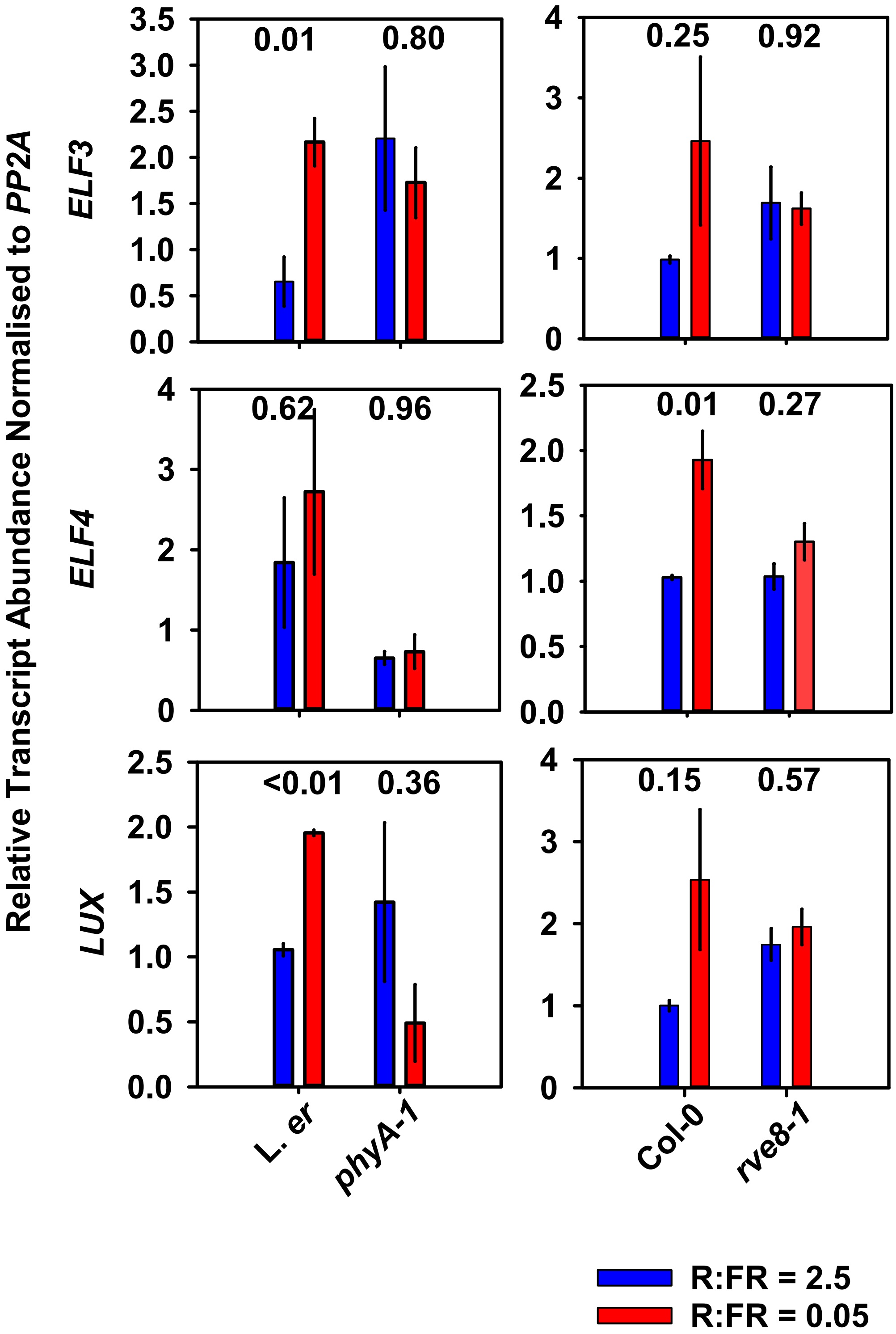

Figure 6.7: phyA and RVE8 regulate transcript abundance of evening complex genes in deep shade. Relative transcript abundance of Evening Complex genes at dusk normalised to *PP2A* in 3 day old *phyA-1* and *rve8-1* mutants grown in PAR = 5 µmol m^{-2} s^{-1} at R:FR = 2.5 and R:FR = 0.05, n = 3, plotted are means +/- 1 S.E.M. Located above the bar charts are p-values from t-tests comparing the ΔΔCT values within genotypes.

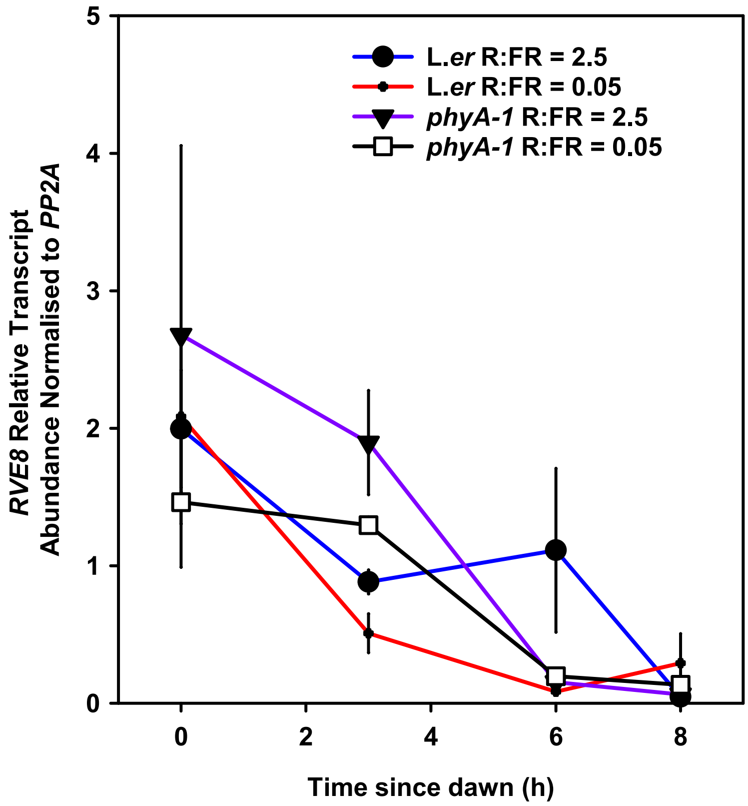

Figure 6.8: In low PAR, low FR did not elevate *RVE8* transcript abundance. Time-course relative transcript abundance of *RVE8* normalised to *PP2A* in 3-day-old L. *er* and *phyA-1* mutants grown in PAR = 5 µmol m^{-2} s^{-1} at R:FR = 2.5 and R:FR = 0.05, n = 3, plotted are means +/- 1 S.E.M.

low R:FR, nor was it phyA-dependent (figure 6.8) . These data suggest that while phyA and RVE8 are required for the upregulation of *TOC1* and evening complex expression, they may not be operating in a linear transcriptional pathway where low R:FR-activated phyA promotes the transcription of RVE8, which promotes the transcription of TOC1.

6.4 TOC1 and RVE8 contribute to phyA-mediated FR inhibition of hypocotyl elongation in deep shade

Martínez-García et al. (2014) reported that phyA was important for the inhibition of hypocotyl elongation in light conditions that simulate plant canopy shade but not neighbour proximity. That is, conditions of low PAR and low R:FR where both B and R light are simultaneously depleted. Additionally, TOC1 has recently been reported to bind to and inhibit PIF3 (Soy et al., 2016) and PIF4 (Zhu et al., 2016) through co-binding to PIF target promoters and the suppression of PIF target gene expression (Soy et al., 2016). Furthermore, Rawat et al. (2011) observed that the fluence rate-dependence of hypocotyl elongation in *rve8-1* mutants resembled mutants in the phyA signalling pathway, while Gray et al. (2017) found that the *REVEILLE* genes inhibited growth of juvenile and adult plants. In this context, the data described above lead to the hypothesis that in low PAR, low R:FR-induced elevation of TOC1 expression may inhibit low PAR-induced hypocotyl elongation. The results described below are from experiments carried out in 12L:12D, 8L:16D and LL photoperiods.

6.4.1 In low PAR, low R:FR-mediated inhibition of hypocotyl elongation is phyA-dependent

phyA-1 plants were grown for 7 days in low PAR at high (2.5) and low (0.05) R:FR ratios under continuous light, 12L:12D or 8L:16D photocycles. Both *phyA-1* and L. *er* seedlings were extremely elongated in all the conditions and photoperiods. Wild-type plants supplemented with FR in a background of low PAR were consistently significantly shorter than plants grown in R:FR = 2.5. The *phyA-1* mutant behaved oppositely, being significantly elongated with FR supplementation, compared to R:FR = 2.5. A two way ANOVA with genotype and R:FR ratio as factors found that there was a highly significant interaction between genotype and R:FR ratio in continuous light (Figure 6.9a), 12L:12D (Figure 6.9b) and 8L:16D (Figure 6.9c) conditions. Taken together, these data confirm previous reports that phyA is responsible for inhibition of hypocotyl elongation in low R:FR in a background of low PAR (Martínez-García et al., 2014).

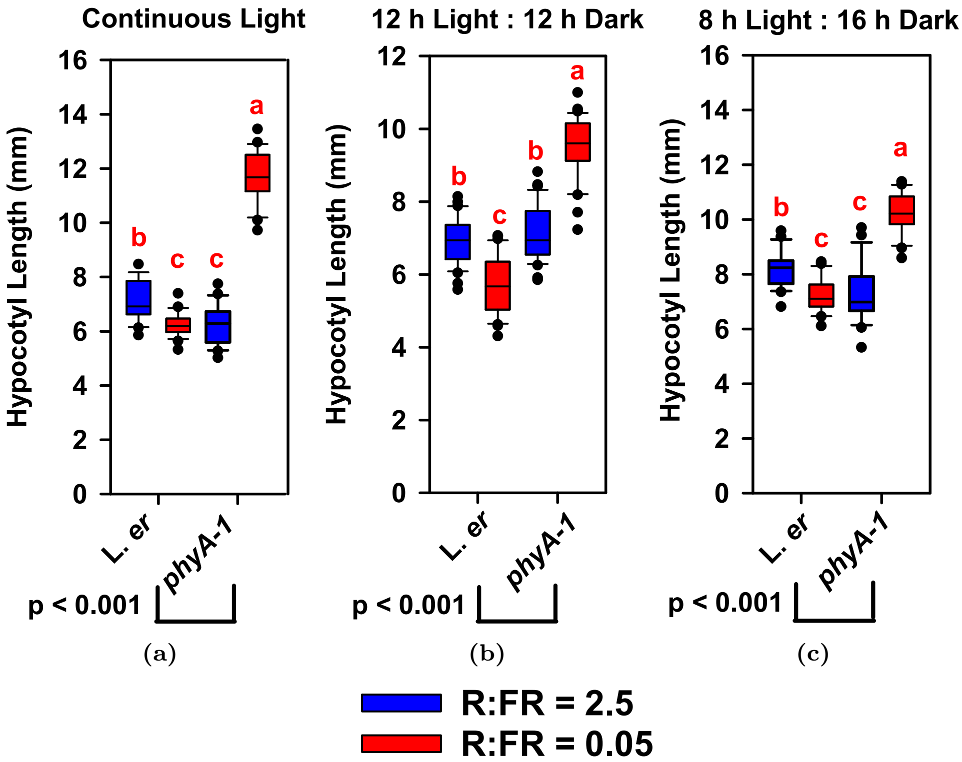

Figure 6.9: In low R:FR with a background of low PAR, phyA inhibits hypocotyl elongation. Seedlings of the *phyA-1* mutant in the L. *er* background were germinated in WL then grown for 7 days in continuous light (6.9a), 12 h light : 12 h dark (6.9b) or 8 h light : 16 h dark (6.9c) under R:FR = 2.5 (blue) or R:FR = 0.05 (red) as indicated. Data are shown as box plots representing the 1st, 2nd and 3rd quartiles with whiskers representing the 10th and 90th percentile. Data are representative of two independent experiments with n = 24. P values for Two-Way ANOVA comparing mutant to wild type using genotype and R:FR ratio as factors are quoted below the box plots. Different red letters above the box plots indicate statistically significant differences by Pairwise Multiple Comparison (Tukey test) at $p < 0.05$.

6.4.2 TOC1 and RVE8 inhibit hypocotyl elongation in deep shade

At low PAR, growth in low R:FR significantly inhibited hypocotyl elongation in WT, *toc1-101* and *rve8-1* mutants in all photoperiods. The magnitude of response to FR supplementation, however, differed depending on photoperiod and genotype (Figure 6.10). In high R:FR, *toc1-101* and *rve8-1* both demonstrated significantly longer hypocotyls than WT in continuous light (Figure 6.10a) and 12L:12D (Figure 6.10b) with *toc1-101* significantly longer than *rve8-1* in both cases. In 8L:16D conditions (Figure 6.10c), *rve8-1* was significantly longer than Col-0 while *toc1-101* in high R:FR did not significantly differ with Col-0 or *rve8-1*. In low R:FR, *toc1-101* and *rve8-1* had significantly longer hypocotyls than WT in continuous light (Figure 6.10a), 12L:12D (Figure 6.10b) and 8L:16D (Figure 6.10c). The hypocotyl phenotypes were significantly longer for *toc1-101* than *rve8-1* in continuous light (Figure 6.10a) and 12L:12D (Figure 6.10b), but in 8L:16D *toc1-101* and *rve8-1* hypocotyl lengths did not significantly differ to each other while both still being significantly elongated compared to WT (Figure 6.10c).

Two-way ANOVA using R:FR ratio and genotype as factors were used to test if the magnitude of hypocotyl inhibition by low R:FR was dependent on genotype. In continuous light, comparing the *toc1-101* mutant to WT found a significant interaction between genotype and R:FR ratio. Similarly, there was a significant interaction between genotype and R:FR when comparing the *rve8-1* mutant to WT. In this instance, the inhibition of hypocotyl elongation in response to low R:FR in the *toc1-101* and *rve8-1* mutants was greater than the response to low R:FR in WT (Figure 6.10a). In 12L:12D, comparing the *toc1-101* mutant to WT found a significant interaction between genotype and R:FR ratio. However, there was not a significant interaction between genotype and R:FR when comparing the *rve8-1* mutant to WT. The inhibition of hypocotyl elongation in response to low R:FR in the *toc1-101* mutant was greater than the response to low R:FR in WT, but not significantly different in the *rve8-1* mutant (Figure 6.10b). In 8L:16D, comparing the *toc1-101* mutant to WT found a significant interaction between genotype and R:FR ratio. Similarly, a two-way ANOVA found a significant interaction between genotype and R:FR when comparing the *rve8-1* mutant to WT. The inhibition of hypocotyl elongation in response to low R:FR in the *toc1-101* and *rve8-1* mutants was less than the response to low R:FR in WT, suggesting that the FR-mediated suppression of hypocotyl elongation was attenuated in 8L:16D photoperiods (Figure 6.10c).

These data demonstrate that both TOC1 and RVE8 inhibit hypocotyl elongation in low PAR in high R:FR and in low R:FR. The observations that both the *toc1-101* and *rve8-1* mutants had significantly attenuated responses to FR supplementation compared to wild-type in 8L:16D suggest that the elevation in TOC1 expression in low R:FR described above contributes to the FR-mediated inhibition of hypocotyl elongation, though statistically significant effects appear to be limited to short day (8L:16D) photocycles.

6.4.3 In deep shade, TOC1 regulation of hypocotyl elongation rate is photoperiod- and R:FR-dependent

Section 6.4.2 demonstrated that the extent of TOC1's role in regulating light-quality-mediated hypocotyl elongation in low PAR is affected by photoperiod length. Previous reports have shown that TOC1 inhibits hypocotyl elongation at the middle and end of night in short day photoperiods, and also gates the shade avoidance response (Soy et al., 2016). The observation that *toc1-101* mutants had a significantly attenuated response to low R:FR compared to wild-type only in short day photoperiods may, therefore, be reflected by differences in elongation rate in 12L:12D and 8L:16D photoperiods. The hypocotyl elongation rate of the *toc1-101* mutant was analysed in low PAR at high and low R:FR and in 12L:12D and 8L:16D photoperiods using timelapse IR photography (figure 6.11). The data presented are from the 48 h period 3 days after germination

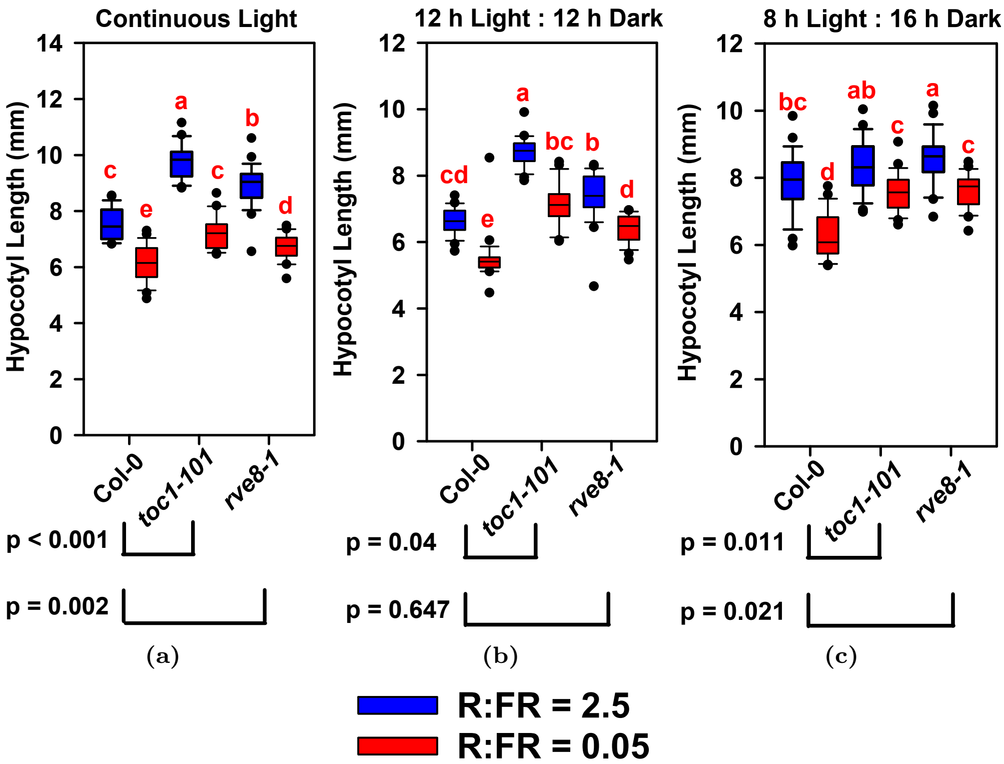

Figure 6.10: TOC1 and RVE8 contribute to the FR-mediated inhibition of hypocotyl elongation in low PAR in a photoperiod dependent manner. Seedlings of *toc1-101* and *rve8-1* in the Col-0 background were germinated in WL then grown for 7 days in continuous light (6.10a), 12 h light : 12 h dark or (6.10b) 8h light : 16h dark (6.10c) under R:FR = 2.5 (blue) or R:FR = 0.05 (red) as indicated. Data are shown as box plots representing the 1st, 2nd and 3rd quartiles with whiskers representing the 10th and 90th percentile. Data are representative of two independent experiments with n = 24. P values for Two-Way ANOVA comparing mutant to wild type using genotype and R:FR ratio as factors are quoted below the box plots. Different red letters above the box plots indicate statistically significant differences by Pairwise Multiple Comparison (Tukey test) at $p < 0.05$.

when the majority of hypocotyl elongation occured.

In 12L:12D, *toc1-101* peak hypocotyl elongation rate, which in both high and low R:FR was greater than Col-0 peak elongation rate, occured around the 4th dawn (24 h) and gradually declined throughout the light period in both high and low R:FR (figure 6.11a,6.11b). In Col-0, peak elongation rate occured at dawn and declined over the course of the light period in high R:FR. In low R:FR, however, elongation rate at dawn was lower than in high R:FR, though still elevated compared to the dark period; and continued to climb until a peak of elongation rate at *c.* 32 h, (which was marginally lower than in high R:FR) when it declined into the dark period. During the dark period, *toc1-101* elongation rate after high R:FR (figure 6.11a) climbed from *c.* 16 h through to dawn at 24 h, whereas after low R:FR (figure 6.11b), the elongation rate started climbing later, from *c.* 20 h until dawn. In Col-0, elongation rate remained low throughout the dark period in both high (figure 6.11a) and low R:FR (figure 6.11b), with elongation rate climbing only in the final *c.* 2 - 3 h before dawn.

In 8L:16D, peak hypocotyl elongation rate occured at dawn in both *toc1-101* and Col-0 in both high and low R:FR, though peak rate, as well as rates in general, were mostly lower in low R:FR compared to high R:FR (figure 6.11c,6.11d). In Col-0, elongation rate was reduced in low R:FR compared to high R:FR at dawn and throughout the light period (figure 6.11c,6.11d). In high R:FR, the elongation rate of *toc1-101* climbed from the start of the dark period until it peaked at dawn, whereas Col-0 elongation rate only started climbing from *c.* 16 h until dawn (figure 6.11c). In low R:FR, elongation rate in *toc1-101* and Col-0 remained low during the dark period until *c.* 20 h when elongation rate climbed sharply in *toc1-101* and only steadily in Col-0 (figure 6.11d). The peak *toc1-101* elongation rate at dawn was higher than Col-0 in low R:FR, with a peak of similar height to Col-0 at dawn in high R:FR (figure 6.11c,6.11d).

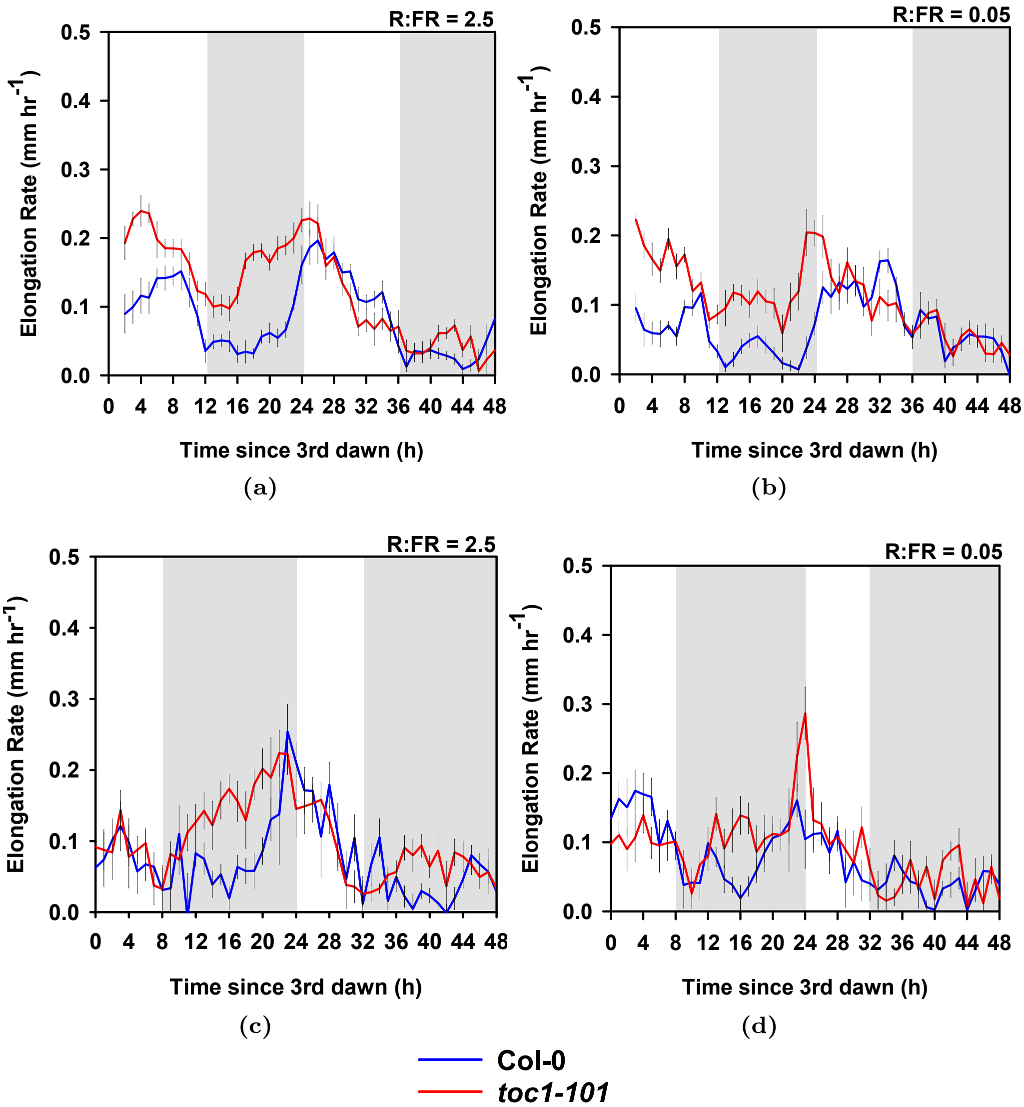

Figure 6.11: In low PAR, TOC1-mediated regulation of hypocotyl elongation rate is R:FR- and photoperiod-dependent. Seedlings of *toc1-101* (red) in the Col-0 (blue) background were germinated in 12L:12D WL then placed into 12L:12D PAR = 5 µmol m^{-2} s^{-1} (6.11a, 6.11b) or were germinated in 8L:16D WL then placed into 8L:16D PAR = 5 µmol m^{-2} s^{-1} (6.11c, 6.11d) at R:FR = 2.5 (6.11a, 6.11c) or R:FR = 0.05 (6.11b, 6.11d). Growth rate was analysed using timelapse IR photography. Plotted are 48 h of hypocotyl elongation rate data starting at dawn on the 3rd day after germination. Data were smoothed using a 3 h rolling average to reduce noise. Unshaded areas indicate the light period whereas shaded areas indicate the dark period, n = 12 +/- 1 S.E.M.

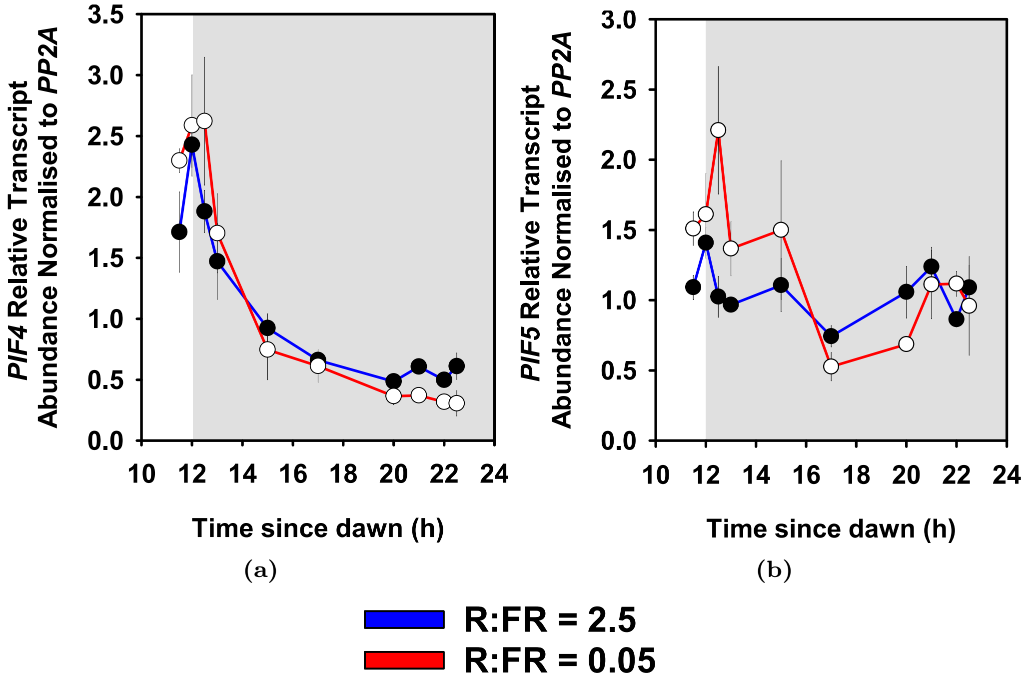

Figure 6.12: *PIF4* and *PIF5* expression is not elevated by FR supplementation in low PAR. Relative transcript abundance of (6.12a) *PIF4* and (6.12b) *PIF5* normalised to PP2A at R:FR = 2.5 and R:FR = 0.05. Col-0 plants were grown in PAR = 5, R:FR = 2.5 or R:FR = 0.05 for 7 days before sampling at the indicated times. Plotted are the means +/- 1 S.E.M. n = 3.

6.5 *PIF4* and *PIF5* transcript abundance is not reduced by FR supplementation in low PAR

Given that the evening complex is reported to suppress *PIF* transcript abundance (Nusinow et al., 2011), the observation that evening complex components had small elevations in transcript abundance with FR supplementation in low PAR (figure 6.7) raised the possibility that low R:FR in low PAR could reduce *PIF* expression. The relative transcript abundance of *PIF4* was unaffected by changing R:FR, whereas *PIF5* transcript abundance was elevated by low R:FR (figure 6.12). As the data above report that low R:FR in a background of low PAR inhibits hypocotyl elongation (section 6.4), these data suggest that *PIF* transcriptional regulation is unlikely to be a component of the mechanism.

6.6 Discussion

The data reported in this chapter show that in a background of low PAR, R:FR ratio affects clock behaviour in driven conditions, which in turn has effects on the circadian regulation of stem elongation. As low R:FR ratio was previously observed to damp circadian oscillations in continuous light but not in driven conditions (where there is a strong entraining stimulus) (chapter 5), it was hypothesised that by weakening the entraining stimulus (by lowering PAR to levels simulating deep shade), low R:FR - induced damping of oscillations might be observed in driven conditions. Results from luciferase assays in low PAR indicated that promoter activity for both *CCA1pro::LUC* and *TOC1pro::LUC* remained rhythmic (figure 6.1), though with peak signal reduced by an order of magnitude compared to growth in higher PAR (compare figures 6.1d & 6.3). It is well-documented that through the process of entrainment, expression of circadian clock components is induced by light either *via* photoreceptors (Oakenfull and Davis, 2017) or through photosynthetic entrainment (Haydon et al., 2013), so it is likely that by reducing the light input into the circadian system, the light-induced activation of circadian clock genes is restricted and hence results in a reduction in peak luciferase bioluminescence.

Unexpectedly, when plants were exposed to low R:FR in low PAR, *TOC1pro::LUC* bioluminescence was augmented and when transferred back into high R:FR, *TOC1pro::LUC* bioluminescence returned to its earlier level (figure 6.1d). FR supplementation specifically increased *TOC1* promoter activity and not *CCA1* (figure 6.1c), suggesting that the increase in amplitude was not simply a general response of the clock to entrainment by higher light levels but rather an upregulation of *TOC1* in low R:FR. Furthermore, while the elevation of *TOC1pro::LUC* bioluminescence seems to be an effect that is low PAR-specific, it is likely that the mechanism still operates at higher PAR, but due to an overall increase in amplitude range of the circadian oscillator in higher PAR, any effects are masked (figure 6.3). The increase in *TOC1* promoter activity in low R:FR correlated with an increase in *TOC1* relative transcript abundance (figure 6.2), it would therefore also be interesting to analyse the effect of low R:FR on TOC1 protein abundance in low PAR. As of the writing of this thesis, optimisation of the TOC1 western blot protocol had not been completed so data on this are unavailable.

One explanation for the elevated expression of circadian clock components could relate to the Emerson effect (Emerson, 1957): long wavelength red light (700 nm) stimulates photosystem (PS) I whereas red (680 nm) light stimulates PSII, meaning that maximum photosynthetic rate is achieved with a combination of these wavelengths. It is possible, therefore, that the addition of FR to the low PAR conditions increases the rate of photosynthesis (which will be extremely low in deep shade conditions) to strengthen sugar entrainment of the circadian clock and hence augment the expression of circadian clock components. In low PAR (< 10 µmol m^{-2} s^{-1}), the addition of sugar to Arabidopsis growth media shortens circadian period in a PRR7-dependent manner (Haydon et al., 2013). To test the involvement of photosynthetic entrainment in the FR-induced elevation of circadian clock gene expression in low PAR, it would be interesting to analyse the behaviour of clock gene promoter-driven luciferase reporters in the *prr7-11* mutant with and without FR supplementation.

Consistent with previous studies (Tepperman et al., 2001; Wenden et al., 2011; Hsu et al., 2013), phyA and RVE8 appear to be responsible for mediating the FR-induced upregulation of *TOC1* as well as evening complex genes in low PAR (section 6.3). Whereas phyA is required for the FR-induced upregulation of *TOC1* transcripts, phyA does not directly associate with the *TOC1* promoter, but it does associate with the *RVE8* promoter to induce *TOC1* expression in response to FR (Chen et al., 2014). RVE8 is a clock-regulated transcriptional activator within the circadian oscillator that mediates histone acetylation at EE-containing promoters (Hsu et al., 2013). The low R:FR-induced elevation at dusk of *TOC1*, and evening complex, transcripts was also dependent on the presence of RVE8 (figure 6.6,6.7). In the conditions used here, low R:FR did not augment *RVE8* transcript abundance in a phyA-dependent manner or otherwise (figure 6.8). Thus, the data reported in section 6.3 suggest that the elevation of *TOC1* and evening complex expression by FR in low PAR is both phyA- and RVE8-dependent but that they do not operate in a linear transcriptional pathway. One possibility is that phyA and RVE8 have post-translational interactions in low R:FR, perhaps leading to an increase in RVE8 movement to the nucleus through the FHY1/FHL pathway, used for nuclear import of phyA (Hiltbrunner et al., 2006; Genoud et al., 2008) resulting in increased expression of evening genes. Another possibility is that phyA could still be associating with the *RVE8* promoter after FR irradiation, but rather than promoting *RVE8* expression, its association may induce alternative splicing of *RVE8* transcripts. Shikata et al. (2014) reported that phyA and phyB can mediate alternative splicing of multiple transcripts in R light, though it is unclear if FR can trigger a similar response. Alternative splicing of circadian clock components in response to environmental stimuli is also not unprecedented as it has been reported that *CCA1* has temperature-dependent splicing variants (Seo et al., 2012). It is interesting that, in spite of having a partially redundant role with RVE4 and RVE6, the *rve8-1* mutation is sufficient to remove the FR-induced elevation of *TOC1* and evening complex expression at dusk (Figure 6.6,6.7). This may be because, according to the ChIP- and RNA-seq dataset made available by Chen et al. (2014), phyA only interacts with the *RVE8* promoter and not with the promoters for *RVE4* and *RVE6*.

Recent studies have found that TOC1 mediates the circadian gating of hypocotyl elongation through direct interaction with PIFs and the suppression of the expression of PIF targets (Soy et al., 2016; Zhu et al., 2016). Given that phyA and RVE8 have also previously been implicated in the control of hypocotyl elongation (Martínez-García et al., 2014; Gray et al., 2017), it was hypothesised that the phyA- and RVE8-dependent augmentation of TOC1 expression by FR may be a mechanism for hypocotyl elongation inhibition in deep shade. In contrast to results from canonical shade avoidance experiments, where supplementation of FR in a background of high PAR provokes hypocotyl elongation (Franklin, 2008), FR supplementation in deep shade inhibited hypocotyl elongation in wild type plants (figure 6.9,6.10). Consistent with previous reports (Martínez-García et al., 2014), phyA inhibits hypocotyl elongation in low R:FR ratio and low PAR. Comparison of wild type and *phyA-1* mutants suggests that phyA is responsible for the majority of the FR-induced inhibition of hypocotyl elongation in deep shade (figure 6.9). The observation that a reduction in R:FR in low PAR promoted hypocotyl elongation in the phyA mutant is likely a consequence of phyB inactivation: The sensitivity of the phyB photoreceptor is such that even at extremely low fluence rates of red light phyB signalling is activated (Reed et al., 1994), the addition of FR to this situation will cause activated phyB to revert to its non-signalling P_r form. The role of phyA, as has been surmised in previous reports (Martínez-García et al., 2014), is likely to be prevention of over-elongation in deep shade, which is an acute resource limiting condition where there is reduced activation of both phyB and cryptochrome photoreceptors (de Wit et al., 2016). End-point hypocotyl elongation data indicate that TOC1 and RVE8 significantly inhibit hypocotyl elongation in deep shade, both with and without FR supplementation. In short day photocycles (8L:16D), there was a significant attenuation of FR-mediated inhibition of hypocotyl elongation in the *toc1-101* and *rve8-1* mutants compared to WT (Figure 6.10), which suggests that in short day conditions, the elevation of TOC1 expression increases the magnitude of FR-induced inhibition of hypocotyl elongation. In longer photoperiod conditions, however, the *toc1-101* and *rve8-1* mutants did not display a significant attenuation of FR-induced inhibition of hypocotyl elongation when compared to wild type controls. This could result from FR supplementation activating multiple phyA-regulated growth repressors, which dominate in the absence of TOC1 or RVE8. This photoperiod dependence could alternatively be explained by rhythmic hypocotyl growth in low PAR. In high R:FR (figure 6.11a,6.11c), peak hypocotyl elongation rate occured around dawn and remained high thoughout the light period due, perhaps, to PIF stabilisation because of a lack of photoreceptor activation in low PAR. In low R:FR (figure 6.11b,6.11d), elongation rate was marginally lower during the light period, maybe because of inhibition through phyA activity in low R:FR. During the dark period, after a high R:FR light period in both day lengths (figure 6.11a,6.11c), *toc1-101* mutant elongation rate climbed earlier in the night than in Col-0, which is consistent with previous reports (Soy et al., 2016). In low R:FR (figure 6.11b,6.11d), however, elongation rate of *toc1-101* mutants during the dark period did not start climbing earlier than Col-0. Instead, *toc1-101* had a higher peak elongation rate at dawn than Col-0, an observation that was particularly clear in the 8L:16D low R:FR condition when *toc1-101* elongation rate climbed sharply between 20 and 24 h to match that of Col-0 peak elongation rate in high R:FR at dawn in 8L:16D (figure 6.11d). The larger difference in peak elongation rate at dawn in low PAR and low R:FR between *toc1-101* and Col-0 in 8L:16D compared to 12L:12D may, therefore, account for the observation that in 8L:16D, mutation of *TOC1* significantly attenuated low R:FR-induced inhibition of hypocotyl elongation (figure 6.10). Furthermore, the observation that the climb in elongation rate of *toc1-101* in low R:FR was delayed compared to *toc1-101* in high R:FR could be consistent with the notion that TOC1 has partial redundancy with the other PRRs to inhibit elongation sequentially through the night (Martín et al., 2018). It would, therefore, be interesting to analyse *PRR5*, *PRR7* and *PRR9* transcript abundance to see if these clock components behave similarly to *TOC1* in low R:FR. Hypocotyl analysis of a PRR knockout mutant, *i.e. prr579* crossed with the *toc1-101* mutant could also be informative, provided the seed is viable.

(Niwa et al., 2009) suggest that the external coincidence model (Nozue et al., 2007) can account for photoperiod-dependent promotion of hypocotyl elongation in short days: Shortening the photoperiod shifts the timing of peak PIF abundance into the night, where it is protected from activated photoreceptors. The combination of short day photoperiods and the low PAR of deep shade reducing photoreceptor activation leaves PIFs predominantly regulated by the circadian clock. As PIF transcript abundance was not reduced by lowering the

R:FR ratio in low PAR (Figure 6.12), FR-induced alterations in the circadian regulation of PIF activity are likely restricted to post-translational interactions with the PRRs (Soy et al., 2016; Martín et al., 2018), and perhaps ELF3 (Nieto et al., 2015).

Neither the *toc1-101* or *rve8-1* mutants fully resembled the *phyA-1* mutant in their responses, suggesting that there is functional redundancy with other phyA-regulated suppressors of elongation. Indeed, given that the PRRs 9, 7 and 5 have been reported to inhibit hypocotyl elongation in a manner very similar to TOC1 (PRR1) (Martín et al., 2018) alongside the finding that PRR5 is RVE8-regulated through the evening element in its promoter (Rawat et al., 2011), it would be interesting to test if these circadian clock genes are also FR-induced and whether they too contribute to the FR-induced inhibition of hypocotyl elongation by phyA. In addition, since the PRRs sequentially repress hypocotyl elongation through their interaction with PIFs (Martín et al., 2018), it would be interesting, as already noted, to see if the relative contributions of the different PRRs to the inhibition of hypocotyl elongation were shade and photoperiod-dependent.

Keeping the circadian clock robustly entrained in low PAR could be another adaptive significance of the FR-induced upregulation of *TOC1* and other evening-phased circadian clock genes. In the absence of FR irradiation in low PAR, the amplitude range of *TOC1pro::LUC* oscillations was limited compared to plants grown in high PAR (compare figures 6.1d & 6.3), yet the addition of FR substantially boosted the peak promoter activity for *TOC1*. Taken alongside the result that a peak in *TOC1* relative transcript abundance at dusk was observed under FR irradiation in low PAR but not in the absence of FR (figure 6.2), it follows that FR light signalling mediated by phyA to the circadian oscillator may become more important in situations of low PAR (like deep shade) for keeping the circadian oscillator entrained. This suggestion is consistent with the hypothesis that by co-opting an array of photoreceptors, the plant circadian clock can entrain to a range of spectral qualities (Somers et al., 1998). If this were the case then the inhibition of hypocotyl elongation by TOC1 after FR irradiation could be a consequence of having a properly entrained circadian clock - rather than purely a direct antagonism of shade avoidance. Correct circadian clock function is dependent on correct entrainment, therefore, an incorrectly entrained circadian clock will have compromised function. In support of this notion, it is likely no coincidence that Arabidopsis lines with disrupted circadian clocks (*e.g. CCA1-OX*) often have long hypocotyls.

The data presented in this chapter make contributions to the understanding of FR signalling to the circadian clock. Mechanistically, whereas ELF4 was previously identified as a potential node for the mediation of FR signalling by phyA to the circadian oscillator (Wenden et al., 2011), the data presented here suggest that RVE8 could link phyA and evening-phased genes (such as *ELF4*) to mediate FR signalling to the circadian clock. In low PAR, FR signalling to the clock may take on an adaptive significance: The depletion of B and R wavelengths in deep shade give reduced external cues to the day/night cycle. The circadian clock has, therefore, recruited a photoreceptor that signals in FR in order to still receive timing information for entrainment in deep shade. Another potential adaptive significance, which may be a by-product of the recruitment of phyA by the circadian clock for entrainment in deep shade, is the contribution, through the FR-induced elevated expression of TOC1, to the inhibition of hypocotyl elongation in low PAR in short day photoperiods. This photoperiod and light combination creates a resource- and external cue-limited situation where plants are at the greatest risk of over-elongation and death; in these conditions limiting hypocotyl elongation, therefore, takes on an acute level of importance.

Chapter 7

General Discussion

As plants cannot move away from unfavourable environmental conditions, they instead adapt their development to improve their chance of survival and reproductive success. The sensing of light conditions is especially important to plants as they are photoautotrophs and for many plant species, shade is harmful. On the perception of shade, or cues that suggest impending shade, shade-avoiding species activate a powerful developmental program that prioritises the elongation of stems and petioles and the elevation of leaves. Shade avoidance responses include several morphological adaptations at every life stage of the plant. In seedlings, hypocotyls elongate; while in adult plants, petioles elongate, leaves are elevated through hyponasty, and flowering is accelerated (Fiorucci and Fankhauser, 2017). Over-elongation is, however, detrimental to plant survival as it leaves them susceptible to lodging, wind damage and water loss. The dramatic morphological changes triggered by shade perception are limited by a number of mechanisms. Several of these mechanisms involve auto-regulatory negative feedback, *e.g.* HFR1 (Hornitschek et al., 2009) or PAR1 and PAR2 (Galstyan et al., 2011). Light quality changes can trigger photoreceptor signaling pathways, which also have the effect of inhibiting elongation and hyponasty. Intuitively, reversing the light quality changes that promote shade avoidance limits elongation, *e.g.* elevating R:FR through short term pulses of

R light to simulate sun flecks inhibits shade avoidance (Sellaro et al., 2012). It has previously been shown that UV-B, perceived by UVR8, inhibits shade avoidance (Hayes et al., 2014). FR, detected by phyA has also been shown to limit elongation and improving seedling survival in low PAR (Yanovsky et al., 1995; Martínez-García et al., 2014). The endogenous plant circadian clock manages a plant's resources to maximise its fitness in rhythmic environments. For instance, the circadian clock regulates starch metabolism such that carbohydrate availability is maintained through the night until the following dawn (**?**). A mechanism through which the clock manages resources is through a process termed circadian gating, where the clock restricts environmental responses to particular phases of the 24 h cycle (Hotta et al., 2007). It has been argued that circadian gating of responses to UV-B can be interpreted as the saving of resources during acclimation to UV-B without negatively impacting fitness (Fehér et al., 2011; Takeuchi et al., 2014). Modern commercial growing environments have the capability to provide supplemental lighting regimes to crops. Knowledge of plant responses to different light qualities and the circadian regulation of these responses may present opportunities to improve the yield and product quality of commercially grown crops without genetic manipulation.

UV-B applied to commercial horticulture

Chapter 4 presents evidence that supplemental low dose UV-B inhibits shade avoidance in Coriander, consistent with previous reports in Arabidopsis (Hayes et al., 2014). Coriander seedlings shade avoid and their hypocotyls were significantly inhibited by supplemental UV-B (figure 4.3). Supplemental UV-B in a background of low R:FR increased the *compactness*, of mature Coriander plants through limiting low R:FR-induced petiole elongation (figure 4.6). PAR and UV-B levels in nature are correlated but are also highly variable due to cloud cover and the height of the sun. Experiments were conducted in the glasshouse to investigate the importance of the UV-B : PAR ratio. Consistent with data presented in section 4.3.1, supplemental UV-B in the glasshouse significantly inhibited hypocotyl elongation when Coriander was grown in dense stands (section 4.5.1). Three different intensities of UV-B delivered for the duration of the photoperiod were similarly effective at inhibiting hypocotyl elongation (section 4.5.2). This result, where low intensity UV-B is as effective as high intensity UV-B, likely reflects the sensitivity of both the UV-B perception mechanism and the mechanism of the inhibition of hypocotyl elongation by UV-B. These data demonstrate that UV-B is a potent brake on shade avoidance in Coriander and that UV-B applied to this commercial crop improves its morphological product quality. It is likely that UV-B treatments limit elongation in other herb crops that have similar branching habits to coriander, such as parsely (*Petroselinum crispum*). Torre et al. (2012) reported that the use of UV-B transparent greenhouse cladding materials allowed growers to reduce the amount of plant growth retardant chemicals used on Poinsettia (*Euphorbia pulcherrima*). It would be interesting to analyse herb growth under UV-B transparent materials to see if these conditions could also give meaningful improvements in product quality as it would avoid energy consumption costs.

Previous reports have suggested that altering R:FR and UV-B irradiation can impact chlorophyll abundance and photosynthetic efficiency (Bartoli et al., 2009; Davey et al., 2012). However, the data reported in figure 4.14 suggest that neither R:FR ratio nor UV-B irradiation significantly affect leaf chlorophyll content in Coriander. It may still be interesting for future work to analyse photosynthetic efficiency, as it is reported that UVR8 increases photosynthetic efficiency in elevated levels of UV-B (Davey et al., 2012). Current opinion sees UV-B as an informational signal that is both a cue for photomorphogenesis and an acclimating signal that activates UV-B defences prior to UV-B damage (Hideg et al., 2013; Jenkins, 2014). Total antioxidant capacity in Coriander was increased by supplemental UV-B in high R:FR, which is consistent with studies in Arabidopsis (Csepregi et al., 2017). In low R:FR, UV-B supplementation did not significantly increase total antioxidant capacity, which may reflect a diverting of resources away from defence and toward elongation (Yang et al., 2016). Alternatively, low R:FR may be interpreted as a signal of reduced light, *i.e.* shade, and hence a reduced risk of photosystem damage from high levels of light (Banaś et al., 2012). Low R:FR signaling may override UV-B signaling in this context as sunlight levels of UV-B alongside a low R:FR would only be experienced by plants on emergence from canopies. Flavonoids absorb UV-B radiation and act as sun-screening compounds in plants (Agati and Tattini, 2010). Figure 4.17 demonstrates that supplemental UV-B increased Coriander flavonol glycoside content in both high and low R:FR, similarly to Arabidopsis. Augmenting the total antioxidant capacity and flavonoid content may have health benefits to consumers (Dou et al., 2017). However, flavonoids such as quercetin are associated with bitter flavours so the aesthetic and nutritious benefits that UV-B supplementation has on Coriander ought to be balanced against potential adverse effects on flavour.

Work in this thesis has therefore shown that UV-B inhibits shade avoidance in Coriander in both controlled climate chambers and glasshouses. It was hypothesised that there may be a time of day when shade-avoiding Coriander is more sensitive to inhibition of elongation by UV-B, and that this may be circadian-regulated. A short dose of UV-B given at that point could provide product quality improvements that avoid the economical, environmental and safety drawbacks of UV-B supplementation for long durations. Timelapse IR photography of Coriander seedlings suggested that peak elongation rate for shade-avoiding Coriander hypocotyls occurred during the light period (section 4.4.1). Furthermore, experiments in Arabidopsis suggested that there was a trend for short dose UV-B treatments at the middle of the day to be more effective than treatments at the start or the end of day (section 3.2.1).

Understanding time-of-day effects in UV-B-mediated hypocotyl inhibition

Experiments on plants over-expressing *CCA1* (figure 3.5) suggested that the inhibition of hypocotyl elongation by UV-B is circadian regulated, like several other reported UV-B responses (Fehér et al., 2011; Takeuchi et al., 2014). A previously suggested component of the mechanism for the antagonism of shade avoidance by UV-B, *GA2ox1* (Hayes et al., 2014), has its UV-B induction gated by the circadian clock with peak transcript occurring at and around 6 - 8 h after dawn and subjective dawn in LD (figure 3.12) and LL (figure 3.9a,figure 3.9b) conditions respectively. In addition, the transcript abundance of the auxin synthesis gene *YUCCA8* (figure 3.16a,3.16b) and the auxin signaling gene *IAA29* (figure 3.17a,3.17b) peaked at 6 - 8 h after dawn in LD in both high and low R:FR. This pattern of transcript abundance in auxin-related genes is probably a consequence of a peak in *PIF* transcript also at 6 - 8 h after dawn in these conditions (figure 3.15), and the likely stabilisation of PIF proteins in low R:FR. At all tested time-points, UV-B irradiation severely reduced transcript abundance for these genes, with the greatest reductions in transcripts occurring 6 - 8 h after dawn. It appears that the trend for the middle of the day 4 h UV-B treatment to give the greatest inhibition of shade avoidance in Arabidopsis is a result of the coincidence of: 1) the circadian gated peak of UV-B-induction of GA catabolism genes, and 2) the observation that UV-B is such a strong inhibitor of auxin signaling that the potential for the greatest reduction in auxin signaling occurs when auxin-related genes would otherwise be at peak expression.

Short 4 h UV-B treatments elicited a significant inhibition of hypocotyl elongation in shade-avoiding Coriander; but unlike in Arabidopsis, applying the treatments at different times of day only produced marginal differences that did not significantly differ (figure 4.8). This observation may reflect species-specific differences in the circadian regulation of hypocotyl elongation and UV-B perception between Arabidopsis and Coriander. Another reason only marginal differences were observed between time points in Coriander could be that as UV-B is such a potent inhibitor of auxin signaling, even short doses of UV-B saturate the suppression pathway. However, the observation that a short dose of UV-B did not inhibit hypocotyl elongation to the same extent as a UV-B dose for the full duration of the photoperiod (figure 4.8) does not support this conclusion and instead suggests that, after UV-B irradiation is stopped, hypocotyl elongation rate increases. This possibility may mean that multiple short doses of UV-B irradiation could be as effective at inhibiting hypocotyl elongation as a single large dose. Further experiments that analyse elongation rate in Coriander during and in the hours after short UV-B treatments would be required to resolve this point. It would also be interesting to test if the most effective time-of-day for UV-B inhibition of hypocotyl elongation were shifted in different photoperiods. For instance, in short photoperiods (8L:16D) peak hypocotyl elongation rate occurs at the end of the night, so a UV-B dose that coincides with this peak may elicit the greatest response. The mechanism for the circadian gating of UV-B responses remains unclear. Previous studies suggest that there is no central mechanism and that the circadian gating of UV-B responses differs gene-by-gene (Fehér et al., 2011; Takeuchi et al., 2014). Given that timings of peak induction by UV-B differs between the genes tested in this thesis (*HY5*, *HYH* and *GA2ox1*), and the observation that UV-B-induced *GA2ox1* transcript damps high whereas *HY5* and *HYH* UV-B-induced transcript damp low, it is likely that they are also gated by separate clock components. It is possible that clock components such as the PRRs may mediate the circadian gating of these genes, perhaps through association with G-box-like motifs in promoters (Liu et al., 2016) or through co-binding at promoters with transcription factors in a manner that inhibits transcriptional activity (Martín et al., 2018). PRRs may mediate the circadian gating of *GA2ox1* (figure 3.18a), but more work, using the *prr579* triple mutant would be required to investigate this. It has previously been suggested that the circadian gating of UV-B responses could be considered as the saving of resources during acclimation to UV-B without loss of fitness (Fehér et al., 2011; Takeuchi et al., 2014). By limiting the peak of UV-B-induction of *HY5*, *HYH* and *GA2ox1* transcripts to the light period the circadian clock is also preventing UV-B responses from occurring at inappropriate times-of-day, *i.e.* at night when there is no sunlight. A very remote possibility is that circadian gating of UV-B responses prevents the stimulation of UVR8 signaling by moonlight. Carver et al. (1974) reported that the moon reflects sunlight rather poorly and as wavelengths decrease, reflectivity also decreases, though interestingly, UV-C is reflected better than UV-B. As UVR8 is sensitive to UV-B at low fluence rates, it may be interesting to test the dimer/monomer status of the UVR8 protein in moonlight levels of UV-B. Over-expression of *CCA1* both altered the pattern and increased the magnitude of the time-of-day differences in UV-B inhibition of hypocotyl elongation (figure 3.5,3.5). An alternative interpretation of these data is that circadian gating of the inhibition of hypocotyl elongation by UV-B acts to minimise time-of-day differences during the light period. Indeed, there may be no adaptive advantage to this process being more sensitive at one point than another during the light period.

Circadian Regulation in Deep Shade

Experiments that tested the circadian gating of UV-B-induced genes led to the unexpected observation that in LL low R:FR, the circadian gating of the UV-B induction of *HY5*, *HYH* and *GA2ox1* transcripts lost the pattern of UV-B-mediated induction that occurred under LL high R:FR (section 3.3.1). While this loss of circadian gating did not extend to plants in LD (section 3.3.2), this result opened up a new avenue of investigation, which aimed to understand why circadian gating was lost in LL low R:FR. Rhythms of *CCA1* and *TOC1* transcripts were also lost in LL low R:FR when compared to LL high R:FR conditions (figure 5.1). Consistent with these observations, luciferase assays showed that rhythms of *CCA1* and *TOC1* promoter activity were both damped in LL low R:FR (figure 5.2). Interestingly, while both *CCA1* transcript and promoter activity damped low (figure 5.2a), *TOC1* transcript and promoter activity damped high (figure 5.2b), which was also consistent with the transcript abundance data (figure 5.1). Previous work has described a similar effect that occurs in monochromatic FR conditions: Wenden et al. (2011) reported that in these conditions, circadian clock genes had damped transcript and promoter activity in a mechanism that involves ELF4. In addition, and consistent with the data reported in this thesis, it was reported that morning gene expression was suppressed whereas evening gene expression was promoted (Wenden et al., 2011). Mechanisms for circadian gating likely include the direct association of clock components with promoters to bring about transcriptional repression or chromatin remodeling. It is, therefore, proposed that damping of oscillations of circadian clock components in LL low R:FR may explain the loss of circadian gating of UV-B-induced genes (section 3.3.1). Questions that remain include: whether more circadian clock components are damped in LL low R:FR, and whether the circadian gating and regulation of the expression of genes beyond UV-B responses are similarly affected. Both possibilities seem likely due to the complex interlocking feedback loop architecture of the clock and the large proportion of genes that have been shown to be circadian regulated (Harmer et al., 2000; Covington et al., 2008; Michael et al., 2008). Another interesting observation was that in LL low R:FR, both *CCA1* and *TOC1* promoter activity had significantly shorter periods than under high R:FR (figure 5.3b,5.3b). It is possible that as increasing the intensity of FR LEDs was used to lower the R:FR ratio, the shortening of period could be a consequence of Aschoff's rule (Aschoff, 1979). Alternatively, increasing FR fluence rate may increase photosynthesis and hence the sugar entrainment of the circadian oscillator (Haydon et al., 2013). The influence of R:FR on the pace of the circadian clock may also be mediated by a hitherto undescribed mechanism. Further experimentation using a range of R:FR ratios without changing the total photon fluence rate would help resolve the question of whether total photons or R:FR alters period length.

Low R:FR was sufficient to damp oscillations of clock components in continuous light, but not in driven conditions at a PAR of *c.* 50 µmol m^{-2} s^{-1}, likely due to the presence of a strong entraining stimulus provided by LD cycles. It was subsequently reasoned that were the entraining stimulus *weakened* through experimenting in low PAR, low R:FR could induce damping of oscillations in driven conditions as well. Propitiously, coupling low PAR to low R:FR also mimicked the ecologically relevant conditions of deep shade. Measurement of PAR and R:FR ratio in deep shade conditions in the field suggested that R:FR of < 0.1 could occur in PAR of < 10 µmol m^{-2} s^{-1} (figure 2.2a,2.2b). In laboratory conditions that mimic deep shade, both *CCA1pro::LUC* and *TOC1pro::LUC* remained rhythmic in LD whether in high or low R:FR. Unexpectedly, the amplitude of *TOC1pro::LUC* oscillations increased in low R:FR when compared to high R:FR (figure 6.1). *TOC1* transcripts in low PAR were also increased in low R:FR when compared to high R:FR such that a peak in *TOC1* transcript abundance was only discernible in low R:FR (figure 6.2). *CCA1pro::LUC* amplitude, however, did not increase in low PAR and low R:FR, which suggests that the increase in *TOC1pro::LUC* amplitude is not simply a consequence of increased light signaling to the circadian clock overall. It is possible that this mechanism also operates at high PAR, but as oscillation amplitudes were an order of magnitude greater in high PAR than in low PAR, any effect is likely to be masked (compare figure 6.3 and figure 6.1d).

The phytochromes detect R:FR and phyA is required for the FR entrainment of the plant circadian clock (Wenden et al., 2011). Figure 6.5 suggested that phyA mediates the low R:FR-induced elevation in *TOC1* transcript abundance. This observation correlates with previous studies, which report that phyA mediates the FR-induction of genes such as *TOC1* in etiolated seedlings (Tepperman et al., 2001). As phyA does not directly associate with the *TOC1* promoter (Chen et al., 2014), it was conjectured that a missing component of the signaling mechanism between phyA and TOC1 is likely to be a positive transcriptional activator. Hsu et al. (2013) proposed that RVE8 binds to the evening element in promoters of evening-phased genes, such as *TOC1* to promote open chromatin through histone acetylation. Furthermore, a publicly-available ChIP-seq dataset suggested that phyA associates with the RVE8 promoter (Chen et al., 2014). Two other studies added weight to the suspicion that RVE8 could be linked to phyA and FR signaling. Firstly, Gray et al. (2017) reported that the *REVEILLE* gene family inhibit growth in seedlings and adult plants. Secondly, Rawat et al.

(2011) speculated that RVE8 may be involved in the low fluence response due to the hypocotyl elongation phenotypes of *RVE8* over-expressing and *rve8-1* lines:

> "*... the RVE8 phenotypes were less obvious at fluence rates of 8 μmol m^{-2} s^{-1} or higher, and almost absent at a fluence rate of 85 μmol m^{-2} s^{-1} ... This type of light-dependent phenotype is reminiscent of mutants in the phyA signaling pathway such as fhy1...*"
> (Rawat et al., 2011)

Indeed, in low PAR, increases in *TOC1* transcript in low R:FR compared to high R:FR required RVE8 (figure 6.6). Furthermore, *ELF3*, *ELF4* and *LUX* transcript abundances were greater in low R:FR than in high R:FR in both a phyA- and RVE8-dependent manner (figure 6.7). These observations are consistent with the characterised role for RVE8 as a circadian transcriptional activator of evening-phased genes (Hsu et al., 2013). While FR signaling to the clock required both phyA and RVE8, they do not appear to be working in a linear transcriptional pathway as low R:FR did not significantly induce *RVE8* transcript nor did mutation of phyA significantly affect *RVE8* transcript abundance (figure 6.8). As phyA perceives and mediates reponses to FR light, (Nagatani et al., 1993; Parks and Quail, 1993; Whitelam et al., 1993), it is likely that phyA signals upstream of RVE8. Further experimentation is required to elucidate the possible interactions between phyA and RVE8, which may involve alternative splicing of *RVE8* or post-translational associations.

The involvement of RVE8 in mediating FR input into the circadian clock could additionally contribute to a mechanistic explanation for both the shortening of period and the damping of oscillations of the circadian clock in continuous low R:FR (chapter 5). Rawat et al. (2011) reported that *rve8-1* mutants have a lengthened period whereas RVE8-OX transgenics have shortened period in LL, which suggests that RVE8 increases the pace of the circadian clock. Were FR supplementation in LL to induce an increase in RVE8 activity, period length in LL might then be expected to shorten, as seen in figure 5.3a. Speculatively, the damping of oscillations in continuous low R:FR light described in chapter 5 could also be consistent with the notion that RVE8 acts like a *rheostat* or variable resistor for the circadian clock (Hsu et al., 2013). Current models of the plant circadian clock take the form of variations on a sequential repressilator system with multiple feedback loops (Pokhilko et al., 2012), where the coincidence of consecutive activators, repressors and repressors of repressors at correct times deliver high amplitude robust circadian oscillations (Shalit-Kaneh et al., 2018). Should RVE8 signaling be increased and left *on* due to its activation by FR, then what is effectively a variable resistor (Hsu et al., 2013) is left in an *open* state, which could partially remove the precision of the oscillations of the circadian clock and hence result in damping of oscillations (whether oscillations damp high or low depend upon the clock component being looked at - *e.g.* *CCA1* damps low whereas *TOC1* damps high in figure 5.1). Oscillations are damped rather than abolished because while this resistor (RVE8) is left *open*, subsequent modulators (that is, repressors) may still be active in their own oscillations. It would be interesting to test the involvement of RVE8 in FR input to the circadian clock using clock promoter-driven luciferase reporters in the *rve8-1* mutant.

TOC1 limits plant shade avoidance in deep canopy shade

In deep canopy shade, phyA signaling inhibits hypocotyl elongation and prevents seedlings from fatally over-elongating due to inactivation of both phyB and cryptochrome photoreceptors (Yanovsky et al., 1995; Martínez-García et al., 2014). The *REVEILLE* gene family inhibits growth (Gray et al., 2017) and the hypocotyls of *rve8-1* mutants bear similarity to mutants in the phyA signaling pathway (Rawat et al., 2011). Furthermore, TOC1 gates hypocotyl elongation through co-binding to PIF3 (Soy et al., 2016) and PIF4 (Zhu et al., 2016) at PIF target promoters to suppress transcription of PIF targets. It was hypothesised, therefore, that the phyA- and RVE8-mediated FR-induction of *TOC1* transcript could be a component of the mechanism of phyA antagonism of hypocotyl elongation in deep shade.

Low R:FR in a background of low PAR inhibited hypocotyl elongation in wild type plants when compared to plants grown in high R:FR (figure 6.9,6.10). Consistent with previous reports (Martínez-García et al., 2014), phyA mutants exhibited elongated hypocotyls under low R:FR when compared to high R:FR, which suggests that phyA mediates the majority of the FR-induced inhibition of hypocotyl elongation in deep shade (figure 6.9). TOC1 and RVE8 inhibit hypocotyl elongation in high and low R:FR in a background of deep shade (figure 6.10). However, only in short day photoperiods (8L:16D) did the absence of TOC1 and RVE8 significantly attenuate the low R:FR-induced inhibition of hypocotyl elongation (figure 6.10c). Analysis of hypocotyl elongation rate in low R:FR and low PAR, showed that *toc1-101* plants in short days had a higher peak elongation rate at dawn than wild type (Col-0) (figure 6.11d). Indeed, this peak of elongation rate in *toc1-101* in low R:FR at dawn (figure 6.11d) was slightly greater than peak elongation rate of Col-0 plants at dawn in high R:FR (figure 6.11c). This observation is consistent with a model whereby elevated levels of TOC1 in low R:FR inhibit hypocotyl elongation at the end of the night. These data suggest that in short days and deep vegetational shade where R:FR is low, FR signaling, mediated by phyA and RVE8, elevates TOC1 expression to augment the inhibition of hypocotyl elongation (figure 7.1). In longer photoperiods, observations that *toc1-101* and *rve8-1* mutants did not display significant attenuations of low R:FR-induced inhibition of hypocotyl elongation may be due to the activation of multiple phyA signaling pathways (Chen et al., 2014), which dominate in their repression of growth in the absence of RVE8 and TOC1.

Observations that the *toc1-101* mutant did not fully resemble the phyA phenotype, and that the *toc1-101* mutant had a delayed climb in elongation rate in low R:FR when compared to high R:FR, are consistent with the possibility that the function of TOC1 in the phyA signaling cascade has functional redundancy with other phyA-regulated suppressors of elongation. *PIF4* and *PIF5* transcripts were not reduced in low R:FR low PAR (figure 6.12), which suggests that *PIF4* and *PIF5* transcriptional regulation by the evening complex (Nusinow et al., 2011) is not likely to play a major role in the low R:FR-induced inhibition of hypocotyl elongation in deep shade. However, ELF3, independently of the evening complex, regulates PIF4 through direct protein interactions (Nieto et al., 2015). It is a possibility, therefore, that increases in *ELF3* transcript in low R:FR (figure 6.7) result in greater ELF3 protein abundance; and that along with TOC1 (Soy et al., 2016), ELF3 regulates PIF protein activity to inhibit hypocotyl elongation in deep shade. It would also be interesting to assay *PRR5* transcript abundance as RVE8 regulates *PRR5* expression through the evening element in its promoter (Rawat et al., 2011) and it has recently been shown that PRR5, 7 and 9 along with PRR1 (TOC1) sequentially co-bind to PIFs and their target promoters to inhibit their transcriptional activity during the night (Martín et al., 2018). An alternative interpretation of the data presented in section 6.4 could be that inhibition of hypocotyl elongation due to the elevated expression of clock components is a beneficial by-product of keeping the circadian oscillator entrained in deep shade conditions. Plants with disrupted circadian clocks often have very elongated hypocotyls, which is a phenotype that survives poorly in deep shade conditions (Yanovsky et al., 1995). As such, the ecological relevance of the signaling mechanisms outlined in chapter 6 and figure 7.1 deserve to be directly clarified through assaying the fitness of TOC1 alleles in deep shade conditions in the field.

Conclusions

This thesis demonstrates that applying continuous supplemental low dose UV-B to the commercially important potted herb Coriander improves product quality morphologically and nutritionally. UV-B applied at different times of day elicited different magnitudes of hypocotyl inhibition in Arabidopsis but not in Coriander. It is highly possible that the time-of-day of peak sensitivity to UV-B inhibition of hypocotyl elongation differs in different photoperiods. Future applications of the suppression of elongation by UV-B in commercial crops should

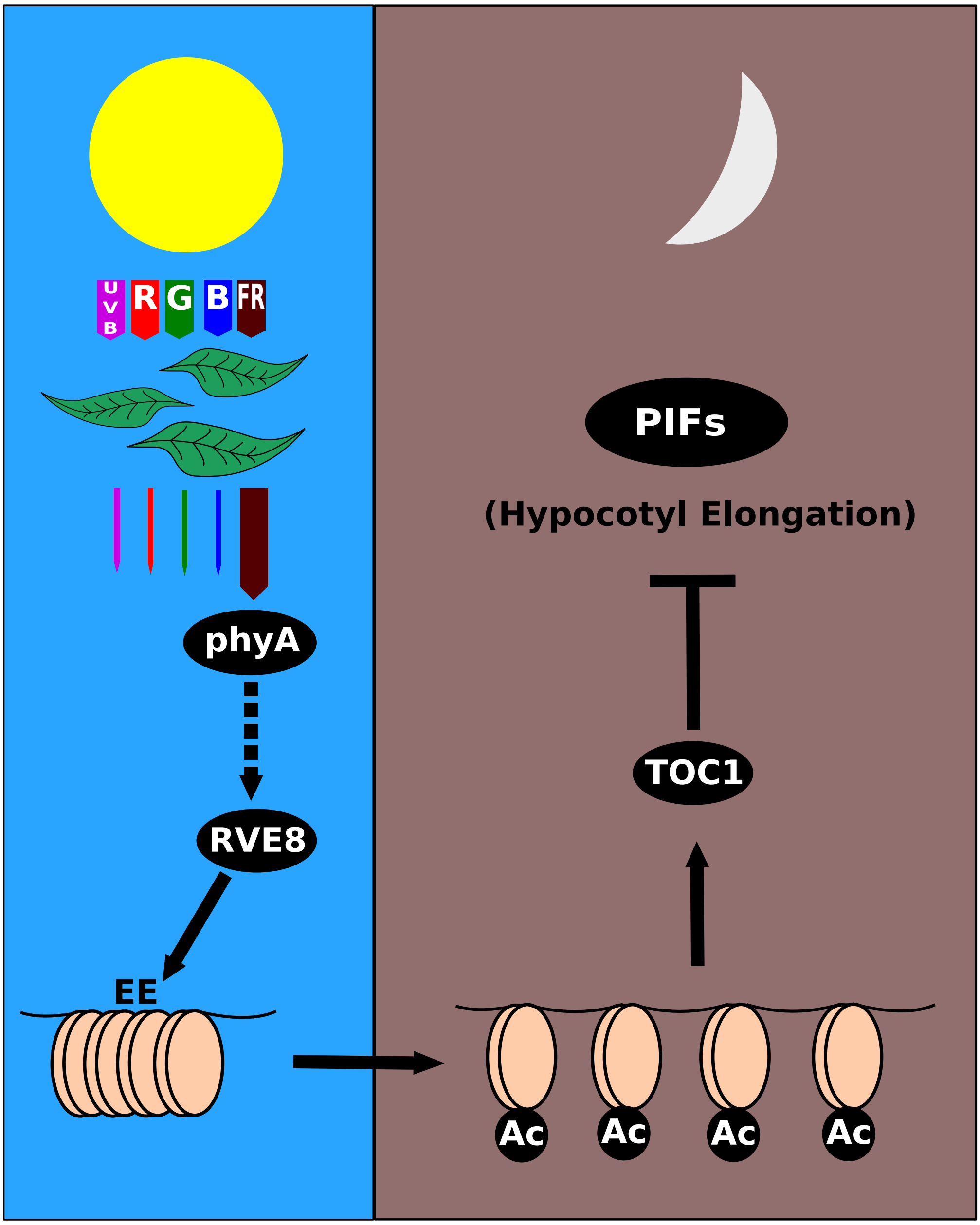

Figure 7.1: Hypothetical model of the TOC1-mediated inhibition of hypocotyl elongation in deep shade. As sunlight passes through a dense canopy, PAR (R, G and B light) and UV-B is depleted to very low levels. FR light is relatively enriched as it is reflected and transmitted through the canopy. phyA is stabilised in low PAR, and signals in FR. In a mechanism that requires the presence of both phyA and RVE8, TOC1 expression is increased at dusk and during the night. The interaction between phyA and RVE8 is yet to be determined, but does not appear to involve increases in *RVE8* transcript. RVE8 associates with the evening element (EE) in promoters of evening-phased genes and stimulates histone acetylation, resulting in open chromatin (Hsu et al., 2013). Increased TOC1 expression inhibits hypocotyl elongation in deep shade in short day conditions, likely through increased inhibition of PIF activity through co-binding at PIF target promoters (Soy et al., 2016; Zhu et al., 2016; Martín et al., 2018).

therefore consider different day lengths as well as light quality. It appears that the inhibition of shade avoidance by UV-B is under circadian regulation, but the mechanism has not been fully clarified. It is likely, given previous suggestions that the clock gates UV-B responses on a *gene-by-gene* basis, that the mechanism for the circadian gating of the UV-B inhibition of shade avoidance is complex and operates at multiple levels of the signaling cascade. A surprising result showing that circadian gating was lost when plants were grown in continuous low R:FR altered the course of this project to consider the effect of shade on the behaviour of the circadian clock. Collectively, the data from this line of inquiry suggest that the loss of gating is caused by damping of the circadian clock, which in turn appears to be an artefact of FR signaling to the oscillator in continuous light. Further experimentation identified a potential adaptive significance for FR signaling to the oscillator, where in driven conditions, FR signaling, mediated by phyA, increases the expression of *TOC1*, which acts to inhibit hypocotyl elongation. This thesis has also identified RVE8 as a key component involved in FR signaling to the circadian clock. The mechanism of the putative interaction between phyA and RVE8 remains to be elucidated, but does not appear to involve increases in *RVE8* transcript abundance. Collectively, this thesis highlights the importance of the interaction between light quality and circadian regulation in plant development in challenging environments.

Bibliography

Abbas, N., Maurya, J. P., Senapati, D., Gangappa, S. N., and Chattopadhyay, S. (2014). Arabidopsis CAM7 and HY5 physically interact and directly bind to the HY5 promoter to regulate its expression and thereby promote photomorphogenesis. *The Plant cell*, 26(3):1036–52.

Achard, P., Liao, L., Jiang, C., Desnos, T., Bartlett, J., Fu, X., and Harberd, N. P. (2007). DELLAs contribute to plant photomorphogenesis. *Plant physiology*, 143(3):1163–72.

Adams, S., Manfield, I., Stockley, P., and Carré, I. A. (2015). Revised Morning Loops of the Arabidopsis Circadian Clock Based on Analyses of Direct Regulatory Interactions. *PLoS ONE*, 10(12):1–11.

Agati, G. and Tattini, M. (2010). Multiple functional roles of flavonoids in photoprotection. *New Phytologist*, 186(4):786–793.

Ahmad, M. and Cashmore, A. (1993). HY4 gene of A. thaliana encodes a protein with characteristics of a blue-light photoreceptor. *Nature*, 366:162–166.

Ahmad, M., Cashmore, A. R., Chan, J., and Lin, C. (1996). CRY2: a second member of the Arabidopsis cryptochrome gene family. *Plant Physiology*, 110:1047.

Al-Sady, B., Ni, W., Kircher, S., Schäfer, E., and Quail, P. H. (2006). Photoactivated phytochrome induces rapid PIF3 phosphorylation prior to proteasome-mediated degradation. *Molecular cell*, 23(3):439–46.

Alabadí, D., Oyama, T., Yanovsky, M. J., Harmon, F. G., Más, P., and Kay, S. A. (2001). Reciprocal Regulation Between TOC1 and LHY / CCA1 Within the Arabidopsis Circadian Clock. *Science*, 293(2001):880–883.

Andronis, C., Barak, S., Knowles, S. M., Sugano, S., and Tobin, E. M. (2008). The clock protein CCA1 and the bZIP transcription factor HY5 physically interact to regulate gene expression in Arabidopsis. *Molecular Plant*, 1(1):58–67.

Aschoff, J. (1979). Circadian Rhythms: Influences of Internal and External Factors on the Period Measured in Constant Conditions 1. *Zeitschrift für Tierpsychologie*, 49(3):225–249.

Aukerman, M., Hirschfeld, M., Wester, L., Weaver, M., Clack, T., Amasino, R. M., and Sharrock, R. (1997). A deletion in the PHYD gene of the Arabidopsis Wassilewskija ecotype defines a role for phytochrome D in red/far-red light sensing. *The Plant Cell*, 9:1317–1326.

Balasubramanian, S., Sureshkumar, S., Agrawal, M., Michael, T. P., Wessinger, C., Maloof, J. N., Clark, R., Warthmann, N., Chory, J., and Weigel, D. (2006). The PHYTOCHROME C photoreceptor gene mediates natural variation in flowering and growth responses of Arabidopsis thaliana. *Nature Genetics*, 38(6):711–715.

Ballaré, C. L., Barnes, P., and Flint, S. (1995). Inhibition of hypocotyl elongation by ultraviolet-B radiation in de-etiolating tomato seedlings. *Physiologia Plantarum*, 93:584–592.

Ballaré, C. L., Scopel, A. L., and Sánchez, R. A. (1990). Far-red radiation reflected from adjacent leaves: an early signal of competition in plant canopies. *Science*, 247(27):329–332.

Banaś, A. K., Aggarwal, C., Łabuz, J., Sztatelman, O., and Gabryś, H. (2012). Blue light signalling in chloroplast movements. *Journal of Experimental Botany*, 63(4):1559–1574.

Banerjee, R. and Batschauer, A. (2005). Plant blue-light receptors. *Planta*, 220:498–502.

Bartoli, C. G., Tambussi, E. A., Diego, F., and Foyer, C. H. (2009). Control of ascorbic acid synthesis and accumulation and glutathione by the incident light red/far red ratio in Phaseolus vulgaris leaves. *FEBS Letters*, 583(1):118–122.

Baudry, A., Ito, S., Song, Y. H., Strait, A. A., Kiba, T., Lu, S., Henriques, R., Pruneda-Paz, J. L., Chua, N. H., Tobin, E. M., Kay, S. A., and Imaizumi, T. (2010). F-Box Proteins FKF1 and LKP2 Act in Concert with ZEITLUPE to Control Arabidopsis Clock Progression. *The Plant Cell*, 22(3):606–622.

Bauer, D., Viczián, A., and Kircher, S. (2004). Constitutive photomorphogenesis 1 and multiple photoreceptors control degradation of phytochrome interacting factor 3, a transcription factor required for light. *The Plant cell*, 3:1433–1445.

Bentsink, L. and Koornneef, M. (2008). Seed Dormancy and Germination. In *The Arabidopsis Book*.

Bernardo-García, S., de Lucas, M., Martínez, C., Espinosa-Ruiz, A., Davière, J.-M., and Prat, S. (2014). BR-dependent phosphorylation modulates PIF4 transcriptional activity and shapes diurnal hypocotyl growth. *Genes & development*, 28(15):1681–94.

Biever, J. J., Brinkman, D., and Gardner, G. (2014). UV-B inhibition of hypocotyl growth in etiolated Arabidopsis thaliana seedlings is a consequence of cell cycle arrest initiated by photodimer accumulation. *Journal of experimental botany*, 65(11):2949–61.

Binkert, M., Crocco, C. D., Ekundayo, B., Lau, K., Raffelberg, S., Tilbrook, K., Yin, R., Chappuis, R., Schalch, T., and Ulm, R. (2016). Revisiting chromatin binding of the Arabidopsis UV-B photoreceptor UVR8. *BMC Plant Biology*, 16(1):42.

Binkert, M., Terecskei, K., Veylder, L. D., Nagy, F., and Ulm, R. (2014). UV-B-Responsive Association of the Arabidopsis bZIP Transcription Factor ELONGATED HYPOCOTYL5 with Target Genes , Including Its Own Promoter. *The Plant Cell*, 26:4200–4213.

Boccalandro, H. E., Mazza, C. A., Mazzella, M. A., Casal, J. J., and Ballaré, C. L. (2001). Ultraviolet B radiation enhances a phytochrome-B-mediated photomorphogenic response in Arabidopsis. *Plant physiology*, 126(2):780–788.

Borthwick, H. A., Hendricks, S. B., and Parker, M. W. (1952a). The reaction controlling floral initiation. *Proceedings of the National Academy of Sciences*, 38:929–934.

Borthwick, H. A., Hendricks, S. B., Parker, M. W., Toole, E. H., and Toole, V. K. (1952b). A reversible photoreaction controlling seed germination. *Proceedings of the National Academy of Sciences*, 38:662–666.

Botto, J. F., Sanchez, R. A., Whitelam, G. C., and Casal, J. J. (1996). Phytochrome A mediates the promotion of seed germination by very low fluences of light and canopy shade light in Arabidopsis. *Plant Physiology*, 110:439–444.

Bradford, M. M. (1976). A rapid and sensitive method for the quantitation of microgram quantities of protein utilizing the principle of protein-dye binding. *Analytical Biochemistry*, 72(1-2):248–254.

Briggs, W. R., Beck, C. F., Cashmore, A. R., Christie, J. M., Hughes, J., Jarillo, J. A., Kagawa, T., Kanegae, H., Liscum, E., Nagatani, A., Okada, K., Salomon, M., Rüdiger, W., Sakai, T., Takano, M., Wada, M., and Watson, J. C. (2001). The phototropin family of photoreceptors. *The Plant cell*, 13(5):993–997.

Brown, B. A., Cloix, C., Jiang, G. H., Kaiserli, E., Herzyk, P., Kliebenstein, D. J., and Jenkins, G. I. (2005). A UV-B-specific signaling component orchestrates plant UV protection. *Proceedings of the National Academy of Sciences*, 102(50):18225–18230.

Brown, B. A. and Jenkins, G. I. (2008). UV-B signaling pathways with different fluence-rate response profiles are distinguished in mature Arabidopsis leaf tissue by requirement for UVR8, HY5, and HYH. *Plant physiology*, 146(2):576–588.

Bu, Q., Zhu, L., Dennis, M. D., Yu, L., Lu, S. X., Person, M. D., Tobin, E. M., Browning, K. S., and Huq, E. (2011). Phosphorylation by CK2 enhances the rapid light-induced degradation of phytochrome interacting factor 1 in arabidopsis. *Journal of Biological Chemistry*, 286(14):12066–12074.

Burgie, E. S., Bussell, A. N., Walker, J. M., Dubiel, K., and Vierstra, R. D. (2014). Crystal structure of the photosensing module from a red/far-red light-absorbing plant phytochrome. *Proceedings of the National Academy of Sciences*, 111(28):10179–84.

Butler, W. L., Norris, K., Siegelman, H. W., and Hendricks, S. B. (1959). Detection, assay, and preliminary purification of the pigment controlling photoresponsive development of plants. *Proceedings of the National Academy of Sciences1*, 45(12):1703–1708.

Caldwell, M. M., Robberecht, R., and Flint, S. D. (1983). Internal filters: Prospects for UV-acclimation in higher plants. *Physiologia Plantarum*, 58(3):445–450.

Carvalho, S. D., Schwieterman, M. L., Abrahan, C. E., Colquhoun, T. A., and Folta, K. M. (2016). Light Quality Dependent Changes in Morphology, Antioxidant Capacity, and Volatile Production in Sweet Basil (Ocimum basilicum).

Carver, J., B.H., H., O'Brien, R., and O'Connor, G. (1974). The Ultraviolet reflectivity of the Moon. *The Moon*, 9:295–303.

Casal, J. J. (2012). Shade avoidance. *The Arabidopsis book / American Society of Plant Biologists*, 10:e0157.

Casati, P., Campi, M., Chu, F., Suzuki, N., Maltby, D., Guan, S., Burlingame, A. L., and Walbot, V. (2008). Histone acetylation and chromatin remodeling are required for UV-B-dependent transcriptional activation of regulated genes in maize. *The Plant cell*, 20(4):827–842.

Casati, P., Stapleton, A. E., Blum, J. E., and Walbot, V. (2006). Genome-wide analysis of high-altitude maize and gene knockdown stocks implicates chromatin remodeling proteins in response to UV-B. *Plant Journal*, 46(4):613–627.

Casson, S. A., Franklin, K. A., Gray, J. E., Grierson, C. S., Whitelam, G. C., and Hetherington, A. M. (2009). phytochrome B and PIF4 Regulate Stomatal Development in Response to Light Quantity. *Current Biology*, 19(3):229–234.

Cerdán, P. D. and Chory, J. (2003). Regulation of flowering time by light quality. *Nature*, 423(6942):881–885.

Chen, D., Xu, G., Tang, W., Jing, Y., Ji, Q., Fei, Z., and Lin, R. (2013). Antagonistic Basic Helix-Loop-Helix/bZIP Transcription Factors Form Transcriptional Modules That Integrate Light and Reactive Oxygen Species Signaling in Arabidopsis. *The Plant Cell*, 25(5):1657–1673.

Chen, F., Li, B., Li, G., Charron, J.-B. J.-B., Dai, M., Shi, X., and Deng, X. W. (2014). Arabidopsis Phytochrome A Directly Targets Numerous Promoters for Individualized Modulation of Genes in a Wide Range of Pathways. *The Plant cell*, 26(5):1949–1966.

Choi, G., Yi, H., Lee, J., Kwon, Y., Soh, M., and Shin, B. (1999). Phytochrome signalling is mediated through nucleoside diphosphate kinase 2. *Nature*, 401(October).

Christie, J. M. (2007). Phototropin blue-light receptors. *Annual review of plant biology*, 58:21–45.

Christie, J. M., Arvai, A. S., Baxter, K. J., Heilmann, M., Pratt, A. J., O'Hara, A., Kelly, S. M., Hothorn, M., Smith, B. O., Hitomi, K., Jenkins, G. I., and

Getzoff, E. D. (2012). Plant UVR8 photoreceptor senses UV-B by tryptophan-mediated disruption of cross-dimer salt bridges. *Science*, 335(March):1492–1496.

Christie, J. M., Salomon, M., Nozue, K., Wada, M., and Briggs, W. R. (1999). LOV (light, oxygen, or voltage) domains of the blue-light photoreceptor phototropin (nph1): binding sites for the chromophore flavin mononucleotide. *Proceedings of the National Academy of Sciences*, 96(15):8779–8783.

Clack, T., Mathews, S., and Sharrock, R. A. (1994). The phytochrome apoprotein family in Arabidopsis is encoded by five genes: the sequences and expression of PHYD and PHYE. *Plant molecular biology*, 25:413–427.

Clack, T., Shokry, A., Moffet, M., Liu, P., Faul, M., and Sharrock, R. A. (2009). Obligate heterodimerization of Arabidopsis phytochromes C and E and interaction with the PIF3 basic helix-loop-helix transcription factor. *The Plant cell*, 21(3):786–799.

Cloix, C. and Jenkins, G. I. (2008). Interaction of the Arabidopsis UV-B-specific signaling component UVR8 with chromatin. *Molecular Plant*, 1(1):118–128.

Cloix, C., Kaiserli, E., Heilmann, M., Baxter, K., Brown, B., O'Hara, A., Smith, B., Christie, J., and Jenkins, G. (2012). C-terminal region of the UV-B photoreceptor UVR8 initiates signaling through interaction with the COP1 protein. *Proceedings of the National Academy of Sciences*, 109(40):16366–16370.

Clough, R. and Vierstra, R. (1997). Phytochrome degradation. *Plant, Cell & Environment*, 20:713–721.

Conte, M., de Simone, S., Simmons, S. J., Ballaré, C. L., and Stapleton, A. E. (2010). Chromosomal loci important for cotyledon opening under UV-B in Arabidopsis thaliana. *BMC plant biology*, 10:112.

Cookson, S. J. and Granier, C. (2006). A dynamic analysis of the shade-induced plasticity in Arabidopsis thaliana rosette leaf development reveals new components of the shade-adaptative response. *Annals of Botany*, 97(3):443–452.

Covington, M. F., Maloof, J. N., Straume, M., Kay, S. A., and Harmer, S. L. (2008). Global transcriptome analysis reveals circadian regulation of key pathways in plant growth and development. *Genome biology*, 9(8):R130.

Csepregi, K., Coffey, A., Cunningham, N., Prinsen, E., Hideg, É., and Jansen, M. A. K. (2017). Developmental age and UV-B exposure co-determine antioxidant capacity and flavonol accumulation in Arabidopsis leaves. *Environmental and Experimental Botany*, 140:19–25.

Cumming, B. G. (1963). The dependence of germination on photoperiod, light quality, and temperature in Chenopodium spp. *Canadian Journal of Botany*, 41:1211–1233.

Czégény, G., Martret, B. L., Pávkovics, D., Dix, P. J., and Hideg, É. (2016a). Elevated ROS-scavenging enzymes contribute to acclimation to UV-B exposure in transplastomic tobacco plants, reducing the role of plastid peroxidases. *Journal of Plant Physiology*, 20(201):95–100.

Czégény, G., Mátai, A., and Hideg, É. (2016b). UV-B effects on leaves-Oxidative stress and acclimation in controlled environments. *Plant Science*, 248:57–63.

Das, D., St Onge, K. R., Voesenek, L. A., Pierik, R., and Sasidharan, R. (2016). Ethylene- and shade-induced hypocotyl elongation share transcriptome patterns and functional regulators. *Plant Physiology*, page pp.00725.2016.

Davey, M. P., Susanti, N. I., Wargent, J. J., Findlay, J. E., Paul Quick, W., Paul, N. D., and Jenkins, G. I. (2012). The UV-B photoreceptor UVR8 promotes photosynthetic efficiency in Arabidopsis thaliana exposed to elevated levels of UV-B. *Photosynthesis Research*, 114(2):121–131.

de Lucas, M. and Prat, S. (2014). PIFs get BRright: PHYTOCHROME INTERACTING FACTORs as integrators of light and hormonal signals. *New Phytologist*, 202:1126–1141.

de Wit, M., Keuskamp, D. H., Bongers, F. J., Hornitschek, P., Gommers, C. M. M., Reinen, E., Martínez-Cerón, C., Fankhauser, C., Pierik, R., Martinez-Ceron, C., Fankhauser, C., and Pierik, R. (2016). Integration of Phytochrome and Cryptochrome Signals Determines Plant Growth during Competition for Light. *Current biology : CB*, 26:3320–3326.

Debrieux, D. and Fankhauser, C. (2010). Light-induced degradation of phyA is promoted by transfer of the photoreceptor into the nucleus. *Plant Molecular Biology*, 73(6):687–695.

Devlin, P., Patel, S., and Whitelam, G. (1998). Phytochrome E influences internode elongation and flowering time in Arabidopsis. *The Plant Cell Online*, 10:1479–1487.

Devlin, P. F., Robson, P. R. H., Patel, S. R., Goosey, L., Sharrock, R., and Whitelam, G. C. (1999). Phytochrome D acts in the shade-avoidance syndrome in Arabidopsis by controlling elongation growth and flowering time. *Plant Physiology*, 119(March):909–915.

Djakovic-Petrovic, T., Wit, M. D., Voesenek, L. A. C. J., and Pierik, R. (2007). DELLA protein function in growth responses to canopy signals. *Plant Journal*, 51(1):117–126.

Dodd, A. N., Salathia, N., Hall, A., Kévei, E., Tóth, R., Nagy, F., Hibberd, J. M., Millar, A. J., and Webb, A. A. R. (2005). Plant circadian clocks increase photosynthesis, growth, survival, and competitive advantage. *Science (New York, N.Y.)*, 309(5734):630–3.

Dou, H., Niu, G., Gu, M., and Masabni, J. (2017). Effects of Light Quality on Growth and Phytonutrient Accumulation of Herbs under Controlled Environments. *Horticulturae*, 3(2):36.

Dowson-Day, M. J. and Millar, A. J. (1999). Circadian dysfunction causes aberrant hypocotyl elongation patterns in Arabidopsis. *The Plant Journal*, 17(1):63–71.

Drewnowski, A. and Gomez-Carneros, C. (2000). Bitter taste, phyonutrients, and the consumer: a review. *Am J Clin Nutr*, 72(22):1424–1435.

Duek, P. D. and Fankhauser, C. (2005). bHLH class transcription factors take centre stage in phytochrome signalling. *Trends in plant science*, 10(2):51–4.

El-Assal, S. E.-D., Alonso-Blanco, C., Peeters, A. J. M., Raz, V., and Koornneef, M. (2001). A QTL for flowering time in Arabidopsis reveals a novel allele of CRY2. *Nature genetics*, 29(4):435–440.

Emerson, R. (1957). Dependence of yield of photo- synthesis in long wave red on wavelength and intensity of supplementary light. *Science*, 125(3251):746–752.

Emerson, R. (1958). The Quantum Yield of Photosynthesis. *Annual Review of Plant Physiology*, 9(1):1–24.

Endo, M. (2016). Tissue-specific circadian clocks in plants. *Current Opinion in Plant Biology*, 29:44–49.

Endo, M., Shimizu, H., Nohales, M. A., Araki, T., and Kay, S. A. (2014). Tissue-specific clocks in Arabidopsis show asymmetric coupling. *Nature*, 515(7527):419–422.

Eriksson, N., Wu, S., Do, C. B., Kiefer, A. K., Tung, J. Y., Mountain, J. L., Hinds, D. A., and Francke, U. (2012). A genetic variant near olfactory receptor genes influences cilantro preference. *Flavour*, 1(22):1–7.

Fankhauser, C., Yeh, K., Clark, J., and Zhang, H. (1999). PKS1, a substrate phosphorylated by phytochrome that modulates light signaling in Arabidopsis. *Science*, 284(May):1539–1542.

Favory, J.-J., Stec, A., Gruber, H., Rizzini, L., Oravecz, A., Funk, M., Albert, A., Cloix, C., Jenkins, G. I., Oakeley, E. J., Seidlitz, H. K., Nagy, F., and

Ulm, R. (2009). Interaction of COP1 and UVR8 regulates UV-B-induced photomorphogenesis and stress acclimation in Arabidopsis. *The EMBO journal*, 28(5):591–601.

Fehér, B., Kozma-Bognár, L., Kevei, E., Hajdu, A., Binkert, M., Davis, S. J., Schäfer, E., Ulm, R., and Nagy, F. (2011). Functional interaction of the circadian clock and UV RESISTANCE LOCUS 8 controlled UV-B signaling pathways in Arabidopsis thaliana. *The Plant Journal*, 67(1):37–48.

Feng, S., Martinez, C., Gusmaroli, G., Wang, Y., Zhou, J., Wang, F., Chen, L., Yu, L., Iglesias-Pedraz, J. M., Kircher, S., Schäfer, E., Fu, X., Fan, L.-M., and Deng, X. W. (2008). Coordinated regulation of Arabidopsis thaliana development by light and gibberellins. *Nature*, 451(7177):475–9.

Fernandez, M. B., Tossi, V. E., Lamattina, L., and Cassia, R. O. (2016). A comprehensive phylogeny reveals functional conservation of the UV-B photoreceptor UVR8 from green algae to higher plants. *Frontiers in plant science*, 7(November):1–6.

Findlay, K. M. W. and Jenkins, G. I. (2016). Regulation of UVR8 photoreceptor dimer/monomer photo-equilibrium in Arabidopsis plants grown under photoperiodic conditions. *Plant, Cell and Environment*, 39(8):1706–1714.

Finlayson, S. A., Krishnareddy, S. R., Kebrom, T. H., and Casal, J. J. (2010). Phytochrome Regulation of Branching in Arabidopsis. *Plant Physiology*, 152(4):1914–1927.

Finlayson, S. A., Lee, I. J., Mullet, J. E., and Morgan, P. W. (1999). The mechanism of rhythmic ethylene production in sorghum. The role of phytochrome B and simulated shading. *Plant physiology*, 119(3):1083–1089.

Fiorucci, A. S. and Fankhauser, C. (2017). Plant Strategies for Enhancing Access to Sunlight. *Current Biology*, 27(17):R931–R940.

Folta, K. M. and Spalding, E. P. (2001). Unexpected roles for cryptochrome 2 and phototropin revealed by high-resolution analysis of blue light-mediated hypocotyl growth inhibition. *Plant Journal*, 26(5):471–478.

Fornara, F., Panigrahi, K. C. S., Gissot, L., Sauerbrunn, N., Rühl, M., Jarillo, J. A., and Coupland, G. (2009). Arabidopsis DOF Transcription Factors Act Redundantly to Reduce CONSTANS Expression and Are Essential for a Photoperiodic Flowering Response. *Developmental Cell*, 17(1):75–86.

Franklin, K., Praekelt, U., Stoddart, W. M., Billingham, O. E., Halliday, K. J., and Whitelam, G. C. (2003a). Phytochromes B, D, and E act redundantly to control multiple physiological responses in Arabidopsis. *Plant Physiology*, 131:1340–1346.

Franklin, K. A. (2008). Shade avoidance. *The New phytologist*, 179(4):930–44.

Franklin, K. A. (2009). Light and temperature signal crosstalk in plant development. *Current opinion in plant biology*, 12(1):63–8.

Franklin, K. A., Davis, S. J., Stoddart, W. M., Vierstra, R. D., and Whitelam, G. C. (2003b). Mutant Analyses Define Multiple Roles for Phytochrome C in Arabidopsis Photomorphogenesis. *The Plant Cell*, 15:1981–1989.

Franklin, K. A., Lee, S. H., Patel, D., Kumar, S. V., Spartz, A. K., Gu, C., Ye, S., Yu, P., Breen, G., Cohen, J. D., Wigge, P. A., and Gray, W. M. (2011). Phytochrome-interacting factor 4 (PIF4) regulates auxin biosynthesis at high temperature. *Proceedings of the National Academy of Sciences*, 108(50):20231–5.

Franklin, K. A. and Quail, P. H. (2010). Phytochrome functions in Arabidopsis development. *Journal of experimental botany*, 61(1):11–24.

Fraser, D. P., Hayes, S., and Franklin, K. A. (2016). Photoreceptor crosstalk in shade avoidance. *Current Opinion in Plant Biology*, 33:1–7.

Frohnmeyer, H. and Staiger, D. (2003). Ultraviolet-B radiation-mediated responses in plants. Balancing damage and protection. *Plant physiology*, 133(4):1420–1428.

Fuglevand, G., Jackson, J., and Jenkins, G. (1996). UV-B, UV-A, and Blue Light Signal Transduction Pathways Interact Synergistically to Regulate Chalcone Synthase Gene Expression in Arabidopsis. *the Plant Cell Online*, 8(12):2347–2357.

Furya, M. and Song, P. S. (1994). Assembly and properties of holophytochrome. In Kendrick, R. and Kronenberg, G., editors, *Photomorphogenesis in Plants*. Springer, Netherlands.

Gallagher, S., Short, T. W., Ray, P. M., Pratt, L. H., and Briggs, W. R. (1988). Light-mediated changes in two proteins found associated with plasma membrane fractions from pea stem sections. *Proceedings of the National Academy of Sciences*, 85(21):8003–8007.

Gallego-Bartolome, J., Minguet, E. G., Grau-Enguix, F., Abbas, M., Locascio, A., Thomas, S. G., Alabadi, D., and Blazquez, M. A. (2012). Molecular mechanism for the interaction between gibberellin and brassinosteroid signaling pathways in Arabidopsis. *Proceedings of the National Academy of Sciences*, 109(33):13446–13451.

Galstyan, A., Cifuentes-Esquivel, N., Bou-Torrent, J., and Martinez-Garcia, J. F. (2011). The shade avoidance syndrome in Arabidopsis: a fundamental role for atypical basic helix-loop-helix proteins as transcriptional cofactors. *The Plant Journal*, 66(2):258–267.

Gangappa, S. N. and Kumar, S. V. (2017). DET1 and HY5 Control PIF4-Mediated Thermosensory Elongation Growth through Distinct Mechanisms. *Cell Reports*, 18(2):344–351.

Gendron, J. M., Pruneda-Paz, J. L., Doherty, C. J., Gross, A. M., Kang, S. E., and Kay, S. A. (2012). Arabidopsis circadian clock protein, TOC1, is a DNA-binding transcription factor. *Proceedings of the National Academy of Sciences*, 109(8):3167–72.

Genoud, T., Schweizer, F., Tscheuschler, A., Debrieux, D., Casal, J. J., Schäfer, E., Hiltbrunner, A., and Fankhauser, C. (2008). FHY1 mediates nuclear import of the light-activated phytochrome A photoreceptor. *PLoS genetics*, 4(8):e1000143.

Goosey, L., Palecanda, L., and Sharrock, R. A. (1997). Differential patterns of expression of the Arabidopsis PHYB, PHYD, and PHYE phytochrome genes. *Plant Physiology*, 115:959–969.

Gould, P. D., Domijan, M., Greenwood, M., Tokuda, I. T., Rees, H., Kozma-Bognar, L., Hall, A. J., and Locke, J. C. W. (2017). Coordination of robust single cell rhythms in the Arabidopsis circadian clock via spatial waves of gene expression. *bioRxiv*, page 208900.

Goyal, A., Karayekov, E., Galvão, V. C., Ren, H., Casal, J. J., and Fankhauser, C. (2016). Shade Promotes Phototropism through Phytochrome B-Controlled Auxin Production. *Current Biology*, pages 3280–3287.

Gray, J. A., Shalit-Kaneh, A., Chu, D. N., Hsu, P. Y., and Harmer, S. L. (2017). The REVEILLE Clock Genes Inhibit Growth of Juvenile and Adult Plants by Control of Cell Size. *Plant Physiology*, 173(4):2308–2322.

Greenham, K. and Mcclung, C. R. (2015). Integrating circadian dynamics with physiological processes in plants. *Nature Publishing Group*, 16(10):598–610.

Gruber, H., Heijde, M., Heller, W., Albert, A., Seidlitz, H. K., and Ulm, R. (2010). Negative feedback regulation of UV-B-induced photomorphogenesis and stress acclimation in Arabidopsis. *Proceedings of the National Academy of Sciences*, 107(46):20132–20137.

Guo, H., Yang, H., Mockler, T. C., and Lin, C. (1998). Regulation of flowering time by Arabidopsis photoreceptors. *Science*, 279(5355):1360–1363.

Hager, A. (1996). Properties of a blue-light-absorbing photoreceptor kinase localized in the plasma membrane of the coleoptile tip region. *Planta*, 198(2):294–299.

Hager, A. and Brich, M. (1993). Blue-light-induced phosphorylation of a plasma-membrane protein from phototropically sensitive tips of maize coleoptiles. *Planta*, 189(4):567–576.

Halliday, K. J., Koornneef, M., and Whitelam, G. C. (1994). Phytochrome B and at Least One Other Phytochrome Mediate the Accelerated Flowering Response of Arabidopsis thaliana L. to Low Red/Far-Red Ratio. *Plant physiology*, 104:1311–1315.

Halliday, K. J., Salter, M. G., Thingnaes, E., and Whitelam, G. C. (2003). Phytochrome control of flowering is temperature sensitive and correlates with expression of the floral integrator FT. *Plant Journal*, 33(5):875–885.

Hao, Y., Oh, E., Choi, G., Liang, Z., and Wang, Z.-Y. (2012). Interactions between HLH and bHLH Factors Modulate Light-Regulated Plant Development. *Molecular Plant*, 5(3):688–697.

Harmer, S. L., Hogenesch, J. B., Straume, M., Chang, H. S., Han, B., Zhu, T., Wang, X., Kreps, J. A., and Kay, S. A. (2000). Orchestrated transcription of key pathways in Arabidopsis by the circadian clock. *Science*, 290(5499):2110–2113.

Haydon, M. J., Mielczarek, O., Robertson, F. C., Hubbard, K. E., and Webb, A. a. R. (2013). Photosynthetic entrainment of the Arabidopsis thaliana circadian clock. *Nature*, 502(7473):689–92.

Hayes, S., Sharma, A., Fraser, D. P., Trevisan, M., Cragg-Barber, C. K., Tavridou, E., Fankhauser, C., Jenkins, G. I., and Franklin, K. A. (2017). UV-B Perceived by the UVR8 Photoreceptor Inhibits Plant Thermomorphogenesis. *Current Biology*, 27(1):120–127.

Hayes, S., Velanis, C. N., Jenkins, G. I., and Franklin, K. A. (2014). UV-B detected by the UVR8 photoreceptor antagonizes auxin signaling and plant shade avoidance. *Proceedings of the National Academy of Sciences*, 111(32):11894–11899.

Heijde, M., Binkert, M., Yin, R., Ares-Orpel, F., Rizzini, L., Van De Slijke, E., Persiau, G., Nolf, J., Gevaert, K., De Jaeger, G., and Ulm, R. (2013). Constitutively active UVR8 photoreceptor variant in Arabidopsis. *Proceedings of the National Academy of Sciences*, 110(50):20326–31.

Heijde, M. and Ulm, R. (2013). Reversion of the Arabidopsis UV-B photoreceptor UVR8 to the homodimeric ground state. *Proceedings of the National Academy of Sciences*, 110(3):1113–8.

Heilmann, M. and Jenkins, G. I. (2013). Rapid reversion from monomer to dimer regenerates the ultraviolet-B photoreceptor UV RESISTANCE LOCUS8 in intact Arabidopsis plants. *Plant physiology*, 161(1):547–55.

Hennig, L., Büche, C., and Schäfer, E. (2000). Degradation of phytochrome A and the high irradiance response in Arabidopsis: A kinetic analysis. *Plant, Cell and Environment*, 23(7):727–734.

Hersch, M., Lorrain, S., de Wit, M., Trevisan, M., Ljung, K., Bergmann, S., and Fankhauser, C. (2014). Light intensity modulates the regulatory network of the shade avoidance response in Arabidopsis. *Proceedings of the National Academy of Sciences*, 111(17):6515–6520.

Hicks, K. A., Millar, A. J., Carre, I. A., Somers, D. E., Straume, M., Meeks-Wagner, R., and Kay, S. A. (1996). Conditional circadian dysfuncion of the Arabidopsis early-flowering 3 mutant. *Science*, 274(November):790–792.

Hideg, É., Jansen, M. A. K., and Strid, Å. (2013). UV-B exposure, ROS, and stress: Inseparable companions or loosely linked associates? *Trends in Plant Science*, 18(2):107–115.

Hiltbrunner, A., Tscheuschler, A., Viczián, A., Kunkel, T., Kircher, S., and Schäfer, E. (2006). FHY1 and FHL act together to mediate nuclear accumulation of the phytochrome A photoreceptor. *Plant and Cell Physiology*, 47(8):1023–1034.

Hoffman, P. D., Batschauer, a., and Hays, J. B. (1996). PHH1 , a novel gene from Arabidopsis thaliana that encodes a protein similar to plant blue-light photoreceptors and microbial phytolyases. *Mol. Gen. Genet.*, 253:259–265.

Holm, M., Ma, L. G., Qu, L. J., and Deng, X. W. (2002). Two interacting bZIP proteins are direct targets of COP1-mediated control of light-dependent gene expression in Arabidopsis. *Genes and Development*, 16(10):1247–1259.

Holmes, M. G. and Smith, H. (1975). The function of phytochrome in plants growing in the natural environment. *Nature*, 254:512–514.

Holmes, M. G. and Smith, H. (1977). The function of phytochrome in the natural environment. II. The influence of vegetation canopies on the spectral energy distribution of natural daylight. *Photochemistry and Photobiology*, 25(6):539–545.

Hornitschek, P., Kohnen, M. V., Lorrain, S., Rougemont, J., Ljung, K., López-Vidriero, I., Franco-Zorrilla, J. M., Solano, R., Trevisan, M., Pradervand, S., Xenarios, I., and Fankhauser, C. (2012). Phytochrome interacting factors 4 and 5 control seedling growth in changing light conditions by directly controlling auxin signaling. *Plant Journal*, 71(5):699–711.

Hornitschek, P., Lorrain, S., Zoete, V., Michielin, O., and Fankhauser, C. (2009). Inhibition of the shade avoidance response by formation of non-DNA binding bHLH heterodimers. *The EMBO journal*, 28(24):3893–902.

Hotta, C. T., Gardner, M. J., Hubbard, K. E., Baek, S. J., Dalchau, N., Suhita, D., Dodd, A. N., and Webb, A. A. R. (2007). Modulation of environmental responses of plants by circadian clocks. *Plant, Cell and Environment*, 30(3):333–349.

Hsu, P. Y., Devisetty, U. K., and Harmer, S. L. (2013). Accurate timekeeping is controlled by a cycling activator in Arabidopsis. *eLife*, 2013(2):1–20.

Hsu, P. Y. and Harmer, S. L. (2014). Wheels within wheels: the plant circadian system. *Trends in Plant Science*, 19(4):240–249.

Huala, E., Oeller, P. W., Liscum, E., Han, I. S., Larsen, E., and Briggs, W. R. (1997). Arabidopsis NPH1: a protein kinase with a putative redox-sensing domain. *Science*, 278(5346):2120–2123.

Huang, W., Perez-Garcia, P., Pokhilko, A., J, M. A., Antoshechkin, I., Piechmann, J., and P, M. (2012a). Mapping the Core of the Arabidopsis Circadian Clock Defines the Network Structure of the Oscillator. *Science*, 337(August):749–754.

Huang, X., Ouyang, X., Yang, P., Lau, O. S., Chen, L., Wei, N., and Deng, X. W. (2013). Conversion from CUL4-based COP1-SPA E3 apparatus to UVR8-COP1-SPA complexes underlies a distinct biochemical function of COP1 under UV-B. *Proceedings of the National Academy of Sciences*, 110(41):16669–74.

Huang, X., Ouyang, X., Yang, P., Lau, O. S., Li, G., Li, J., Chen, H., and Deng, X. W. (2012b). Arabidopsis FHY3 and HY5 positively mediate induction of COP1 transcription in response to photomorphogenic UV-B light. *The Plant cell*, 24(11):4590–606.

Huot, B., Yao, J., Montgomery, B. L., and He, S. Y. (2014). Growth-defense tradeoffs in plants: A balancing act to optimize fitness. *Molecular Plant*, 7(8):1267–1287.

Huq, E., Al-Sady, B., Hudson, M., Kim, C., Apel, K., and Quail, P. (2004). Phytochrome-interacting factor 1 is a critical bHLH regulator of chlorophyll biosynthesis. *Science*, 305:1937–1942.

Huq, E., Kang, Y., and Halliday, K. (2000). SRL1: a new locus specific to the phyB signaling pathway in Arabidopsis. *The Plant Journal*, 23(4):461–470.

Ito, S., Song, Y. H., and Imaizumi, T. (2012). LOV domain-containing F-box proteins: Light-dependent protein degradation modules in Arabidopsis. *Molecular Plant*, 5(3):573–582.

James, A. B., Monreal, J. A., Nimmo, G. A., Kelly, C. L., Herzyk, P., Jenkins, G. I., and Nimmo, H. G. (2008). The Circadian Clock in Arabidopsis. *Science*, (December):1832–1835.

Jansen, M. A., Gaba, V., and Greenberg, B. M. (1998). Higher plants and UV-B radiation: Balancing damage, repair and acclimation. *Trends in Plant Science*, 3(4):131–135.

Jenkins, G. I. (2009). Signal transduction in responses to UV-B radiation. *Annual review of plant biology*, 60:407–431.

Jenkins, G. I. (2014). The UV-B Photoreceptor UVR8 : From Structure to Physiology. *The Plant Cell*, 26(1):21–37.

Jenkins, G. I. (2017). Photomorphogenic responses to ultraviolet-B light. *Plant Cell and Environment*, 40(11):2544–2557.

Jenkins, G. I., Long, J. C., Wade, H. K., Shenton, M. R., and Bibikova, T. N. (2001). UV and blue light signalling: pathways regulating chalcone synthase gene expression in Arabidopsis. *New Phytologist*, 151(1):121–131.

Jiménez-Gómez, J. M., Wallace, A. D., and Maloof, J. N. (2010). Network analysis identifies ELF3 as a QTL for the shade avoidance response in arabidopsis. *PLoS Genetics*, 6(9):e1001100.

Johnson, E. and Bradley, M. (1994). Photoresponses of light-grown phyA mutants of Arabidopsis. *Plant Physiology*, 105:141–149.

Jordan, B. R. (2002). Molecular responses of plant cells to UV-B radiation. *Functional Plant Biology*, 29:909–916.

Jung, J. H., Domijan, M., Klose, C., Biswas, S., Ezer, D., Gao, M., Khattak, A. K., Box, M. S., Charoensawan, V., Cortijo, S., Kumar, M., Grant, A., Locke, J. C., Schäfer, E., Jaeger, K. E., and Wigge, P. A. (2016). Phytochromes function as thermosensors in Arabidopsis. *Science*, 354(6314):886–889.

Kaczorowski, K. (2004). *Mutants in phytochrome-dependent seedling photomorphogenesis and control of the Arabidopsis circadian clock*. PhD thesis, University of California, Berkeley, CA, USA.

Kaiserli, E. and Jenkins, G. I. (2007). UV-B promotes rapid nuclear translocation of the Arabidopsis UV-B specific signaling component UVR8 and activates its function in the nucleus. *The Plant cell*, 19(8):2662–2673.

Kamioka, M., Takao, S., Suzuki, T., Taki, K., Higashiyama, T., Kinoshita, T., and Nakamichi, N. (2016). Direct Repression of Evening Genes by CIRCADIAN CLOCK-ASSOCIATED1 in the Arabidopsis Circadian Clock. *The Plant Cell*, 28(3):696–711.

Kasahara, M., Kagawa, T., Oikawa, K., Suetsugu, N., Miyao, M., and Wada, M. (2002). Chloroplast avoidance movement reduces photodamage in plants. *Nature*, 420(6917):829–832.

Kasperbauer, M. J. (1971). Spectral distribution of light in a tobacco canopy and effects of end-of-day light quality on growth and development. *Plant physiology*, (1971):775–778.

Kegge, W. and Pierik, R. (2010). Biogenic volatile organic compounds and plant competition. *Trends in Plant Science*, 15(3):126–132.

Keiller, D. and Smith, H. (1989). Control of carbon partitioning by light quality mediated by phytochrome. *Plant Science*, 63(1):25–29.

Keller, M. M., Jaillais, Y., Pedmale, U. V., Moreno, J. E., Chory, J., and Ballaré, C. L. (2011). Cryptochrome 1 and phytochrome B control shade-avoidance responses in Arabidopsis via partially independent hormonal cascades. *Plant Journal*, 67(2):195–207.

Keuskamp, D. H., Pollmann, S., Voesenek, L. A. C. J., Peeters, A. J. M., and Pierik, R. (2010). Auxin transport through PIN-FORMED 3 (PIN3) controls shade avoidance and fitness during competition. *Proceedings of the National Academy of Sciences*, 107(52):22740–22744.

Keuskamp, D. H., Sasidharan, R., Vos, I., Peeters, A. J. M., Voesenek, L. a. C. J., and Pierik, R. (2011). Blue-light-mediated shade avoidance requires combined auxin and brassinosteroid action in Arabidopsis seedlings. *Plant Journal*, 67(2):208–217.

Khanna, R., Huq, E., and Kikis, E. (2004). A novel molecular recognition motif necessary for targeting photoactivated phytochrome signaling to specific basic helix-loop-helix transcription factors. *The Plant Cell*, 16:3033–3044.

Khanna, R., Shen, Y., Marion, C. M., Tsuchisaka, A., Theologis, A., Schäfer, E., and Quail, P. H. (2007). The basic helix-loop-helix transcription factor PIF5 acts on ethylene biosynthesis and phytochrome signaling by distinct mechanisms. *The Plant Cell*, 19(12):3915–3929.

Kiba, T., Henriques, R., Sakakibara, H., and Chua, N.-H. (2007). Targeted degradation of PSEUDO-RESPONSE REGULATOR5 by an SCFZTL complex regulates clock function and photomorphogenesis in Arabidopsis thaliana. *The Plant cell*, 19(8):2516–2530.

Kim, B., Tennessen, D., and Last, R. (1998). UV-B-induced photomorphogenesis in Arabidopsis thaliana. *The Plant Journal*, 15(5):667–674.

Kim, D. H., Yamaguchi, S., Lim, S., Oh, E., Park, J., Hanada, A., Kamiya, Y., and Choi, G. (2008). SOMNUS, a CCCH-type zinc finger protein in Arabidopsis, negatively regulates light-dependent seed germination downstream of PIL5. *The Plant cell*, 20(5):1260–77.

Kim, J.-I., Bhoo, S.-H., Han, Y.-J., Zarate, X., Furuya, M., and Song, P.-S. (2006). The PAS2 domain is required for dimerization of phytochrome A. *Journal of Photochemistry and Photobiology A: Chemistry*, 178(2-3):115–121.

Kim, K., Kook, H.-S., Jang, Y.-J., Lee, W.-H., Kamala-Kannan, S., Chae, J.-C., Lee, and Kui-Jae (2013). The Effect of Blue-light-emitting Diodes on Antioxidant Properties and Resistance to Botrytis cinerea in Tomato. *Journal of Plant Pathology & Microbiology*, 4(9).

Kim, T.-W. and Wang, Z.-Y. (2010). Brassinosteroid signal transduction from receptor kinases to transcription factors. *Annual review of plant biology*, 61:681–704.

Kim, W. Y., Fujiwara, S., Suh, S. S., Kim, J., Kim, Y., Han, L., David, K., Putterill, J., Nam, H. G., and Somers, D. E. (2007). ZEITLUPE is a circadian photoreceptor stabilized by GIGANTEA in blue light. *Nature*, 449(7160):356–360.

Kinoshita, T., Doi, M., Suetsugu, N., Kagawa, T., Wada, M., and Shimazaki, K. (2001). Phot1 and phot2 mediate blue light regulation of stomatal opening. *Nature*, 414(6864):656–660.

Kircher, S., Gil, P., and Kozma-Bognár, L. (2002). Nucleocytoplasmic partitioning of the plant photoreceptors phytochrome A, B, C, D, and E is regulated differentially by light and exhibits a diurnal rhythm. *The Plant Cell ...*, 14(July):1541–1555.

Kircher, S., Kozma-Bognar, L., and Kim, L. (1999). Light quality dependent nuclear import of the plant photoreceptors phytochrome A and B. *The Plant Cell*, 11(August):1445–1456.

Kliebenstein, D. J., Lim, J. E., Landry, L. G., and Last, R. L. (2002). Arabidopsis UVR8 regulates ultraviolet-B signal transduction and tolerance and contains sequence similarity to human regulator of chromatin condensation 1. *Plant physiology*, 130(1):234–243.

Kolmos, E., Herrero, E., Bujdoso, N., Millar, A. J., Toth, R., Gyula, P., Nagy, F., and Davis, S. J. (2011). A Reduced-Function Allele Reveals That EARLY FLOWERING3 Repressive Action on the Circadian Clock Is Modulated by Phytochrome Signals in Arabidopsis. *the Plant Cell Online*, 23(9):3230–3246.

Koorneef, M., Rolff, E., Spruit, C., Koornneef, M., Rolff, E., and Spruit, C. (1980). Genetic Control of Light-inhibited Hypocotyl Elongation in Arabidopsis thaliana (L.) Heynh. *Zeitschrift für Pflanzenphysiologie*, 100(2):147–160.

Krizek, D. T. (2004). Influence of PAR and UV-A in determining plant sensitivity and photomorphogenic responses to UV-B radiation. *Photochemistry and photobiology*, 79(4):307–315.

Kumar, G. and Pandey, A. (2017). Effect of UV-B Radiation on Chromosomal Organisation and Biochemical Consituents of Coriandrum sativum L. *Jordan Journal of Biological Sciences*, 10(2):85–93.

Lau, O. S. and Deng, X. W. (2012). The photomorphogenic repressors COP1 and DET1: 20 years later. *Trends in plant science*, 17(10):584–93.

Legris, M., Klose, C., Burgie, E. S., Rojas, C. C. R., Neme, M., Hiltbrunner, A., Wigge, P. A., Schäfer, E., Vierstra, R. D., and Casal, J. J. (2016). Phytochrome B integrates light and temperature signals in Arabidopsis. *Science*, 354(6314):897–900.

Leivar, P. and Monte, E. (2014). PIFs: systems integrators in plant development. *The Plant cell*, 26(1):56–78.

Leivar, P., Monte, E., Cohn, M. M., and Quail, P. H. (2012a). Phytochrome Signaling in Green Arabidopsis Seedlings: Impact Assessment of a Mutually Negative phyB - PIF Feedback Loop. *Molecular Plant*, 5(3):734–749.

Leivar, P., Monte, E., Oka, Y., Liu, T., and Carle, C. (2008). Multiple phytochrome-interacting bHLHtranscription factors repress premature seedling photomorphogenesis in darkness. *Current Biology*, 18(23):1815–1823.

Leivar, P., Tepperman, J. M., Cohn, M. M., Monte, E., Al-Sady, B., Erickson, E., and Quail, P. H. (2012b). Dynamic Antagonism between Phytochromes and PIF Family Basic Helix-Loop-Helix Factors Induces Selective Reciprocal Responses to Light and Shade in a Rapidly Responsive Transcriptional Network in Arabidopsis. *The Plant Cell*, 24(4):1398–1419.

Li, G., Siddiqui, H., Teng, Y., Lin, R., Wan, X. Y., Li, J., Lau, O. S., Ouyang, X., Dai, M., Wan, J., Devlin, P. F., Deng, X. W., and Wang, H. (2011). Coordinated transcriptional regulation underlying the circadian clock in Arabidopsis. *Nature Cell Biology*, 13(5):616–622.

Li, K., Yu, R., Fan, L.-M., Wei, N., Chen, H., and Deng, X. W. (2016). DELLA-mediated PIF degradation contributes to coordination of light and gibberellin signalling in Arabidopsis. *Nature Communications*, 7(May):11868.

Li, L., Ljung, K., Breton, G., Schmitz, R. J., Pruneda-Paz, J., Cowing-Zitron, C., Cole, B. J., Ivans, L. J., Pedmale, U. V., Jung, H. S., Ecker, J. R., Kay, S. A., and Chory, J. (2012a). Linking photoreceptor excitation to changes in plant architecture. *Genes and Development*, 26(8):785–790.

Li, Q.-F., Wang, C., Jiang, L., Li, S., Sun, S. S. M., and He, J.-X. (2012b). An Interaction Between BZR1 and DELLAs Mediates Direct Signaling Crosstalk Between Brassinosteroids and Gibberellins in Arabidopsis. *Science Signaling*, 5(244):ra72–ra72.

Liang, T., Mei, S., Shi, C., Yang, Y., Peng, Y., Ma, L., Wang, F., Li, X., Huang, X., Yin, Y., and Liu, H. (2018). UVR8 Interacts with BES1 and BIM1 to Regulate Transcription and Photomorphogenesis in Arabidopsis. *Developmental Cell*, 44(4):512–523.e5.

Lin, C., Robertson, D. E., Ahmad, M., Raibekas, A. A., Jorns, M. S., Dutton, P. L., and Cashmore, A. R. (1995). Association of flavin adenine dinucleotide with the Arabidopsis blue light receptor CRY1. *Science*, 269(5226):968–970.

Lin, C., Yang, H., Guo, H., Mockler, T., Chen, J., and Cashmore, a. R. (1998). Enhancement of blue-light sensitivity of Arabidopsis seedlings by a blue light receptor cryptochrome 2. *Proceedings of the National Academy of Sciences*, 95(5):2686–2690.

Linkosalo, T. and Lechowicz, M. J. (2006). Twilight far-red treatment advances leaf bud burst of silver birch (Betula pendula). *Tree physiology*, 26(10):1249–1256.

Liou, M.-Y. and Storz, P. (2010). Reactive oxygen species in cancer. *Free Radic Res.*, 44(5):479—-96.

Liscum, E. and Briggs, W. R. (1995). Mutations in the NPH1 locus of Arabidopsis disrupt the perception of phototropic stimuli. *The Plant cell*, 7(4):473–485.

Liu, T. L., Newton, L., Liu, M.-J., Shiu, S.-H., and Farré, E. M. (2016). A G-Box-Like Motif Is Necessary for Transcriptional Regulation by Circadian Pseudo-Response Regulators in Arabidopsis. *Plant Physiology*, 170(1):528–539.

Liu, X. L., Covington, M. F., Fankhauser, C., Chory, J., and Wagner, D. R. (2001). ELF3 encodes a circadian clock-regulated nuclear protein that functions in an Arabidopsis PHYB signal transduction pathway. *The Plant cell*, 13(6):1293–1304.

Liu, Z., Zhang, Y., Liu, R., Hao, H., Wang, Z., and Bi, Y. (2011). Phytochrome interacting factors (PIFs) are essential regulators for sucrose-induced hypocotyl elongation in Arabidopsis. *Journal of Plant Physiology*, 168(15):1771–1779.

Lois, R. (1994). Accumulation of UV-absorbing flavonoids induced by UV-B radiation in Arabidopsis thaliana L. *Planta*, 194(4):498–503.

Lorrain, S., Allen, T., Duek, P. D., Whitelam, G. C., and Fankhauser, C. (2008). Phytochrome-mediated inhibition of shade avoidance involves degradation of growth-promoting bHLH transcription factors. *The Plant journal : for cell and molecular biology*, 53(2):312–23.

Lucas, M., Davière, J.-M., Rodríguez-Falcón, M., Pontin, M., Iglesias-Pedraz, J. M., Lorrain, S., Fankhauser, C., Blázquez, M. A., Titarenko, E., Prat, S., de Lucas, M., Davière, J.-M., Rodríguez-Falcón, M., Pontin, M., Iglesias-Pedraz, J. M., Lorrain, S., Fankhauser, C., Blázquez, M. A., Titarenko, E., and Prat, S. (2008). A molecular framework for light and gibberellin control of cell elongation. *Nature*, 451(7177):480–484.

Ma, D., Li, X., Guo, Y., Chu, J., Fang, S., Yan, C., Noel, J. P., and Liu, H. (2015). Cryptochrome 1 interacts with PIF4 to regulate high temperature-mediated hypocotyl elongation in response to blue light. *Proceedings of the National Academy of Sciences*, 113(1):224–229.

Makino, S., Matsushika, A., Kojima, M., Yamashino, T., and Mizuno, T. (2002). The APRR1/TOC1 quintet implicated in circadian rhythms of Arabidopsis thaliana: I. Characterization with APRR1-Overexpressing Plants. *Plant & cell physiology*, 43(1):58–59.

Manivannan, A., Soundararajan, P., Halimah, N., Ko, C. H., and Jeong, B. R. (2015). Blue LED light enhances growth, phytochemical contents, and antioxidant enzyme activities of Rehmannia glutinosa cultured in vitro. *Horticulture, Environment, and Biotechnology*, 56(1):105–113.

Martín, G., Rovira, A., Veciana, N., Soy, J., Toledo-Ortiz, G., Gommers, C. M., Boix, M., Henriques, R., Minguet, E. G., Alabadí, D., Halliday, K. J., Leivar, P., and Monte, E. (2018). Circadian Waves of Transcriptional Repression Shape PIF-Regulated Photoperiod-Responsive Growth in Arabidopsis. *Current Biology*, pages 1–8.

Martínez-García, J. F., Gallemí, M., Molina-Contreras, M. J., Llorente, B., Bevilaqua, M. R. R., and Quail, P. H. (2014). The Shade Avoidance Syndrome in Arabidopsis: The Antagonistic Role of Phytochrome A and B Differentiates Vegetation Proximity and Canopy Shade. *PLoS ONE*, 9(10):e109275.

Martínez-García, J. F., Huq, E., Quail, P. H., Martinez-Garcia, J., Huq, E., and Quail, P. H. (2000). Direct targeting of light signals to a promoter element-bound transcription factor. *Science*, 288(May):859–864.

Más, P. (2008). Chromatin remodelling and the Arabidopsis biological clock. *Plant Signaling and Behavior*, 3(2):121–123.

Más, P., Kim, W.-Y., Somers, D. E., and Kay, S. A. (2003). Targeted degradation of TOC1 by ZTL modulates circadian function in Arabidopsis thaliana. *Nature*, 426(6966):567–570.

Mathews, S., Lavin, M., and Sharrock, R. A. (1995). Evolution of the phytochrome gene family and its utility for phylogenetic analyses of angiosperms. *Annals of the Missouri Botanical Garden*, 82(2):296–321.

Mathews, S. and Sharrock, R. A. (1997). Phytochrome gene diversity. *Plant, Cell and Environment*, 20(6):666–671.

Matsushika, A., Makino, S., Kojima, M., Yamashino, T., and Mizuno, T. (2002). The APRR1/TOC1 Quintet Implicated in Circadian Rhythms of Arabidopsis thaliana: II. Characterization with CCA1-Overexpressing Plants. *Plant and Cell Physiology*, 43(1):58–69.

Mazza, C. and Ballaré, C. (2015). Photoreceptors UVR8 and phytochrome B cooperate to optimize plant growth and defense in patchy canopies. *New Phytologist*.

Mazza, C. A., Giménez, P. I., Kantolic, A. G., and Ballaré, C. L. (2013). Beneficial effects of solar UV-B radiation on soybean yield mediated by reduced insect herbivory under field conditions. *Physiologia Plantarum*, 147(3):307–315.

McClung, C. R. (2006). Plant circadian rhythms. *The Plant cell*, 18(4):792–803.

Michael, T. P., Mockler, T. C., Breton, G., McEntee, C., Byer, A., Trout, J. D., Hazen, S. P., Shen, R., Priest, H. D., Sullivan, C. M., Givan, S. A., Yanovsky, M., Hong, F., Kay, S. A., and Chory, J. (2008). Network discovery pipeline elucidates conserved time-of-day-specific cis-regulatory modules. *PLoS Genetics*, 4(2).

Michael, T. P., Salomé, P. A., Yu, H. J., Spencer, T. R., Sharp, E. L., McPeek, M. A., Alonso, J. M., Ecker, J. R., and McClung, C. R. (2003). Enhanced Fitness Conferred by Naturally Occurring Variation in the Circadian Clock. *Science*, 302(5647):1049–1053.

Millar, A. J., Carre, I. A., Stayer, C. A., Chua, N.-H., and Kay, S. A. (1995a). Circadian Clock Mutants in Arabidopsis Indentified by Luciferase Imaging. *Science*, 267(February):1161–1163.

Millar, A. J., Short, S. R., Chua, N.-H., and Kay, S. A. (1992). A Novel Circadian Phenotype Based on Firefly Luciferase Expression in Transgenic Plants. *the Plant Cell Online*, 4(9):1075–1087.

Millar, A. J., Straume, M., Chory, J., Chua, N.-H., and Kay, S. A. (1995b). The Regulation of Circadian Period by Photo Transduction Pathways in Arabidopsis. *Science*, 267(February):1163–1166.

Miransari, M. and Smith, D. L. (2014). Plant hormones and seed germination. *Environmental and Experimental Botany*, 99:110–121.

Mishra, P. and Panigrahi, K. C. (2015). GIGANTEA-An emerging story. *Frontiers in Plant Science*, 6:1–15.

Monte, E., Ecker, J. R., Zhang, Y., Li, X., Young, J., Austin-Phillips, S., and Quail, P. H. (2003). Isolation and Characterization of phyC Mutants in Arabidopsis Reveals Complex Crosstalk between Phytochrome Signaling Pathways. *The Plant Cell*, 15:1962–1980.

Moon, J., Zhu, L., Shen, H., and Huq, E. (2008). PIF1 directly and indirectly regulates chlorophyll biosynthesis to optimize the greening process in Arabidopsis. *Proceedings of the National Academy of Sciences*, 105(27):9433–9438.

Morgan, D. C., O'Brien, T., and Smith, H. (1980). Rapid photomodulation of stem extension in light-grown Sinapis alba L. *Planta*, 150(2):95–101.

Morgan, D. C. and Smith, H. (1976). Linear relationship between phytochrome photoequilibrium and growth in plants under simulated natural radiation. *Nature*, 262:210–212.

Morgan, D. C. and Smith, H. (1978). The relationship between phytochrome-photoequilibrium and Development in light grown Chenopodium album L. *Planta*, 193(1978):187–193.

Morgan, D. C. and Smith, H. (1981). Control of Development in Chenopodium Album L. By Shadelight: the Effect of Light Quantity (Total Fluence Rate) and Light Quality (Red.Far-Red Ratio). *New Phytologist*, 88(2):239–248.

Murashige, T. and Skoog, F. (1962). A Revised Medium for Rapid Growth and Bio Assays with Tobacco Tissue Cultures. *Physiologia Plantarum*, 15(3):473–497.

Nagatani, A., Chory, J., and Furuya, M. (1991). Phytochrome B is not detectable in the hy3 mutant of Arabidopsis, which is deficient in responding to end-of-day far-red light treatments. *Plant and Cell Physiology*, 32(7):1119–1122.

Nagatani, A., Reed, J. W., and Chory, J. (1993). lsolation and lnitial Characterization of Arabidopsis Mutants That Are Deficient in Phytochrome A. *Plant Physiology*, 102:269–277.

Nagel, D. H. and Kay, S. A. (2012). Complexity in the wiring and regulation of plant circadian networks. *Current Biology*, 141(4):520–529.

Nakamichi, N., Kiba, T., Henriques, R., Mizuno, T., Chua, N. H., and Sakakibara, H. (2010). PSEUDO-RESPONSE REGULATORS 9, 7, and 5 Are Transcriptional Repressors in the Arabidopsis Circadian Clock. *The Plant Cell*, 22(3):594–605.

Nakamichi, N., Kita, M., Ito, S., Yamashino, T., and Mizuno, T. (2005). PSEUDO-RESPONSE REGULATORS, PRR9, PRR7 and PRR5, Together play essential roles close to the circadian clock of Arabidopsis thaliana. *Plant and Cell Physiology*, 46(5):686–698.

Naznin, M. T., Lefsrud, M., Gravel, V., and Hao, X. (2016). Different ratios of red and blue LED light effects on coriander productivity and antioxidant properties. *Acta Horticulturae*, 1134:223–230.

Nelson, D. C., Lasswell, J., Rogg, L. E., Cohen, M. A., and Bartel, B. (2000). FKF1, a clock-controlled gene that regulates the transition to flowering in Arabidopsis. *Cell*, 101(3):331–340.

Ni, M., Tepperman, J., and Quail, P. (1998). PIF3, a phytochrome-interacting factor necessary for normal photoinduced signal transduction, is a novel basic helix-loop-helix protein. *Cell*, 95:657–667.

Ni, M., Tepperman, J., and Quail, P. (1999). Binding of phytochrome B to its nuclear signalling partner PIF3 is reversibly induced by light. *Nature*, 450:781–784.

Ni, W., Xu, S.-L., Chalkley, R. J., Pham, T. N. D., Guan, S., Maltby, D. A., Burlingame, A. L., Wang, Z.-Y., and Quail, P. H. (2013). Multisite light-induced phosphorylation of the transcription factor PIF3 is necessary for both its rapid degradation and concomitant negative feedback modulation of photoreceptor phyB levels in Arabidopsis. *The Plant cell*, 25(7):2679–98.

Ni, W., Xu, S.-L., Tepperman, J. M., Stanley, D. J., Maltby, D. A., Gross, J. D., Burlingame, A. L., Wang, Z.-Y., and Quail, P. H. (2014). A mutually assured destruction mechanism attenuates light signaling in Arabidopsis. *Science*, 344(6188):1160–1164.

Nieto, C., Lopez-Salmeron, V., Daviere, J.-M., and Prat, S. (2015). ELF3-PIF4 Interaction Regulates Plant Growth Independently of the Evening Complex. *Current Biology*, 25:187–193.

Niwa, Y., Yamashino, T., and Mizuno, T. (2009). The circadian clock regulates the photoperiodic response of hypocotyl elongation through a coincidence mechanism in Arabidopsis thaliana. *Plant & cell physiology*, 50(4):838–854.

Nozue, K., Covington, M. F., Duek, P. D., Lorrain, S., Fankhauser, C., Harmer, S. L., and Maloof, J. N. (2007). Rhythmic growth explained by coincidence between internal and external cues. *Nature*, 448(7151):358–61.

Nusinow, D. A., Helfer, A., Hamilton, E. E., King, J. J., Imaizumi, T., Schultz, T. F., Farré, E. M., and Kay, S. A. (2011). The ELF4-ELF3-LUX complex links the circadian clock to diurnal control of hypocotyl growth. *Nature*, 475:398–402.

Oakenfull, R. J. and Davis, S. J. (2017). Shining a light on the Arabidopsis circadian clock. *Plant, Cell & Environment*, (January):2571–2585.

Oh, E., Kang, H., Yamaguchi, S., Park, J., Lee, D., Kamiya, Y., and Choi, G. (2009). Genome-wide analysis of genes targeted by PHYTOCHROME INTERACTING FACTOR 3-LIKE5 during seed germination in Arabidopsis. *The Plant cell*, 21(2):403–19.

Oh, E., Kim, J.-i., Park, E., and Kim, J. (2004). PIL5, a phytochrome-interacting basic helix-loop-helix protein, is a key negative regulator of seed germination in Arabidopsis thaliana. *The Plant Cell*, 16(November):3045–3058.

Oh, E., Yamaguchi, S., Hu, J., Yusuke, J., Jung, B., Paik, I., Lee, H.-S., Sun, T.-P., Kamiya, Y., and Choi, G. (2007). PIL5, a phytochrome-interacting bHLH protein, regulates gibberellin responsiveness by binding directly to the GAI and RGA promoters in Arabidopsis seeds. *The Plant cell*, 19(4):1192–208.

Oh, E., Zhu, J. Y., and Wang, Z.-Y. (2012). Interaction between BZR1 and PIF4 integrates brassinosteroid and environmental responses. *Nat Cell Biol*, 14(8):802–809.

Ohgishi, M., Saji, K., Okada, K., and Sakai, T. (2004). Functional analysis of each blue light receptor, cry1, cry2, phot1, and phot2, by using combinatorial multiple mutants in Arabidopsis. *Proceedings of the National Academy of Sciences*, 101(8):2223–2228.

Oravecz, A., Baumann, A., Máté, Z., Brzezinska, A., Molinier, J., Oakeley, E. J., Adám, E., Schäfer, E., Nagy, F., and Ulm, R. (2006). CONSTITUTIVELY PHOTOMORPHOGENIC1 is required for the UV-B response in Arabidopsis. *The Plant cell*, 18(8):1975–1990.

Orient, A., Donkó, Á., Szabó, A., Leto, T. L., and Geiszt, M. (2007). Novel sources of reactive oxygen species in the human body. *Nephrology Dialysis Transplantation*, 22(5):1281–1288.

Osterlund, M. T., Hardtke, C. S., Wei, N., and Deng, X. W. (2000). Targeted destabilization of HY5 during light-regulated development of Arabidopsis. *Nature*, 405(6785):462–466.

Oyama, T., Shimura, Y., and Okada, K. (1997). The Arabidopsis HY5 gene encodes a bZIP protein that regulates stimulus- induced development of root and hypocotyl. *Genes and Development*, 11(22):2983–2995.

Palmer, J. M., Short, T. W., and Briggs, W. R. (1993). Correlation of Blue Light-Induced Phosphorylation to Phototropism in Zea mays L. *Plant physiology*, 102(4):1219–1225.

Park, D. H., Somers, D. E., Kim, Y. S., Choy, Y. H., Lim, H. K., Soh, M. S., Kim, H. J., Kay, S. A., and Nam, H. G. (1999). Control of circadian rhythms and photoperiodic flowering by the Arabidopsis GIGANTEA gene. *Gene. Science*, 285(September):1579–1582.

Park, E., Park, J., and Kim, J. (2012). Phytochrome B inhibits binding of Phytochrome-Interacting Factors to their target promoters. *The Plant Journal*, 72(4):537–546.

Parks, B. and Quail, P. (1993). hy8, a new class of arabidopsis long hypocotyl mutants deficient in functional phytochrome A. *The Plant Cell*, 5:39–48.

Paul, N. D., Jacobson, R. J., Taylor, A., Wargent, J. J., and Moore, J. P. (2005). The Use of Wavelength - selective Plastic Cladding Materials in Horticulture: Understanding of Crop and Fungal Responses Through the Assessment of Biological Spectral Weighting Functions. *Photochemistry and Photobiology*, 81(5):1052–1060.

Pedmale, U., Huang, S.-s., Zander, M., Cole, B., Hetzel, J., Ljung, K., Reis, P., Sridevi, P., Nito, K., Nery, J., Ecker, J., and Chory, J. (2015). Cryptochromes Interact Directly with PIFs to Control Plant Growth in Limiting Blue Light. *Cell*, pages 1–13.

Peer, W. A. and Murphy, A. S. (2007). Flavonoids and auxin transport: modulators or regulators? *Trends in Plant Science*, 12(12):556–563.

Penfield, S., Josse, E.-M., and Halliday, K. J. (2010). A role for an alternative splice variant of PIF6 in the control of Arabidopsis primary seed dormancy. *Plant molecular biology*, 73(1-2):89–95.

Penfield, S., Josse, E.-M., Kannangara, R., Gilday, A. D., Halliday, K. J., and Graham, I. A. (2005). Cold and light control seed germination through the bHLH transcription factor SPATULA. *Current biology : CB*, 15(22):1998–2006.

Pérez-García, P., Ma, Y., Yanovsky, M. J., and Mas, P. (2015). Time-dependent sequestration of RVE8 by LNK proteins shapes the diurnal oscillation of anthocyanin biosynthesis. *Proceedings of the National Academy of Sciences*, 112(16):5249–5253.

Pfaffl, M. W. (2001). A new mathematical model for relative quantification in real-time RT-PCR. *Nucleic Acids Research*, 29(9):45e–45.

Pfeiffer, A., Nagel, M.-K., Popp, C., Wüst, F., Bindics, J., Viczián, A., Hiltbrunner, A., Nagy, F., Kunkel, T., and Schäfer, E. (2012). Interaction with plant transcription factors can mediate nuclear import of phytochrome B. *Proceedings of the National Academy of Sciences*, 109(15):5892–7.

Pham, V. N., Kathare, P. K., and Huq, E. (2018). Phytochromes and Phytochrome Interacting Factors. *Plant Physiology*, 176:pp.01384.2017.

Pierik, R. and De Wit, M. (2014). Shade avoidance: Phytochrome signalling and other aboveground neighbour detection cues. *Journal of Experimental Botany*, 65(11):2815–2824.

Pierik, R., Djakovic-Petrovic, T., Keuskamp, D. H., de Wit, M., and Voesenek, L. A. (2009). Auxin and Ethylene Regulate Elongation Responses to Neighbor Proximity Signals Independent of Gibberellin and DELLA Proteins in Arabidopsis. *Plant Physiology*, 149(4):1701–1712.

Pierik, R., Whitelam, G. C., Voesenek, L. A. C. J., De Kroon, H., and Visser, E. J. W. (2004). Canopy studies on ethylene-insensitive tobacco identify ethylene as a novel element in blue light and plant-plant signalling. *Plant Journal*, 38(2):310–319.

Pizzino, G., Irrera, N., Cucinotta, M., Pallio, G., Mannino, F., Arcoraci, V., Squadrito, F., Altavilla, D., and Bitto, A. (2017). Oxidative Stress: Harms and Benefits for Human Health. *Oxidative Medicine and Cellular Longevity*, 2017.

Podolec, R. and Ulm, R. (2018). Photoreceptor-mediated regulation of the COP1/SPA E3 ubiquitin ligase. *Current Opinion in Plant Biology*, 45:18–25.

Pokhilko, A., Fernández, A. P., Edwards, K. D., Southern, M. M., Halliday, K. J., and Millar, A. J. (2012). The clock gene circuit in Arabidopsis includes a repressilator with additional feedback loops. *Molecular Systems Biology*, 8(574):1–13.

Pucciariello, O., Legris, M., Costigliolo, C., José, M., Esteban, C., Dezar, C., Vazquez, M., Yanovsky, M. J., Finlayson, S. A., Prat, S., and Casal, J. J. (2018). Rewiring of auxin signaling under persistent shade. *Proceedings of the National Academy of Sciences*, (May):1721110115.

Rausenberger, J., Tscheuschler, A., Nordmeier, W., Wüst, F., Timmer, J., Schäfer, E., Fleck, C., and Hiltbrunner, A. (2011). Photoconversion and nuclear trafficking cycles determine phytochrome A's response profile to far-red light. *Cell*, 146(5):813–25.

Rawat, R., Takahashi, N., Hsu, P. Y., Jones, M. A., Schwartz, J., Salemi, M. R., Phinney, B. S., and Harmer, S. L. (2011). REVEILLE8 and PSEUDO-REPONSE REGULATOR5 form a negative feedback loop within the arabidopsis circadian clock. *PLoS Genetics*, 7(3).

Reed, J. W., Nagatani, A., Elich, T., Fagan, M., and Chory, J. (1994). Phytochrome A and Phytochrome B Have Overlapping but Distinct Functions in Arabidopsis Development. *Plant Physiology*, 104(4):1139–1149.

Rice-Evans, C. A., Miller, N. J., and Paganga, G. (1996). Structure-antioxidant activity relationships of flavonoids and phenolic acids. *Free Radical Biology and Medicine*, 20(7):933–956.

Rizzini, L., Favory, J.-J., Cloix, C., Faggionato, D., O'Hara, A., Kaiserli, E., Baumeister, R., Schäfer, E., Nagy, F., Jenkins, G. I., and Ulm, R. (2011). Perception of UV-B by the Arabidopsis UVR8 protein. *Science*, 332:103–106.

Robson, P., Whitelam, G. C., and Smith, H. (1993). Selected Components of the Shade-Avoidance Syndrome Are Displayed in a Normal Manner in Mutants of Arabidopsis thaliana and Brassica rapa Deficient in Phytochrome B. *Plant physiology*, 102(4):1179–1184.

Rockwell, N. C., Su, Y. S., and Lagarias, J. C. (2006). Phytochrome Structure and Signaling Mechanisms. *Annual review of plant biology*, 57(26):837–858.

Roland, W. S. U., Buren, L. V., Gruppen, H., Driesse, M., Gouka, R. J., Smit, G., and Vincken, J.-p. (2013). Bitter Taste Receptor Activation by Flavonoids and Iso fl avonoids: Modeled Structural Requirements for Activation of hTAS2R14 and hTAS2R39. *Journal of Agricultural and Food Chemistry*, 61:10454–66.

Rolauffs, S., Fackendahl, P., Sahm, J., Fiene, G., and Hoecker, U. (2012). Arabidopsis COP1 and SPA genes are essential for plant elongation but not for acceleration of flowering time in response to a low red light to far-red light ratio. *Plant Physiology*, 160(4):2015–27.

Rozema, J., van de Staaij, J., Björn, L. O., and Caldwell, M. (1997). UV-B as an environmental factor in plant life: stress and regulation. *Trends in Ecology and Evolution*, 12(1):22–28.

Ryan, K. G., Markham, K. R., Bloor, S. J., Bradley, J. M., Mitchell, K. A., and Jordan, B. R. (1998). UVB Radiation Induced Increase in Quercetin: Kaempferol Ratio in Wild-Type and Transgenic Lines of Petunia. *Photochemistry and Photobiology*, 68(3):323–330.

Sadanandom, A., Ádám, É., Orosa, B., Viczián, A., Klose, C., Zhang, C., Josse, E.-M., Kozma-Bognár, L., and Nagy, F. (2015). SUMOylation of phytochrome-B negatively regulates light-induced signaling in. *Proceedings of the National Academy of Sciences*, 112(35):11108–13.

Saijo, Y., Zhu, D., Li, J., Rubio, V., and Zhou, Z. (2008). Arabidopsis COP1/SPA1 complex and phytochrome A signaling intermediates associate with distinct phosphorylated forms of phytochrome A in balancing. *Molecular Cell*, 31(4):607–613.

Sakai, T., Kagawa, T., Kasahara, M., Swartz, T. E., Christie, J. M., Briggs, W. R., Wada, M., and Okada, K. (2001). Arabidopsis nph1 and npl1: blue light receptors that mediate both phototropism and chloroplast relocation. *Proceedings of the National Academy of Sciences*, 98(12):6969–6974.

Sakai, T., Wada, T., Ishiguro, S., and Okada, K. (2000). RPT2. A signal transducer of the phototropic response in Arabidopsis. *The Plant cell*, 12(2):225–236.

Sakalauskaite, J., Viskelis, P., Dambrauskiene, E., Sakalauskiene, S., Samuoliene, G., Brazaityte, A., Duchovskis, P., and Urbonaviciene, D. (2012). The effects of different UV-B radiation intensities on morphological and biochemical characteristics in Ocimum basilicum L. *Journal of the Science of Food and Agriculture*, 93(6):1266–1271.

Sakamoto, K. and Briggs, W. R. (2002). Cellular and subcellular localization of phototropin 1. *The Plant cell*, 14(8):1723–1735.

Sakamoto, K. and Nagatani, A. (1996). Nuclear localization activity of phytochrome B. *The Plant Journal*, 10(5):859–868.

Salter, M. G., Franklin, K. A., and Whitelam, G. C. (2003). Gating of the rapid shade-avoidance response by the circadian clock in plants. *Nature*, 426(6967):680–3.

Sancar, G. B. (1990). DNA photolyases: Physical properties, action mechanism, and roles in dark repair. *Mutation Research/DNA Repair*, 236(2-3):147–160.

Sanchez, S. E., Cagnola, J. I., Crepy, M., Yanovsky, M. J., and Casal, J. J. (2011). Balancing forces in the photoperiodic control of flowering. *Photochemical & photobiological sciences : Official journal of the European Photochemistry Association and the European Society for Photobiology*, 10(4):451–460.

Sanchez, S. E. and Kay, S. A. (2016). The Plant Circadian Clock : From a Simple Timekeeper to a Complex Developmental Manager. *Cold Spring Harbor Perspectives in Biology*, 8:a027748.

Sasidharan, R., Chinnappa, C. C., Staal, M., Elzenga, J. T. M., Yokoyama, R., Nishitani, K., Voesenek, L. A. C. J., and Pierik, R. (2010). Light Quality-Mediated Petiole Elongation in Arabidopsis during Shade Avoidance Involves Cell Wall Modification by Xyloglucan Endotransglucosylase/Hydrolases. *Plant Physiology*, 154(2):978–990.

Schaffer, R., Ramsay, N., Samach, A., Corden, S., Putterill, J., Carré, I. A., and Coupland, G. (1998). The late elongated hypocotyl mutation of Arabidopsis disrupts circadian rhythms and the photoperiodic control of flowering. *Cell*, 93(7):1219–1229.

Schindelin, J., Arganda-Carreras, I., Frise, E., Kaynig, V., Longair, M., Pietzsch, T., Preibisch, S., Rueden, C., Saalfeld, S., Schmid, B., Tinevez, J. Y., White, D. J., Hartenstein, V., Eliceiri, K., Tomancak, P., and Cardona, A. (2012). Fiji: An open-source platform for biological-image analysis. *Nature Methods*, 9(7):676–682.

Schultz, T. F., Kiyosue, T., Yanovsky, M., Wada, M., and Kay, S. A. (2001). A role for LKP2 in the circadian clock of Arabidopsis. *The Plant cell*, 13(12):2659–2670.

Sellaro, R., Crepy, M., Trupkin, S. A., Karayekov, E., Buchovsky, A. S., Rossi, C., and Casal, J. J. (2010). Cryptochrome as a sensor of the blue/green ratio of natural radiation in Arabidopsis. *Plant Physiology*, 154(September):401–409.

Sellaro, R., Pacín, M., and Casal, J. J. (2012). Diurnal dependence of growth responses to shade in Arabidopsis: Role of hormone, clock, and light signaling. *Molecular Plant*, 5(3):619–628.

Seo, H. and Watanabe, E. (2004). Photoreceptor ubiquitination by COP1 E3 ligase desensitizes phytochrome A signaling. *Genes & Development*, 18:617–622.

Seo, P. J., Park, M.-J., Lim, M.-H., Kim, S.-G., Lee, M., Baldwin, I. T., and Park, C.-M. (2012). A Self-Regulatory Circuit of CIRCADIAN CLOCK-ASSOCIATED1 Underlies the Circadian Clock Regulation of Temperature Responses in Arabidopsis. *The Plant Cell*, 24(6):2427–2442.

Sessa, G., Carabelli, M., and Sassi, M. (2005). A dynamic balance between gene activation and repression regulates the shade avoidance response in Arabidopsis. *Genes & Development*, 19(23):2811–2815.

Shalit-Kaneh, A., Kumimoto, R. W., Filkov, V., and Harmer, S. L. (2018). Multiple feedback loops of the Arabidopsis circadian clock provide rhythmic robustness across environmental conditions. *Proceedings of the National Academy of Sciences*, June:201805524.

Sharrock, R. A. and Clack, T. (2002). Patterns of expression and normalized levels of the five Arabidopsis phytochromes. *Plant Physiology*, 130:442–456.

Sharrock, R. A. and Clack, T. (2004). Heterodimerization of type II phytochromes in Arabidopsis. *Proceedings of the National Academy of Sciences*, 101(31):11500–5.

Sharrock, R. A. and Quail, P. H. (1989). Novel phytochrome sequences in Arabidopsis thaliana: structure, evolution, and differential expression of a plant regulatory photoreceptor family. *Genes & Development*, 3(11):1745–1757.

Sheerin, D. J., Menon, C., zur Oven-Krockhaus, S., Enderle, B., Zhu, L., Johnen, P., Schleifenbaum, F., Stierhof, Y.-D., Huq, E., and Hiltbrunner, A. (2015). Light-activated phytochrome A and B interact with members of the SPA family to promote photomorphogenesis in Arabidopsis by reorganizing the COP1/SPA complex. *The Plant cell*, 27(1):189–201.

Shen, H., Moon, J., and Huq, E. (2005). PIF1 is regulated by light-mediated degradation through the ubiquitin-26S proteasome pathway to optimize photomorphogenesis of seedlings in Arabidopsis. *Plant Journal*, 44(6):1023–1035.

Shikata, H., Hanada, K., Ushijima, T., Nakashima, M., Suzuki, Y., and Matsushita, T. (2014). Phytochrome controls alternative splicing to mediate light responses in Arabidopsis. *Proceedings of the National Academy of Sciences*, 111(52):18781–18786.

Shin, A. Y., Han, Y. J., Baek, A., Ahn, T., Kim, S. Y., Nguyen, T. S., Son, M., Lee, K. W., Shen, Y., Song, P. S., and Kim, J. I. (2016). Evidence that phytochrome functions as a protein kinase in plant light signalling. *Nature Communications*, 7(May):1–13.

Shinomura, T., Nagatani, A., Chory, J., and Furuya, M. (1994). The induction of seed germination in Arabidopsis thaliana is regulated principally by phytochrome B and secondarily by phytochrome A. *Plant physiology*, 104(1994):363–371.

Shinomura, T., Nagatani, A., Hanzawa, H., Kubota, M., Watanabe, M., and Furuya, M. (1996). Action spectra for phytochrome A- and B-specific photoinduction of seed germination in Arabidopsis thaliana. *Proceedings of the National Academy of Sciences of the United States of America*, 93(15):8129–8133.

Shor, E., Paik, I., Kangisser, S., Green, R., and Huq, E. (2017). PHYTOCHROME INTERACTING FACTORS mediate metabolic control of the circadian system in Arabidopsis. *New Phytologist*, 215:217–228.

Short, T. W. and Briggs, W. R. (1990). Characterization of a Rapid, Blue Light-Mediated Change in Detectable Phosphorylation of a Plasma Membrane Protein from Etiolated Pea (Pisum sativum L.) Seedlings. *Plant physiology*, 92(1):179–185.

Shrestha, S. H. T. and Warren, G. (2016). CORIANDER VARIETY CN CORI 6003.

Smith, H. (1982). Light Quality, Photoperception, and Plant Strategy.

Smith, H. and Holmes, M. G. (1977). The Function of Phytochrome in the Natural Environment - III. Measurement and Calcualtion of Phytochrome Photoequilibria. *Photochemistry and Photobiology*, 25(6):547–550.

Smith, H. and Whitelam, G. C. (1997). The shade avoidance syndrome: multiple responses mediated by multiple phytochromes. *Plant, Cell and Environment*, 20(6):840–844.

Solomon, S., Ivy, D. J., Kinnison, D., Mills, M. J., Iii, R. R. N., and Schmidt, A. (2016). Emergence of healing in the Antarctic ozone layer. *Science*, 353(6296):269–274.

Solovchenko, A. and Schmitz-Eiberger, M. (2003). Significance of skin flavonoids for UV-B-protection in apple fruits. *Journal of Experimental Botany*, 54(389):1977–1984.

Somers, D. E. (2012). The Arabidopsis clock: Time for an about-face? *Genome Biology*, 13(4):2–5.

Somers, D. E., Devlin, P. F., and Kay, S. A. (1998). Phytochromes and cryptochromes in the entrainment of the Arabidopsis circadian clock. *Science*, 282(5393):1488–1490.

Somers, D. E., Schultz, T. F., Milnamow, M., and Kay, S. A. (2000). ZEITLUPE encodes a novel clock-associated PAS protein from Arabidopsis. *Cell*, 101(3):319–329.

Somers, D. E., Sharrock, R. A., Tepperman, J. M., and Quail, P. H. (1991). The hy3 long hypocotyl mutant of Arabidopsis is deficient in phytochrome B. *The Plant Cell*, 3:1263–1274.

Soriano, G., Cloix, C., Heilmann, M., Núñez-Olivera, E., Martínez-Abaigar, J., and Jenkins, G. I. (2018). Evolutionary conservation of structure and function of the UVR8 photoreceptor from the liverwort Marchantia polymorpha and the moss Physcomitrella patens. *New Phytologist*, 217(1):151–162.

Southern, M. M. and Millar, A. J. (2005). Circadian Genetics in the Model Higher Plant, Arabidopsis thaliana. In Young, M. W., editor, *Circadian Rhythms*, volume 393 of *Methods in Enzymology*, pages 23–35. Academic Press.

Soy, J., Leivar, P., González-Schain, N., Martín, G., Diaz, C., Sentandreu, M., Al-Sady, B., Quail, P. H., and Monte, E. (2016). Molecular convergence of clock and photosensory pathways through PIF3 - TOC1 interaction and co-occupancy of target promoters. *Proceedings of the National Academy of Sciences*.

Soy, J., Leivar, P., González-schain, N., Sentandreu, M., Prat, S., Quail, P. H., and Monte, E. (2012). Phytochrome-imposed oscillations in PIF3 protein abundance regulate hypocotyl growth under diurnal light dark conditions in Arabidopsis. *Plant Journal*, 71(3):390–401.

Steindler, C., Matteucci, a., Sessa, G., Weimar, T., Ohgishi, M., Aoyama, T., Morelli, G., and Ruberti, I. (1999). Shade avoidance responses are mediated by the ATHB-2 HD-zip protein, a negative regulator of gene expression. *Development (Cambridge, England)*, 126(19):4235–4245.

Stephenson, P. G., Fankhauser, C., and Terry, M. J. (2009). PIF3 is a repressor of chloroplast development. *Proceedings of the National Academy of Sciences*, 106(18):7654–7659.

Stracke, R., Favory, J. J., Gruber, H., Bartelniewoehner, L., Bartels, S., Binkert, M., Funk, M., Weisshaar, B., and Ulm, R. (2010a). The Arabidopsis bZIP transcription factor HY5 regulates expression of the PFG1/MYB12 gene in response to light and ultraviolet-B radiation. *Plant, Cell and Environment*, 33(1):88–103.

Stracke, R., Jahns, O., Keck, M., Tohge, T., Niehaus, K., Fernie, A. R., and Weisshaar, B. (2010b). Analysis of production of flavonol glycosides-dependent flavonol glycoside accumulation in Arabidopsis thaliana plants reveals MYB11-, MYB12- and MYB111-independent flavonol glycoside accumulation. *New Phytologist*, 188(4):985–1000.

Strahan, S. E. and Douglass, A. R. (2018). Decline in Antarctic Ozone Depletion and Lower Stratospheric Chlorine Determined From Aura Microwave Limb Sounder Observations. *Geophysical Research Letters*, 45(1):382–390.

Suesslin, C. and Frohnmeyer, H. (2003). An arabidopsis mutant defective in UV-B light-mediated responses. *The Plant Journal*, 33(3):591–601.

Sun, J., Qi, L., Li, Y., Zhai, Q., and Li, C. (2013). PIF4 and PIF5 transcription factors link blue light and auxin to regulate the phototropic response in Arabidopsis. *The Plant cell*, 25(6):2102–14.

Takeuchi, T., Newton, L., Burkhardt, A., Mason, S., and Farré, E. M. (2014). Light and the circadian clock mediate time-specific changes in sensitivity to UV-B stress under light/dark cycles. *Journal of Experimental Botany*, 65(20):6003–12.

Tao, Y., Ferrer, J. L., Ljung, K., Pojer, F., Hong, F., Long, J. A., Li, L., Moreno, J. E., Bowman, M. E., Ivans, L. J., Cheng, Y., Lim, J., Zhao, Y., Ballaré, C. L., Sandberg, G., Noel, J. P., and Chory, J. (2008). Rapid Synthesis of Auxin via a New Tryptophan-Dependent Pathway Is Required for Shade Avoidance in Plants. *Cell*, 133(1):164–176.

Tepperman, J. M., Zhu, T., Chang, H.-S., Wang, X., and Quail, P. H. (2001). Multiple transcription-factor genes are early targets of phytochrome A signaling. *Proceedings of the National Academy of Sciences*, 98(16):9437–9442.

Thomas T.T., D. and Puthur, J. T. (2017). UV radiation priming: A means of amplifying the inherent potential for abiotic stress tolerance in crop plants. *Environmental and Experimental Botany*, 138:57–66.

Toledo-Ortiz, G., Huq, E., and Quail, P. (2003). The Arabidopsis basic/helix-loop-helix transcription factor family. *The Plant Cell*, 15:1749–1770.

Toledo-Ortiz, G., Johansson, H., Lee, K. P., Bou-Torrent, J., Stewart, K., Steel, G., Rodríguez-Concepción, M., and Halliday, K. J. (2014). The HY5-PIF regulatory module coordinates light and temperature control of photosynthetic gene transcription. *PLoS genetics*, 10(6):e1004416.

Tong, H., Leasure, C. D., Hou, X., Yuen, G., Briggs, W., and He, Z.-H. (2008). Role of root UV-B sensing in Arabidopsis early seedling development. *Proceedings of the National Academy of Sciences*, 105(52):21039–21044.

Torre, S., Roro, A. G., Bengtsson, S., Mortensen, L. M., Solhaug, K. A., Gislerød, H. R., and Olsen, J. E. (2012). Control of plant morphology by UV-B and UV-B-temperature interactions. *Acta Horticulturae*, 956:207–214.

Tóth, R., Kevei, E., Hall, A., Millar, A. J., Nagy, F., and Kozma-Bognár, L. (2001). Circadian Clock-Regulated Expression of Phytochrome and Cryptochrome Genes in Arabidopsis 1. *Plant physiology*, 127:1607–1616.

Troein, C., Locke, J. C. W., Turner, M. S., and Millar, A. J. (2009). Weather and Seasons Together Demand Complex Biological Clocks. *Current Biology*, 19(22):1961–1964.

Ulm, R., Baumann, A., Oravecz, A., Máté, Z., Adám, E., Oakeley, E. J., Schäfer, E., and Nagy, F. (2004). Genome-wide analysis of gene expression reveals function of the bZIP transcription factor HY5 in the UV-B response of Arabidopsis. *Proceedings of the National Academy of Sciences*, 101(5):1397–1402.

Uttara, B., Singh, A. V., Zamboni, P., and Mahajan, R. T. (2009). Oxidative stress and neurodegenerative diseases: a review of upstream and downstream antioxidant therapeutic options. *Current neuropharmacology*, 7(1):65–74.

Van Buskirk, E. K., Decker, P. V., and Chen, M. (2012). Photobodies in light signaling. *Plant physiology*, 158(1):52–60.

van Zanten, M., Snoek, L. B., Proveniers, M. C. G., and Peeters, A. J. M. (2009). The many functions of ERECTA. *Trends in Plant Science*, 14(4):214–218.

Wang, F. F., Lian, H. L., Kang, C. Y., and Yang, H. Q. (2010). Phytochrome B is involved in mediating red light-induced stomatal opening in arabidopsis thaliana. *Molecular Plant*, 3(1):246–259.

Wang, W., Barnaby, J. Y., Tada, Y., Li, H., Tör, M., Caldelari, D., Lee, D. U., Fu, X. D., and Dong, X. (2011). Timing of plant immune responses by a central circadian regulator. *Nature*, 470(7332):110–115.

Wang, Z. Y. and Tobin, E. M. (1998). Constitutive expression of the CIRCADIAN CLOCK ASSOCIATED 1 (CCA1) gene disrupts circadian rhythms and suppresses its own expression. *Cell*, 93(7):1207–1217.

Wargent, J. J. (2016). UV LEDs in horticulture: from biology to application. *Acta Horticulturae*, 1134:25–32.

Wargent, J. J., Elfadly, E. M., Moore, J. P., and Paul, N. D. (2011). Increased exposure to UV-B radiation during early development leads to enhanced photoprotection and improved long-term performance in Lactuca sativa. *Plant Cell and Environment*, 34:1401–1413.

Weigel, D. and Glazebrook, J. (2002). *Arabidopsis: A Laboratory Manual.* Cold Spring Harbor Laboratory Press, New York, 1 edition.

Wellmann, E. (1976). Specific ultraviolet effects in plant morphogenesis. *Photochemistry and photobiology*, 24(6):659–660.

Welsh, D. K., Imaizumi, T., and Kay, S. A. (2005). Real-time reporting of circadian-regulated gene expression by luciferase imaging in plants and mammalian cells. *Methods in Enzymology*, 393:269–288.

Wenden, B., Kozma-Bognár, L., Edwards, K. D., Hall, A. J. W., Locke, J. C. W., and Millar, A. J. (2011). Light inputs shape the Arabidopsis circadian system. *The Plant journal : for cell and molecular biology*, 66(3):480–91.

Wenden, B., Toner, D. L. K., Hodge, S. K., Grima, R., and Millar, A. J. (2012). Spontaneous spatiotemporal waves of gene expression from biological clocks in the leaf. *Proceedings of the National Academy of Sciences*, 109(17):6757–6762.

Whitelam, G. C., Johnson, E., Peng, J., Carol, P., L., A. M., Cowl, J. S., and Harberd, N. P. (1993). Phytochrome A Null Mutants of Arabidopsis Display a Wild-Type Phenotype in White Light. *The Plant Cell*, 5(7):757–768.

Wilson, K. E., Wilson, M., and Greenbergt, B. M. (1998). Identification of the Flavonoid Glycosides that Accumulate in Brassica napus L. cv. Topas Specifically in Response to Ultraviolet B Radiation. *Photochem. photobiol.*, 67(5):547–553.

Winkel-Shirley, B. (2001). Flavonoid Biosynthesis. A Colorful Model for Genetics, Biochemistry, Cell Biology, and Biotechnology. *Plant Physiology*, 126(2):485–493.

Winkel-Shirley, B., Kubasek, W. L., Storz, G., Bruggemann, E., Koornneef, M., Ausubel, F. M., and Goodman, H. M. (1995). Analysis of Arabidopsis mutants deficient in flavonoid biosynthesis. *The Plant Journal*, 8(5):659–671.

Witham, F. H., Blaydes, D. F., and Devlin, R. M. (1971). *Experiments in Plant Physiology*.

Wu, M., Eriksson, L. a., and Strid, Å. (2013). Theoretical prediction of the protein-protein interaction between Arabidopsis thaliana COP1 and UVR8. *Theoretical Chemistry Accounts*, 132(7):1–11.

Xie, Q., Wang, P., Liu, X., Yuan, L., Wang, L., Zhang, C., Li, Y., Xing, H., Zhi, L., Yue, Z., Zhao, C., McClung, C. R., and Xu, X. (2014). LNK1 and LNK2 Are Transcriptional Coactivators in the Arabidopsis Circadian Oscillator. *The Plant Cell*, 26(7):2843–2857.

Yakir, E., Hassidim, M., Melamed-Book, N., Hilman, D., Kron, I., and Green, R. M. (2011). Cell autonomous and cell-type specific circadian rhythms in Arabidopsis. *Plant Journal*, 68(3):520–531.

Yamaguchi, R., Nakamura, M., Mochizuki, N., Kay, S. a., and Nagatani, A. (1999). Light-dependent translocation of a phytochrome B-GFP fusion protein to the nucleus in transgenic Arabidopsis. *The Journal of Cell Biology*, 145(3):437–445.

Yang, C., Xie, F., Jiang, Y., Li, Z., Huang, X., and Li, L. (2018). Phytochrome A Negatively Regulates the Shade Avoidance Response by Increasing Auxin/Indole Acidic Acid Protein Stability. *Developmental Cell*, 44(1):29–41.e4.

Yang, D., Seaton, D. D., Krahmer, J., and Halliday, K. J. (2016). Photoreceptor effects on plant biomass, resource allocation, and metabolic state. *Proceedings of the National Academy of Sciences*, 113(27):7667–7672.

Yanovsky, M. J., Casal, J. J., and Whitelam, G. C. (1995). Phytochrome A, phytochrome B and HY4 are involved in hypocotyl growth responses to natural radiation in Arabidopsis: weak de-etiolation of the phyA mutant under dense canopies. *Plant, Cell & Environment*, 18(7):788–794.

Yao, L. H., Jiang, Y. M., Shi, J., Tomás-Barberán, F. A., Datta, N., Singanusong, R., and Chen, S. S. (2004). Flavonoids in food and their health benefits. *Plant foods for human nutrition (Dordrecht, Netherlands)*, 59(3):113–122.

Yu, X., Liu, H., Klejnot, J., and Lin, C. (2010). The Cryptochrome Blue Light Receptors. In *The Arabidopsis Book*, pages 1–27.

Yue, J., Qin, Q., Meng, S., Jin, H., Gou, X., Li, J., and Hou, S. (2016). TOPP4 Regulates the Stability of Phytochrome Interacting Factor 5 during Photomorphogenesis in Arabidopsis. *Plant Physiology*, 170(March):1381–1397.

Zagotta, M. T., Hicks, K. A., Jacobs, C. I., Young, J. C., Hangarter, R. P., and Meeks-Wagner, D. R. (1996). The Arabidopsis ELF3 gene regulates vegetative photomorphogenesis and the photoperiodic induction of flowering. *Plant Journal*, 10(4):691–702.

Zeng, X., Ren, Z., Wu, Q., Fan, J., Peng, P.-P., Tang, K., Zhang, R., Zhao, K.-h., and Yang, X. (2015). Dynamic Crystallography Reveals Early Signalling Events in Ultraviolet Photoreceptor UVR8. *Nature Plants*, 1:1–14.

Zhang, B., Holmlund, M., Lorrain, S., Norberg, M., Bakó, L. S., Fankhauser, C., and Nilsson, O. (2017). BLADE-ON-PETIOLE proteins act in an E3 ubiquitin ligase complex to regulate PHYTOCHROME INTERACTING FACTOR 4 abundance. *eLife*, 6:1–19.

Zhang, Y., Mayba, O., Pfeiffer, A., Shi, H., Tepperman, J. M., Speed, T. P., and Quail, P. H. (2013). A Quartet of PIF bHLH Factors Provides a Transcriptionally Centered Signaling Hub That Regulates Seedling Morphogenesis through Differential Expression-Patterning of Shared Target Genes in Arabidopsis. *PLoS Genetics*, 9(1):11–13.

Zhen, S. and van Iersel, M. W. (2017). Far-red light is needed for efficient photochemistry and photosynthesis. *Journal of Plant Physiology*, 209:115–122.

Zhong, S., Shi, H., Xue, C., Wang, L., Xi, Y., Li, J., Quail, P. H., Deng, X. W., and Guo, H. (2012). A molecular framework of light-controlled phytohormone action in arabidopsis. *Current Biology*, 22(16):1530–1535.

Zhu, J.-Y., Oh, E., Wang, T., and Wang, Z.-Y. (2016). TOC1 - PIF4 interaction mediates the circadian gating of thermoresponsive growth in Arabidopsis. *Nature Communications*, 7:13692.

Zhu, Y., Tepperman, J. M., Fairchild, C. D., and Quail, P. H. (2000). Phytochrome B binds with greater apparent affinity than phytochrome A to the basic helix-loop-helix factor PIF3 in a reaction requiring the PAS domain of PIF3. *Proceedings of the National Academy of Sciences*, 97(24):13419–24.